

**PHYSICAL CHARACTERIZATION OF OLEIC ACID
POLYOL BASED POLYURETHANE COATINGS**

THAMIL SELVI VELAYUTHAM

SUBMISSION OF RESEARCH THESIS FOR THE
FULFILMENT OF THE DOCTOR OF PHILOSOPHY

UNIVERSITY OF MALAYA

2009

UNIVERSITI MALAYA
ORIGINAL LITERARY WORK DECLARATION

Name of Candidate: **Thamil Selvi Velayutham** (I.C/Passport No:
720226-01-5332)

Registration/Matric No: **SHC030012**

Name of Degree: **Doctor of Philosophy**

Title of Project Paper/Research Report/Dissertation/Thesis ("this Work"):

**"Physical Characterization of Oleic Acid Polyol Based Polyurethane
Coatings"**

Field of Study: **Physics (Material Science)**

I do solemnly and sincerely declare that:

- (1) I am the sole author/writer of this Work;
- (2) This Work is original;
- (3) Any use of any work in which copyright exists was done by way of fair dealing and for permitted purposes and any excerpt or extract from, or reference to or reproduction of any copyright work has been disclosed expressly and sufficiently and the title of the Work and its authorship have been acknowledged in this Work;
- (4) I do not have any actual knowledge nor do I ought reasonably to know that the making of this work constitutes an infringement of any copyright work;
- (5) I hereby assign all and every rights in the copyright to this Work to the University of Malaya ("UM"), who henceforth shall be owner of the copyright in this Work and that any reproduction or use in any form or by any means whatsoever is prohibited without the written consent of UM having been first had and obtained;
- (6) I am fully aware that if in the course of making this Work I have infringed any copyright whether intentionally or otherwise, I may be subject to legal action or any other action as may be determined by UM.

Candidate's Signature

Date

Subscribed and solemnly declared before,

Witness's Signature

Date

Name:

Designation:

ABSTRACT

The research studies focus on physical characterization of oleic acid polyol based polyurethane (PUR) coatings. Basically, polyurethanes are derived from the reactions between polyols and isocyanates. The most common polyols used in PUR production are made from petroleum derivatives. In this research, a new technology has been developed which results in producing PUR coatings based on polyols synthesized from oleic acid.

Three different polyols, with various oleic acid contents were used in the preparation of polyurethane (PUR) coatings. The polyols were designated as Alk28, Alk40 and Alk65, in which 28, 40 and 65 represents the oleic acid percentage of the polyols formulation. These polyols were reacted with aromatic isocyanate (toluene 2, 4-diisocyanate, TDI) to form PUR coatings. Properties such as acid number and hydroxyl value of the polyols have been determined. The polyols were characterized by Infrared (IR) spectroscopic. By varying the oleic acid content in the polyols, the amount of flexible side chains incorporated in the polymer was varied. On the other hand, the NCO/OH ratios of the PURs samples were varied to see the cross-linking effects as the ratios increased.

The characterization of PURs coating were carried out by IR spectroscopy, DSC analysis, TGA analysis and XRD analysis. Physico-chemical properties such as drying time, pencil hardness, adhesion properties, solvent resistance and corrosion/chemical resistant determination were reported. The PUR made from the lowest oleic acid content exhibited the best overall physical properties followed by the medium and the highest oleic acid content. The properties were enhanced as the NCO/OH ratio increased.

A part of the research was concentrated on electrical properties of the materials. Two types of conductivity measurement were performed which involved alternative current, ac and direct current, dc. The purpose of performing the ac and dc conductivity measurements for the PURs was to investigate the alternating current response as a function of the frequency to the applied field in order to study the dielectric behaviour of the material. The nature of conduction mechanism involved in the PUR was also determined. Mechanical and creep properties of the samples were also determined in the studies. The analysis revealed that the PURs made with polyols of the lowest oleic acid content have the best mechanical and creep properties due to introduction of higher degree of cross-linking.

ABSTRAK

Tesis ini mengkaji pencirian fizikal salutan polyurethane yang diperbuat daripada poliol asid oleik. Poliuretane (PUR) adalah polimer disintesis daripada poliol dan isocyanate. Kebanyakan poliol di pasaran dunia adalah hasil daripada bahan petroleum. Dalam tesis ini satu teknologi baru telah dibina yang menghasilkan salutan PUR diperbuat daripada poliol asid oleik.

Tiga jenis poliol dengan pelbagai kandungan asid oleik telah digunakan dalam penyediaan salutan PUR. Poliol tersebut telah dilabelkan sebagai Alk28, Alk40 dan Alk65 yang mana nombor 28, 40 dan 65 mewakili peratusan oleik acid dalam formulasi poliol. Poliol-poliol ini bertindakbalas dengan isocyanate aromatic (toluene 2, 4-diisocyanate, TDI) untuk menghasilkan penyalutan PUR. Pengelasan seperti nombor asid dan nilai hidroksil bagi poliol telah dikenal pasti. Kesemua poliol dikategorikan dengan menggunakan spektroskopik infra merah. Peningkatan peratusan kandungan asid oleik dalam poliol menghasilkan PUR yang mempunyai rantai polimer bercabang yang fleksibel. Selain itu, nisbah NCO kepada OH bagi sampel PUR juga dipelbagaikan untuk melihat kesan sambung-silang (crosslinking) molekul polimer apabila nisbah tersebut bertambah.

Pengelasan penyalut PUR dilakukan dengan spektroskopik infra merah, analisis DSC, TGA dan XRD. Ciri kimia-fizik seperti masa pengeringan salutan, ujian kekerasan pensil, ciri kelekatan penyalut PUR, kerintangan pelarut dan pengoksidaan dalam air dan pelarut kimia telah dilaporkan. PUR diperbuat daripada kandungan asid oleik terendah (28%) menunjukkan ciri fizikal keseluruhan yang terbaik berbanding dengan kandungan asid oleik sederhana (40%) dan tinggi (65%). Ciri kimia-fizik yang disebutkan diatas semakin ketara apabila nisbah NCO kepada OH bertambah.

Sebahagian dari kajian ini mefokuskan kepada ciri-ciri elektrik bagi bahan tersebut. Dua jenis pengukuran konduktiviti telah dijalankan yang melibatkan arus ulang-alik dan arus terus. Pengukuran ini bertujuan untuk menyelidik kesan tindakbalas arus ulang alik didalam medan elektrik. Sifat mekanisma konduksi yang terlibat dalam PUR juga dikenal pasti. Selain dari itu, ciri mekanikal dan rayapan PUR juga dikaji. Analisa menunjukkan PUR yang diperbuat daripada poliol dengan kandungan asid oleik terendah mempunyai ciri rayapan dan mekanikal terbaik disebabkan oleh peningkatan sambung-silang polimer molekul PUR.

ACKNOWLEDGEMENTS

I would like to express the deepest gratitude to my supervisors, Professor Dr. Wan Haliza Abdul Majid of Physics Department, and Professor Dr. Gan Seng Neon of Chemistry Department, Faculty of Science for their constant encouragement, supervision and effort in directing me in this research. Their wisdom, knowledge and commitment has inspired and motivated me to the highest standards. Without their guidance and persistent help this dissertation would not have been possible.

I am grateful to Associate Professor Dr Abu Bakar Ahmad, for his encouragement, discussion and constructive comment during the preliminary stage of the research. I would also like to thank the late En. Md Salleh bin Zakariah for his kind technical assistance in Material Science Laboratory. I am grateful to Mr Gan Yik Kang, Polymer Lab, Chemistry Department, University Malaya for synthesizing and characterizing the polyols. Heartfelt thanks to all my friends and colleague for their useful suggestions and invaluable support.

Special thanks to my beloved husband for his love, support, constant patience and sacrifice. I would also like to convey deepest appreciation to my parents and family members for their unfailing encouragement.

The financial support of this research by PASCA fellowship and award of research grant (Vot F F0161/2004) under University of Malaya are fully acknowledged.

LIST OF PUBLICATIONS

1. T. S. Velayutham, W. H. Abd Majid, A. B. Ahmad, Yik Kang Gan, Seng Neon Gan, 2009. **The physical and mechanical properties of polyurethanes from oleic acid polyols.** *Journal of Applied Polymer Science*, **112**(6), 3554-3559.
2. T. S. Velayutham, A. B. Ahmad, W. H. Abd Majid, Gan Seng Neon, 2008. Electrical properties of polyurethane graphite composites. *Jurnal Fizik Malaysia*, **29**, 25- 28.
3. T. S. Velayutham, W.H.Abd Majid, A.B.Ahmad, Gan Yik Kang, Gan, S.N. Synthesis and characterization of polyurethane coatings derived from polyols synthesized with glycerol, phthalic anhydride and oleic acid. *Progress in Organic Coatings*, **66**, 367-371.
4. T. S. Velayutham, W. H. Abd Majid, A. B. Ahmad, Gan Seng Neon. Dielectric behavior of **polyurethane coatings derived from polyols synthesized with glycerol, phthalic anhydride and oleic acid.** Submitted to the *Journal of Physics D: Applied Physics*.
5. T. S. Velayutham, W. H. Abd Majid, A. B. Ahmad, Gan Seng Neon. The dielectric and mechanical properties of polyurethanes synthesized from oleic acid polyols. Submitted to the *Journal of Applied Polymer Science*.

TABLE OF CONTENTS

<i>Abstract</i>	<i>i</i>
<i>Abstrak</i>	<i>ii</i>
<i>Acknowledgement</i>	<i>iii</i>
<i>List of Publications</i>	<i>iv</i>
<i>Table of Contents</i>	<i>v</i>
<i>List of Figures</i>	<i>ix</i>
<i>List of Tables</i>	<i>xiv</i>

CHAPTER 1: INTRODUCTION

Introduction.....	1
References.....	7

CHAPTER 2: LITERATURE REVIEW

2.1	Introduction.....	8
2.2	Types of coatings	10
	2.2.1 Conventional solvent borne coatings.....	13
	2.2.2 Water borne coatings.....	15
	2.2.3 High solid coatings.....	17
2.3	Basic curing mechanism.....	19
2.4	Raw materials.....	22
	2.4.1 Polyol.....	24
	2.4.2 Isocyanate.....	26
2.5	Renewable resources.....	28
	2.5.1 Structure of triglyceride oil.....	30
	2.5.2 Polyurethane from vegetable oil.....	31
	2.5.3 Palm oil and PUR.....	32
	2.5.3.1 Palm kernel oil (PKO) & palm olein.....	35
2.6	Alkyd resin / polyol.....	36
	2.6.1 Process of alkyd making.....	37

2.7	Conclusion.....	39
	References.....	40

CHAPTER 3: EXPERIMENTALS AND STRUCTURAL CHARACTERIZATION OF POLYURETHANE

3.1	Introduction.....	54
3.2	Sample preparation	
3.2.1	Raw materials.....	55
3.2.2	Procedure of polyol synthesis.....	55
3.2.3	Procedure of PUR prepolymer synthesis.....	57
3.2.4	Preparation of coating and free films for testing.....	59
3.3	Polyols and PURs reaction schemes.....	60
3.4	Common techniques used in PUR films characterization	
3.4.1	FTIR.....	63
3.4.2	XRD.....	64
3.4.3	DSC.....	64
3.4.4	TGA.....	66
3.5	Results and Discussion	
3.5.1	FTIR Analysis.....	69
3.5.2	XRD Analysis.....	72
3.5.3	DSC Analysis.....	75
3.5.4	TGA Analysis.....	77
3.6	Conclusion.....	85
	References.....	86

CHAPTER 4: CHARACTERIZATION OF THE PUR COATING

4.1	Introduction.....	88
4.2	Coating on mild steel panel.....	89
4.3	Tests on coatings	
4.3.1	Adhesion test.....	92
4.3.2	Pencil hardness test.....	93
4.3.3	Water immersion testing.....	94
4.3.4	Acid resistance testing.....	95

4.3.5	Alkali resistance testing.....	96
4.3.6	Salt water resistance testing.....	96
4.3.7	Solvent resistance test (solvent rubs).....	97
4.4	Results.....	98
4.4.1	Coatings appearance.....	99
4.4.2	Curing time.....	99
4.4.3	Adhesion measurement by tape test.....	101
4.4.4	Pencil hardness.....	101
4.4.5	Water resistance.....	101
4.4.6	Acid, alkali and salt resistance.....	102
4.4.7	Solvent rub test.....	104
4.5	Discussion.....	105
4.6	Conclusion.....	110
	References.....	112

CHAPTER 5: ELECTRICAL PROPERTIES OF POLYURETHANE

5.1	Introduction.....	114
5.2	AC conductivity studies	
5.2.1	Theory.....	115
5.2.2	Experimental setup.....	121
5.2.3	Results.....	122
5.2.4	Discussion.....	136
5.2.4.1	The effect of oleic acid content.....	137
5.2.4.2	The effect of NCO/OH ratio.....	138
5.2.4.3	Polarization.....	139
5.3	DC conductivity studies	
5.3.1	Theory of conductivity.....	142
5.3.2	Experimental setup.....	147
5.3.3	Results.....	148
5.3.4	Discussion.....	162
5.4	Conclusion.....	167
	References.....	168

CHAPTER 6: MECHANICAL PROPERTIES OF PUR

6.1	Introduction.....	174
6.2	Literature review.....	175
6.3	Background	
6.3.1	Polymers classification.....	178
6.3.2	Molecular forces and chemical bonding.....	179
6.3.3	Solid state properties of polymers.....	180
6.3.4	Mechanical properties.....	181
6.4	Experimental setup	
6.4.1	Tensile testing.....	185
6.4.2	Creep and recovery testing at constant load and time.....	188
6.5	Results	
6.5.1	Tensile studies.....	189
6.5.2	Creep and recovery studies.....	194
6.6	Discussion	
6.6.1	Tensile test	200
6.6.2	Creep test.....	204
6.7	Conclusion.....	206
	References.....	208

CHAPTER 7: CONCLUSION AND SUGGESTION FOR FUTURE WORK

Conclusion and suggestion for future work.....	211
---	------------

APPENDIX

LIST OF FIGURES

- Figure 1.1** Simple PUR containing urethane linkage at its backbone chain
- Figure 2.1** A triglyceride molecule
- Figure 2.2** Synthesis of triglyceride
- Figure 3.1** Apparatus set-up during the pre-polymerization process of PUR
- Figure 3.2** The FTIR spectra of polyols Alk28, Alk40, Alk65 and oleic acid
- Figure 3.3** The FTIR spectra of PUR with NCO/OH ratios of 1.2, 1.4, 1.6.
- Figure 3.4** XRD profiles of PURs with various NCO/OH ratios
- Figure 3.5** TG and DTG curve versus temperature of PUalk28 (1.2)
- Figure 3.6** TG and DTG curve versus temperature of PUalk28 (1.4)
- Figure 3.7** TG and DTG curve versus temperature of PUalk28 (1.6)
- Figure 3.8** TG and DTG curve versus temperature of PUalk40 (1.2)
- Figure 3.9** TG and DTG curve versus temperature of PUalk40 (1.4)
- Figure 3.10** TG and DTG curve versus temperature of PUalk40 (1.6)
- Figure 3.11** TG and DTG curve versus temperature of PUalk65 (1.2)
- Figure 3.12** TG and DTG curve versus temperature of PUalk65 (1.4)

- Figure 3.13** TG and DTG curve versus temperature of PUalk65 (1.6)
- Figure 4.1** Classifications of adhesion test results
- Figure 4.2** Schematic diagram of a sheen pencil hardness tester kit
- Figure 4.3** The relationship between dry hard time in log scale and NCO/OH ratios for PUalk28, PUalk40 and PUalk65.
- Figure 5.1** Frequency dependence of real and imaginary components of the dielectric permittivity for PUalk28 (1.6) measured at room temperature
- Figure 5.2** Variation of real permittivity (ϵ') with frequency for PUalk28 with NCO/OH ratio of 1.2, 1.4 and 1.6 measured at room temperature
- Figure 5.3** Variation of real permittivity (ϵ') with frequency for PUalk40 with NCO/OH ratio of 1.2, 1.4 and 1.6 measured at room temperature
- Figure 5.4** Variation of real permittivity (ϵ') with frequency for PUalk65 with NCO/OH ratio of 1.4 and 1.6 measured at room temperature.
- Figure 5.5** Frequency dependence of the imaginary permittivity (ϵ'') for PUalk28 at NCO/OH 1.2, 1.4 and 1.6 measured at room temperature.
- Figure 5.6** Frequency dependence of the imaginary permittivity (ϵ'') for PUalk40 at NCO/OH ratio 1.2, 1.4 and 1.6 measured at room temperature.
- Figure 5.7** Frequency dependence of the relative permittivity (ϵ'') for PUalk65 at NCO/OH ratio 1.4 and 1.6 measured at room temperature.
- Figure 5.8** Real permittivity ϵ' vs frequency for PUalk28, PUalk40 and PUalk65 at NCO/OH ratio 1.6 measured at room temperature.
- Figure 5.9** Imaginary permittivity ϵ'' vs frequency for PUalk28, PUalk40 and PUalk65 of NCO/OH ratio 1.6 measured at room temperature.

- Figure 5.10** The asymmetrical Havriliak-Negami plots of the dispersion curves for (i) PUalk28 (ii) PUalk40 and (iii) PUalk65 measured at RT
- Figure 5.11** The asymmetrical Havriliak-Negami plots of the dispersion curves for PUalk28, PUalk40 and PUalk65 at fixed ratio of 1.6 measured in RT
- Figure 5.12** Frequency-dependent conductivity σ_{ac} vs frequency for PUR at room temperature. Dots are experimental points and continuous lines correspond to simulated fit.
- Figure 5.13** Four possible electrons band structures in solid at 0 K
- Figure 5.14** Arrhenius plots of PUalk28 with NCO/OH ratio of 1.2, 1.4 and 1.6
- Figure 5.15** Arrhenius plots of PUalk40 with NCO/OH ratio of 1.2, 1.4 and 1.6
- Figure 5.16** Arrhenius plots of PUalk65 with NCO/OH ratio of 1.2, 1.4 and 1.6
- Figure 5.17** Exponential plot at various temperatures for (i) PUalk28 (1.6), (ii) PUalk40 (1.6), (iii) PUalk65 (1.6).
- Figure 5.18** Schottky plot of (i) PUalk28 (1.6), (ii) PUalk40 (1.6) and (iii) PUalk65 (1.6) at various temperatures
- Figure 5.19** Typical hyperbolic sine function model fit performed on (i)PUalk28 (1.2) (ii) PUalk28 (1.6). Dots are experimental points and continuous lines corresponds to simulated fit.
- Figure 5.20** Typical hyperbolic sine function model fit performed on (i) PUalk40 (1.2) (ii) PUalk40 (1.6). Dots are experimental points and continuous lines corresponds to simulated fit.
- Figure 5.21** Typical hyperbolic sine function model fit performed on (i)PUalk65 (1.2) (ii) PUalk65 (1.6). Dots are experimental points and continuous lines corresponds to simulated fit.

- Figure 5.22** Plot of hopping distance, λ as a function of temperature (i) PUalk28 (ii) PUalk40 (iii) PUalk65 for NCO/OH ratio 1.2, 1.4, 1.6
- Figure 5.23** Plot of hopping distance, λ as a function of temperature at fixed ratios (i) 1.2 (ii) 1.4 (iii) 1.6 for all the PURs
- Figure 6.1** Secondary bonding
(Adapted from Szycher M., 1999)
- Figure 6.2** Schematic stress-strain curve for a plastic polymer showing how tensile strength, elongation at break, ϵ_{Fmax} , rupture strength and E modulus are determined
- Figure 6.3** Typical stress-strain curves for (a) rigid and brittle, (b) plastic, (c) highly elastic (elastomeric) polymers
- Figure 6.4** Typical extension-time curve for creep studies
- Figure 6.5** Specimen dimension according to ASTM D638 – type IV. The entire dimension is in mm.
- Figure 6.6** Stress (MPa) versus Strain (%) curves for oleic acid polyol based PUR
- Figure 6.7** The effect of NCO/OH ratios on the tensile strength for PUR
- Figure 6.8** The effect of NCO/OH ratios on the elongation at break for PUR
- Figure 6.9** Extension (%) versus Time (min) curve for PUalk28 (1.2)
- Figure 6.10** Extension (%) versus Time (min) curve for PUalk28 (1.4)
- Figure 6.11** Extension (%) versus Time (min) curve for PUalk28 (1.6)
- Figure 6.12** Extension (%) versus Time (min) curve for PUalk40 (1.2)

Figure 6.13 Extension (%) versus Time (min) curve for PUalk40 (1.4)

Figure 6.14 Extension (%) versus Time (min) curve for PUalk40 (1.6)

Figure 6.15 Extension (%) versus Time (min) curve for PUalk65 (1.4)

Figure 6.16 Extension (%) versus Time (min) curve for PUalk65 (1.6)

LIST OF TABLES

Table 2.1	Some fatty acids in natural oils (Adapted from F. Seniha Güner et al., 2006)
Table 2.2	Classification of alkyd resins
Table 3.1	Composition of PA, glycerol and oleic acid used in the preparation of polyols.
Table 3.2	Properties of oleic acid polyols
Table 3.3	Composition of polyols and TDI used in the preparation of PUR
Table 3.4	Thermal dissociation temperatures of linkages found in polyurethanes
Table 3.5	The vibration modes and wavenumbers of PUR from IR spectrum
Table 3.6	Glass transition temperatures of PUR samples
Table 3.7	Thermal behavior of PUR at nitrogen atmosphere
Table 4.1	Classification of water immersion test results
Table 4.2	Classification of acid, alkali and salt water resistance test results
Table 4.3	Set-to-touch, dry-to-touch and dry-hard time observed for the oleic acid based polyols PUR coatings
Table 4.4	Results of pencil hardness, adhesion and water immersion testing
Table 4.5	The PUR coatings resistance to NaCl 5%, 0.1M HCl and 0.1M NaOH
Table 4.6	Result of solvent resistance test on PUR coatings

Table 5.1	The static permittivity, ϵ_s , induced permittivity ϵ_∞ , dielectric strength, $\Delta\epsilon$, α and β parameters at room temperature derived from HN plots
Table 5.2	The experimental and fitted results of dc conductivity at room temperature derived from power law plots
Table 5.3	Activation energies derived from Arrhenius plot
Table 6.1	Summary of results from tensile measurement
Table 6.2	Material's characteristic and percentage recovery during the creep test

CHAPTER 1: INTRODUCTION

The development of plastics in history signifies that man constantly needs newer and better material with which to work in order to continue his progress. Each individual polymer was born as an idea, a theory and even sometimes as by-product of unrelated research work. However, the end results presented to industry or consumer were efforts of many men as a total contribution. The polyurethane that we know today was first invented by Professor Dr. Otto Bayer as a fiber-forming polymer in 1937 (LN Philips et al., 1964). He synthesized it by reacting an aliphatic 1,8-octane diisocyanate with 1,4-butanediol. It was known that the early study of PUR was to improvise the properties as a polymer fiber to compete with nylon. However, later the versatility of this new organic polymer and its ability to substitute for scarce materials, spurred numerous applications such as PUR foams, elastomers and surface coatings.

Numerous technical papers, articles and patents on PUR materials have routed development on PURs. Although most of the details are not entirely clear today, however few historical events of PUR developments are considered important and compiled in this thesis. In 1937, I.G Farbenindustrie applied for the first PUR patent in German titled “A process for the production of polyurethanes and polyureas” (Bayer O et al., 1942, German Patent 728981), in 1938 Rinke et al., awarded the first US patent 2511544 on “diol-diisocyanate high molecular polymerization products”, in 1941 the first PUR coating was developed, in 1955 estane thermoplastic elastomer was approved for US patent (Charles SS et al., 1959, US Patent 2871218), in 1971 patent on PUR silicone elastomer for medical application was awarded (Emery et al., 1971, US Patent

3562352) and in 1993, aliphatic biostable PUR elastomer was patented in US (Michael S et al., 1993, US Patent 5254662).

Most plastics industries realized that PUR have a very promising future. Commercially, the development of polyurethanes closely coincided with the consumption of the material as end product in the market. In the 1950s, the world annual consumption of PUR was only 8 million pounds. In 1960s, the amount reached 600 millions in various applications. The versatilities of the material and wide range of physical properties from soft flexible foam to hard foam and to long wearing coatings have resulted in many end use applications. Consequently, the worldwide demand for the material reached 6652 million pounds in 1980's (Kenneth N Edwards, 1980). In 1995, it was estimated that the world's polyurethane amount was approximately 16 billion pounds, which constituted about 5% of the total amount of plastics produced worldwide (Szycher, 1999). The plastic industry is becoming more and more aware of the importance of PUR, thus there are many ongoing developmental work and research on these polymers.

In general, polyurethanes consist of several polymer structures with repeating urethanes (-NH-CO-O-) linkages. It is obtained from the reaction of isocyanates and any hydroxyl bearer compounds such as polyester or polyether, polycarbonates, polyacetals, castor oil and simple glycols. Figure 1.1 shows simple polyurethane structure. There are many kinds of raw materials that can be used to synthesize PUR. For the isocyanates component, one can choose bi or polyisocyanate. The adduct or trimers of diisocyanates are the polyisocyanate and are used frequently to minimize the evaporation of the toxic isocyanates to the atmosphere. Diisocyanate can be classified into aliphatic and aromatic diisocyanate. Aromatic isocyanates are very reactive and

cheaper than aliphatic isocyanates but polyurethanes made from aliphatic diisocyanates are more resistant to hydrolysis, UV light degradation and heat degradation (E. N Doyle, 1972).

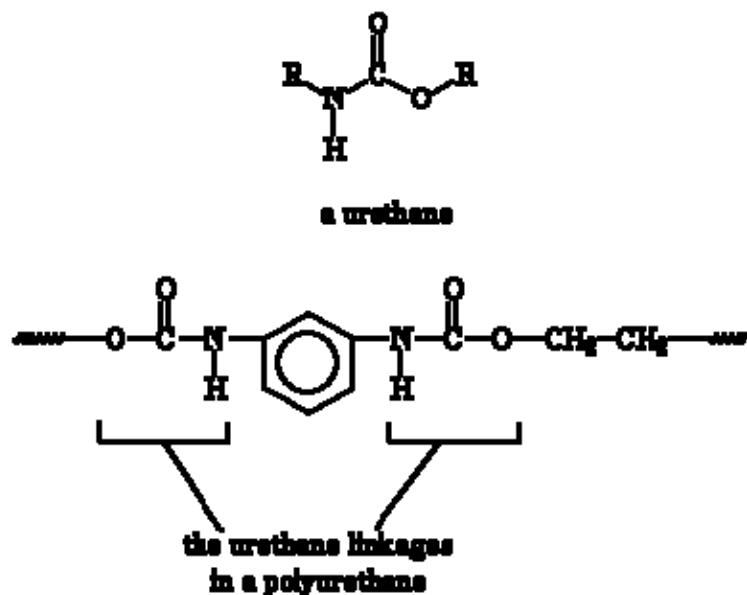


Figure 2.1 Simple PUR Containing Urethane Linkage at his Backbone Chain

As for polyols, they can be classified as polyether polyol, polyester polyol and other hydroxyl containing compounds. Most commonly used polyols in industries are the polyester and polyether polyols. Generally, polyester polyols are used to make coatings and elastomers and polyether polyols are used to make foams, elastomers and sealants. Almost all commercial polyols are obtained from petroleum derivatives. Presently, the scientific community has become very interested in developing material originating from renewable resources. The main vegetable oil used to manufacture PURs of excellent properties is castor oil. There are other oils such as soya, sunflower, linseed, canola and safflower used in the production of PUR.

Palm oil is a vegetable oil abundant in our country. In fact, Malaysia is one of the world largest producers and exporters of palm oil. Palm oil industry has adopted efficient techniques to diversify the uses of palm oil in many areas. Since PURs are one of highly priced and valuable polymer, the transformation of palm oil into PURs provides the possibilities of obtaining the biggest economic profit per unit of the products. In this present research, an attempt has been made to develop polyols with palm oleic acid to synthesize PUR coating.

Polyurethane coatings, which generally exhibit excellent abrasion resistance, high adhesion performance and solvent resistance, are widely used in our daily life and industrial environments. Compared to other coating in the market, PUR has many advantages. PUR coatings have good decorative and protective performance, elasticity of the material varies considerably and chemical and water resistance properties of the material are considerably very good. The many advantages of the material is the main reason for it to be the market leader for coating various substrates in the end use such as automotive refinish, aircraft, chemical resistant coatings, industrial maintenance and appliances. Besides that, the major usage of PUR is in the electrical field - wire coating and encapsulation of delicate component.

The main aim of this research is to synthesize and characterize a series of PUR coatings derived from palm oleic acid based polyols. The polyols are prepared by varying the oleic acid content in the samples to 28, 40 and 65%. The content of oleic acid in the polyols ensures incorporation of flexible side chains in the polymer. On the other hand, the NCO/OH ratios of the PURs samples are varied to see the cross-linking effects as the ratios increased. The effects of both variations on physical characteristics such as

structural, coating, electrical and mechanical properties of the PUR samples are studied and reported in this thesis.

Chapter 2 of this thesis describes the literature review of PUR materials. The chapter begins by reviewing the types of PUR coatings, followed by curing mechanism and raw materials used in PUR industry. Subsequently, the usage of renewable resources, palm oil relevancy and techniques in the synthesis of polyols are also described in detailed.

Chapter 3 deals on experimental set-up carried out in the research. The formulation of the samples along with the preparation methods of polyol and PUR prepolymers are presented in the chapter. In addition, the measurements such infra-red spectroscopy, x-ray diffraction, differential scanning calorimetry and thermogravimetry which have been carried out in the investigation on the physical properties of PUR, are also described and analyzed in this chapter.

Chapter 4 solely indulges on PUR coatings. The chapter begins with the coating method on mild steel panel and the measurement of film thickness are described. The curing of the coatings are investigated and reported. Focus is then given to coating testing such as adhesion test, pencil hardness tests, and chemical resistance test. The results and analysis of the testing are presented in the chapter.

The next chapter, Chapter 5, focus on the experimental techniques and associated theories involved in measuring the electrical properties of PUR coatings prepared in thick films. Two types of conductivity measurement were performed which involved alternative current, AC and direct current, DC. The natures of conduction mechanism

involved in PUR on both methods are investigated and the informations pertaining to the dielectric behaviour of the material are presented in this chapter.

Next, mechanical properties of polyurethane are addressed in chapter 6. Two types of testing, firstly tensile measurement and secondly, the creep and recovery of material at constant load and time are determined. The details of literature review, theory, experimental set-up, results and discussion on the testing performed are outlined and discussed in this chapter.

Finally, Chapter 7 concludes this thesis with a summary of the research findings which was previously discussed in the other chapters. This chapter also explores on the possible future research activities on polyurethane.

References

Bayer O, Siefkin W, Orther L, Schild H., 1942. A process for the production of polyurethanes and polyureas. German Patent 728981.

Charles S Schollenberger, Cuyahoga Falls, Ohio (BF Good Company NY), 1959. Simulated vulcanizates of polyurethane elastomers. US patent 2871218.

Emery Nyilas, Bedford, 1971. Polysiloxane-PUR Block copolymers. US Patent 3562352.

E. N Doyle, 1972. The development and use of polyurethane products. McGraw-hill, 1971, pg 2-92.

Kenneth N Edwards, 1980. Urethane Chemistry and Applications. ACS Symposium series 172, pg 9.

LN Phillips , DBV Parker, 1964. Polyurethanes – Chemistry, Technology & Properties. London Iliffe Books Ltd, pg 1.

Michael Szycher, Lynnfield, 1993. Biostable PUR products. US Patent 5254662.

Rinke H, Schild H, Siefken W (IG Farbenindustrie), 1938. Diol-dilsoocyanate high molecular polymerization products. US Patent 2511544

Szycher, M., 1999. Szycher's handbook of polyurethanes, CRC Press, pg 1-7.

CHAPTER 2: LITERATURE REVIEW

2.1 Introduction

The demand for polyurethanes (PUR) in the coating industry is growing rapidly and in some applications they dominate the market. PUR films have outstanding properties such as toughness, flexibility, abrasion resistance, and solvent resistance, plus the ability to be customized. Typical uses of the coating include leather coatings, fabric coatings and adhesives, industrial maintenance and corrosion resistant finishes, floor varnishes, seamless flooring, marine finishes, magnet wire coating and concrete sealing.

Like any other coatings, PUR coatings are made from a variety of chemicals. The main raw materials used in the production of PUR are polyols, polyisocyanates and additives. About 90% of the polyols currently used for the production of PUR worldwide are based on polyethers derived from ethylene and propylene oxide. However, as the oil crisis and global warming deepen, there is a growing interest to produce polymers by the use of natural renewable resources to substitute petrochemicals. Triglyceride oils are one of the most important sources for green polyols. Polyurethane materials created from triglyceride oils such as cast resins and rigid foams are not something new and have been in existence for some time (Saggese EJ et al., 1967; Khoe et al., 1972; CK Lyon et al., 1974; Hoefer et al., 1989, Chian KS et al., 1998; ^bPetrovic ZS et al., 2000).

The wide application of petroleum in producing polyols are restricted because major issues associated with the extensive use of petroleum in our society such as, depleting reserves, national scarcity issues, price uncertainty and growing environmental concern

over the combustion of fossil fuel. However, vegetable oil is a sustainable resource and available almost every country in the world. The production of vegetable-based polyols has low capital - raw material and processing cost if compared to petroleum based polyol.

Technologies to produce polyols from palm oil, palm olein and palm kernel oil that are economically competitive to petroleum based polyols have been developed in Malaysia. The polyols are produced from palm oil, palm kernel oil and their derivatives. The reaction between these polyols with polyisocyanate produces polyurethane. To date polyols from palm oil have been used to produce flexible and rigid PUR foam successfully (^bSalmiah, A et al., 1995, Tuan Noor Maznee et al., 2001). The effort to prepare PUR coatings from palm oil based polyols are still under development.

There are several types of PUR coatings. Conventional PUR coatings are solvent - based coatings and over recent decades, this system has dominated the industrial coating market. However, more stringent regulations concerning emissions of volatile organic compounds (VOCs) continue to threaten this position. Hence, paint manufacturers and raw material suppliers are developing alternative technologies that are more respectful of the environment while offering the same level of performance.

Earlier efforts to formulate low-VOC of high solids coating were mainly focus on the development of the resin however the reduction in viscosity is often achieved by the reduction of molecular weight of resin which has less satisfactory properties. Over the past few years, a new generation of low viscosity polyisocyanate such as hexamethylene diisocyanate, HDI dimer (uretidione) is manufactured to reduce the

viscosity without affecting PUR reaction and performance. Recently reactive diluents such as oxazolidine and aldimine are becoming available to replace conventional solvent. Other alternatives are water-borne PUR coatings and powder coatings which are gaining popularity.

This chapter reviews the development of PUR coatings. A brief description of low VOC PUR coatings, moisture cured PUR coatings, waterborne and high solid PUR coatings and there is given. The review also focus on the chemistry aspect of PUR, the importance of side products such as biuret and allophanate formation as well as the raw materials used in the synthesis of the PUR coatings. A portion of the review is also devoted to bio-based PUR and their development. In bio-based polymers, the review covers the structure, property and modification of triglyceride oils and synthesis of PUR. Palm oil and palm kernel oil properties and their development in producing PUR are also elaborated in the review.

2.2 Types of coatings

There are many ways to compare coatings. ASTM D16 Standard (ASTM D16-00, Dieterich D et al., 1993) categorized six different PUR coatings which are related to the curing mechanism. ASTM classification of urethane coatings is summarized and adapted from ^aD.K. Chattopadhyay et al. 2007, Michael Szycher, 1999 and Dieter Stoye et al., 1998 as described in the next section.

ASTM classification of PUR types of coatings

One Component PUR coatings

- Type I (Urethane-modified alkyd coatings - “Urethane oils”) - produced by reacting diisocyanates with polyol-modified drying or semidrying oils. The process is analogous to that used in alkyd manufacture in which a proportion of the dicarboxylic acid is replaced by diisocyanate produces an upgraded drying oil. Curing is accomplished by oxidation of the unsaturated oil. Urethane oil and alkyd do not contain free isocyanate. Generally, the resultant films have faster drying capacity, better mechanical properties and higher solvent resistance.
- Type II (Moisture cured urethane) - Isocyanates are polymerized with diols and triols such as polyethers, polyhydric alcohols and castor oil products. These are PUR prepolymers, finished at free NCO content around 3 - 4% at nonvolatile level of 40 - 50%. In this system, prepolymers are prepared with unreacted terminated isocyanate groups that react with atmospheric moisture to form the finished cross-linked urea groups. The films produced from this method have excellent resistance to chemical and mechanical attacks.
- Type III (Blocked urethane - heat cured) – Reaction of isocyanate groups with polyols is blocked with certain blocking agents making it unreactive at room temperature but easily eliminated under the action of heat. The stoving temperatures vary from 120-220⁰C depending on the blocking agent but can be lowered by using catalyst such as dibutyl tin dilaurate for certain case. Blocking agents include phenol, oxime (Wicks Jr. et al., 1975), butanone, ϵ -caprolactam (Katsobashvili VYa et al., 1976), imidazoline (Rainer G et al., 1979), tetra-

hydropyrimidine, imidazole (Nasar AS et al., 1999), pyrazole (Muhlebach A et al., 1994), etc.

- Type VI (Non reactive lacquer) – Fully polymerized PUR dissolved in solvents and the forming of films occurs as the solvent evaporates from the surface of substrate. These types of coatings are thermoplastic polymer with relatively high molecular weight.

Two Component PUR coatings

- Type IV (Prepolymer plus catalyst) – Isocyanate prepolymer is similar to Type II, provides with a separate catalyst to accelerate the cure. One package contains the isocyanate adducts or prepolymers, and the second package contains a small amount of highly reactive diamine compound and other ingredients or additives to promote flow, bubble release and etc.
- Type V (Prepolymer plus polyol) - Isocyanates are reacted with relatively low-molecular weight polyols such as alcohol to form adducts. These adduct then form one part of a two-component system and another part is isocyanate rich. Reaction occurs when the two components were reacted where chain extension and curing are obtained.

There are many types of PUR coatings in the market. However, most commonly used coatings are conventional solvent-borne coatings, high solids coatings and water-borne coatings. Noting their importance in practical applications, these types of coatings are briefly reviewed in the next section.

2.2.1 Conventional solvent borne coatings

Traditionally, PUR coatings are formulated in solvents, which upon their evaporation and the reaction of isocyanate groups with hydroxyl groups, PUR coating is formed. Solvent borne PUR coatings, also known as moisture-cured polyurethanes, contain isocyanate (NCO) terminated PUR prepolymer (Hofacker S et al., 2004) which cures on exposure to atmospheric moisture to produce highly cross-linked networks. In terms of composition, this coating comprises 50 – 70 percent solvent content or in terms 30 - 50 percent solid content.

Solvents are an integral component of coating formulations, providing control over flow, wetting, coalescing and drying characteristics. The word “conventional” in conventional solvent borne coatings refers to the fact that these coatings have been in use much longer than the other two systems that are compared here. In fact solvent borne PUR systems have been used successfully in a wide variety of applications. These coatings are more readily available than other types simply because they are well established in the market.

Although solvent borne PUR coatings can be categorized into one component and two components system but conventional solvent borne PUR coatings in this section refers to one component system. The advantages of solvent borne PUR coatings have been summarized by G.J. Gardner, 1996. According to him, the advantage of the system is that it can be manufactured as a one-package system that can be readily used and their applications are far easier than two component systems. Secondly, the formulation has less VOC than two-component system since the salient reactant is water. In comparison of two-component polyurethanes, the moisture-cured polyurethanes/polyurea coatings

have good adhesion, abrasion resistance, thermal stability, hardness, chemical and solvent resistance and high humidity tolerance (Hai Ni et.al 2000).

As for two component solvent borne coatings, utilizing aliphatic isocyanate and polyester or acrylic polyols has become the industry standard for weatherable topcoats (S Bassner et al., 1996 and RR. Rosler et al., 1996). This type of coatings is widely used in applications where high requirement are specified (such as automotive refinish, aircraft finishing, industrial coatings and corrosion protection) in terms of film appearance and resistance properties due to their high percentage of urea groups in the polymer structure.

The current standard for topcoats and clear coats in car refinish in Europe is 3.5 VOC solvent borne as determined by the directive in force as of 2007. The binders in 3.5 VOC are acrylic polyols and sometimes combined with polyester oligomers and cross-linkers mostly based on HDI trimer. An improvement in the design of the above polyols was the introduction of branched polyether oligomers with at least four functional groups to get the overall property balance. Jos TH. et al., 2006 prepared the polyester polyols by ring opening polyetherification giving narrow functionality (F) and molecular weight distributions and a favourable solids-viscosity relation. They have even shown how the final clear coat properties correlate with some initial oligomers properties in view of M_w , T_g and F of oligomers and type of polyisocyanate hardener.

Graft copolymers have been used for many important applications in the polymer industry. However, reports on the application of graft copolymers to coatings, particularly to two-component PUR coatings have been scarce. The synthesis and

properties of the graft copolymers as acrylic polyol in PUR coatings were obtained and the uses of it are reported by Yoshizumi M. et al., 1999.

2.2.2 Water borne coatings

When it comes to having high performance and environmentally acceptable coatings, waterborne polyurethanes are the first choice. Waterborne polyurethanes can be one- or two component systems or binders cured by ultra-violet radiation. Until the late 1980s, it was still unthinkable to produce waterborne two-component PUR coatings. The main obstacle was the undesired secondary reaction of water with isocyanate. The growing success of waterborne two component PUR coatings lies in the development of raw materials such as water reducible polyisocyanate hardeners, improved binder dispersion based on polyacrylates and polyester – PUR, and etc.

There has been a wide range of work done in the synthesis and characterizations of waterborne PUR (A.K. Nanda et al, 2005, S.S.Yoon et al, 2005, T.C.Wen et al, 1999). Generally, the waterborne PUR can be prepared in the ionomer, nonionomer and anionomer. Li-Hong Bao et al 2006 studied the structure and properties of aqueous PUR dispersion with ionic group in the soft segments. B.K Kim et al, 2003 synthesized PUR ionomer dispersions containing ionic groups in soft segment and compared it with the conventional ones which contain ionic groups in hard segments. They found ionic soft segments gave a significantly lower solution viscosity, smaller particle size and greater dispersion viscosity. Xin Wei et al., 1997 synthesized a series of PUR ionomers with different contents of sodium sulfonate groups in the soft segments and found that as the ionization level increased, the compatibility of the hard and soft segments increased and the glass transition region of the soft segment became broader.

Waterborne polyurethanes often contain N-methyl pyrrolidone (NMP), an organic solvent that is used in the processing of the resin. Another development of waterborne PUR coating is NMP free coatings. According to upcoming European legislation, products containing more than 0.5 NMP will have to be labelled as being irritant and toxic. Dr. Dirk Mestach et al., 2006 disclosed in his paper some novel NMP-free waterborne PURs and compared their performance with NMP containing products.

Fire retardant polyurethane coatings system (Hongsoo Park et al., 1996, Park, H.S., et al., 1996, Ying-Ling Liu et al., 1997, Kuo et al., 1998, ^bWang TZ et al., 1999, ^aWang TZ et al., 2001) are also becoming very popular. Flame retardants can be classified as organic materials such as halogenated compounds and inorganic materials like metal oxides, metal hydroxides and metal borates. Funda Celebi et al., 2003 reported that the flame resistance of polyurethane can be improved by incorporating either reactive or non reactive fire retardants. Funda Celebi produced phosphorus-containing flame retardant water dispersed PUR coatings by incorporating different amounts of a phosphorus compound onto the PUR main chain.

Aqueous PUR dispersion has been investigated by many researches, however, relatively little systematic work has been reported in detail on chain extension process. Therefore, Young-Kuk Jhon et al., 2001, had taken initiatives to report in detail the chain extension process. Their work describes the reaction of chain extension step as the variation of residual NCO group and subsequent weight average molecular weight of the PUR during the chain extension step. They have prepared the PUR dispersion by neutralization emulsification method and the dispersion was prepared with different average particle sizes.

2.2.3 High solid coatings

As mentioned before, since the 1980s, the main challenge for solvent borne coatings is to increase the solid content. In order to achieve this objective, the approach adapted was to lower the viscosity of the binder, add reactive diluents or lower the viscosity of polyisocyanate cross-linking agent (Renz H et al., 2001). The most used polyols in two component high solid coatings are hydroxyl-terminated polyester and hydroxyl-functional acrylic resins and they are cross-linked through the isocyanate group.

Lowering the viscosity of the acrylic polyols are done by decreasing the molecular weight or by decreasing the weight distribution. This is done by two processes (C.A. Zezza et al., 1996). The first process is a special process where polymerization done at high temperature by using chain transfer agents and special initiators. Whereas the second process is modification of the polymer composition such as glass transition temperature T_g , and functionality by special monomers. However, decreasing binder viscosity leads to some disadvantages such as slower physical drying of the coatings compared with the standard PUR system and requires special hazards handling due to higher contents of acrylic oligomers.

Hood et al., 1986 and Wicks et al., 1992 have disclosed that generally polyether can achieve higher solid, better adhesion to metals and greater solvent resistance than acrylic resins. Controlling molecular weight or use of low molecular weight compounds which have lower viscosity resulting in minimum solvent usage in application (Williams, 1993 and SM Lee et al 1995), selecting the number of functional groups, using hydrogen bond acceptor solvents and reducing the ratio of aromatic/aliphatic diacids are the four approaches reported by Belote et al., 1981 and Ni H et al., (2002) to

obtain low VOC for traditional polyester in polyester-urethane two component coatings. Moreover, to achieve higher solids aliphatic polyurethane coating system, GN Robinson et al., 1994 suggested the use of reactive diluents and Jeffrey Kramer et al., 1994 suggested the use of new polyurethane pre-polymers.

Some of the industrially important low viscous polyisocyanate cross-linker for making PUR coatings are polymeric MDI, HDI- biuret, HDI trimer, asymmetric-trimer and etc. The preparation of low viscosity allophanates by reacting compounds containing urethane groups and mono isocyanates was reported by BW Ludwig et al., 2006.

Recent development of this coating for pipeline protective coatings are high temperature resistant PUR coating (^aGuan, Dr. S., 1994), low cost but high performance wastewater internal PUR coating (^bGuan, Dr. S., 1995) and underground fuel tanks coatings (Kennedy H., 1995).

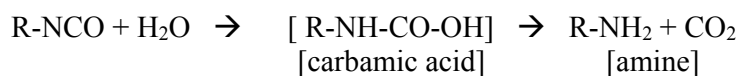
A big problem encountered during the formulation of ultra high solid PUR coatings, is the result of an unacceptable short potlife in the can and cure speed on the substrate (Arie Noomen, 2002). Arie Noomen suggested that bicyclic orthoesters (BOE) are a class of compounds that can be used to increase the potlife of the coating. BOE is non-shrinking monomers in ring opening polymerization reaction. BOE in the can cause the rings to stay close and no functional hydroxyl groups are available for reaction with the isocyanate cross-linker. However, after applied on substrate a fast hydrolysis occurs in the presence of an acid catalyst and the polyol-isocyanate cross-linking reaction starts.

2.3 Basic curing mechanism

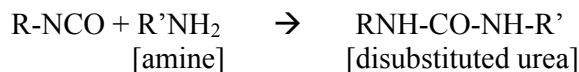
Isocyanate is one of the important components for the PUR coatings. Hence, understanding on basic reactions of diisocyanate with different reagents is very important. A few basic reaction of diisocyanate with some important compounds are stated below as mentioned in reference Michael Szycher, 1999.

1. Compounds containing OH groups or water.

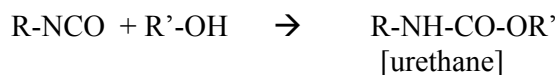
- a. Isocyanate + water = urea + carbon dioxide (CO₂)



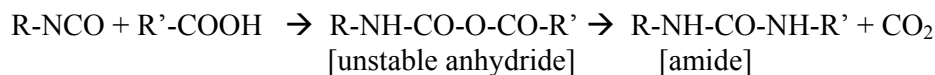
The amine reacts immediately with additional isocyanates to form disubstituted urea:



- b. Isocyanate + alcohol = urethane (RNHCOOR')

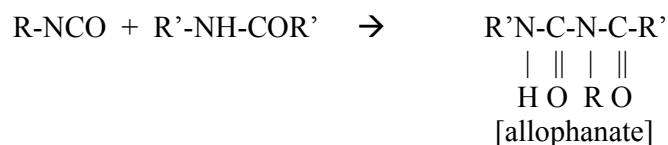


- c. Isocyanate + carboxylic acids = amide + carbon dioxide



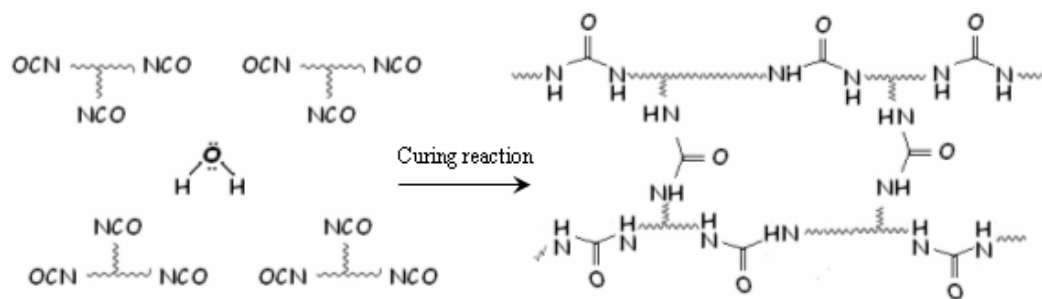
2. Urethanes

Isocyanate + urethanes = allophanate



The process of curing in a coating defines the properties of the finished coating material. ^{b,c}D.K. Chattopadhyay et al., 2005 & 2006, Dzierza W., 1978, Li W et al. 2002, Elwell MJ et al., 1996, ^aSanchez-Adsuar MS., 2000, Aaserud Ni H et al., 2000, ^aPetrovic ZS et al., 1989 disclose that temperature, humidity level and state of cure are the key aspects for a better understanding and controlling of the coating performance. Therefore, for developing custom tailored properties of moisture cured PUR coatings the determination of cure condition is an important factor and were discussed by R. Lomölder, et al., 1997, S.D. Seneker et al., 1991, B.W Ludwig et al., 1996, GN. Robinson et al., 1994, AM. Heintz et al., 2003 and R. Narayan et al., 2002 in their paper.

Moisture cures PUR systems contain isocyanate-capped low molecular weight prepolymers prepared from reacting polyols with excess isocyanates. Moisture from atmosphere diffuses into the prepolymer, and the nucleophilic attack of water on NCO-terminated prepolymer produces carbamic acid. Carbamic acid is unstable at room temperature and decomposes into carbon dioxide and primary amine. Primary amine reacts further with NCO-terminated prepolymer and produces urea (DW Duff et al., 1991, Cui et al., 2002, Kościelecka, 1991 and P.I. Kordomenos et al., 1987). This reaction leads to development of three-dimensional network in the presence of a tri-functional monomer in the reactive prepolymers (^{a,b}J. Comyn et al., 1998). Cross-linking reaction is also possible between urea, urethane and residual isocyanates end group to form biuret and allophanate linkages. Biuret and allophanates are more thermally stable than polyurethane/urea network. It also alters the interconnectivity of the hard segments (Nierzwicki W et al., 1980), thermal properties (Thames SF et al., 1990) and adhesive behaviour. Scheme 2.1 shows the synthesis of moisture cured PUR-urea polymer and their curing reaction (^{a,c}DK Chattopadhyay et al., 2005 & 2006).



Scheme 2.1 The Moisture Curing Reaction and Film Formation of NCO-terminated PUR Prepolymer (^{a,c}DK Chattopadhyay et al., 2005 & 2006).

YanJun et al., 2003 studied isocyanate-terminated urethane prepolymer based on oligoester or oligoether diols. They have shown that the curing process in saturated humidity level can be evaluated by the second-order autocatalytic model. Ana Luisa et al., 2005 have studied the content of free isocyanates on the adhesive properties of reactive trifunctional polyether urethane quasi-prepolymers. The results of the studies disclosed that the free isocyanate content produced quasi-prepolymers with lower average chain length and less intermolecular interactions between polymer chains. Urethane prepolymers containing higher free isocyanate content (15-30 wt %) are called isocyanates quasi-prepolymers because only part of the isocyanates molecules contributes to the formation of the backbone oligomer (Michael Szycher, 1999). Somani KP et al., 2003 and few others have studied the correlation between the isocyanate content and the adhesion properties of the quasi-prepolymers.

The major disadvantage of moisture cured system is their lower storage stability and shelf life. These is due to the presence of side products such as allophanate and isocyanurate which increase the viscosity of the prepolymer and changes the onset of

gelation during cure and lower the storage stability of the product (Querat et al., 1996 & Kościelecka, 1991).

Urska Sebenik et al., 2006 had studied the influence of soft segment length and content on the synthesis properties of isocyanate-terminated urethane prepolymers prepared from monomeric diphenylmethane-4,4'-diisocyanate, difunctional polypropyleneglycol polyols and their mixtures. They have disclosed that increasing hard segment (NCO) in prepolymers increase the formation of urethane groups. Katsuhiko N et al., 1999 studied the effect on functional groups on interfacial properties and structure of segmented PUR. They have synthesized a series of segmented PUR having carboxyl (COOH) groups in the hard segment and disclosed that phase mixing brought high molecular motion in segmented PUR which stimulates the more localization of COOH groups onto PET interface.

2.4 Raw materials

Bayer, Du Pont and Mobay were the companies involved in the developmental and research on PUR in the early stages. E.N.Doyle reported that in 1971 there were more than 10 companies engaged in manufacturing basic diisocyanate and more than 50 companies producing the wide variety of hydroxyl-bearing material which are the important raw material in producing PUR (E.N.Doyle, 1971).

In the last few decades, researchers have varied the chemical composition, structure and molecular weight of the raw materials to modify urethane properties as well as to gain an insight into the fundamental structure-property relationship (Somani et al., 2003, ^{a,c}DK Chattopadhyay et al., 2005 & 2006, Daniel da Silva AL et al., 2006, ^{a,b}Sanchez-

Adusar et al., 2000). The effect of reaction temperature on the molecular weight distribution and the extent of side reaction have also been studied (A.M Heintz et al., 2003).

Many other materials may be required to obtain a well balanced formulation for a specific end product. There are catalysts which promote or accelerate the reaction of the components in the formulation. Wicks Z.W., 1992 reported that commonly used catalyst for the reaction of isocyanates with alcohol, include tertiary amines, diazabicyclo [2,2,2] octane (DABCO) and organotin compounds such as dibutyltin dilaurate (DBTDL). In contrast, J.H.Saunders, 1962 stated that acid catalyst were mild catalyst or in other words not as active as tertiary amines and organotin compounds in catalyzing the reaction. However, Hai Ni et al., 2000, in their research indicated that the acid catalyst enhanced the adhesive properties of the hybrid coating. They have used *para*-toluene sulfonic acid (*p*-TSA) as a catalyst to catalyze the moisture curing of an organic/inorganic hybrid coating system. The organic phase was based on isocyanates of 1, 6-hexamethylene diisocyanate (HDI) and the inorganic phase was based on prepolymerized oligomers of tetraethyl orthosilicate (TEOS).

Commonly used catalyst for the reaction of alcohol with isocyanates can also be used to catalyze reaction of water and isocyanates (Hai Ni et al., 2000). Seneker et al., 1991 investigated the catalyst effects in the reaction of dicyclo-hexylmethane diisocyanate with water. P.J. Walker, 1980, A. Sabata et al., 1993, and G.L.Witucki, 1993 studied organofunctional alkoxysilanes and stated that it enhances adhesion and corrosion resistance in organic coatings.

There are also several different types of treated silica and synthetic materials available for use in urethanes (E.N. Doyle, 1971). The properties of the PUR formulation may be adequately modified by adding these compounds. Ana M. Torro-Palau et al., 2001 studied the characteristics of PUR containing four different silica namely two fumed and two precipitated silica which are hydrophilic and hydrophobic.

Pigments and fillers may enhance the properties of PUR coatings as well as reduce the cost. Conventional PUR exhibits poor resistance to heat and limits its applications (Fabris, H, 1976). Attempts to improve thermal stability of PUR involved the chemical modification of its structure by thermally stable heterocyclic groups (Zuo et al, 1999, Masiulonis et al, 1985) and use of organoclays (Tien et al 2001, Zilg et al 1999, Jin-Hae et al 2002). Conducting carbon black fillers in PUR have a lot of applications in the field of electric and electronics industry (Fengkui Li et al 2000). B Guiffard et al 2006 studied improvement of electric field-induced thickness strain of PUR elastomer films by carbon black nanopowder incorporation in the polymer matrix.

2.4.1 Polyol

One of the major ingredients for PUR is polyols. Polyols or polyhydric alcohols are compounds having more than two hydroxyl groups. Polyols give the flexibility to the backbone of the network chains and therefore they are called soft segments or domains in PUR. There are two major categories of polyols in the urethane industry, namely polyether polyol and polyester polyol. More than 90% of polyol usages in the industry are polyether type, 9% on polyesters and approximately 1% was based on other specialty polyols.

Polyether polyols are the products of reaction between alkali initiators and monomers such as ethylene oxide and propylene oxide. Examples of polyfunctional polyether are polyethylene glycol, polypropylene glycol and polycaprolactone diol. U. Sebenik et al., 2006 studied the synthesis and structure – property relationship of NCO-terminated urethane prepolymers prepared from difunctional polypropylene polyols and monomeric diphenylmethane-4,4'-diisocyanate. They have disclosed that the prepolymers which contained longer polyol segments have a higher number of average molecular weight, while Brookfield viscosity is lower due to a higher content of the soft segments which made the urethane chain more flexible.

Polyester polyols can be synthesized in several routes such as polycondensation of hydroxyl acids or diacids and a diol or by ring-opening polymerization of lactone. In commercial applications, the polyester prepared from a mixture of two or more diacids reacted with different glycols are common to obtain a complex product (Wamprecht C. et al., 2002, Santos D. et al., 2001, James MB et al., 2004).

It is possible to customize the formulation of polyols tailored to the end properties of PUR. The polyester polyols according to the invention with an average equivalent weight in the range from 200 to 4,000, which were prepared by reacting α , ω -dicarboxylic acids with butane 1,4-diol, hexane 1,6-diol, propane 1,3-diol or pentane 1,5-diol and with polyols having 3 to 6 hydroxyl groups, are used for the preparation of PUR pourable elastomers with improved resistance to hydrolysis (James Micheal, 2004).

Unsaturated polyester is of great commercial importance due to their low cost and easy processing. The inclusion of unsaturated bond into the polymer backbone gives a

polymeric material with improved physico-chemical properties. Hydroxy terminated polybutadiene (HTPB) has been used in the synthesis of polyesters, polyurethane, poly(urethane-imide)s and poly(urethane-urea) (Desai S. et al., 2000, Sekkar V et al., 2000, Gnanarajan TP et al., 2002 & Rama Rao M. et al., 2000). Synthesis of unsaturated poly(ester-imide)s based on HTPB is reported by P. Banu et al., 2004. When the soft segment is polybutadiene instead of polyether / polyester, the resultant polymer can be synthesized with unique properties such as high hydrolytic stability, high solvent and chemical resistant and excellent low temperature flexibility.

2.4.2 Isocyanate

Isocyanates are among the most heavily produced specialty organic chemical in the polyurethane industry. The first synthetic route of isocyanates was reported by Wurtz A. in 1848 where he demonstrated the preparation of monoisocyanate. Subsequently other alternative synthetic approaches were achieved by Hoffmann, Curtius and Hentschel, in year 1884. They have highlighted the phosgene-amine approach. Staudinger H et al., 1921 elucidated the structural similarities between isocyanates and ketenes. However, in 1945 when the world was pressed for alternative to natural rubber, that synthetic route to isocyanates became commercially important.

Commercially available organic isocyanates are aliphatic, aromatic, cycloaliphatic, araliphatic and heterocyclic polyisocyanates. Some examples of isocyanates are ethylene diisocyanate, 1,4-tetramethylene diisocyanate, 1,6-hexamethylene diisocyanate, 1,12-dodecane diisocyanate; cyclobutane-1'3-diisocyanate, cyclohexane-1,3 and -1,4 diisocyanate and etc (Michael Szycher, 1999). Aromatic isocyanates have higher reactivity than aliphatic or cycloaliphatic diisocyanate. Polyurethane prepared

from aromatic diisocyanate is more rigid than that prepared from aliphatic. However, the disadvantage of aromatic diisocyanate is its lower stability in sunlight and the PUR gets discoloured when exposed to sunlight. The polymer has lower oxidative and ultraviolet stability (JH Saunders et al., 1962).

Da-Kong Lee et al., 2000 studied the properties of segmented PUR derived from various diisocyanate. They have used 4,4'-diphenylmethane diisocyanate (MDI), 2,4-toluene diisocyanate (TDI) and its isomers, hydrogenated 4,4'-diphenylmethane diisocyanate (HMDI) and 1,6-hexane diisocyanate (HDI) and disclosed that the diisocyanate structure influences the mechanical properties of the PUR significantly. They described that the effect was due to symmetry and chemical structure of the hard segment.

Caraculacu AA et al., 2001 proposed a new general classification of multiple possible addition processes of isocyanates based on the interatomic bond type changes. Starting from the latest achievement of the physico-chemical methods, new aspects regarding the isocyanates structure and different hydroxyl compound associations form as part of the addition processes were revealed. The intramolecular hydrogen bonding in the symmetrical diols was found to determine a significant difference between their two-OH group reactivities. Recent kinetic and other reactivity measurement, extended to polyfunctional systems reported in some macromolecular synthesis was presented in their paper.

2.5 Renewable resources

Petrochemicals serve as raw materials for the chemical industry in the production of solvents, lubricants, paints, lacquers and other chemicals. The oil crisis in the 1970s, depleting reserves, national scarcity issues, price uncertainty, and growing environmental concern over the combustion of fossil fuels highlight major issues associated with the extensive use of petroleum in our society (K.D. Maher et al., 2007). Therefore, the petrochemical resources are becoming tense and the use of renewable resources as substitutes for petrochemical derivatives has attracted more attention of many researchers (H.D. Rozman et al, 2003, J. Huang et al, 2002). It is well known that triglyceride based vegetable oils or animal fats have the potential to be a suitable source of fuel. Vegetable oils have a number of excellent properties which could be utilized in producing valuable polymeric materials such as epoxy, polyesteramide, alkyd and polyurethane in addition to its many application in other areas.

The seeds of many plants contain large amount of oils which could be a viable alternative resources for many applications (N. Dutta et al., 2004). For example, N Dutta et al., used Nahar (a plant that produces high oil content seeds) seed oil to synthesize polyester resin. Other traditional seeds such as linseed (Sharif Ahmad et al., 2002), soybean (Andrew Guo et al., 2002, Andrew Guo et al., 2006, Ahamed Shabeer, 2006), amaranth (CK Lyon et al., 1987), castor (P. Knaub et al., 1986, Hamid Yeganeh et al., 2004 & Guo Qipeng et al., 1990), sunflower kernels (J.A. Robertson et al., 1988), cashew nut (H.P. Bhunia et al., 1999), karanja (P.G. Shende et al., 1997), *annonasquamosa* have been used or still under development for the synthesis of different kinds polymeric resin such as polyurethane, polyester amide and alkyd resins.

Oils are relatively un-reactive and therefore must be functionalized to serve as building blocks for polymers. Hydroxyl functionality of polyol plays an important role in the formation of PUR. Network properties would depend on the cross-linking density, the number of hydroxyl groups in the polyols, their distribution in the polyol and the position in the chain. Thus, the properties are expected to depend on the type of vegetable oil used in the production of the polyols (Alisa Z. et al., 2004). They have studied the effect of structure of six vegetable oils, canola, midoleic sunflower, soybean, linseed, sunflower and corn oil on the properties of polyols and the resulting polyurethane networks. They have concluded that, canola, corn, soybean and sunflower oils gave PUR resins of similar cross-linking density, glass transitions and mechanical properties despite of the different distribution of fatty acids. CK Lyon et al., 1987 reported the pilot scale extraction of oil from the seed of *Amaranthus cruentus* and study the refining and bleaching of this oil.

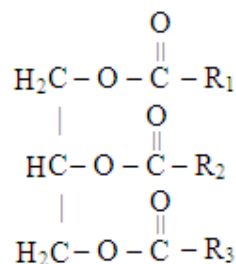
Several studies have dealt with the incorporation of lignin or its derivatives as the natural polymer into PUR (^aSaraf et al., 1984, ^bSaraf et al., 1985, ^aYoshida et al., 1987, ^bYoshida et al., 1990). The lignins used for the studies were usually obtained as by-products from pulping. The source, molecular mass distribution and OH group content restrict the types of lignin suitable for the PURs.

Liquefaction of wood materials using polyhydric alcohols (polyols) is one of the processes utilizing wood waste as raw materials for PUR resins. Wood liquefaction using polyols is a technique to convert whole wood into liquid. The resulting products through solvolysis were directly used as polyol for PUR (^{b,c}Kurimoto et al., 1992, 2001, ^{a,b}Yao et al., 1995, 1996). ^aKurimoto et al., 1999 disclosed that almost all wood wastes

could be used for the liquefaction because the primary components of various wood species have similar chemical structures.

2.5.1 Structure of triglyceride oil

The word “oil” is used for triglycerides that are liquid at ordinary temperature and a water insoluble product of plants. It is an ester product obtained from one molecule of glycerol and three molecules of fatty acids (F. Seniha Güner et al., 2006). Some fatty acids are saturated where it has no double bonds. Some of them are unsaturated which have one or more double bonds.



R₁, R₂, R₃: fatty acid chain

Figure 2.1 A triglyceride molecule

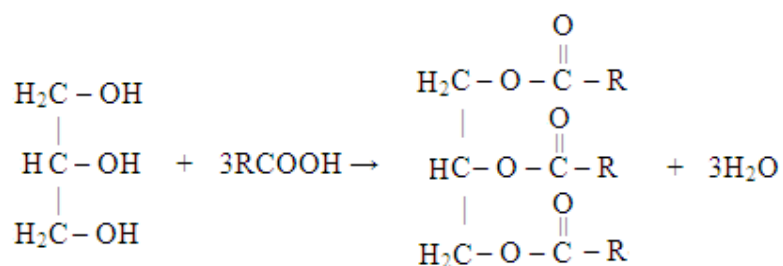


Figure 2.2 Synthesis of triglyceride

The double bonds are called isolated if the double bonds in the carbon chain are separated by at least 2 carbon atoms (eg. $-\text{CH}_2-\text{CH}=\text{CH}-\text{CH}_2-\text{CH}=\text{CH}-\text{CH}_2-$). On the other hand, the double bonds are called conjugated if single and double bonds alternate between carbon atoms (eg. $-\text{CH}_2-\text{CH}=\text{CH}-\text{CH}=\text{CH}-\text{CH}_2-$). The most common fatty acids in natural oils are shown in Table 2.1.

2.5.2 Polyurethane from vegetable oil

Castor oil is one of the vegetable oils which has become a competitive material in PUR industry (R.K. Mendes et al., 2002, Qi Zhou et al., 2002, Keyur P. Somani et al., 2003, Shelby F. Thames et al., 2000, Petrovic ZS et al., 1984, Hong-Quan Xie et al., 2002). Castor oil possesses both unsaturated bond and hydroxyl functional groups. In castor oil, the greater part of fatty acid is ricinoleic acid (87.5%) and followed by oleic acid (5%), linoleic acid (4%), palmitic acid, stearic acid and linolenic acid (F. Seniha Güner et al., 2006). Hamid Yageneh et al., 2004, synthesized millable polyurethane elastomers based on castor oil and studied the physical, thermal and mechanical properties of the elastomer. He has reported that the properties of the castor oil based PUR could be tailor made to fulfill industrial needs. Keyur P. Somani et al., 2003 have synthesized PUR adhesives from castor oil and studied the effect of NCO/OH ratios, types of isocyanate adducts and chain length of glycols by determining wood-to-wood adhesion strength.

Table 2.1 Some fatty acids in natural oils
(Adapted from F. Seniha Güner et al., 2006)

Name	Formula	Structure
Myristic acid	$C_{14}H_{28}O_2$	$CH_3(CH_2)_{12}COOH$
Palmitic acid	$C_{16}H_{32}O_2$	$CH_3(CH_2)_{14}COOH$
Palmitoleic acid	$C_{16}H_{30}O_2$	$CH_3(CH_2)_5CH=CH(CH_2)_7COOH$
Stearic acid	$C_{18}H_{36}O_2$	$CH_3(CH_2)_{16}COOH$
Oleic acid	$C_{18}H_{34}O_2$	$CH_3(CH_2)_7CH=CH(CH_2)_7COOH$
Linoleic acid	$C_{18}H_{32}O_2$	$CH_3(CH_2)_4CH=CH-CH_2-CH=CH(CH_2)_7COOH$
Linolenic acid	$C_{18}H_{30}O_2$	$CH_3CH_2-CH=CH-CH_2-CH=CH-CH_2-CH=CH(CH_2)_7COOH$
α -Eleostearic acid	$C_{18}H_{30}O_2$	$CH_3-(CH_2)_3-CH=CH-CH=CH-CH=CH(CH_2)_7COOH$
Ricinoleic acid	$C_{18}H_{33}O_3$	$CH_3(CH_2)_4CH-CH-CH_2-CH=CH(CH_2)_7COOH$ $\begin{array}{c} \\ OH \end{array}$
Vernolic acid	$C_{18}H_{32}O_3$	$CH_3(CH_2)_4CH-CH-CH_2-CH=CH(CH_2)_7COOH$ $\begin{array}{c} \diagdown \diagup \\ O \end{array}$
Licanic acid	$C_{18}H_{28}O_3$	$CH_3(CH_2)_3CH=CH-CH=CH-CH=CH(CH_2)_4C-(CH_2)_2COOH$ $\begin{array}{c} \\ O \end{array}$

Sandip D. Desai et al., 2003 prepared polyester polyol for use in PUR adhesive from potato starch and natural oils by tranesterification reaction. They have concluded that vegetable oil – based PUR adhesive give superior bonding properties to commercially available adhesives for wood joints.

Other polyurethane materials created from vegetable oils such as cast resins and rigid foams have been in existence for some time.

2.5.3 Palm oil and PUR

Palm oil originates from West Africa and was introduced in Malaysia at the beginning of the 20th century and commercially produced in 1917. Today, Malaysia's oil palm plantations cover 40% of its cultivated land, and it has become the world's largest producer and exporter of palm oil. Indonesia has also embarked on a massive oil palm

plantation programme, and having a much bigger land base, it is expected to catch up soon with Malaysia.

Palm oil's unique composition makes it versatile in its application in food manufacturing and in the chemical, cosmetic and pharmaceutical industries. Its non-cholesterol quality and digestibility make it popular as source of energy, while its technical and economic superiority makes it preferable as base material in the manufacture of various non-edible products.

Palm oil is one of the 17 major oils traded on the world market. Oleochemicals are one of the most important non-food uses for palm products. The basic oleochemical produced from palm oil are fatty acids, esters, alcohols, glycerin, and sodium soap. The Malaysian oleochemical industry began in 1980 with 10,000 tonne of capacity but now has the potential to produce about 20% of world capacity. The Advanced Oleochemical Technology Centre of the Palm Oil Research Institute Malaysia (PORIM) has achieved another breakthrough with the production of the world's first palm oil-based polyurethane foam for the application in industries such as construction, automotive, furniture and packaging (Ahmad, S et al.,1995).

Production of palm oil based polyester polyols has many advantages for our country such as lower capital on raw material and processing costs. The Malaysian Palm Oil Board (MPOB) first produced polyol from epoxidized palm oil (Hassan et al., 1993). A process to produce polyol from palm oil was patented in Malaysia, Singapore and Indonesia (^{a,b}Salmiah et al., 1995 & 2002). According to Salmiah et al., 800 kg batch⁻¹ pilot plant to produce palm-based polyol was commissioned by Malaysian Palm Oil Board (MPOB) in July 2000. The palm-based polyols from MPOB pilot plant were

used to produce PU for a variety of applications such as insulator in refrigerator, roof insulator, wall panels, ceiling panels, cornices, flower foams and lazy foams. The process involved in the production of palm-based polyols, the properties of the polyols and the final foam products and briefly on the pilot plant development were discussed by Parthiban S et al., 1999.

Additives are also used in the production of the foam to control and modify both the PUR reactions and properties of the final polymer. Tuan Noor Maznee et al., 2001 have done a preliminary study on the effects of some additives on the properties such as density, hardness and curing of palm-based polyurethane foam. The additives used were Ethacure 100, Amisol CDE and KD-1, N-methyl-2,2'-iminodiethanol (MDEA) and phthalic anhydride. In a separate study, ^bNorin Zamiah et al., 2006 have described the properties of moulded flexible foams incorporated with phthalate and two other additives. They had reported that the flexible foams from total palm-based polyols had tear strength of 140-150 Nm⁻¹ and therefore can only be used in automotive parts such as carpet underlay and thermal insulator. Better foams were produced from blended polyol (50:50 palm based to petrochemical polyether polyols). ^aNorin Zamiah et al., 2004, have described the effect of triethanolamine on the strength properties of flexible PUR produced from two palm-based polyols and MDI.

PORIM is also looking at other application of palm oil based PUR foam both for rigid and flexible foams. In the case of rigid foam, Khairiah Badri et al., 2006 investigated the influence of oil palm empty fruit bunch on the mechanical properties of high density rigid polyurethane. The palm kernel oil based polyester is mixed with tetramethylethylenediamine as curing agent, silicone-type of surfactant and EFB fiber as filler to make the resin. The resin was then reacted with MDI to produce high density

rigid PUR. Excellent water resistance and optimum flexural and impact strength were observed in the biocomposites. Other studies such as microbial degradation of the flexible foams have been conducted by Razmah Ghazali et al., 2005. The study showed that palm-based flexible foam can be degraded by *Aspergillus niger* in the presence of sufficient nutrients.

2.5.3.1 Palm kernel oil (PKO) & palm olein

In the world of oils and fats, the lauric oils are the unique ones and there are very few of them. Among the seventeen major oils and fats in world trade, there are only two lauric oils, namely coconut oil and palm kernel oil. The major fatty acid in their composition is lauric acid which is about 50%. The palm fruit looks like a plum where the outer fleshy mesocarp gives the palm oil, while the inner hard shell gives palm kernel oil. It is rather strange that the oils from the same fruit have entirely different fatty acid compositions and properties. The major fatty acids in PKO is about 48% of lauric acid (C12), 16% of myristic acid (C14) and 15% of oleic acid (C18:1) (Pantzaris, T.P et al., 2001).

Even after full hydrogenation, the melting point of palm kernel oil does not raise much and fractionation gives a stearin, which has even sharper melting point. This is the outstanding property of lauric oil which determines its use in the edible field. Palm kernel oil is about 82% saturated compared to the other major liquid oils such soybean which is only 16% saturated or sunflower oil 12% saturated. If compared to coconut oil, because of their similarity in composition and properties, palm kernel oil has similar uses; however PKO is more unsaturated than the coconut oil and thus can be hydrogenated to a wider range of products. Furthermore, coconut oil has greater content

of shorter chain fatty acids which makes it a little more valuable for the oleochemical industry (Pantzaris, T.P et al., 2001).

Palm kernel oil and its hydrogenated and fractionated products are widely used in biscuits, ice creams, cake icings, margarines, etc. Palm kernel oil is also used in synthesizing detergent and soaps. A very large amount of palm kernel oil is now used for manufacturing the short chain fatty acids, fatty alcohols, methyl ester, fatty amines and amides for use in detergents, cosmetics and other products.

Palm olein is widely used as cooking oil and it blends perfectly with other popular vegetable oils that are traditionally used in many parts of the world. For example, in Japan, refined palm olein is blended with rice bran and in Malaysia; it is blended with groundnut oil. Palm olein is also widely used as a frying oil due to its good resistance to oxidation and formation of breakdown products at frying temperatures and longer shelf life of finished products.

2.6 Alkyd resin / polyol

Alkyd resin is the reaction of a polyfunctional alcohol with a polybasic acid together with a mono-functional acid. The term “alkyd” describes the resinous products of di- and polyhydric alcohols and acids. Hence, from the combination of acid and alcohol came the term “alkyd,” with the letter “k” employed to give the desired phonics. Polymeric ester compounds were first synthesized in 1847 by Berzelius. He prepared the compound by the reaction of glycerol and tartaric acid. In 1922, Roy Kienle of General Electric Co. prepared a fatty acid modified polyester composition and this basic composition called “alkyd” (Joe Maty, 2004; Patton TC., 1962). Kienle was granted a patent for this oil-modified polyester resin but was invalidated later in the court, according to historical accounts of the early development of alkyds. The first

alkyd resins sold commercially were marketed as “Glyptals” by General Electric (Joe Maty, 2004).

Alkyds are commonly manufactured from vegetable oils. Oil modified alkyd resin may also be made from fatty acids rather than from oils. This resin has special properties which include improved drying, better water resistance or maximum colour retention. The ratio of the ingredients is expressed by the oil length or phthalic content of the product. Table 2.2 shows the approximate classification of the alkyd resins. Percentage oil length refers to oil portion of an alkyd. It is equal to the weight of any fatty acid in the alkyd and the weight of the polyol needed to completely esterify this fatty acid and expressed as a percentage of the solids content of the finished alkyd (Patton TC., 1962). It is noted that the weight taken is a minus weight of evolved water of esterification.

Table 2.2 Classification of alkyd resins

Alkyd Resins	Phthalic Anhydride (%)	Fatty Acid or Oil (%)
Short oil length	40-50	30-40
Medium oil length	30-40	40-50
Long oil length	20-30	Over 50

2.6.1 Process of alkyd making

Four methods have been used to manufacture alkyds, where each method has some commercial advantages over the other.

- i) The acidolysis process
- ii) The fatty acid/oil process
- iii) The fatty acid process
- iv) The alcoholysis or monoglyceride process

The fatty acid process is discussed here because the oleic acid alkyds used in this project were prepared through this method. Fatty acid process is often called the “high polymer technique”. In this process polyol, dibasic acid and the monobasic acid are reacted simultaneously at temperature 220-260⁰C until the required degree of polymerization is reached. This method can be simplified into two steps:

- 1) Glycerol and phthalic anhydride are reacted together at 180⁰C until a soft clear viscous resin is obtained. Then, the warm fatty acids are added and heated with the resin at 180-220⁰C.
- 2) All the raw materials are mixed together and heated to the reaction temperature. During the reaction, foaming occurs due to evolution of water. Other volatile products are also evolved, including some phthalic anhydride that sublimes. Heater will be turned off after water collected approaches the predicted amount in the formulation.

The advantage of this process is that there is a greater freedom in formulation when fatty acid is being used. The fatty acids from natural whole oils have been separated and refined. By selecting the fatty acids from the raw material the unwanted acid such as linolenic acid (causes yellowing) and the palmitic and stearic acid can be eliminated. The disadvantage of this method is the fatty acids derived from the glyceride oils are rather expensive. Fatty acids are also more sensitive to discolouration during storage and have high congealing point. This requires heating facilities to maintain the acid in a liquid condition during cold weather.

2.7 Conclusion

The efforts of both industrialized and developing countries to use and cultivate natural oils as renewable resources for food and foodstuff manufacture have led to an expansion of natural oils as raw material for industrial application. To use natural oils to produce polyurethane requires multiple hydroxyl functionality. Hydroxyl functionality occurs naturally for some natural oils i.e. castor oil and some can be introduced synthetically in natural oils in various ways. Generally, oleochemical polyols are used when the final application requires flexible coatings with good abrasion resistance and stability against acid, alkali and organic solvents. Palm based polyols now opens a new era of possibilities for new applications and partial replacement of petrochemical based polyols with palm based polyols. According to UK-based market research firm Merchant Research & Consulting Ltd., global demand for polyurethane has been growing at a steady pace over the recent years. Chinese PUR is forecast to grow by 10% to become the world's largest by 2015. The demand for PUR materials grew by an average rate of 5% within 1998-2004. This rate varied from 3% in Europe to 10% in Asia Pacific (www.MarketPublishers.com Feb, 2008). In Malaysia all the raw material for PUR are imported. Hence, the market potential for palm oleic acid based polyol and PUR will be large as partial replacement for current polyols and PUR for new applications. The future of palm based PUR market is therefore, very bright.

References

- Ahmad, S, Siwayanan, P, Ooi, T L, Intermed Sdn Bhd, 1995. Characteristic of polyurethane foams derived from palm oil products. Paper presented at 21st World Congress and Exhibition of the International Society of Fat Research (ISF), The Hague, The Netherlands.
- A.K.Nanda, D.A. Wicks, S.A Madbouly, Joshua U. Otaigbe, 2005. Effect of ionic content, solid content, degree of neutralization, and chain extension on aqueous polyurethane dispersions prepared by prepolymer method. *Journal of Applied Polymer Science*, **98**(6), 2514-2520.
- A.M. Heintz, D.J. Duffy, S.L.Hsu, Suen W, Chu W, Paul CW 2003. Effects of Reaction Temperature on the Formation of Polyurethane Prepolymer Structures. *Macromolecules*. **36**, 2695-2704.
- A.Sabata, W.J.V. Ooij, R.J. Koch, 1993. The interphase in painted metals pretreated by functionalsilanes. *Journal of Adhesion Science Technology*, **7**(11), 1153.
- Aaserud Ni H, Simonsick DJ, Soucek Jr MDWJ., 2000. Preparation and characterization of alkoxysilane functionalized isocyanurates. *Polymer*, **41**, 57-71.
- Ahamed Shabeer, 2006. Manufacturing and characterization of soy-based resin and nanocomposites, Dissertation of Doctor Philosophy in Mechanical Engineering, University of Missouri-Rolla.
- Aliza Zlatanić, Charlene Lava, Wei Zhang, Zoran S. Petrović, 2004. Effects of structure on properties of polyols and PUR based different vegetable oils. *Journal Polymer Science: Part B: Polymer Physics*, **42**, 809-819.
- Ana Luisa Daniel da Silva, Jose Miguel Martin-Martinez, Joao Carlos Moura Bordado, 2006. Influence of the free isocyanates content in the adhesive properties of reactive trifunctional polyether urethane quasi-prepolymer. *International Journal of Adhesion & Adhesive*, **26**: 355-362.
- Ana M. Torro-Palau, Juan C. Fernandez-Garcia, A. Cesar Orgiles-Barcelo, 2001. Characterization of PUR containing different silicas. *International Journal of Adhesion & Adhesive*, **21**, 1-9.

Andrew Guo, Dima Demydov, Wei Zhang, Zoran S. Petrovic, 2002. Polyols and polyurethanes from hydroformylation of soybean oil. *Journal of Polymers and the Environment*, 10 (112), 49-52.

Andrew Guo, Wei Zhang, Zoran S. Petrovic, 2006. Structure-property relationships in polyurethanes derived from soybean oil. *Journal of Material Science*, **41**, 4914-4920.

Arie Noomen, 2002. Bicyclic orthoesters as binders with latent hydroxyl functionality. *Progress in Organic Coating*, **45**, 225-230.

ASTM Standard D16-00. Technology for paint, related coatings materials and applications.

Dieterich D, Grigat E, Hahn W, Hespe H, Schmelzer HG 1993. Principles of polyurethane chemistry and special applications. In: Oertel G, Polyurethane handbook. Munich: Hanser Publishers; p. 11-53

B Guiffard, L Seveyrat, G Sebald and D Guyomar, 2006. Enhanced electric field-induced strain in non-percolative carbon nanopowder/polyurethane composites. *Journal of Physics D: Applied Physics*, **39**, 3053-3057.

B.K Kim, J.S. Yang, S.M. Yoo et al., 2003. Waterborne polyurethanes containing ionic groups in soft segments. *Colloid & Polymer Science*, **281**, 461-468.

BW. Ludwig, Urban, 1996. Quantitative Determination of Isocyanate Concentration in Cross-linked Polyurethane Coatings. *Journal of Coating Technology*, **68**(857):93

Belote SN, Blount WW 1981. Optimizing resins for low VOC. *Journal of Coating Technology*, **53** (681), 33-7.

Caraculacu A.A., Coseri S., 2001. Isocyanates in polyaddition processes. Structure and reaction mechanisms. *Progress in Polymer Science*, **26**, 799-851.

C.A. Zezza, Kimberly D. Talmo, May 1996. Viscosity Reduction via Monomer Selection in Solvent Borne High Solids Styrene/Acrylic Coating Resins. *Journal of Coating Technology*, **68** (856), 49.

CK Lyon, R. Becker, 1987. Extraction and refining of oil from Amaranth seed. *Journal of the American Oil Chemists' Society (JAOCs)*, **64** (2), 283

Chian KS, Gan LH, 1998. Development of rigid polyurethane foam from palm oil. *Journal of Applied Polymer Science*, **68**(3), 509-515.

Cui Y, Chen D, Wang X, Tang X, 2002. Crystalline structure in isocyanate reactive hot melt adhesives. *International Journal of Adhesion & Adhesive*, **22**, 317.

^aD.K Chattopadhyay, KVS N Raju, 2007. Structural engineering of polyurethane coatings for high performance applications. *Progress in Polymeric Science*, **32** 352-418.

^bD.K. Chattopadhyay, B. Sreedhar, K.V.S.N.Raju, 2005. Thermal stability of chemically cross-linked moisture-cured polyurethane coatings. *Journal of Applied Polymer Science*, **95**(6), 1509-1518.

^cD.K. Chattopadhyay, B. Sreedhar, K.V.S.N.Raju, 2006. Influence of varying hard segments on the properties of chemically cross-linked moisture-cured polyurethane-urea. *Journal of Polymer Science Part B: Polymer Physics*, **44**(1), 102-118.

^dD.K. Chattopadhyay, B. Sreedhar, K.V.S.N.Raju, 2006. The phase mixing studies on moisture cured polyurethane-urea during cure. *Polymer*, **47**, 3814-3825.

^eD.K. Chattopadhyay, P.S.R. Prasad, B. Sreedhar, K.V.S.N.Raju, 2005. The phase mixing of moisture cured polyurethane-urea during cure. *Progress in Organic Coating*, **54**, 296-304.

D.W. Duff, G.E. Macial, 1991. Monitoring postcure reaction chemistry of residual isocyanate in 4,4'-methylenebis(phenyl isocyanate) based isocyanurate resins by nitrogen-15 and carbon-13 CP/MAS NMR. *Macromolecules*, **24**, 387-397.

Da-Kong Lee, Hong-Bing Tsai, 2000. Properties of segmented PUR derived from different diisocyanates. *Journal of Applied Polymer Science*, **75**(1), 167-174.

Daniel da Silva AL, Martin-Martinez JM, Bordado JCM, 2006. Influence of the free isocyanate content in the adhesive properties of reactive trifunctional polyether urethane quasi-prepolymers. *International Journal of Adhesion & Adhesive*, **26**, 355-62.

Desai S, Thakore IM, Sarawade BD, Devi S, 2000. Effect of polyols and diisocyanates on thermo-mechanical and morphological properties of polyurethanes. *European Polymer Journal*, **36**, 711-725.

Dieter Stoye, Werner Freitag, 1998. Paints, Coatings and Solvents. Wiley VCH Weinheim, Chapter 2, pg 66-67

Dr. Dirk Mestach, Nuplex Resins BV, Bergen op Zoom, 2006. New Approaches for Solvent-Free Waterborne Polyurethanes. *European Coating Conference*.

Dzierza W, 1978. Mechanical properties of cross-linked polyurethanes. *Journal of Applied Polymer Science*, **22**, 1331-42.

E.N.Doyle, 1971. "The development and use of Polyurethane products" McGraw-Hill US: Chapter 1, pg 3

Elwell MJ, Ryan AJ, Grunbauer HJM, Van Lieshout HC 1996. *In-Situ* Studies of Structure Development during the Reactive Processing of Model Flexible Polyurethane Foam Systems Using FT-IR Spectroscopy, Synchrotron SAXS, and Rheology. *Macromolecules*, **29**, 2960-68.

F. Seniha Güner, Yusuf Yağci, A. Tuncer Erciyes, 2006. Polymers from triglyceride oils. *Progress in Polymer Science*, **31**, 633-670.

Fabris, H., 1976. Advances in Urethane Science and Technology. *Technomic*: New York.

Fengkui Li, Lanying Qi, Jiping Yang, Mao Xu, Xiaolie Luo, Dezhu Ma, 2000. Polyurethane/conducting carbon black composites: Structure, electric conductivity, strain recovery behavior, and their relationships. *Journal of Applied Polymer Science*, **75(1)**, 68-77.

Funda Celebi, Leyla Aras, Güngör Gündüz, Idris M. Akhmedov, Sept 2003. Synthesis and characterization of waterborne and phosphorus-containing flame retardant PUR coatings. *Journal of Coatings Technology*, **75**, 944.

G.J. Gardner, 1996. *Journal of Protective Coating Linings* **13(2)**, 81

G.L. Witucki, 1993. A Silane Primer: Chemistry and Applications of Alkoxy Silanes. *Journal of Coating Technology*, **65** (822), 57.

GN. Robinson, etc., Dec. 1994. High Performance PUR Coating Systems Utilizing Oxazolidine-Based Reactive Diluents. *Journal of Coatings Technology*, **69**, Vol. 66.

Gnanarajan TP, Padmanabha Iyer N, Nasar AS, Radhakrishnan G, 2002. Preparation and properties of poly(urethane-imide)s derived from amine-blocked-polyurethane prepolymer and pyromellitic dianhydride. *European Polymer Journal*, **38**, 487-495.

^aGuan, Dr. S., 1994. Test Report on Corroclad 2000 HT. Milton, ON: Madison Chemical Industries Inc.

^bGuan, Dr. S., 1995. Wasteliner Test Report. Milton, ON: Madison Chemical Industries Inc.

Guo Qipeng, Fan Shixia and Zhang Qingyu, 1990. Polyurethanes from 2,4-toluene diisocyanate and a mixture of castor oil and hydroxyether of bisphenol-A. *European Polymer Journal*, **26(11)**, 1177 – 1180.

H.D.Rozman, Y.S.Yeo, G.S. Tay et al., 2003. The mechanical and physical properties of polyurethane composites based on rice husk and polyethylene glycol. *Polymer Testing*, **22**, 617-623.

H.P. Bhunia, G.B. Nando, T.K. Chaki, A. Basak, S. Lenka, P.L. Nayak, 1999. Synthesis and characterization of polymers from cashewnut shell liquid (CNSL), a renewable resource II. Synthesis of polyurethanes. *European Polymer Journal*, **38**, 1381-1391.

Hai Ni, Allen D. Skaja, Mark D. Soucek, 2000. Acid-catalyzed moisture-curing polyurea/polysiloxane ceramer coatings. *Progress In Organic Coatings*, **40**, 175-184.

Hamid Yeganeh and Mohammad Reza Mehdizadeh, 2004. Synthesis and properties of isocyanate curable millable polyurethane elastomers based on castor oil as a renewable resource polyol. *European Polymer Journal*, **40 (6)**, 1233-1238.

Hassan, HA; Yeong, SK and Ahmad,S, 1993. Palm-based polyols for polyurethane foams. *Proceedings of the 1993 PORIM International Palm Oil Conference (Chemistry and Technology)*, 227-235.

Hoefer, R, Gruber, B, Meffert, A, Gruetzmacher, R, 1989. Polyurethane casting resin. US Patent 4826944.

Hofacker S, Gertzmann R, Fleck O, Ruttman G, Brummer H., 2004. NCO prepolymers prepared from isophorone diisocyanate and having low monomer content. US patent 6825376

Hong-Quan Xie, Jun-Shi Guo, 2002. Room temperature synthesis and mechanical properties of two kinds of elastomeric interpenetrating polymer network based on castor oil. *European Polymer Journal*, **38**, 2271-2277.

Hongsoo Park, Janghyoun Keun, Kisay Lee 1996. Syntheses and physical properties of two-component polyurethane flame-retardant coatings using chlorine-containing modified polyesters. *Journal of Polymer Science: Part A : Polymer Chemistry*, **34**, 1455

Hood JD, Blount WW, Sade WT., 1986. Polyester resin synthesis techniques for achieving lower VOC and improved coating performance. *Journal of Coating Technology*, **58** (739), 49-52

^aJ. Comyn, 1998. Moisture cure of adhesives and sealants. *International Journal of Adhesion & Adhesive*, **18**, 247-253.

^bJ. Comyn, F. Brady, R.A Dust, M. Graham, A. Haward, 1998. Mechanism of moisture-cure of isocyanate reactive hot melt adhesives. *International Journal of Adhesion & Adhesive*, **18**, 51-60.

J. Huang and L. Zhang, 2002. Effects of NCO/OH molar ratio on structure and properties of graft-interpenetrating polymer networks from polyurethane and nitrolignin. *Polymer*, **43**, 2287-2294.

J.A. Robertson, B.G. Lyon, W.H. Morrison, J.F. Miller, 1988. Sensory and chemical evaluation of stored oil-roasted, high oleic nano oil sunflower kernels. *Journal of the American Oil Chemists' Society (JAOCs)*, **65** (6), 985.

J.H. Saunders, K.C. Frisch, 1962. Polyurethanes Chemistry and Technology. Part I: Chemistry, Interscience, New York: Wiley, vol. **XVI**, p. 161.

James Micheal Barnes, Michael Schneider, Andreas Hoffmann, 2004. Polyester polyols and the use of polyester for producing polyurethane cast elastomers that have an improved resistance to hydrolysis. US Patent 6809172.

Jeffery Kramer and Sherri Bassner, Aug. 1994. Using Novel PUR Prepolymers in VOC- Compliant, Two-Component Weatherable Topcoats. *Paint & Coatings Industry*, 42.

Jin-Hae Chang, Yeong UK An, 2002. Nanocomposites of PUR with various organoclays: Thermo-mechanical properties, morphology and gas permeability. *Journal of Polymer Science: Part B: Polymer Physics*, **40**, 670-677.

Joe Maty, 2004. In the 1920s: Alkyd resin roars into prominence. *Paint & Coatings Industry*, **20(3)**, 32-33.

Jos T. Huybrechts, Leen M. Tanghe, 2006. 2.1 VOC solvent borne 2K clear coats based on star oligoethers. *Progress in Organic Coatings*, **58**, 217-226.

K.D. Maher, D.C. Bressler, 2007. Pyrolysis of triglyceride materials for the production of renewable fuels and chemicals. *Bioresource Technology*, **98**, 2351-2368.

Katsobashvili VYa, Babkin BM, Salnikova GA, Simonova NI, Eremina TN, Kulikova TN, et al., 1976. Blocked isocyanate. *USSR patent* 508449.

Katsuhiko N, Takashi Nishino, Seiji Asaoka, Sudaryanto, 1999. Relationship between interfacial properties and structure of segmented polyurethane having functional groups. *International Journal of Adhesion & Adhesive*, **19**, 345-351.

Kennedy, H., 1994. Over 200,000 sti-P3 tanks Installed. Milton, ON: Madison Chemical Industries Inc.

Keyur P. Somani, Sujata S. Kansara, Natvar K. Patel, Animesh K. Rakshit, 2003. Castor oil based polyurethane adhesive for wood-to-wood bonding. *International Journal of Adhesion & Adhesive*, **23**, 269-275.

Khairiah Badri, Khairul Anuar Mat Amin, 2006. Biocomposites from oil palm resources. *Journal of Oil Palm Research*, **Special Issue**, 103-113.

Khoe, TH, Otey FH, Frankel EN., 1972. Selective hydroformylation of polyunsaturated fats with a rhodium-triphenylphosphine catalyst. *Journal of the American Oil Chemists' Society*, **49**, 615-618.

Kościelecka, 1991. Thermal stability of polyurethanes with allophanate and isocyanurate cross-links. *Acta Polymerica*. **42**, 221-225.

Kuo, P., Chang, J.M., and Wang, T.L., 1998. Flame-retarding materials - I. Syntheses and flame-retarding property of alkylphosphate-type polyols and corresponding polyurethanes. *Journal of Applied Polymer Science*, **69**, 1635

^aKurimoto, Y., Doi, S., Tamura, Y., 1999. Species effects on wood-liquefaction in polyhydric alcohols. *Holzforschung*, **53**, 617-622.

^bKurimoto, Y., Koizumi, A., Doi, S., Tamura, Y., Ono, H., 2001. Wood species effects on the characteristics of liquefied wood and the properties of PUR films prepared from liquefied wood. *Biomass and Bioenergy*, **21**, 381-390.

^cKurimoto, Y., Shirakawa, K., Yoshioka, M., Shiraishi, N., 1992. Liquefaction of untreated wood with polyhydric alcohols and its application to PUR foams. In: New Zealand Forest Research Institute, Bulletin No. 176, pg 163-172.

Li W, Ryan AJ, Meier IK., 2002. Effect of Chain Extenders on the Morphology Development in Flexible Polyurethane Foam. *Macromolecules*; **35**, 6306-6312.

Li-Hong Bao, Yun-Jun Lan and Shu-Fen Zhang, 2006. Synthesis and properties of Waterborne PUR dispersions with ions in the soft segments. *Journal of Polymer Research*, **13**, 507-514.

Ludewig M, Weikard J, Stoeckel N., 2006. Allophanate-containing modified PUR. US patent 7001973.

Masiulonis B, Zielinski R, 1985. Mechanical, thermal, and electric properties of polyurethaneimide elastomers. *Journal of Applied Polymer Science*, **30**, 2731-41.

Michael Szycher, 1999. Szycher's Handbook of Polyurethane. CRC Press LLC. Chapter 20, (pg 1), chpt 1, pg 3-7.

Muhlebach A, 1994. Pyrazoles-a novel class of blocking agents for isocyanates. *Journal of Polymer Science: Part A: Polymer Chemistry*, **32**, 753-65.

N. Dutta, N. Karak, S.K. Dolui, 2004. Synthesis and characterization of polyester resins based Nahar seed oil. *Progress in Organic Coatings*, **49**, 146-152.

Nasar AS, Subramani S, Radhakrishnan G, 1999. Synthesis and properties of imidazole-bocked diisocyanates. *Polymer International*, **48**, 614-20.

Ni H, Daum JL, Thilgen PR, Soucek MD, Simonsick Jr WJ, Zhong W et al., 2002. Cycloaliphatic polyester-based high solids PUR coatings; II The effect of difunctional acid. *Progress in Organic Coating*, **45**, 49-58.

Nierzwicki W, Wysocka E, 1980. Microphase separation and properties of urethane elastomers. *Journal of Applied Polymer Science*, **25**, 739-46.

^aNorin Zamiah et al., Ooi Tian Lye, Salmiah Ahmad, June 2004. Effect of triethanolamine on the properties of palm-based flexible polyurethane foams. *Journal of Oil Palm Research*, **16**, 66-71.

^bNorin Zamiah Kassim Shaari, Ooi Tian Lye, Salmiah Ahmad, June 2006. Production of moulded palm-based flexible polyurethane foams. *Journal of Oil Palm Research*, **18**, 198-203.

P. Banu, G. Radhakrishnan, 2004. Unsaturated poly(ester-imide)s from hydroxyl-terminated polybutadiene, dianhydride and diisocyanate. *European Polymer Journal*, **40**, 1887-1894.

P. Knaub and Y. Camberlin, 1986. Castor oil as a way to fast-cured polyurethane ureas. *European Polymer Journal*, **22** (8), 633-635.

P.G. Shende, S.B. Dabhade, 1997. Polymer synthesis and applications, in: D.K. Vohra, D. Singh, P. Singh (Eds.), *Proceedings of National Seminar on Polymers*, Allied Publishers Ltd., 104-110.

P.I. Kordomenos, J.E. Kresta, K.C. Frisch, 1987. Thermal stability of isocyanate-based polymers. 2. Kinetics of the thermal dissociation of model urethane, oxazolidone, and isocyanurate block copolymers. *Macromolecules*. **20**, 2077-2083.

P.J. Walker, 1980. Organo Silanes as Adhesion Promoters for Organic Coatings. *Journal of Coating Technology*, **52** (670) 49.

Pantzaris, T.P and Mohd Jaaffar Ahmad, 2001. Properties and utilization of palm kernel oil. *Palm Oil Developments*, **35**, 11-23.

Park, H.S., Hahm, H.S., and Park, E.K., 1996. Preparation and characteristics of two-component polyurethane flame retardant coatings using 2,3-dibromo modified polyesters. *Journal of Applied Polymer Science*, **61**, 421-429.

Parthiban Siwayanan, Ooi Tian Lye, Norin Zamiah Kassim Shaari, Salmiah A, Dieter Wiese & Chua Meng Choo, 1999. Recent Developments in palm-based polyols. *Proceedings of the 1999 PORIM International Palm Oil Congress (Oleochemicals)*, **5**, 59-64.

Patton, Temple C., 1962. Alkyd Resin Technology: Intersec Publication

^aPetrovic ZS, Javni I., 1989. The effect of soft –segment length and concentration on phase separation in segmented polyurethanes. *Journal of Polymer Science Part B: Polymer Physics*, **27**(3), 545-560.

^bPetrovic ZS, Guo, A Javni I., 2000. Process for the preparation of vegetable oil-based polyols and electron insulating casting compounds created from vegetable oil-based polyols. US Patent 6107433

^cPetrovic ZS, Dragica Fajnik, 1984. Preparation and properties of castor oil based polyurethanes. *Journal of Applied Polymer Science*, **29**, 1031-1040.

Qi Zhou, Lina Zhang, Ming Zhang, Bo Wang, Shaojie Wang, 2002. Miscibility, free volume behavior and properties of blends from cellulose acetate and castor oil-based polyurethane. *Polymer*, **44**, 1733-1739.

Querat E, Tighzert L, Pascault JP, Dusek K. 1996. *Angew Macromol. Chem*; **242**: 1
R. K. Mendes, S. Claro-Neto, E.T.G. Cavalheiro, 2002. Evaluation of new rigid carbon-castor oil polyurethane composite as an electrode material. *Talanta*, **57**, 909-917.

R Narayan, DK Chattopdhyay, B Sreedhar, KVS N Raju, 2002. Cure, Viscoelastic and Mechanical Properties of Hydroxylated Polyester Melamine High Solids Coatings. *Journal of Material Science*, **37**, 4911.

R. Lomölder, F. Plogmann, P. Speier, 1997. Selectivity of isophorone diisocyanate in the urethane reaction influence of temperature, catalysis, and reaction partners. *Journal of Coating Technology*, **69**(868), 51-57.

RR. Rosler and P.R Hergenrother, Jan 1996. Two component PUR coatings. *Journal of Coatings & Linings*, p 83-94.

Rainer G, Johann O, Elmar W, Guenter D, 1979. Protective coating for glass surfaces. Ger Offen DE 2740253, 19790315.

Rama Rao M, Scariah KJ, Varghese A, Naik PV, Swamy KN, Sastry KS, 2000. Evaluation of criteria for blending hydroxy terminated polybutadiene (HTPB)

polymers based on viscosity build-up and mechanical properties of gumstock. *European Polymer Journal*, **36**, 1645-51.

Razmah Ghazali, Lai Choon MEi, Norin Zamiah Kassim Shaari, Mohtar Yusof, Salmiah Ahmad, 2005. Preliminary study on microbial degradation of flexible polyurethane foams- physico-mechanical and weight changes during fungal deterioration. *Journal of Oil Palm Research*, **17**, 103-109.

Renz H, Bruchmann B, 2001. Pathway targeting solvent-free PUR coatings. *Progress in Organic Coating*, **43**, 32-40.

S. Bassner and C.R Hegedus, September 1996. A review of two component water-borne PUR coatings for industrial applications. *Journal of Coatings & Linings*, p52-65.

S.D. Seneker, T.A. Potter, 1991. Solvent and Catalyst Effects in the Reaction of Dicyclohexyl-methane. Diisocyanate with Alcohols and Water. *Journal of Coating Technology* **63** (793):19.

S.M. Lee, etc., 1995. Aldimine-Isocyanate Chemistry: A Foundation for High Solids Coating. *Proc. Twenty-Second Waterborne, Higher Solids and Powder Coatings Symp.*, New Orleans, LA,1.

S.S.Yoon and S.C Kim, 2005. Modification of aqueous polyurethane dispersions by polybutadiene. *Journal of Applied Polymer Science*, **95**(5), 1062-1068.

Saggese EJ, Scholnick F, Zubillaga M, Ault WC, Wrigley AN (1965). Urethane Foams from Animal Fats I. Oxyethylated 9,10-Dihydroxystearic Acid. *Journal of the American Oil Chemists' Society (JAOCS)*, **42**(6), 553-556.

^aSalmiah Ahmad, OOi Tian Lye, Norin Zamiah Kassim Shaari & Tuan Noor Maznee Tuan Ismail, 2002. Palm based polyols and polyurethanes. *MPOB Information Series*, **170**, MPOB TT No 153.

^bSalmiah Ahmad, Parthiban Siwayanan, & Dieter Wiese, 1995. Polyurethane foams from palm oil and palm oil products. Patent Singapore (55223), Malaysia (MY-114189-A) and Indonesia (patent application: P962884).

^aSanchez-Adusar MS., 2000. Influence of the composition on the crystallinity and adhesion properties of thermoplastic polyurethane elastomers. *International Journal of Adhesion & Adhesive*, **20**, 291-298.

^bSanchez-Adusar MS, Martin-Martinez JM, 2000. Structure, composition, and adhesion properties of thermoplastic polyurethane adhesives. *Journal of Adhesion Science Technology*, **14**(8), 1035-1055.

Sandip D. Desai, Jigar V. Patel, Vijay Kumar Sinha, 2003. Polyurethane adhesive system from biomaterial-based polyol for bonding wood. *International Journal of Adhesion & Adhesives*, **23**, 393-399.

Santos D, Manuel A, 2001. Polyester polyols and their use as the polyol component in two-component polyurethane paints. US Patent 6184332.

^aSaraf, V. P., Glasser, W.G., 1984. Engineering plastics from lignin. III. Structure property relationships in solution cast PUR films. *Journal of Applied Polymer Science*, **29**, 1831-1841.

^bSaraf, V. P., Glasser, W.G., Wilkes, G.L., McGrath, J.E., 1985. Engineering plastics from lignin. VI. Structure-property relationships of peg-containing PUR network. *Journal of Applied Polymer Science*, **30**, 3809-3823.

Sekkar V, Ninan KN, Krishnamurthy VN, Jain SR, 2000. Thermal decomposition studies on copolyurethanes based on hydroxyl terminated polybutadiene and poly(12-hydroxy stearic acid-co-TMP) ester polyol. *European Polymer Journal*, **36**, 2437-2448.

Sharif Ahmad, S.M. Ashraf, E. Sharmin, F. Zafar and Abdul Hasnat, 2002. Studies on ambient cured polyurethane modified epoxy coatings synthesized from sustainable resource. *Progress in Crystal Growth and Characterization of Materials*, **45**, 83-88.

Shelby F. Thames, Haibin Yu, Ramesh Subramaniam, 2000. Cationic ultraviolet curable coatings from castor oil. *Journal of Applied Polymer Science*, **77**(1), 8-13.

Somani KP, Kansara SS, Patel NK, Rakshit AK, 2003. Castor oil based polyurethane adhesives for wood-to-wood bonding. *International Journal of Adhesion & Adhesive*, **23**, 269-75.

Staudinger H., and Hauser, E., 1921. Über neue organische Phosphorverbindungen IV Phosphinimine. *Helvetica Chimica Acta*, **4**, 861-868.

T.C. Wen, Y.J. Wang, T.T. Cheng and Ch. H. Yang, 1999. The effect of DMPA units on ionic conductivity of PEG-DMPA-IPDI waterborne polyurethane as single-ion electrolytes. *Polymer*, **40**, 3979-3988.

Thames SF, Boyer PC, 1990. AC impedance in predicting the corrosion behavior of metallic spots contained in polymer films. *Journal of Coating Technology*, **62**, 51.

Tien YI, Wei KH, 2001. Hydrogen bonding and mechanical properties in segmented montmorillonite/polyurethane nanocomposites of different hard segment ratios. *Polymer*, **42**, 3213-3221.

Tuan Noor Maznee, T I, Norin, Z K S, Ooi, T L, Salmiah, A and Gan LH, 2001. Effects of additives on palm-based polyurethane foams. *Journal of Oil Palm Research*, **13**, 7-15.

Urska Sebenik, Matjaz Krajnc, 2006. Influence of the soft segment length and content on the synthesis and properties of isocyanate-terminated urethane prepolymers. *International Journal of Adhesion & Adhesive*, **Article in Press**.

Wamprecht C, Sonntag M, 2002. Polyester polyols and their use as a binder component in two-component polyurethane coating composition. US Patent 6423816.

^aWang, TZ., Cho, Y.L., and Kuo, P.L., 2001. Flame-retarding materials. II. Synthesis and flame-retarding properties of phosphorus-on-pendent and phosphorus-on-skeleton polyols and the corresponding polyurethanes. *Journal of Applied Polymer Science*, **82**(2), 343-357.

^bWang, TZ and Chen, K.N., 1999. Introduction of covalently bonded phosphorus into aqueous-based polyurethane system via postcuring reaction. *Journal of Applied Polymer Science*, **74**(10), 2499-2509.

Wicks Jr ZW, 1975. Blocked isocyanate. *Progress in Organic Coating*, **3**, 73-99.

Wicks ZW, Jones FN, Pappas SP., 1992. Organic coating science and technology. In: Film formation, components and appearance, vol I. New York: Wiley; (Chapter 8 & Chapter 12)

Williams J.L., 1993. High solids PUR coatings: Past, Present, and Future. *Proc. Twentieth Waterborne, Higher-Solids and Powder Coatings Symposium*, New Orleans, LA, 1.

Xin Wei and Xuehai Yu, 1997. Synthesis and properties of sulfonated polyurethane ionomers with anions in the polyether soft segments. *Journal of Polymer Science Part B: Polymer Physics*, **35**, 225-232.

YanJun, Ling Hong, Xinling Wang, Xiaozhen Tang, 2003. Evaluation of the cure kinetics of isocyanate reactive hot-melt adhesives with differential scanning calorimetry. *Journal of Applied Polymer Science*, **89**(10), 2708-2713.

^aYao Y., Yoshioka, M., Shiraishi, N., 1995. Rigid PUR foams from combined liquefaction mixture of wood and starch. *Mokuzai Gakkaishi*, **41**(7), 659-668.

^bYao, Y., Yoshioka, M., Shiraishi, N., 1996. Water-absorbing PUR foams from liquefied starch. *Journal of Applied Polymer Science*, **60**, 1939-1949.

Ying-Ling Liu, Ging-Ho Hsiue, Chih-Wein Lan, Yie-Shun Chiu, 1997. Flame-retardant polyurethanes from phosphorus-containing isocyanates. *Journal of Polymer Science: Part A : Polymer Chemistry*, **35** (9), 1769.

^aYoshida, H., Morck, R., Kringstad, K.P., Hatekeyama, H., 1987. Kraft lignin in PUR. I. Mechanical properties of PUR from kraft lignin-polyether triol-polymeric MDI system. *Journal of Applied Polymer Science* **34**, 1187-1198.

^bYoshida, H., Morck, R., Kringstad, K.P., Hatekeyama, H., 1990. Kraft lignin in PUR. II. Effects of the molecular weight of kraft lignin on the properties of PUR from kraft lignin-polyether triol-polymeric MDI system. *Journal of Applied Polymer Science*, **40**, 1819-1832.

Yoshizumi M., Takato Adachi, Nobushige Numa, 1999. Application of graft copolymers using macromonomer method to two-component polyurethane coatings. *Progress in Organic Coatings*, **35**, 117-127.

Young-Kuk Jhon, In-Woo Cheong, Jung-Hyun Kim, 2001. Chain extension study of aqueous PUR dispersions. *Colloids and Surfaces A: Physicochemical and Engineering Aspects*, **179**, 71-78.

Zilg C, Thomann R, Mülhaupt R, Finter J, 1999. Polyurethane Nanocomposites Containing Laminated Anisotropic Nanoparticles Derived from Organophilic Layered Silicates. *Advanced Material*, **11**, 49-52.

Zuo M, Takeichi, 1999. Preparation and characterization of poly(urethane-imide) films prepared from reactive polyimide and polyurethane prepolymer. *Polymer*, **40**, 5153-5160.

CHAPTER 3: EXPERIMENTALS AND STRUCTURAL CHARACTERIZATION OF POLYURETHANE

3.1 Introduction

This chapter describes the synthesis procedure, formulations and experimental techniques used for preparation of polyols and PUR prepolymer in the research. A series of PUR were prepared in coatings and also in a form of free films by varying the polyols and NCO/OH ratios. Overall, measurements such as infra-red spectroscopy, x-ray diffraction, differential scanning calorimetry and thermogravimetry have been carried out with the purpose of investigating the properties of PUR. The aims of these studies conducted are to clarify the effect of oleic acid content and NCO/OH ratios on the physical properties of PUR coatings.

Knowledge of structure and physical properties of coating materials is a fundamental relevance in formulating the coating for a specific usage. Infra-red spectroscopy technique has been used as a tool to investigate the functional groups present in polyols and PUR samples, whereas x-ray diffraction results inferred about the structure of the material and differential scanning calorimetry technique is used to investigate thermal transition or the changes that occurs in PUR when they are heated. Lastly, thermogravimetry measurement was conducted to study the thermal stability of PUR samples.

3.2 Sample preparation

3.2.1 Raw materials

Oleic acid (purity 99.5%) and glycerol (purity 99.5%) were obtained from Cognis Oleochemical (M) Sdn. Bhd. Phthalic anhydride, PA (P.T. Petrowidada, Indonesia) and toluene diisocyanate, TDI (Aldrich, USA) (80:20; 2,4-toluene diisocyanate:2,6-toluene diisocyanate) mixture of the two isomers were used as received. Toluene (JT Baker, USA) was used as solvent; it was dried over activated molecular sieve overnight before use. Silicone surfactant used was L6900 (Air Products, USA) and defoamer BYK-088 was from BYK Chemie, Germany. The syntheses of the polyols were preceded in Polymer Lab, Chemistry Department, University Malaya by Mr Gan Yik Kang, a postgraduate student.

3.2.2 Procedure of polyol synthesis

Pre-weighed PA, glycerol and oleic acid were charged into a 2 litre four neck round bottom reactor flask. The mixture was stirred and heated up to a temperature of 120°C to 130°C while a slow stream of nitrogen gas was bubbled through the mixture for 30 minutes. The temperature was then increased to 180-200°C when the reaction could proceed readily with the evolution of water, which was collected at the decanter arm. Sample was taken periodically to check the acid number until it fell below 50 mg KOH g⁻¹. The reaction was considered complete after the water of reaction collected was as predicted in the formulation. Three different formulations of polyols were synthesized by varying contents of oleic acid into 28%, 40% and 65%. The samples

were named as Alk28, Alk40 and Alk65 respectively in accordance with the percentage of oleic acid in the samples. The compositions and characteristic of polyols are summarized in Table 3.1 and Table 3.2. The formulations were based on the method as described in reference (T.C.Patton 1962), and the targeted alkyds would have similar hydroxyl value and acid numbers.

Table 3.1 Composition of PA, glycerol and oleic acid used in the preparation of polyols

	Alk28	Alk40	Alk65
Glycerol / g	456	256	145
Phtalic Anhydride / g	700	338	103
Oleic Acid / g	452	400	460
Projected OH Value (mg KOH/g resin)	142	142	143

The polyols were characterized by Fourier Transform Infrared (FTIR) spectroscopy (Perkin-Elmer FTIR spectrum RX-1 spectrometer) and differential scanning calorimetry (DSC Mettler 821e) from -40 to 150°C at a heating rate of 10°C/min under nitrogen atmosphere. Acid number and hydroxyl value of polyols were also determined by standard methods which are ASTM D1639-90 and ASTM D1957-90 respectively. The molecular weights of the polyols were determined by gel permeation chromatography (GPC, Waters, polystyrene standards) in THF (elution rate: 1 ml/min) at 35°C. The viscosity of the polyols were measured using a Brookfield model RVT plate and cone viscometer (serial no 206505) at room temperature. The end properties of the samples are shown in the Table 3.2. It was noticed that polyol with the lowest

percentage of oleic acid content (short oil length) was very viscous and had to be heated in the oven before it could be poured out of the bottle.

Table 3.2 Properties of oleic acid polyols

Properties	Alk28	Alk40	Alk65
Colour	dark brownish	brownish	light brownish
Viscosity	12800 cps	8000 cps	2800 cps
Stability	> 6 months	> 6 months	> 6 months
Acid Number (mg KOH)	48.2	40.4	33.5
OH value (mg KOH)	132	134	135
T _m (°C)	-28.4	-28.5	-28.4
M _n	999	953	859
M _w	2322	2251	1441
M _p	1171	1070	1092
Poly dispersity	2.44	2.25	1.68

3.2.3 Procedure of PUR prepolymer synthesis

The polyol and additives were dried under reduced pressure at 80°C for 2 hours before being poured into a 3 neck flat bottom flask equipped with thermometer, dropping funnel and magnetic stirrer. The apparatus used is shown in Figure 3.1. Polyol was allowed to react with a calculated amount of TDI in the presence of toluene, surfactant

and defoamer. TDI was added dropwise into the reaction mixture at 80°C over 3 hours with constant stirring. The partially reacted sample formed a viscous solution, which was then poured into a rectangular mould of 12 cm x 12 cm to cure under ambient temperature overnight to form film of 0.5 mm thickness and left in the oven at 60°C for two days to evaporate off all the solvent (discussed in detail in Section 3.2.4).

Coatings of PUR cured at ambient temperature were prepared by draw down method stated in ASTM D4147-93 on mild steel panel 70 x 200 mm (explained in detail in section 4.2 chapter 4) The composition and designation codes of the polyurethane systems are shown in Table 3.3.

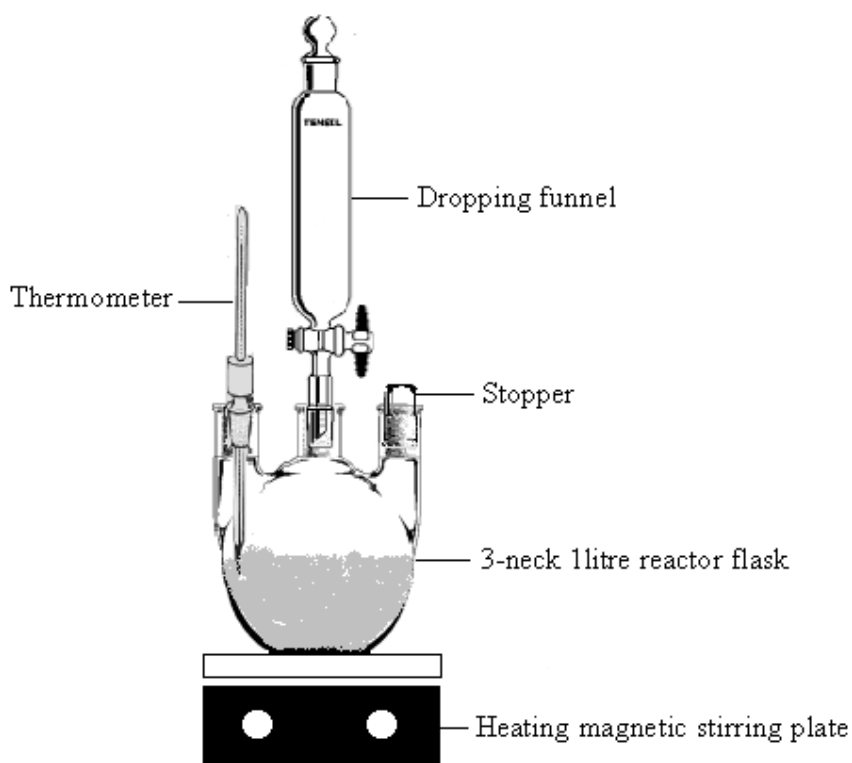


Figure 3.1 Apparatus set-up during the pre-polymerization process of PUR

Table 3.3 Composition of polyols and TDI used in the preparation of polyurethanes

Type of polyol	Designation of PU composition code	NCO/OH ratio	Amount of polyol (g)	Toluene (g)	L6900 (g)	BYK-088 (g)	Amount of isocyanates adduct (g)	Available NCO in prepolymer (%)
Alk28	PUalk28(1.2)	1.2	397.89	200.91	0.24	0.24	104.40	10.17
	PUalk28(1.4)	1.4	397.89	218.27	0.25	0.25	121.8	19.67
	PUalk28(1.6)	1.6	397.89	225.28	0.26	0.26	139.20	28.54
Alk40	PUalk40(1.2)	1.2	399.59	211.68	0.24	0.24	104.40	10.14
	PUalk40(1.4)	1.4	399.59	218.98	0.25	0.25	121.8	19.60
	PUalk40(1.6)	1.6	399.59	226.29	0.26	0.26	139.20	28.45
Alk65	PUalk65(1.2)	1.2	400.46	262.53	0.24	0.24	104.40	10.12
	PUalk65(1.4)	1.4	400.46	271.58	0.25	0.25	121.8	19.57
	PUalk65(1.6)	1.6	400.46	280.62	0.26	0.26	139.20	28.41

3.2.4 Preparation of coating and free films for testing

Free films are required for physical, tensile and electrical testing. There are a number of ways to produce films of uniform and reproducible thickness. The technique used in preparing the free films was arrived by trial-and-error method after many trials on producing films with the best even thickness. A rectangular mould of 12 cm x 12 cm was prepared and the prepolymer was poured into it to cure under ambient temperature overnight to form film of 0.5 mm thickness and left in the oven at 60°C for two days to evaporate off all the solvent. The base of the oven tray where the mould was seated was adjusted so that it is as flat as possible to ensure the films were in even thickness. Some of the PUR films were very brittle; hence aluminum foil was used to simplify the peeling process of PUR films from the surface of the mould without breaking the

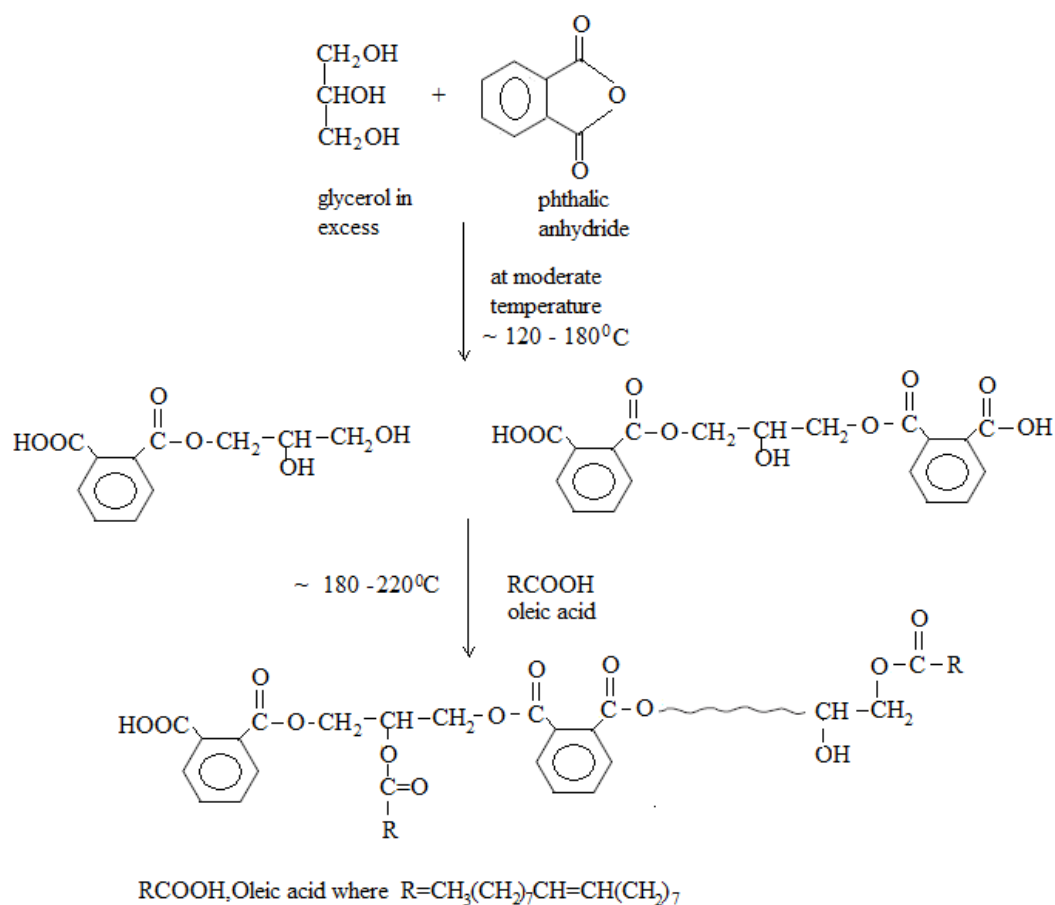
samples. The samples were kept at least 30 days in room temperature before conducting any test on them.

3.3 Polyols and PURs reaction schemes

i. Polyols

In the preparation of polyols, the reaction of phthalic anhydride involves two distinct steps. The first step is the reaction between anhydride and glycerol to form a half ester and a free carboxylic group. This ring opening of phthalic anhydride does not evolve any water and could occur quite readily at moderate temperature around 120°C to 130°C. In this series of polyols, there was an excessive amount of glycerol over the phthalic anhydride at the initial stage which led to the formation of a mixture of oligomers with terminal carboxylic and excess hydroxyl groups. At this stage there was no noticeable reaction between free -COOH and -OH as no water was evolved. At the second stage, the temperature was raised to 180-200°C. Both the carboxylic acid of the half ester and oleic acid would compete to react with hydroxyl group to form ester linkages with liberation of water. The oleic acid is incorporated as flexible side chains. The resulting low molecular weight polyols are viscous liquids. From the results, it can be noted that viscosity and molecular weight of the resin decreases as the oleic acid content increases. These steps and the predicted polyols structure are represented in Scheme 3.1.

Scheme 3.1 Reaction of phthalic anhydride, glycerol and oleic acid to form polyol



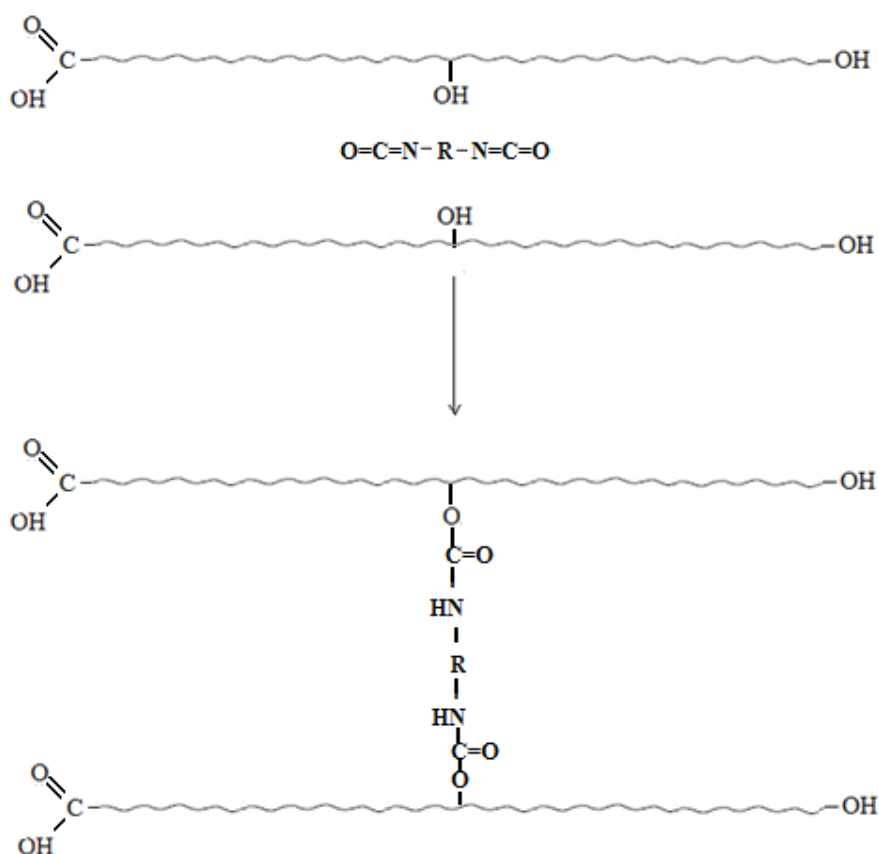
ii. Polyurethanes

Formation of the PUR occurs by simultaneous solvent evaporation (physical process) and chemical reactions of -NCO group with -OH group (Eram S et al., 2007, S. Ahmad et al., 2001) as represented in Scheme 3.2. Polymerization of polyurethane is known as condensation polymerizations or as a functional group polymerization. Functional groups on each end of monomer molecules (e.g., -NCO group from 2,4 toluene diisocyanate) react with functional groups on the end of another monomer (e.g., -OH from polyols or alkyds) to form linkages (e.g., urethanes). There are no inherent initiations or chain transfer reactions, only

propagation. In this case the polymerization proceeds, the structure of the main chain consist of urethane back bone with oleic acid as flexible side chain as shown in Scheme 3.2.

Good film formation, which was non-sticky to touch, after 48 h curing required the use of excess equivalent amount of isocyanate. The excess of diisocyanate (for NCO/OH ratio of 1.2-1.6) introduced allophanate and polyisocyanurate structures, which were effectively bonding between polymer chains giving rise to cross-linking.

Scheme 3.2 Reaction of polyols with isocyanates to form polyurethanes



3.4 Common techniques used in PUR films characterization

3.4.1 FTIR

Infrared spectroscopy is a spectroscopic technique where molecular vibrations are analyzed. Typically when a molecule is exposed to infra-red (IR) radiation, it absorbs specific frequencies of radiation. The frequencies are dependent upon the functional groups within the molecule and the symmetry of the molecule. IR radiation can only be absorbed by bonds within a molecule, if the radiation has exactly the right energy to induce a vibration of the bond. This is the reason only specific frequencies are absorbed.

Infrared spectroscopy focuses on electromagnetic radiation in the frequency range of 400-4000 cm^{-1} , where cm^{-1} is known as wavenumber (1/wavelength), which is a unit of measure for the frequency.

Polyols Alk28, Alk40 and Alk65 were analyzed by FTIR from a thin film on a sodium chloride cell using a Perkin Elmer FTIR Spectrum RX-1 spectrometer at wavenumber from 4000 – 400 cm^{-1} . As for PUR, all infrared measurements have been taken using Nicolet Magna-IR 550 spectrometer at wavenumber from 4000 – 400 cm^{-1} with 1 cm^{-1} resolution from a thin film coated on Potassium Bromide, KBr disc. The bench is controlled via Nicolets's Omnic software with a full diagnostics analysis system. Background effects due to atmospheric water (H_2O), carbon dioxide (CO_2) and other volatiles were subtracted. The source is a tungsten-halogen source.

3.4.2 XRD

An x-ray diffractometer illuminates a sample of material with x-rays of known wavelength, moving the sample and detector in order to measure the intensity of the diffracted radiation as a function of beam and sample orientation. The measurement is generally not straightforward, and the inference required to make useful observations on the sample is quite subtle. All the diffractometer can tell us is the spacing between atomic layers and when combined with enough other information, in particular knowledge of crystal symmetries, remarkably complete understanding of the sample can be achieved.

The XRD equipment used in this research was Siemens D5000 X-Ray Diffractometer. The D5000 measures atomic spacing in crystals using diffraction of approximately monochromatic x-radiation. It can be used to characterize solid samples ranging in size from about 1 millimeter square up to intact four-inch wafers. The radiation source used is copper k-alpha with a wavelength of 1.5418 Angstroms.

3.4.3 DSC

Differential scanning calorimetry (DSC) is a technique used to investigate thermal transition or the changes that occurs in a polymer when they are heated. DSC measures the temperatures and heat flow associated with transitions in materials as a function of time and temperature in a controlled atmosphere. These measurements provide quantitative and qualitative information about physical and chemical changes that involve endothermic or exothermic processes, or change in heat capacity.

In thermal transition, there are glass transition temperature T_g , polymers crystallization temperature T_c and polymer's melting temperature, T_m . However, not all of the above will be shown in DSC plot. Complete amorphous polymers won't show T_c or T_m but polymers with both crystalline and amorphous domains will show all the features.

The glass transition is the temperature where the polymer goes from a hard, glass like state to a rubber like state. Glass transition occurs in amorphous and semicrystalline polymers and this is due to a reduction in motion of large segments of molecular chains with decreasing temperature. DSC defines the glass transition as a change in the heat capacity as the polymer matrix goes from the glass state to the rubber state. This is a second order endothermic transition (requires heat to go through the transition) so in the DSC, the transition appears as a step transition and not a peak such as might be seen with a melting transition.

Crystallization is the process where a liquid melt having a highly random molecular structure becomes an ordered solid phase upon cooling. Temperature when the molecules spontaneously arrange themselves into a crystalline form is known as crystallization temperature. This transition from amorphous solid to crystalline solid is an exothermic process, and results in a peak in the DSC signal.

Melting of a polymer crystal corresponds to transformation of a solid material having an ordered structure of aligned molecular chains to a viscous liquid in which the structure is highly random (WD Callister, 2004). The melting process results in an endothermic peak in the DSC curve.

3.4.4 TGA

A technique where the weight of a substance heated at a controlled rate recorded as a function of time or temperature is defined as Thermogravimetry (TGA). Basic instrumental requirements for thermogravimetry are a precision balance, a furnace capable of being programmed for a linear rise of temperature with time and a recorder (Cyril K, 1969). Results of the programmed operation of a thermobalance may be presented in a plot of weight versus temperature (or time) referred to as the thermogravimetry TG curve and a plot of the rate of weight loss versus temperature which is referred as derivative thermogravimetric curve or DTG curve. Thermogravimetry widely used to study the thermal stability of a wide range of organic polymers. For example, Newkirk, 1960 heated a series of polymers under nitrogen and showed that an increasing order of stability was readily observable for poly(methyl methacrylate), polystyrene, Mylar, nylon and polyethylene.

Organic macromolecules as well as low molecular weight organic molecules are stable only below a certain limiting temperature usually from 100 to 200°C. If the temperature is increased to certain temperature, organic molecules may vaporize or decompose into small fragments. Molecules are composed of atoms linked together by covalent bonds. Dissociation energies of single bonds in the ground state are in the order of 150-400 kJ per mol at 25°C and other typical values of dissociation energy depicted from Szycher M., 1999 are O-O:147 kJ/mol, C-H: 320-420 kJ/mol, C-C:260-400 kJ/mol and C-O:330 kJ/mol.

Thermal cracking of short chain hydrocarbons occurs at high temperatures (400 to 600°C) and therefore significant degradation conversion of most polymers is also

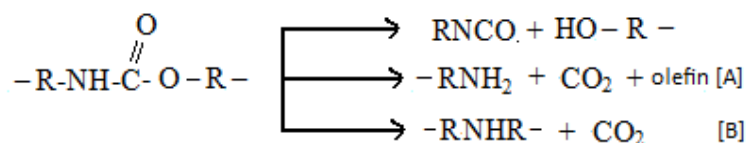
expected at these temperatures. At lower temperature (150 to 300°C) bond scissions are less frequent. However, chemical reaction initiated at these temperature and conversions can be achieved at slightly elevated temperature, especially if the chemical reactions proceeded by a chain mechanism.

Dissociation of PUR begins at 115 to 125°C where biuret linkage starts to dissociate around these temperatures. The aromatic based urethane bond begins its thermal dissociation around 180°C, which is prior to the urea linkage which is about 160 to 200°C. Urethane can dissociate into the isocyanate and polyol from which it was formed. The second reaction produces a primary amine and an olefin. The third reaction produces a secondary amine. The latter reactions generate CO₂, which is lost as a gas as they are irreversible. The thermal dissociation relationships are summarized in Table 3.4.

Table 3.4 Thermal dissociation temperatures of linkages found in polyurethanes (Adapted from Szycher M., 1999)

Linkage	Onset of dissociation (°C)
Aliphatic allophanate	85 - 105
Aromatic allophanate	100 -120
Aliphatic biuret	100 - 110
Aromatic biuret	115 - 125
Aliphatic urea	140 - 180
Aromatic urea	160 - 200
Aliphatic urethane	160 - 180
Aromatic urethane	180 - 200
Disubstituted urea	235 – 250

The urethane linkage may undergo three separate types of thermal degradation: (1) the formation of the precursor isocyanate and the precursor alcohol; (2) the cleavage of the oxygen of the alpha CH₂ group and association of one hydrogen on the second CH₂ group would lead to the carbamic acid and an olefin with subsequent carbamic acid decomposition to give a primary amine and CO₂ or referred as mechanism [A]; and (3) the formation of a urethane and secondary amine and referred to as mechanism [B]. Thermal degradation of PUR is summarized in Scheme 3.3.



Scheme 3.3 Thermal degradation of urethane linkages

Thermodegradation of PUR occurs depending upon the factors such as structure of the urethane, the reacting conditions and the environment. As for coatings, thermogravimetry was used to investigate the thermal stability of the coatings and also to select a suitable cure temperature that would not lead to degradation (TB Yeow, 2000).

3.5 Results and Discussion

3.5.1 FTIR Analysis

FTIR analysis is performed in this study to confirm the composition expected for polyols and PUR prepolymers. Figures 3.2 and 3.3 show the infrared spectra of polyols and PUR respectively. From the overlay spectra of Alk28, Alk40, Alk65 and oleic acid shown in Figure 3.2, the stretching band at $3460 - 3480\text{ cm}^{-1}$ indicates the presence of free hydroxyl groups which is absent in oleic acid. The rest of the peaks in the spectra of oleic acid did not show any noticeable changes if compared to the alkyds. The band observed in alkyds at 2925 cm^{-1} is due to the -CH- stretching. Typical ester C=O peak was observed at wavelength 1730 cm^{-1} and the 1599 cm^{-1} was the “breathing mode” of the aromatic ring. The peak at 1580 cm^{-1} represent C-C multiple band for aromatic substitution, peak at 854 cm^{-1} was due to C=C bending and 744 cm^{-1} was from C-H aromatic substitution bending.

The FTIR spectra of the polyurethanes PUalk28, PUalk40 and PUalk65 were given in Figure 3.3. The absorption peaks resulting from NH stretching and bending vibrations were observed at $3350\text{-}3380\text{ cm}^{-1}$ and $1540\text{-}1550\text{ cm}^{-1}$ respectively. In the spectra, the characteristic carbonyl stretching was observed at $1734\text{-}1745\text{ cm}^{-1}$. The formation of urethane linkages is clearly indicated by the disappearance of -OH- absorbance band associated with the polyol within the range of $3460 - 3480\text{ cm}^{-1}$ and the appearance of a -NH- band of PUR at 3360 cm^{-1} . The presence of isocyanurates (2283 cm^{-1}) from trimerization of isocyanates was observed for some of the sample. The bands in the PURs spectra are obtained from the literature (DK Chattopadhyay et al., 2005, 2006; MM Coleman et al., 1986) and in this work are tabulated in Table 3.5.

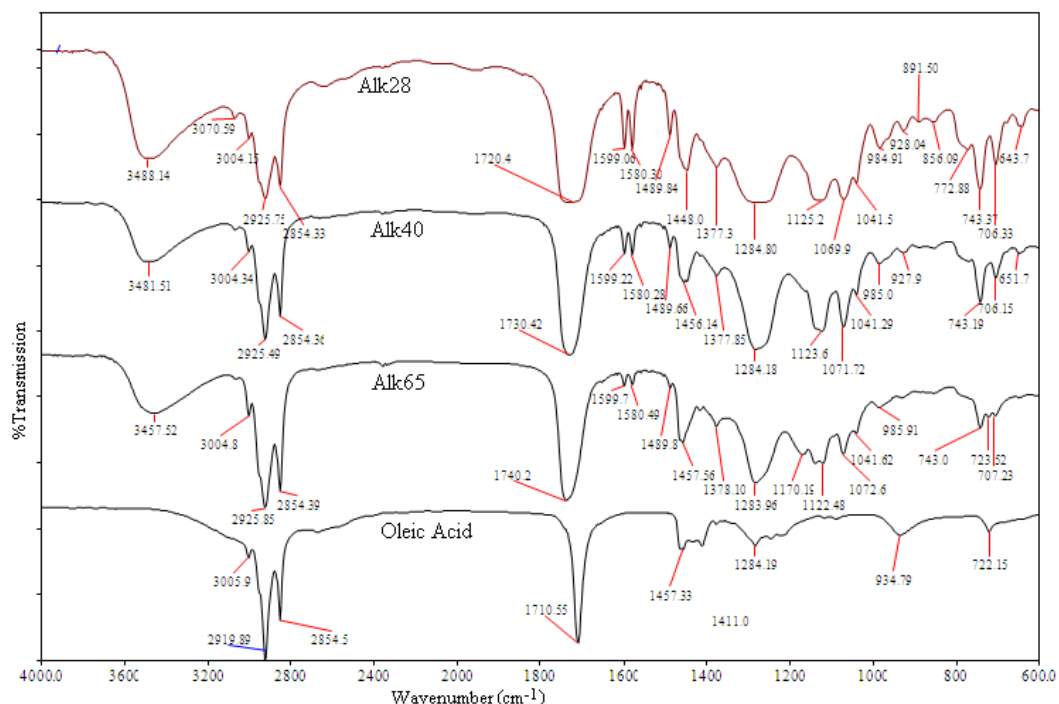


Figure 3.2 The FTIR spectra of polyols Alk28, Alk40, Alk65 and oleic acid.

Amide I vibration consists of several components reflecting C=O groups in different environments and is sensitive on the specificity and magnitude of hydrogen bonding. Amide I mode (DK Chattopadhyay et al., 2006) is a complex vibration mode involving the contribution of C=O stretching, C-N stretching and C-C-N deformation vibration. Amide II mode (MM Coleman et al., 1986) is a mixed contribution of N-H in-plane bending, the C-N stretching and C-C stretching vibrations. Amide II mode is sensitive to chain conformation and intermolecular hydrogen bonding. As for Amide III mode, it involves the stretching vibration of the C-N group. This mode is highly mixed and complicated by coupling with NH deformation modes.

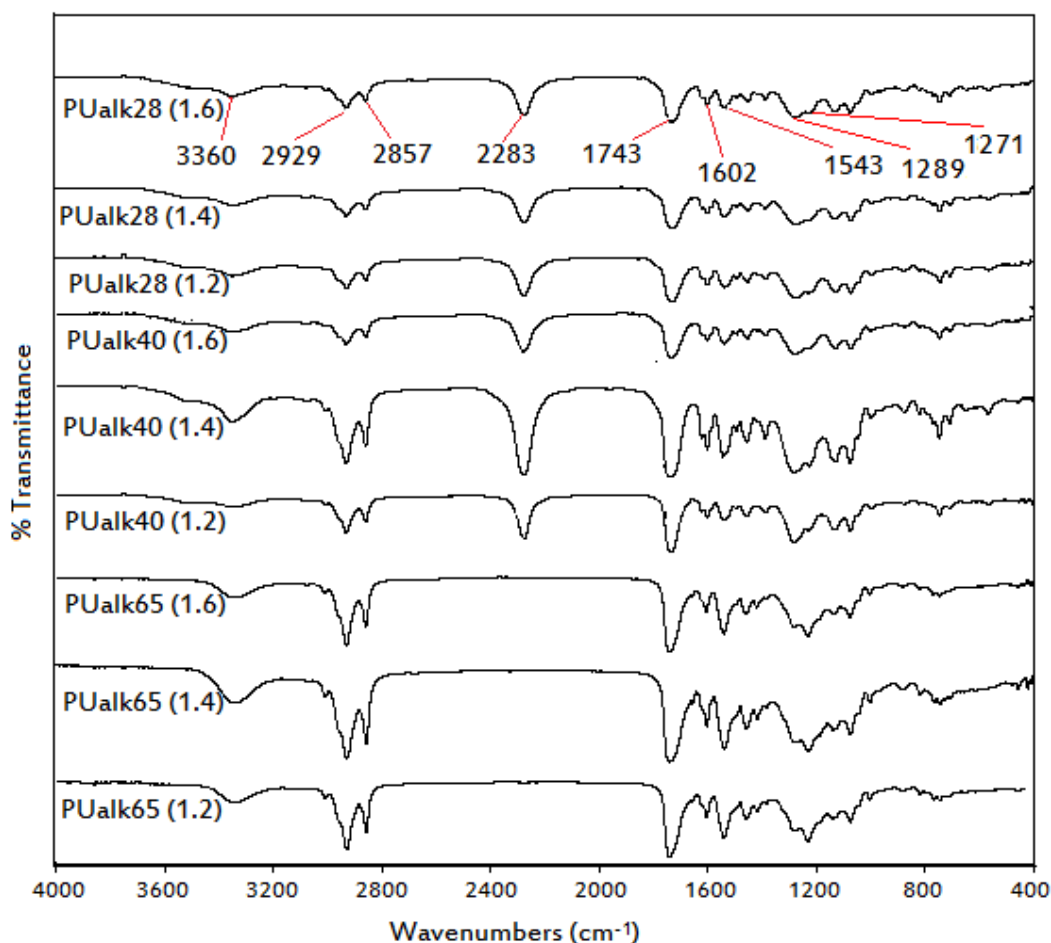


Figure 3.3 The FTIR spectra of PUR with NCO/OH Ratios 1.2, 1.4, 1.6.

Reaction occurs between polyol O-H groups ($3460 - 3480 \text{ cm}^{-1}$) and diisocyanate $\text{N}=\text{C}=\text{O}$ groups (2283 cm^{-1}) forming urethane groups and thus, forming signals such as N-H bond at 3360 cm^{-1} , Amide modes of I, II and III as shown in Figures 3.2 and 3.3. The appearance of OH groups $3460 - 3480 \text{ cm}^{-1}$ in the polyols of Figure 3.2 and disappearance of it in Figure 3.3 may be concluded that all hydroxyl groups were consumed in the reaction of polyols and TDI.

Table 3.5 The vibration modes and wavenumbers of PUR from IR spectrum (DK Chattopadhyay et al., 2005, 2006; MM Coleman et al., 1986)

Modes of vibration	Wavenumbers (cm⁻¹)	Wavenumbers (cm⁻¹) obtained experimentally
N-H stretching	3150 - 3600	3360
C-H stretching Anti-Symmetric & Symmetrical stretching of methylene groups	2800 - 3000	2929, 2857
NCO	2300 - 2270	2283
Amide I (C=O stretching)	1600 - 1760	1743, 1602
Amide II ($\delta_{\text{N-H}} + \nu_{\text{C-N}} + \nu_{\text{C-C}}$)	1540	1543
Amide III ($\nu_{\text{C-N}}$)	1226-1292	1271, 1281

3.5.2 XRD Analysis

Figure 3.4 illustrates the x-ray diffractogram of PUR films. Broad scattering halos between 5° and 80° of 2 θ are observed. The XRD pattern without any strong diffraction peak exhibits the amorphous nature of the polymer.

The probability of a polymer to exhibit crystallinity is determined primarily by the chemical nature of the polymer chains. Furthermore, crystallinity is more likely to occur if the polymer is capable of strong intermolecular attraction advantageously distributed along the polymer chains. However, polymer chains contain bulky side groups or branching would prevent close packing and interfere crystalline formation.

The diffraction patterns in Figure 3.4 exhibit broad peaks at approximately 2 θ = 23° for all the samples which indicates that the samples are amorphous in nature at room temperature. Some amount of crystalline phase exists due to the presence of hard

segments which are indicated by the broad single diffraction peaks observed in the spectrums. This small amount of crystallinity is overshadowed by the presence of long hydrocarbon chain of polyols and the hydrogen bonding between -OCONH- groups of PUR. Hence, the PUR exhibit overall amorphous character.

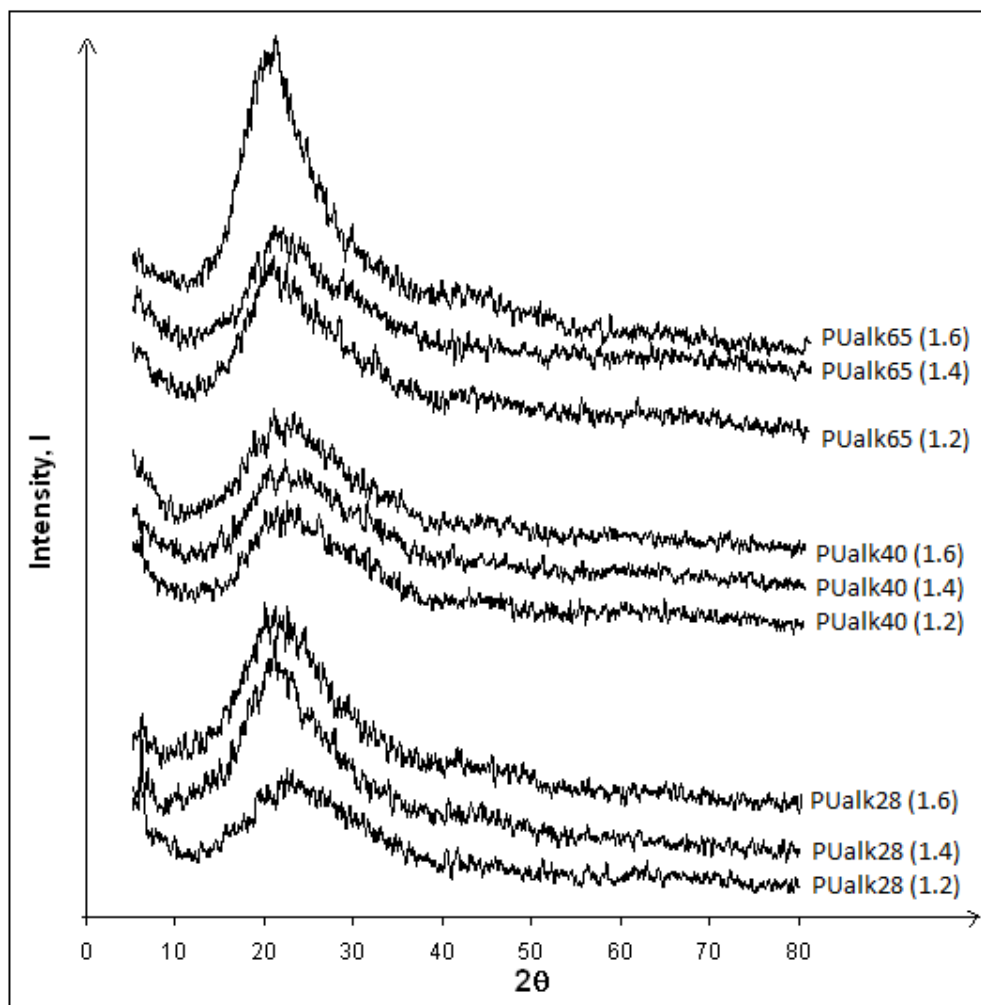


Figure 3.4 XRD profiles of PURs with various NCO/OH ratios

In general, the intensity of the peaks increases (at approximately $2\theta = 23^\circ$) as the NCO/OH ratios increase with no evidence of diffraction angle shift. As the NCO/OH ratio increases, the percentages of hard segments increase in the polymer. These crystalline regions (hard segments) are surrounded by a matrix of amorphous soft

segments in which the chains are more random and entangled. The increase in the intensity of the highest NCO/OH ratio represents the ordered structure of hard segments which increase as the ratio increases. However the samples still exhibit overall amorphous character due to the presence of soft segments.

However, comparing the x-ray results for PUR with polyols of different oleic acid content, the intensity increase of the peaks are not very significant for PUalk28 and PUalk40 except for PUalk65. In general, the three polyols have similar main chain structure formed from the reaction of PA and glycerol with the attachment of some oleic acid as flexible side chains. As the oleic acid content increases, the percentages of flexible side chain increase in the system. PUalk65 contains higher percentage of oleic acid and thus, presumably have a higher amount of flexible side chain. Flexible side groups have no effect on mobility of the main chain. However they increase the inter-chain distance and decrease the inter-chain interaction (Marcel M, 1996). Therefore it may be concluded that the samples are more amorphous as the oleic acid content increases.

In summary, crystalline structure of PUR samples diminishes as the oleic acid content of the polyols increased and crystallinity remains existent, though insignificantly, in the fully cured polyurethane-urea cross-linked matrices. Increased in NCO/OH ratio increases the cross-linking, thus increases the crystallinity of the polymer. However, as for the highest NCO/OH ratio in which in this case 1.6 shows segmental PUR structure where the hard segment, has an orderly structure. The increase in oleic acid content of the soft segments increases the amorphous structure of the samples. Overall, at room temperature, the palm olein oleic acid based PUR has an amorphous nature with some amount of crystalline phase due to the presence of hard segments.

3.5.3 DSC Analysis

DSC technique was used to investigate the thermal properties of the synthesized PUR. The glass transition temperature (T_g) of each PUR film was measured using a differential scanning calorimeter. The samples were tested by using DSC 6 Perkin Elmer. About 5 to 10 mg of the samples were weighed and sealed in aluminum crucibles during the testing process. First, the samples were heated from 35°C to 150°C at 20°C/min to eliminate the thermal history or effect of enthalpy relaxation (Rials et al., 1984, Yoshida et al., 1990) of the samples. The second and third heating from 35°C to 150°C at 20°C/min were performed to confirm the T_g values for the PUR samples. The glass transition was sometimes difficult to observe, but the strength of the transition could be enhanced somewhat by quenching from the melt at the fastest cooling rate to increase the amorphous fraction of the sample. The DSC signals obtained through this method are displayed in Appendix A for PUalk28 (1.2), PUalk28 (1.4), PUalk28 (1.6), PUalk40 (1.2), PUalk40 (1.4), PUalk40 (1.6), PUalk65 (1.2), PUalk65 (1.4), PUalk65 (1.6) individually.

In the PUR, the soft segments are from the polyester polyol, whereas the hard segments are formed by the diisocyanate with urethane linkages. Therefore, polyurethanes, urethane prepolymers or urethane-urea copolymers derived from polyols of higher molecular weight are softer. If the soft and hard segments arrange themselves in separate domains, the resulting phase segregated polymer will have two respective glass transition temperatures (T_g), one at a lower temperature corresponding to soft segments and the other at a higher temperature belonging to hard segments. However, if extensive mixing between the two types of segments occurs, only one T_g is usually observed which is located between those of pure soft and hard segments. If the mixing

is not extensive, one broad glass transition or two transitions are located between those of pure soft and hard segments (Urška Šebenik et al., 2006).

The melting temperature (T_m) are -28.4°C , -28.5°C and -28.4°C for Alk28, Alk40 and Alk65 respectively (shown in Appendix A, Figure X, XI & XII). Polyols synthesized from different percentage of oleic acids content had almost identical T_m values around -28°C regardless their oleic acid percentage. For all the PUR samples synthesized and analyzed in this work, only a single broad T_g was observed and the T_g values are tabulated in Table 3.6. All the PUR samples exhibited one glass transition temperature over the temperature range studied. The single T_g for each sample suggests that there are less visible phase separations between soft and hard domains. There are no endothermic peaks appearing in the scans, indicating that crystalline regions do not exist in our samples. Both phase separation and crystalline formation may have been inhibited by the presence of chemical cross-links. This fact further confirms the amorphous nature of the PUR as discussed in the XRD analysis section 3.4.2.

Table 3.6 Glass transition temperatures of PUR samples

Samples	$T_g \pm 0.2 (^{\circ}\text{C})$		
	NCO/OH = 1.2	NCO/OH = 1.4	NCO/OH = 1.6
PUalk28	122.8	122.5	122.9
PUalk40	122.8	123.7	123.2
PUalk65	123.1	123.0	122.7

Furthermore, the oleic acid percentage and NCO/OH ratio does not influence the T_g . The T_g values remain at 123°C regardless of NCO/OH ratios and the increment of oleic

acid percentage. The T_g obtained is presumed from the main chain of the polymer as the structure of main chain is the same for all the nine PURs in the research. The only significant change in the structure of main PUR chain is the side branch of oleic acid and in this case the side chain does not contribute significantly to the T_g of the sample.

In summary, the absence of endothermic peaks in the scans indicates that both phase separation and crystalline formation may have been inhibited by the presence of chemical cross-links. Higher percentage of oleic acid content has higher percentage of flexible side chains and the flexible side chains of the polyols refrains cross-linking from increasing, thus the T_g values of PURs remain constant regardless of NCO/OH ratio increment.

3.5.4 TGA Analysis

Samples of PURs (8-10mg) were tested in a thermogravimeter (Rheometric Scientific TGA instrument, Model 1000+) at a heating rate of 20°C /min from room temperature to 900°C under N₂ gas flow. TGA data gives only qualitative indication of the thermal stability of the material concerned. Typical TGA measurement for PUalk28(1.2), PUalk28(1.4), PUalk28(1.6), PUalk40(1.2), PUalk40(1.4), PUalk40(1.6), PUalk65(1.2), PUalk65(1.4) and PUalk65(1.6) are shown in Figures 3.5 to 3.13 respectively. Three to five steps degradation stages were observed for the nine PUR samples. The polymers are stable up to 170°C and rapid weight loss starts at approximately 170°C up to 700°C. Table 3.8 shows the decomposition temperature at various weight loss percentages for all the degradation stages.

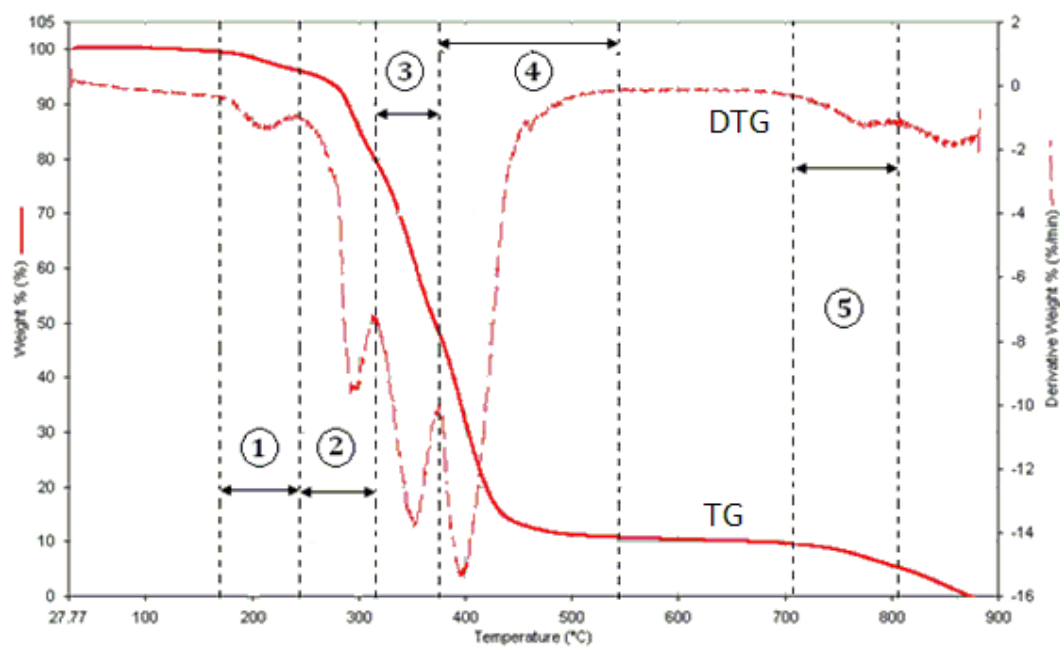


Figure 3.5 TG and DTG curve versus temperature of PUalk28 (1.2)

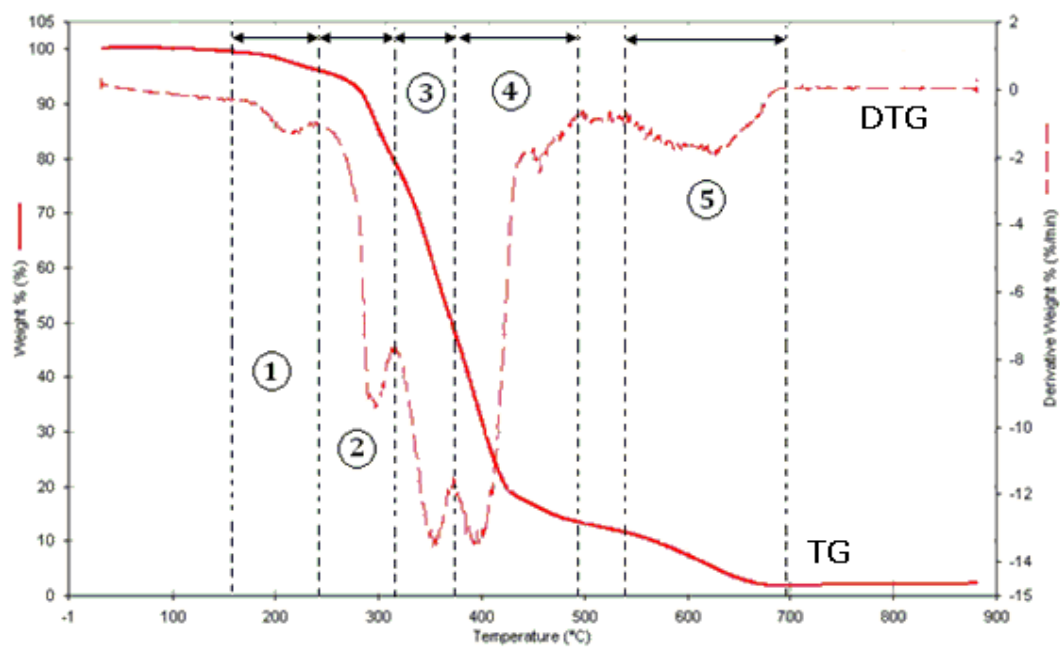


Figure 3.6 TG and DTG curve versus temperature of PUalk28 (1.4)

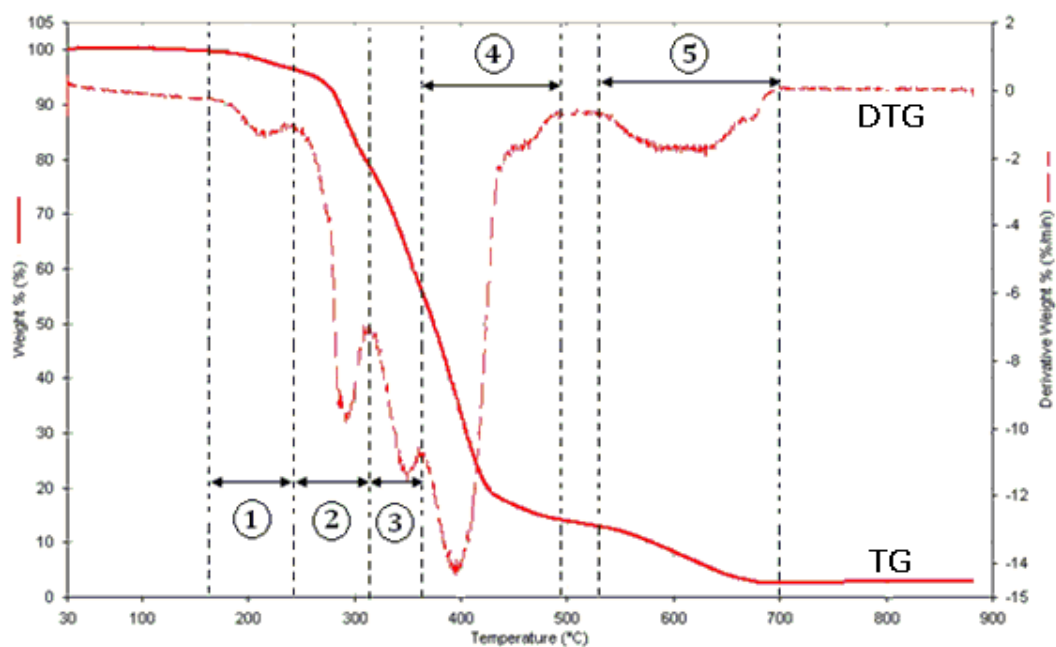


Figure 3.7 TG and DTG curve versus temperature of PUalk28 (1.6)

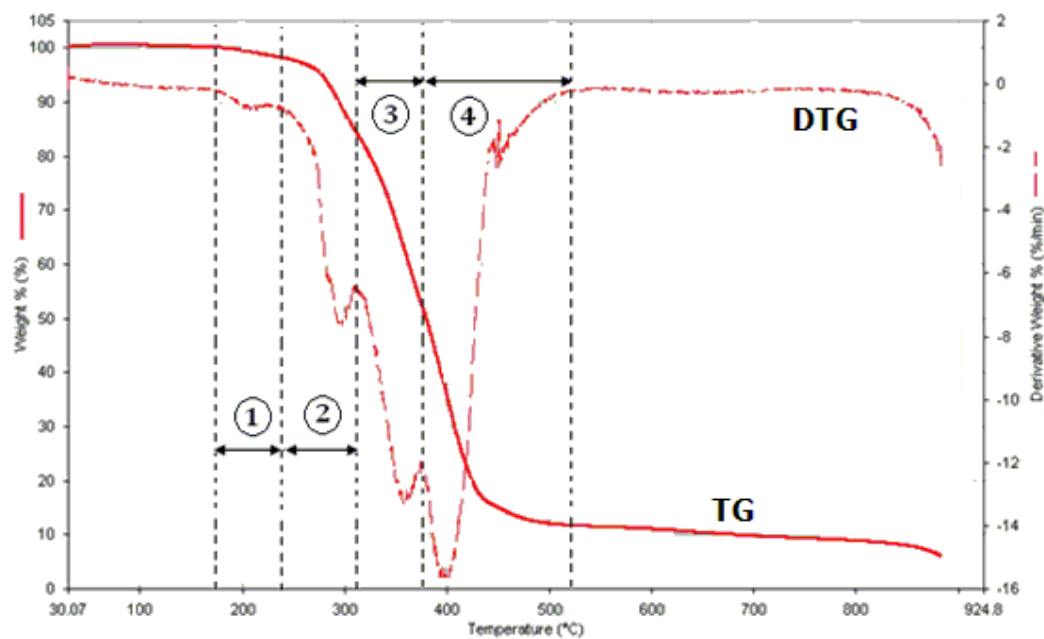


Figure 3.8 TG and DTG curve versus temperature of PUalk40 (1.2)

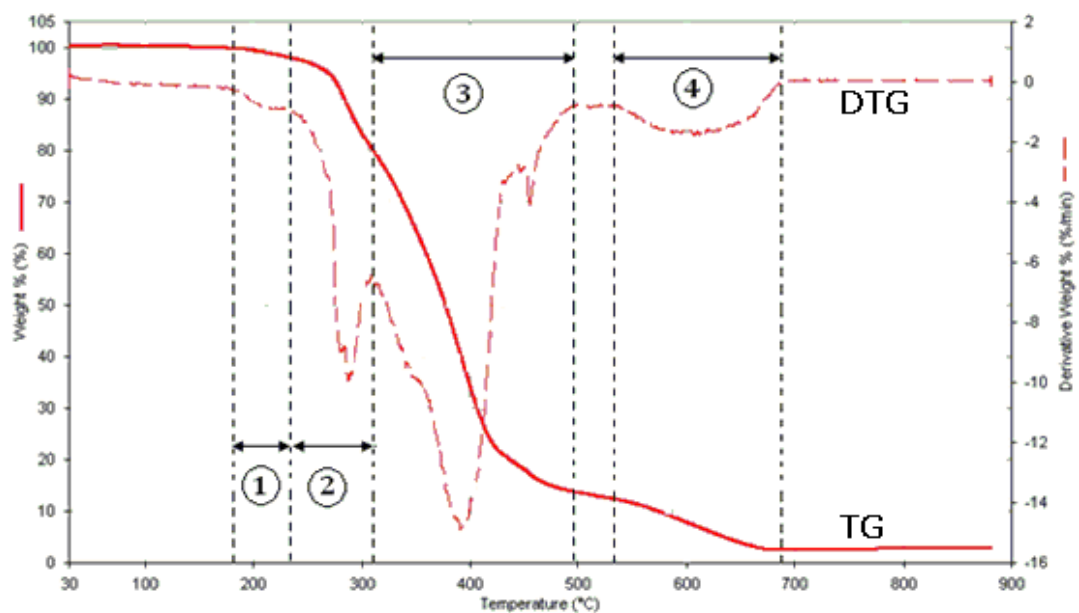


Figure 3.9 TG and DTG curve versus temperature of PUalk40 (1.4)

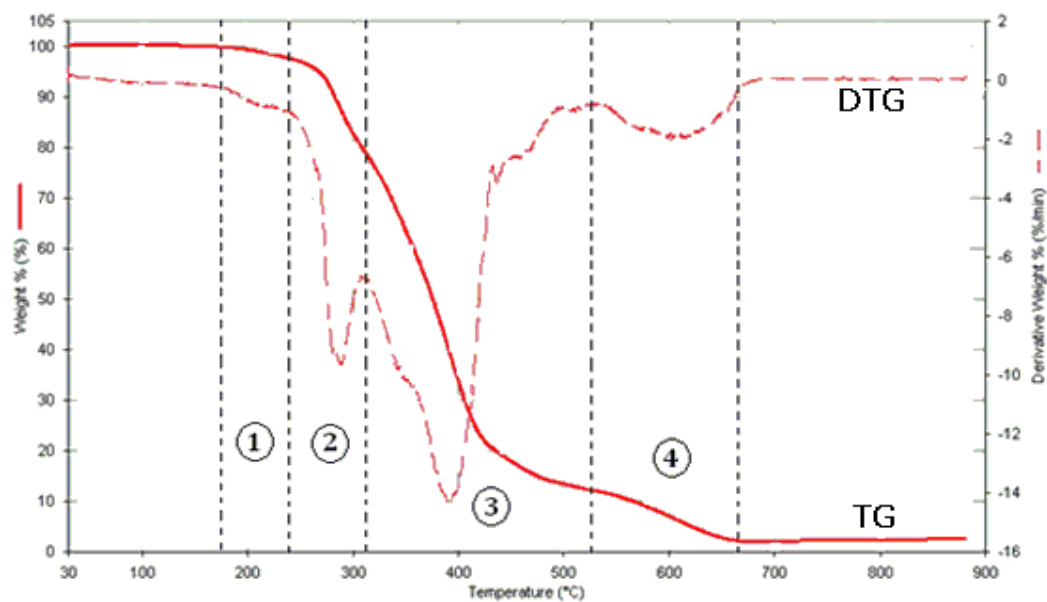


Figure 3.10 TG and DTG curve versus temperature of PUalk40 (1.6)

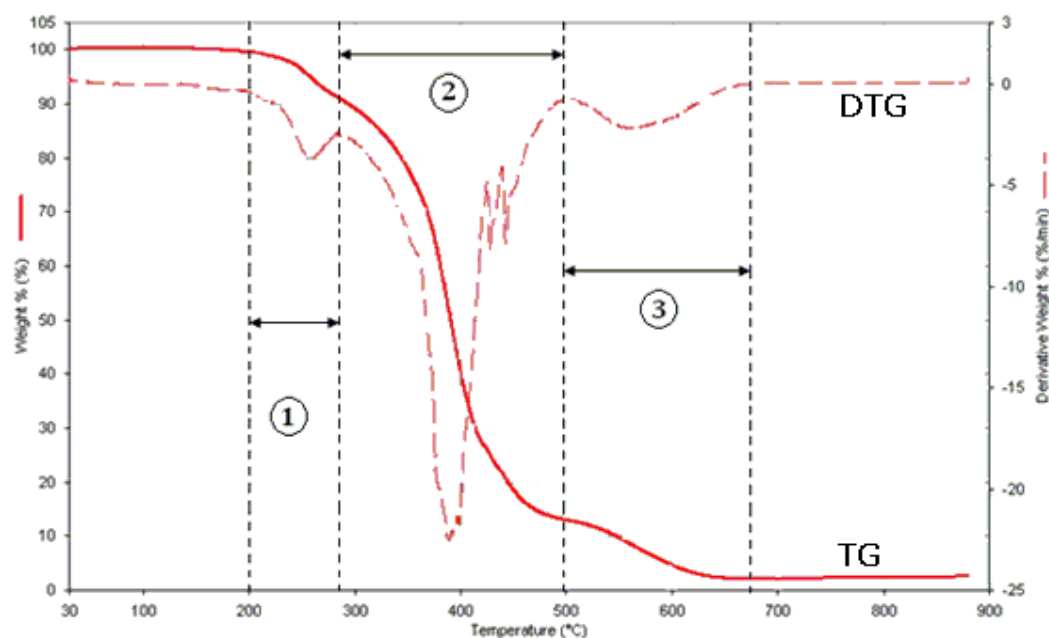


Figure 3.11 TG and DTG curve versus temperature of PUalk65 (1.2)

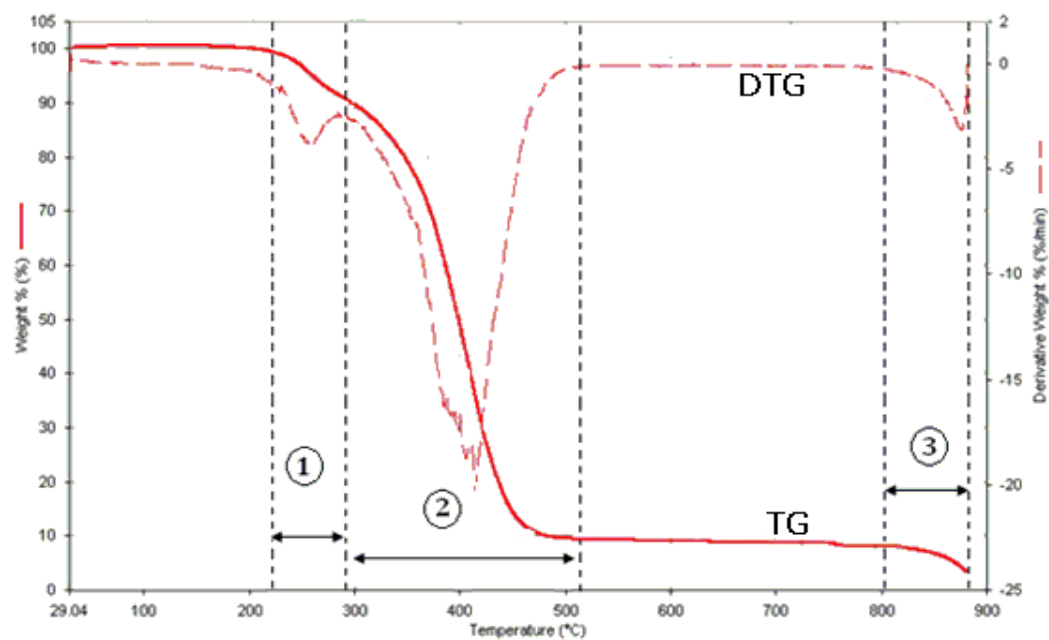


Figure 3.12 TG and DTG curve versus temperature of PUalk65 (1.4)

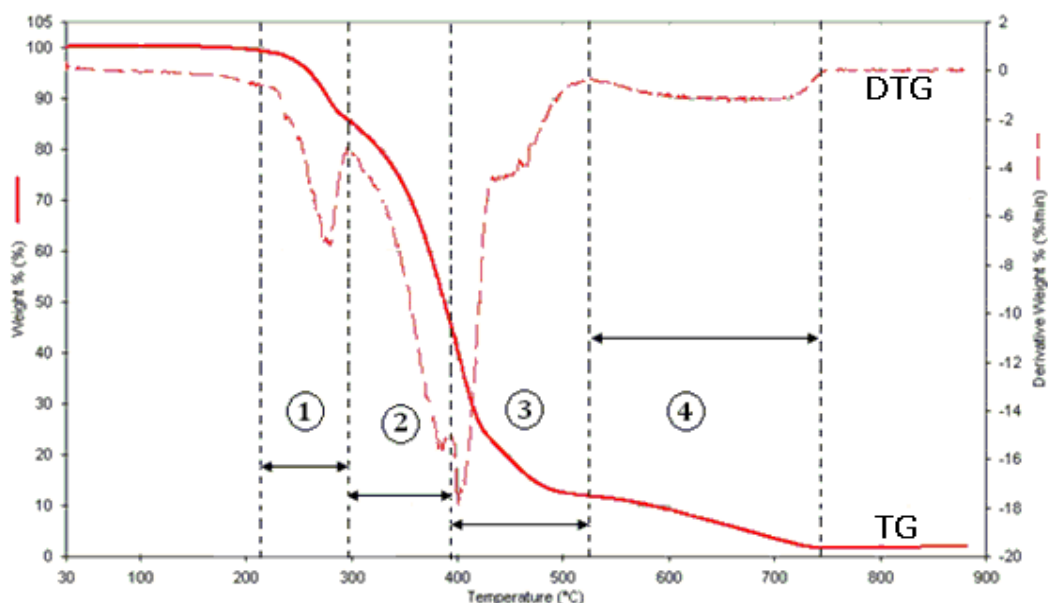


Figure 3.13 TG and DTG curve versus temperature of PUalk65 (1.6)

As for PUalk28, there are five stages of degradation observed. An initial weight loss starts at 160°C to 170°C. At the first step, the polymer remains almost intact and mainly gaseous compound was released. Rapid weight loss starts at approximately 240°C up to 700°C. Primary decomposition of isocyanates in urethane polymer occurs at stage '3' (including the peaks at approximately 360°C) as indicated in Figure 3.5. This is based on the report that the isocyanate decomposition of urethane elastomer showed peaks ranging from 290°C to 370°C by the analyses of DSC thermograms by Long et al., 1976.

Most of DTG curves show a broad peak in the region of 500–700 °C related to degradation of the polymer carbon backbone (A. Fainleiba et al., 2002). It should be mentioned that, due to thermal destruction of the urethane group (near 200 °C) with subsequent recovery of highly reactive NCO groups, the process of cross-linked PUR thermal-oxidative destruction can be accompanied by chemical transformations without degradation (carbodiimide and/or isocyanurate formation).

Table 3.7 Thermal behavior of PUR at nitrogen atmosphere

Sample	Stages	Decomposition Temperature		Weight percentage
		T ₁	T ₂	ΔW
PUalk28 (1.2)	1	170	243	3.31
	2	243	316	16.43
	3	316	375	31.51
	4	376	533	37.17
	5	699	878	10.10
PUalk28 (1.4)	1	172	241	3.33
	2	241	316	16.82
	3	316	372	30.00
	4	372	507	36.42
	5	541	690	9.60
PUalk28 (1.6)	1	178	244	3.17
	2	244	313	17.30
	3	313	364	23.26
	4	365	510	41.49
	5	538	701	10.06
PUalk40 (1.2)	1	171	239	1.89
	2	238	311	13.54
	3	311	375	31.76
	4	375	541	41.37
PUalk40 (1.4)	1	198	244	1.85
	2	245	311	17.44
	3	311	503	16.55
	4	537	698	9.73
PUalk40 (1.6)	1	199	234	1.48
	2	236	310	18.04
	3	311	523	67.11
	4	539	689	9.57
PUalk65 (1.2)	1	201	288	8.95
	2	290	499	77.44
	3	499	677	10.90
PUalk65 (1.4)	1	201	289	9.08
	2	289	514	81.57
	3	801	871	3.11
PUalk65 (1.6)	1	213	298	13.74
	2	301	392	40.86
	3	396	598	37.89
	4	526	749	10.12

At the initial temperature, thermal degradation of PU films increases as the NCO/OH ratio has increased; for instance PUalk28 (1.2) starts to degrade at 170°C, PUalk28 (1.4) at 172°C and PUalk28 (1.6) at 178°C. Similar trend was observed for PUalk40 and PUalk65. When the NCO/OH ratio was increased from 1.2 to 1.6, the decomposition of isocyanates occurs in urea polymer and isocyanate ring structures. It is well established that the isocyanate-based polymers provide their thermostability in the order of isocyanurate > urea > urethane > biuret > allophanate (Fabris 1976, Y Kurimoto et al., 2001). In this investigation the PURs excess isocyanate would lead to formation of urea therefore the thermostability increases as the NCO/OH ratio increased.

As for the effect of oleic acid content in polyols, when the percentage of oleic acid content is increased, the thermostability increases too. For example at NCO/OH ratio of 1.2, PUalk28 starts to degrade at 170°C, PUalk40 at 171°C and PUalk65 at 201°C. As for NCO/OH ratio 1.4, the initial degradation temperature is in the rank of 172, 198 and 201°C for PUalk28, PUalk40 and PUalk65 respectively. The most plausible explanation for this phenomenon could be due to the thermostability of the films corresponded to the decomposition of oleic acid fragment in the films. The increase in the contribution of oleic acid to PUR network formations resulted in higher thermo stability.

In summary, from the TGA results it can be concluded that the degradation of oleic acid polyols based PUR starts from the temperature 170°C. The thermostability of the samples increases in small amount as the NCO/OH ratio increases and also as the oleic acid content in polyols is increased.

3.6 Conclusions

Three different polyester polyols from oleic acid and glycerol were synthesized. These polyols were reacted with toluene diisocyanate by varying the NCO/OH ratios 1.2, 1.4 and 1.6 to form PUR prepolymer. The prepolymers were coated on mild steel panel to form PUR coatings. Nine different PUR samples were prepared in coatings and free film and the characteristics of the samples were analyzed. From the FTIR results of polyols (the appearance of OH groups) and PUR (disappearance of OH groups and appearance of NH bond) it can be concluded that reaction occurs between polyol O-H groups ($3460-3480\text{ cm}^{-1}$) and diisocyanate $\text{N}=\text{C}=\text{O}$ groups (2283 cm^{-1}) forming urethane groups and thus, forming a signal such as N-H bond at 3360 cm^{-1} . From the appearance of OH groups and the disappearance of it one concludes that all hydroxyl groups were consumed in the reaction of polyols and TDI. From the XRD results, the PUR samples in the research are confirmed as an amorphous polymer where cross-linking diminishes the crystallinity structure of the samples. The amorphous nature of the samples was further confirmed by the DSC analysis. The TGA results of the PUR samples indicate that the degradation of the oleic acid polyols based PUR starts from the temperature 170°C . The thermostability of the samples increases in small amount as the NCO/OH ratios and the oleic acid content in polyols are increased.

References

- A. Fainleiba*, N. Kozaka, O. Grigoryevaa, Yu. Nizelskiia, V. Grytsenkoa, P. Pissisb, G. Boiteuxc, 2002. Structure–thermal property relationships for polycyanurate–polyurethane linked interpenetrating polymer networks. *Polymer Degradation and Stability*, **76**, 393–399.
- Cyril Keattch, 1969. An introduction to thermogravimetry. Heyden & Son Ltd, Great Britain, pg1-23.
- DK Chattopadhyay, PSR Prasad, B Sreedhar, KVSJN Raju, 2005. The phase mixing of moisture cured polyurethane-urea during cure. *Progress in Organic Coating*, **54**, 296-304.
- DK Chattopadhyay, B Sreedhar, KVSJN Raju, 2006. The phase mixing studies on moisture cured polyurethane-urea during cure. *Polymer*, **47**, 3814-3825.
- E.N. Doyle, 1971. The development and use of polyurethane products. Mcgraw-hill, pg 2-92.
- Eram Sharmin, S.M. Ashraf, Sharif Ahmad, 2007. Synthesis, characterization, antibacterial and corrosion protective properties of epoxies, epoxy-polyols and epoxy-polyurethane coatings from linseed and *Pongamia glabra* seed oils. *Biological Macromolecules*, **40**, 407-422.
- Fabris HJ., 1976. Thermal and oxidative stability of urethanes. *Advances in Urethane Science and Technology* **4**, 89-111.
- Long, T.S., Pisney, JJ., 1976. Characterization of polyurethane using infrared and thermal analysis. *Plastic Engineering*, **22**, 398-403.
- Marcel Mulder, 1996. Basic principles of membrane technology. Kluwer Academic Publishers (2nd edition), pg 33-35.
- MM Coleman. KH Lee, DJ Skrovanek, PC Painter, 1986. Hydrogen bonding in polymers: Infrared temperature studies of a simple polyurethane. *Macromolecules*, **19**, 2149.
- Newkirk AE, 1960. Thermogravimetric Measurements. *Analytical Chemistry*, **32**(12), 1558–1563.

Rials TG, Glasser WG, 1984. Engineering plastics from lignin. IV. Effects of cross-link density on polyurethane film properties – variation in NCO/OH ratio. *Holzforschung* **38**, 191-199.

S. Ahmad, S.M. Ashraf, A. Hasnat, S. Yadav, A. Jamal, 2001. Studies on urethane-modified alumina-filled polyesteramide anticorrosive coatings cured at ambient temperature. *Journal of Applied Polymer Science*, **82**, 1855-1865.

Szycher Michael, 1999. Szycher's Handbook of Polyurethane. CRC Press LLC. Chapter 2, pg 1-17.

TB Yeow, 2000. Alkyd from crude palm oil. Dissertaion of MSc,UM, pg 106.

TC Patton, 1962. Alkyd Resin Technology: Intersec Publication.

Urška Šebenik, Matjaž Krajnc, 2006. Influence of the soft segment length and content on the synthesis and properties of isocyanate-terminated urethane prepolymers. *International Journal of Adhesion & Adhesives*, Article In Press.

William D. Callister, 2004. Material Science and Engineering, An Introduction. Sixth Ed., John Wiley & Sons, pg 500.

Y Kurimoto, M Takeda, S Doi, Y Tamura, H Ono, 2001. Network structures and thermal properties of polyurethane films prepared from liquefied wood. *Biosource Technology*, **77**, 33-40.

Yoshida H, Morck R, Kringstad KP, Hatakeyama H., 1990. Kraft lignin in polyurethanes. II. Effects of the molecular weight of kraft lignin on the properties of polyurethanes fromkraft lignin-polyether triol-polymeric MDI system. *Journal of Applied Polymer Science*, **40**, 1819-1832.

CHAPTER 4: CHARACTERIZATION OF THE PUR COATING

4.1 Introduction

In many industries, organic and metallic coatings are used to protect engineering systems and structures. The life of these components is frequently determined by the performance of the coating. Tremendous financial losses are incurred every year as a result of premature failure of paints and coatings. Costs of such failures far outweigh the initial costs of painting due to the complexity of repairs and the liability associated with downtime to correct the problems.

It is possible to evaluate the performance of coatings simply by visual inspection, but a more quantitative approach is needed for an objective evaluation. Organizations such as American Standard Testing Method (ASTM), have established standardized methods for testing coatings. Paint and Coating Testing Manual (Gardner-Sward Handbook) is also an excellent reference which provides a wide range of tests methods and summaries of each major class of properties as well as background information and comparisons of the utility of various tests. These references are generally useful in understanding the performance and failure of a coating. Many important properties of paint or coating are difficult to be defined in scientific units. There is no fully reliable testing to assess the application and appearance of coated products although much progress has been made in recent years in introducing instrumentation of paint testing.

The testing of a coating or paint has three main objectives in the paint industries. The first objective is the use as a means of quality control in production; secondly to satisfy the requirement of user specifications and lastly as a tool of research and development.

Selecting a coating system that will perform well over time in a given environment is not always a clear cut decision. The type of substrate, service environment, durability, abrasive resistance, and long term appearance, are all important factors that should be taken into consideration before a coating system is adopted. For example, resistance to indentation and scratching are important in a coating system and therefore poor scratch resistance is definitely a limiting factor for the service life of any polymer or polymer coated product.

Noting the importance of quality testing of a coating system, there are few quality tests that have been performed on the oleic acid PUR coating. This chapter solely indulges in the report and tests that have been conducted on the coatings to assess the characteristic and quality of the films. Initially, the mild steel panel for coating has been prepared and resin is coated onto it. The curing of the coatings are investigated and reported in section 4.2.1. Testing such as adhesion test, pencil hardness tests and chemical resistance test are conducted after two weeks of the application to ensure the coatings are thoroughly dried. The results and analysis of the tests are discussed in the following sections. The summary and conclusion of the results are presented in the last section of the chapter.

4.2 Coating on mild steel panel

The metal and surface characteristics of the metal can have a major effect on adhesion of a coating. Metal surfaces are normally contaminated with oil and such surfaces can have a very low surface tension (Zeno W. Wicks et al., 1999). Surface of the panel should be perfectly cleaned and freed of greases in order to obtain the best results (C.J.

A. Taylor et al., 1965). B.M. Perfetti, 1994, provides a review of metal surface characteristics, cleaning and treatments.

There are many ways to clean the surface of a metal. Sometimes, the metal is wiped with rags wet with solvent. Panel preparation for coating in this research is done according to IS (Indian Standard Methods of Test for Readymade Paints and enamels 1964). Mild steel panels of 7cm x 20cm are used for coating the resin. A clean cotton cloth is soaked into xylene and used for removing oil or grease from the surface of the panel. Then, the surface is abraded and smoothened with emery cloth to remove loose rust scale. The surface is wiped again with a piece of fresh cotton cloth, soaked in xylene until fresh portions of the cloth show no discolouration. The prepared test panels are stored in a desiccator for not more than 24 hours prior to use.

There are number of ways to produce films of uniform and reproducible thickness. The drawdown method that is stated in ASTM D4147-93 has been used. A flat mild steel panel is secured on a firm horizontal surface. A pool of coating is poured across one end of the panel and then the drawdown bar is placed behind the coating. The drawdown bar is rotated to 30 to 60° in the coating to ensure complete wetting of the coating in the threads of the bar. The bar is then drawn uniformly along the length of the panel with a smooth steady motion to apply a uniform film. Films of 50 µm wet film thickness are coated on panels and then left to cure at room temperature. The wet film thickness produced is dependent on the volume shrinkage of the coating. Dry film thickness can be calculated from the wet film thickness and the content of non-volatile percentage.

Various stages and rates of film formation in the drying or curing of organic coatings are determined by using the testing method stated in ASTM D1640-83. In order to determine set-to-touch time, the tested films are lightly touched with the tip of a clean finger and immediately placed against a clean piece of clear glass. Observation is noted if any coating is transferred to the glass. Pressure of the fingertip against the coating is made in such a manner that is no greater than that is required to transfer a spot of the coating, between 3 mm to 5 mm in cross-section. The film is set-to-touch when it is still in a tacky condition, but does not adhere to the finger.

The second testing is carried out to determine dry-to-touch time. The film is considered dry when it no longer adheres to the finger and does not seem rubbed up when the finger is lightly rubbed across the surface. Finally, dry-hard time is determined. The end of thumb resting on the test film with the forefinger supporting the test panel, a maximum downward pressure (without twisting) of the thumb on the film is exerted. The contacted area is lightly polished with a soft cloth. The film is considered dry-hard when any mark left by the thumb is completely removed after the polishing operation. Visual observation of the films and results of the set-to-touch time, dry-to-touch time and dry hard time are tabulated in Table 4.3, section 4.4.2.

After the coating is dried completely, the thickness of the film is measured using thickness gauge (Sheen - Ecotest Plus B FN2, type 121-17-00). Dry film thicknesses of $(30 \pm 5) \mu\text{m}$ are obtained. The cured panels are then subjected to further tests as described in section 4.3 at 30 days of cure under ambient conditions.

4.3 Tests on coatings

There are few types of tests commonly performed on PUR coatings. These include adhesion test, hardness, water immersion, solvent resistance, acid resistance, alkali resistance and salt water resistance tests. For each formulation, six replicates are tested for pencil hardness, crosshatch adhesion, chemical resistant and water resistant. The best results of each test are then reported.

4.3.1 Adhesion test

This test is designed to assess the adherent strength of the cured paint film. The procedure of test is conducted according to ASTM D 3359-93. The panel is placed on a firm base and a criss-cross lattice pattern with eleven cuts in each direction is made with 1 mm spacing. All cuts are approximately 20 mm long. The film is cut through the substrate in one steady motion using sufficient pressure on the cutting tool to have the cutting edge reaching the substrate. After making the required cuts, the film is brushed lightly with a soft camel brush to remove any detached flakes of the coatings.

Two complete laps of pressure-sensitive tape are detached and discarded. A piece of 75 mm in length is removed and the centre of the tape is placed over the grid and smoothened into place with a finger. The tape is rubbed firmly with an eraser to ensure good contact with the film. The tape is removed within (90 ± 30) seconds of application by seizing the free end and rapidly pulling it off at as close to an angle of 180° as possible. The grid area is inspected by visual inspection for removal of coating from the substrate. The adhesion is rated according to the scale illustrated in Figure 4.1 adapted from ASTM D3359-93.

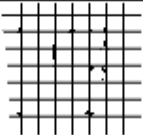



Classification	Surface of cross-cut area from which flaking has occurred
5B	None
4B	
3B	
2B	
1B	
0B	Greater than 65%

Figure 4.1 Classifications of adhesion test results

4.3.2 Pencil hardness test

The hardness of a surface coating can be assessed by the results of this test. The test procedure is done according to ASTM D3363-92a using a Sheen Pencil Hardness Kit with a set of calibrated wood pencils meeting the following scale of hardness.

6B 5B 4B 3B 2B B HB F H 2H 3H 4H 5H 6H
 Softer Harder

The pencil is sharpened to remove approximately 5 mm – 6 mm wood to expose about 3 mm length of pencil lead. The sharpened pencil is rubbed to an abrasive paper at angle of 90° to obtain a flat, smooth and circular cross-section, free of any chips or nicks in the edge of the cross-section. The pencil is moved over the surface using the pencil tester which has been fixed at pressure and angle of 45°. The schematic diagram

of the pencil tester and test conducted is shown in the Figure 4.2. Usually a mid range pencil will be chosen at first for e.g. 2H. The pencil will be inserted into the hole given in the pencil tester until its point touches the flat surface of the panel. Clamping screw is tightened to hold the pencil firmly at a 45° angle.

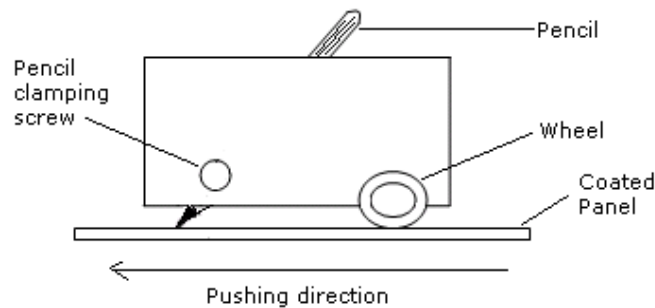


Figure 4.2 Schematic diagram of a sheen pencil hardness tester kit (K.C. Hui, 2005)

The coated panel is placed on a flat level surface with the coated side upward. The pencil tester is placed gently on the panel and pushed forward by 6-12 mm in a steady motion away from the operator. The coating is examined for any indentation or scratching. If there is no scratching or indentation then the test will be repeated with a harder pencil 3H and if there is scratching, then the test is repeated with a softer pencil e.g. H. The process is repeated until a pair of pencils with one which indents the coating and the other which does not indent the coating, is obtained. The testing is repeated for at least two times for each panel. A newly sharpened pencil lead is used for each test.

4.3.3 Water immersion testing

Immersion in water can degrade the coatings. Knowledge on how coating resists water immersion is very helpful in predicting its service life. Failure in a water immersion test

may be caused by a number of factors including a deficiency in the coating itself, contamination of the substrate or inadequate surface preparation (^bC.J. A. Taylor et al., 1966). The method of water immersion test that has been used is according to ASTM D 1647-89. The purpose of this test is to ascertain the behaviour of a film when the water is present for prolonged periods. The testing should be done at the temperature which may be encountered by the coating in its service life but in the absence of special condition (ex. specified temperature by the end user for certain application); the test in this study is carried out at room temperature (^aC.J.A. Taylor et al., 1965).

A beaker containing distilled water 2.5 inches in height is prepared. The cured panels are immersed in the water at room temperature for 18 hours. After 18 hours, the panels are taken off and allowed to dry thoroughly. The results are stated in a scale as shown in the Table 4.1.

Table 4.1 Classification of water immersion test results

Classification	Descriptions
1	Not visibly affected
2	Whitening disappears within 20 minutes
3	Whitening appears in 20 minutes but disappears within 2 hours
4	Whitening appears in 2 hours but disappears within 4 hours

4.3.4 Acid resistance testing

Acid resistance testing is done according to procedure described by K.P Somani et al., 2003. Solution of acid hydrochloric 0.1M (HCl) is prepared in a beaker and is heated up to 80°C. The coated panels are then placed with the edge of about 5cm on the

bottom of the beaker and the top of the panel resting against the side. A separate beaker is used for each test panel. The coated panels are immersed in the solution for about an hour. Throughout the testing period, the temperature is maintained at 80°C. At the end of the specified time, the panel is removed from the solution. The panel is then dried at room temperature for 24 hours before examination for deterioration is performed.

4.3.5 Alkali resistance testing

This alkali resistance testing procedure is also conducted as stated in K.P Somani et al., 2003. Solution of Sodium Hydroxide 0.1M (NaOH) is prepared in a beaker and is heated up to 80°C. The coated panels are placed with the edge about 5cm on the bottom of the beaker and the top of the panel resting against the side. Panels are tested in separate beakers. The panels are immersed in the solution for about an hour at a constant temperature; 80°C. At the end of the specified time, the panel is removed from the solution and is dried at room temperature for about 24 hours before examination for any deterioration is performed.

4.3.6 Salt water resistance testing

The resistance of coatings to marine conditions can be assessed by salt water immersion test. The testing method for salt water immersion test is adapted from K.P Somani et al., 2003. A solution of 5% sodium chloride is prepared in a beaker and is heated up to 80°C. The coated panels are then placed with the edge about 5cm on the bottom of the beaker and the top of the panel resting against the side. A separate beaker is used for each test panel. The coated panels are immersed in the solution for about an hour. Throughout the testing period, the temperature is maintained at 80°C. At the end

of the specified time, the panel is removed from the solution and examined for deterioration. The classification of test results on acid, alkali and salt water resistance testing is stated in Table 4.2.

Table 4.2 Classification of acid, alkali and salt water resistance test results

Classification	Descriptions
1	No effects
2	Whitening of films
3	Shrinkage of films
4	Wrinkles at several spots
5	Removal of films

4.3.7 Solvent resistance test (solvent rubs)

Polyurethane coating chemically changes during the curing process and becomes more resistant to solvents as they cure. Rubbing with a cloth saturated with appropriate solvent is one way to determine when a specific level of solvent resistance is reached. However, the time required to reach a specific level of solvent resistance can be influenced by temperature, film thickness, air movement and humidity (ASTM D5402-93).

The solvent resistance testing is done according to ASTM D5402-93. An area of 150mm long on the coated surface is selected for the test. The surface area is then cleaned with tap water to remove any loose material and is allowed to dry. The dry-film

thickness of the coating in the selected area is measured. On the undamaged cleaned surface area of the coated panel, a rectangular test area of 150mm x 25mm is marked using a pencil. A cotton cloth is folded into a pad of double thickness and soaked into a specified solvent. A protected index finger is placed into the center of the pad at an angle of 45° to the test surface while holding excess cloth with the thumb and remaining fingers of the same hand. The rectangular test area is rubbed with moderate speed in forward and backward motion. One forward and backward motion is considered as one double rub. Each double rub should be completed at the rate of approximately 1/s. The test area is continuously rubbed for a total of 25 double rubs in the rectangular test area. The area is immediately inspected for any visual changes in appearance and fingernail hardness comparing the rubbed area with an adjacent unrubbed area. The film thickness of the rubbed area is measured and noted. The cloth is visually examined for any indication of coating removal.

4.4 Results

Polyol constitutes a major component in polyurethane and plays a very important role in the finishing of a coating. On the other hand, NCO/OH ratio will have effect on cross- linking of the film. As mentioned before, three types of polyols are used in synthesizing the polyurethane namely Alk28, Alk40 and Alk65. These polyols differ by the oleic acid content of the materials where Alk28 has the lowest oleic acid content (28%), Alk40 has 40% oleic acid content and finally Alk65 has the highest oleic acid content (65%). The NCO/OH ratio and the oleic acid content of polyols are varied, and the influence of these two factors on coating characteristic is studied. It is expected that these factors give significant change either in appearance or performance of the

finishing of coatings. The results of the properties tested are discussed in the next sections.

4.4.1 Coatings appearance

Generally the best overall visual appearance of the clear coat films is obtained with oleic acid based PUR. Each film has a very good appearance in term of clarity and glossiness. However, a slight tinge of yellowness is detected in PUalk40 samples. The yellowness of the coating is very obvious for PUalk65 compared to that of PUalk40. As the NCO/OH ratio is increased, the yellowness of the coatings seems to remain the same. The results indicate that as the oleic acid content of the alkyd increases the coating turned yellow. However, excess NCO would cause further yellowing of the sample if exposed to the sun. TDI is an aromatic isocyanate which is very unstable under the sun. The yellowing could be masked by using pigments in the formulation of the coating.

4.4.2 Curing time

Set-to-touch, dry-to-touch and dry-hard time for the specified samples are summarized in Table 4.3. Time in seconds were measured by using stopwatch with an error of ± 0.1 s. Coatings based on formulation of polyester Alk28 achieved the shortest time curing, followed by Alk40 and Alk65. From the table, it is noticed that changes in set-to-touch, dry-to-touch and dry-hard time of coatings are very much dependent upon NCO/OH ratios and the polyols oleic acid content.

Set-to-touch, dry-to-touch and dry-hard time cure time decreases overall as the NCO/OH ratio increases for all the three PUR. For example, the dry hard time for NCO/OH ratio from 1.2 to 1.6 for the PUR coatings PUalk28, PUalk40 and PUalk65, decreases about 20%, 37% and 75% respectively. However, as the oleic acid content of the polyester increases, the time of air drying of the films increases as well. This relationship is shown clearly in the Figure 4.3 in log time scale.

Table 4.3 Set-to-touch, dry-to-touch and dry-hard time observed for the oleic acid based polyols PUR coatings.

Sample	NCO/OH	Set-to-touch time	Dry-to-touch time	Dry-hard time
PUalk28	1.2	12.0 s	30.0 s	35.0 s
	1.4	10.0 s	28.0 s	32.0 s
	1.6	6.0 s	25.0 s	28.0 s
PUalk40	1.2	40.0 s	129.0 s	215.0 s
	1.4	33.0 s	109.0 s	181.0 s
	1.6	25.0 s	83.0 s	135.0 s
PUalk65	1.2	144 hrs	168 hrs	192 hrs
	1.4	24 hrs	36hrs	48 hrs
	1.6	22 hrs	35hrs	45 hrs

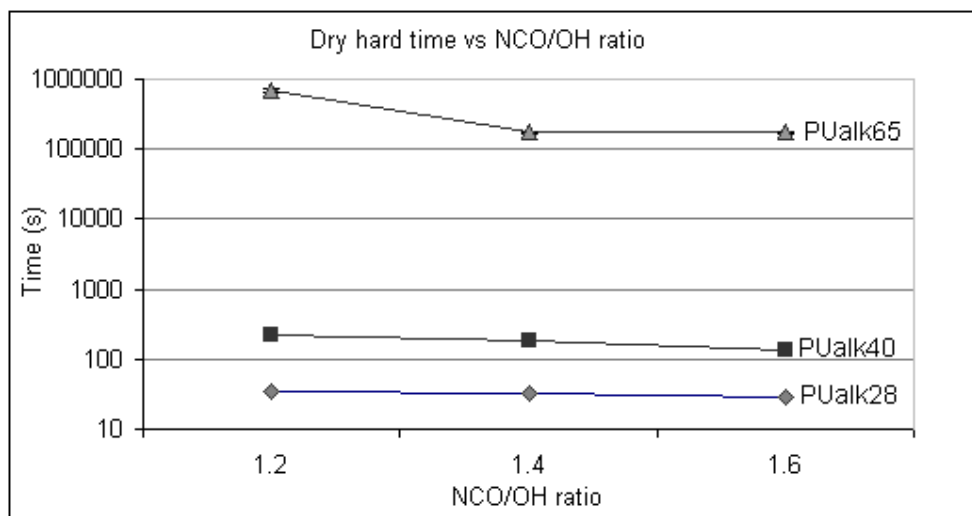


Figure 4.3 The relationship between dry hard time in log scale and NCO/OH ratios for PUalk28, PUalk40 and PUalk65.

4.4.3 Adhesion measurement by tape test

Table 4.4 shows the adhesion measurement results for the clear coat onto the metal substrate at ambient temperature. Excellent adhesion performance is denoted by 5B while a very poor performance with more than 65% detachment is denoted by 0B. Generally, a value of 3B and higher would be considered good and acceptable. PUR coatings from oleic acid polyester polyol have achieved an excellent adhesion performance on mild steel panel.

4.4.4 Pencil hardness

Table 4.4 also summarizes the results of pencil hardness test on the clear PUR coatings. Generally, the hardness of the film is increased as the oleic acid content of polyester polyol decreases. For specific composition such as PUalk28 and PUalk40, the pencil hardness increases with the NCO/OH ratios. However, exception occurs for PUalk65 where the NCO/OH ratio does not contribute much on the hardness of the coating.

Hence, from the results it can be concluded that PUalk28 (1.6) has the best hardness followed by PUalk40 (1.6) and PUalk65.

4.4.5 Water resistance

The results of water resistance of the films are tabulated in Table 4.4. PUalk28 films are unaffected by immersion in water for 18 hours. As for PUalk40 and PUalk65, water immersion caused whitening of films but the whiteness disappear in 4 hours. However, as the ratio of NCO/OH increases to 1.6, the water resistance of the films improves.

Table 4.4 Results of pencil hardness, adhesion and water immersion testing

Sample	NCO/OH ratio	Pencil Hardness	Tape Test	Water resistance
PUalk28	1.2	2H	5B	1
	1.4	3H	5B	1
	1.6	4H	5B	1
PUalk40	1.2	B	5B	4
	1.4	HB	5B	4
	1.6	2H	5B	1
PUalk65	1.2	2B	5B	4
	1.4	2B	5B	4
	1.6	2B	5B	1

4.4.6 Acid, alkali and salt resistance

The next result to be discussed is the effect of acid, alkali and salt on the coatings. Table 4.5 below shows the effect of PUR coatings on the abovementioned material. The coatings are immersed in acid (0.1M HCl) and alkali (0.1M NaOH) and salt water (NaCl). As for the acid solution, the results indicate that PUR coatings have a good overall resistance to acid. In detail, all three PUalk28 have the best resistant to acid compared to PUalk40 and PUalk65. However, the acid solution had the worst negative effect on PUalk65. For example, wrinkles occurred for PUalk65 (1.2) and (1.4) coatings. The acid solution has no effect on PUalk65 with the NCO/OH ratio 1.6.

As for the alkali solutions, the films deteriorate to some extent where the results still depends on the polyester and NCO/OH ratios. PUalk28 has the highest deterioration rate where the film is removed from the panel. Wrinkles occurred after the films of PUalk28 (1.4) and (1.6) are immersed in the alkali solution. Overall, PUalk40 shows the best alkali resistance followed by PUalk65 and PUalk28. NCO/OH ratios also determine the alkali resistance of the film, where as the ratio increases from 1.2 to 1.6 the resistance of the film to alkali increased to a certain extent.

On perusal of Table 4.5, it has been found that salt water immersion caused wrinkles at several spots for most of the film. The resistance of the films to salt water for PUalk28 and PUalk40 are improved when the NCO/OH ratio is increased. However, for PUalk65, even at NCO/OH ratio 1.6 has shown no improvement in deterioration effect on the film.

Table 4.5 The PUR coatings resistance to NaCl 5%, 0.1M HCl and 0.1M NaOH

Sample	NCO/OH	NaCl 5%	0.1M HCl	0.1M NaOH
PUalk28	1.2	4	1	5
	1.4	4	1	4
	1.6	1	1	4
PUalk40	1.2	4	2	2
	1.4	1	1	2
	1.6	1	1	2
PUalk65	1.2	4	4	5
	1.4	4	4	2
	1.6	4	1	1

4.4.7 Solvent rub test

The results from solvent rub test are tabulated in Table 4.6. On perusal of Table 4.6, it is observed that PUalk28 thin films have better solvent resistance compared to the rest of PUR films. PUalk65 thin films have the worst effect where film removal occurs when rubbed with all the solvents. It is also noticed that the films lost their glossiness after the test. As the NCO/OH ratio increases, the resistance of the films to solvent improved; however, there is still a slight removal of films. As for PUalk40, a slight removal of films occurs when they are rubbed with solvents, such as methyl ethyl ketone and ethyl acetate. However, the films have better resistance to acetone. Hence, generally, it can be concluded that PUR films synthesized from oleic acid have better solvent resistance as the oleic acid content of polyol decreases and the NCO/OH ratio increases.

Table 4.6 Result of solvent resistance test on PUR coatings

Sample	NCO/OH	Acetone	Methyl ethyl ketone	Ethyl acetate
PUalk28	1.2	Passed 25 rubs	Passed 25 rubs	Passed 25 rubs
	1.4	Passed 25 rubs	Passed 25 rubs	Passed 25 rubs
	1.6	Passed 25 rubs	Passed 25 rubs	Passed 25 rubs
PUalk40	1.2	Passed 25 rubs	Slight removal of films, loss of gloss	Slight removal of films, loss of gloss
	1.4	Passed 25 rubs	Slight removal of films, loss of gloss	Slight removal of films, loss of gloss
	1.6	Passed 25 rubs	Slight removal of films, loss of gloss	Slight removal of films, loss of gloss
PUalk65	1.2	Removal of films, loss of gloss	Removal of films, loss of gloss	Removal of films, loss of gloss
	1.4	Removal of films, loss of gloss	Removal of films, loss of gloss	Removal of films, loss of gloss
	1.6	Removal of films, loss of gloss	Removal of films, loss of gloss	Removal of films, loss of gloss

4.5 Discussion

The polyols were synthesized by fatty acid procedure. Generally, polyols cooked from this method are said to be more viscous with lighter colour than those cooked by conventional method (T.C Patton, 1962). The chemical reaction schemes of the polyols and polyurethanes were presented in Schemes 3.1 and 3.2, Chapter 3. The properties of the polyols differ depending on synthesis procedure. Goldsmith AH., 1948 explained that the difference was due to the differential reactions between - OH and - COOH groups, depending on their location on the parent molecules. In fatty acid preparation method, all groups are added at the beginning such that there is a competition among the -COOH groups from phthalic anhydride and the fatty acids used. The reaction may be random in real situation and the structure might differ because of many factors.

The hydroxyl values for the polyols are 140.99, 140.39 and 140.09 for Alk28, Alk40 and Alk65 respectively. The greater the excess of hydroxyl content, the greater the

number of available sites for cross-linking and subsequent cures. The number of hydroxyl groups in the polyols, their distribution in the fatty acid and the position in fatty acid chain (in the middle or closer to the end of the chain) affect the network properties on the cross-linking density of PUR (Alisa Z. et al., 2004).

Phthalic anhydride, oleic acid and glycerol are used for synthesis of the polyols. Generally, the synthesis of polyester with phthalic anhydride and glycerol gives a very clear end product. However as oleic acid is included, the end product, polyols has a tinge of yellowness due to the nature of palm oil itself. The yellowness of PUalk65 PUR films is higher than the rest of the thin films due to higher percentage of fatty acid in the formulation of the highest oleic acid content polyols.

According to Alisa Z. et al., 2004, every oil or fat has a fatty acid characteristic profile which is unique to the type of oil. Variability in composition is expected even in the same type of oil, depending on the local weather condition, soil and plant characteristics. The principle variation in fatty acids composition of the oils results in a variation of chain length and also the degree of unsaturation. Consequently, there is a variation in the length of elastically active network chains and dangling chains in polyurethane network. Dangling chain acts as plasticizer in a polymer structure which are elastically inactive and do not support stress when the sample is under load. Dangling chains result from saturated fatty acids.

Oleic acid is unsaturated fatty acid and the reactive sites in oleic acid located on 9th or 10th carbon. The formula of the oleic acid is $\text{CH}_3(\text{CH}_2)_7\text{CH}=\text{CH}(\text{CH}_2)_7\text{COOH}$. The double bond of this acid is non-conjugated. The drying mechanism of non-conjugated oil is believed to involve the reaction with oxygen (or free radicals) without loss of

unsaturation. Oxygen does attack the double bonds, but the hydroperoxide formations and rearrangement of the bonds occur simultaneously, resulting in no loss of unsaturation (Turner GPA., 1967). Iodine values serve as a measure of the double bond content in fatty acid. To a great extent, the performance of polyol is affected by oleic acid content. Oleic acid content determines the properties of polyester with resin like properties (the lowest oleic acid content) dominating at one extreme and oil like properties (the highest oleic acid content) dominating the other end. Optimum durability is considered to occur at near 50% oil modification with even weight mixture of resin-like and oil-like properties (T.C Patton, 1962).

Alk28 has resin-like properties and Alk65 has oil-like properties. It is expected that as the oleic acid content of an alkyd decreases, the colour retention and the gloss retention increase, and vice versa. This factor can be obviously seen in the reported results where PUalk28 with polyester of lower oleic acid content produces films with the best appearance compared to PUalk65 with the highest oleic acid content.

PUR formation in the research using the polyol with the lowest, intermediate and the highest oleic acid content consist of reaction between isocyanates from TDI and hydroxyl from polyol. The polyol having lower oleic acid content cures rapidly and in contrast with the polyols with the highest oleic acid content, take a longer time to cure. Polyols with increasing oleic acid content have more side chains in the PUR system. More oleic acid side chains introduce greater amount of stearic hindrance for the isocyanates to react with OH hence slowing down the rate of reaction.

The PUR coating was cured by chemical reactions of -NCO group with -OH group as represented in Scheme 3.2 chapter 3. The first stage of curing occurs by solvent

evaporation (physical process). The extremely thin coats (30 μm) on the steel panel allow the toluene to evaporate off fairly quickly. It is suggested that there are two functionalities which participate in the curing reactions of PUR films, free -NCO and unsaturation of fatty triester chains. The free -NCO groups of PUR prepolymers react with moisture in the air leading to surface drying of coated panels. The mechanism involves reaction of free -NCO groups with moisture to form an amino group through primary addition reaction (Eram Sharmin et al., 2007, ^aS Ahmad et al., 2001). The amino group reacts rapidly with an -NCO group present in another molecule and most of them get consumed in this process. Thus, the two molecules are cross-linked together.

From the results reported, the drying time of the films reduces as the NCO/OH ratio increases for all the films. Excess of diisocyanate (NCO/OH ratio > 1) introduce allophanate or biuret bond between polymer chains. It may cause chain branching and chemical cross-linking. When multifunctional components of polyol or diisocyanate are used, highly developed cross-linking can be obtained (^bS Ahmad et al., 2002). It has been found that upon increasing the loading of TDI in the polymer, the drying time decreases. The cross-linking continues to increase with increased loading of TDI which reduces the time required for drying the films.

Generally, all the PUR films from palm oil in this research have adhered well on mild steel panel. Adhesion of films to substrate is dependent on cross-linking density of the polymeric chain. Excess NCO presence in the formulation of the coatings and it apparently remains well distributed within PUR to give a cross-linked network having good adhesion strength (S.D. Desai et al, 2003). By increasing the TDI amount in the formulation of PUR provides additional isocyanate moieties which causes extra cross-

linking sites. Therefore, the number of polar urethane linkages per unit chain increases which in turn increases the cross-link density as well as adhesion of the film to the substrate.

The pencil hardness also increases upon increasing the concentration of TDI. The scratch hardness of polymer mainly depends upon the cross-linking density. On increasing the amount of TDI, reactive sites for cross-linking increase causing an increase in the scratch hardness. Above certain percentage in the addition of TDI, considerable cross-linking occurs between PUR chains which results into their stiffening (Oprea S et al., 2000). Increase of intermolecular interactions and cross-linking efficiency with higher chain extender content and increase in intermolecular entanglement with more oil content having long pendent alkyl group (H. Yeganeh et al., 2004) reduces slipping of chains. The pencil hardness increases with the increase in isocyanate due to the presence of rigid aromatic moiety in the polymer chain. Polyols are block copolymers. Polyol of low glass transition temperature forms soft segment, while diisocyanate comprise hard segment. The hard segments give the mechanical strength to the PUR, whereas soft block domain formed from soft segments gives high extensibility and resiliency (H.C. Jung et al., 2000).

The cured polyurethanes from polyester are vulnerable to water, especially hot water in where they hydrolyze readily during prolonged immersion (MYL. Chew, 2003). However, in this case PUR films from Alk28 have better water resistance compared to the rest. So from the results it can be assumed that PUalk40 and PUalk65 hydrolyze readily as immersed in the water but the hydrolyzation can be improved as the NCO/OH ratios of the formulation are increased.

Acid decreases coating performance to some extent and alkali has the most detrimental effect on coating performance. PUR based on highly cross-linked polyester polyol has better chemical resistance than PUR with less cross-linked structure. Acid shows very high deterioration on PUalk65 compared to the rest of the films. But as the percentage of isocyanate increases, it enhances the physico-mechanical and anticorrosive properties of the polymer films. This phenomenon occurs probably because polyols with the highest oleic acid content is easily detached in the presence of acid.

As for alkali resistance, the film with lower NCO/OH ratio is generally strongly affected when immersed in alkali solution when the films were removed from the steel panel. As the NCO/OH ratio increases, the sample becomes more resistant to alkali solution. Generally, the polymer chains are protected against acid and base and other chemicals by the urethane groups in the PUR coatings. Urethane groups are resistant to chemical especially to hydrolysis due to existence of high density of hydrogen bonding which form a stable physical network (Martin MC., 2000).

Salt resistance of palm oil PUR coating is very poor compared to acid and alkali resistance. Wrinkles occur at several spots on the films after immersion of panels in the salt solution. It can be therefore concluded that salt also has deteriorating effect on oleic acid-based polyol PUR films to a certain extent.

As for solvent resistance, PUalk28 performs satisfactorily under solvent rub test for acetone, methyl ethyl ketone and ethyl acetate. PUalk28 seems to be unaffected under 25 rubs of solvents. However, for PUalk40, deterioration is slightly observed. PUalk65 deteriorates the worst in solvents. Loss of glossiness and removal of films are also observed. Polyol with higher percentage of oil generally performs less satisfactorily on

the resistant to solvent test compared to lower oleic acid content polyol. This is presumably due to the higher amount of flexible side chain rendering the film less compact.

4.6 Conclusion

The studies on physico-mechanical and chemical resistance of oleic acid based polyol PUR coatings reveal many interesting properties of the films. Generally, the physico-mechanical and chemical resistance of the coatings improve with the increase in TDI content. These studies also reveal that scratch hardness, adhesion properties are inter-dependent. Factors that govern the physico-mechanical properties of the coatings are also directly determined their chemical resistance behaviour. The properties of the coatings are largely determined by the oleic acid composition of the starting material.

PUalk28 exhibits far superior coating properties followed by PUalk40 and finally PUalk65. Another factor contributing to the superior coating properties is the loading percentage of TDI content in the formulation. However, when higher percentage of TDI in the formulation is used, brittle end product due to the excess cross-linking density is produced.

References

Alisa Zlatanovic, Charlene Lava, Wei Zhang, Zoran S. Petrovic, 2004. Effect of structure on properties of polyols and polyurethanes based on different vegetable oils. *Journal of Polymer Science: Part B: Polymer Physics*, **42**, 809-819.

Annual Book of ASTM Standards, 1993. Standard Practice for Assessing the Solvent Resistance of Organic Coatings Using Solvent Rubs. D5402-93, pg 547.

Annual Book of ASTM Standards, 1993. Standard Practice for Applying Coil Coatings Using the Wire-Wound Drawdown Bar. D 4147-93, pg 256.

Annual Book of ASTM Standards, 1993. Standard Test Methods for Film Hardness by Pencil Test. D 3363-92a, pg 442.

Annual Book of ASTM Standards, 1993. Standard Test Methods for Measuring Adhesion by Tape Test. D 3359-93, pg 433.

B.M. Perfetti, 1994. Metal Surface Characteristics Affecting Organic Coatings. Federation of Societies for Coatings Technology, Blue Bell, PA.

^aC.J. A. Taylor and S. Marks, 1965. Testing of Paints, part five, Chapman & Hall; London, pg101.

^bC.J. A. Taylor and S. Marks, 1966. Convertible Coatings, part three, Chapman & Hall; London, pg164.

Eram Sharmin, S.M. Ashraf, Sharif Ahmad, 2007. Synthesis, characterization, antibacterial and corrosion protective properties of epoxies, epoxy-polyols and epoxy-polyurethane coatings from linseed and *Pongamia glabra* seed oils. *Biological Macromolecules*, **40**, 407-422.

Goldsmith, A.H., 1948. Alpha- and beta hydroxyls of glycerol in preparation of alkyd resins. *Industrial Engineering Chemistry*, **40**, 1205.

H. Yeganeh, M.R. Mehdizadeh, 2004. Synthesis and properties of isocyanate curable millable polyurethane elastomers based on castor oil as a renewable resource polyol. *European Polymer Journal*, **40(6)**, 1233-1238.

H.C. Jung, SJ Kang, WN Kim, YB Lee, KH Choe, SH Hong, SB Kim, 2000. Properties of cross-linked polyurethanes synthesized from 4,4'-Diphenylmethane

diisocyanate and polyester polyol. *Journal of Applied Polymer Science*, **78**, 624-630.

K.P. Somani, Sujata S. Kansara, Natvar K.Patel, Animesh K. Rakshit, 2003. Castor oil based polyurethane adhesives for wood-to-wood bonding. *International Journal of Adhesion & Adhesives*, **23**, 269-275.

M.Y.L Chew, 2003. The effects of some chemical components of polyurethane sealants on their resistance against hot water. *Building and Environment*, **38**, 1381-1384.

Martin Mel Chiors, Micheal Sonntag, Claus Kobusch, Eberhard Jurgens, 2000. Recent development in a queous two component PUR (2K) coatings. *Progress in Organic Coating*, **40**, 99-109.

Oprea S, Stelian Vlad, Stanciu A, Macoveanu M, 2000. Epoxy urethane acrylate. *European Polymer Journal*, **36**, 373-378.

^aS. Ahmad, S.M. Ashraf, A. Hasnat, S. Yadav, A. Jamal, 2001. Studies on urethane-modified alumina-filled polyesteramide anticorrosive coatings cured at ambient temperature. *Journal of Applied Polymer Science*, **82**, 1855-1865.

^bS. Ahmad, S.M. Ashraf, E. Sharmin, F. Zafar and Abdul Hasnat, 2002. Studies on ambient cured polyurethane modified epoxy coatings synthesized from sustainable resource. *Progress in Crystal Growth and Characterization of Materials*, 83-88.

S.D. Desai, Jigar V.P, Vijay K.S., 2003. Polyurethane adhesive system from biomaterial-based polyol for bonding wood. *International Journal of Adhesion & Adhesives*, **23**, 393-399.

Standard Practice for Testing Water Resistance of Coatings Using Water, Annual Book of ASTM Standards, Vol 06.01, D 1647-89, pg 133.

T.C Patton, 1962. Alkyd resin technology. Interscience Publishers, pg 21,177.

Turner G.P.A, 1967. Introduction to paint chemistry. *Science Paperbacks*.

Zeno W. Wicks, JR., Frank N. Jones, S. Peter Pappas, 1999. Organic Coatings, Science and Technology. 2nd Edition, Wiley-Interscience, pg 113.

5.1 Introduction

This chapter describes the experimental techniques and associated theories involved in measuring the electrical properties of PUR coatings prepared in thick films. Two types of conductivity measurement were performed which involved alternative current, ac and direct current, dc. The purpose of performing the ac and dc conductivity measurement for PUR is to determine the nature of conduction mechanism involved in PUR and also to investigate the alternating current response as a function of the frequency of the applied field to obtain the complimentary information regarding the dielectric behaviour of the material.

Dielectric spectroscopy technique is used to characterize the dielectric characteristic of PUR. Dielectric spectroscopy or often called impedance spectroscopy measures the dielectric properties of a medium as a function of frequency. The frequency range is from 100Hz to 40MHz at room temperature. The dielectric polarization theory and relaxation phenomena related to PUR are also discussed.

This chapter also indulges in electrical conductivity of PUR which is determined by the dc conductivity measurement at temperature ranging from 28 to 108°C. Electrical conduction may occur through the movement of either electrons or ions. The possible electrical conduction mechanisms in PUR, the relation with activation energy and glass transition temperature of the material are also discussed. The possible conduction mechanism, which is related to PUR sample, is determined and discussed in detail.

5.2 AC conductivity studies

5.2.1 Theory

(1) Dielectric Characterization

Dielectric spectroscopy technique is used to characterize the dielectric characteristic of a dielectric material. Dielectric spectroscopy is sensitive to dipolar species and localised charges in material and it determines their strength, kinetics and interactions. The advantage of this technique is that it is non-invasive and can be used to follow the dynamics of paint film drying without inhibiting the drying process of the films (Dissado et al., 1989). The dielectric properties measured through this technique are normally described by dielectric permittivity (real permittivity) ϵ' , loss factor (imaginary permittivity) ϵ'' and dielectric breakdown strength. Permittivity describes the interaction of a material with an electric field. Permittivity is caused by the polarization of dielectric materials. Polarization is the alignment of permanent or induced atomic or molecular dipole moments with an externally applied electric field. If the field applied is time dependent, polarization will also be time dependent. There are three types of polarization; electronic, ionic and orientation. Dielectric materials ordinarily exhibit at least one of these types of polarization depending on the material and on the manner of the external field applied.

The real permittivity value, ϵ' can be calculated from the equation 5.1

$$\epsilon' = \frac{Cd}{\epsilon_0 A} \quad (5.1)$$

The parameters C , ϵ_0 , A , and d are the capacitance (F) of the dielectric (dependent on the nature of the material and dimension of the electrodes), absolute permittivity of free space ($8.85 \times 10^{-12} \text{ Fm}^{-1}$), the area of electrode (m^2) and the thickness of the sample (m)

respectively. From equation 5.1, the real permittivity of the material can be calculated at each frequency.

Resistance to motions of atoms in the dielectric material causes a delay between changes in the field and polarization and this delay often stated as a phase shift or loss angle δ . Dielectric loss tangent ($\tan \delta$) or dissipation factor D is the imaginary part of dielectric constant which determines the loss factor of the medium. Equation 5.2 relates the real permittivity with the dielectric loss tangent of the dielectrics.

$$D = \tan \delta = \frac{\epsilon''}{\epsilon'} \quad (5.2)$$

where ϵ'' is the loss factor or imaginary permittivity of the dielectric material.

Dielectric relaxation is the result of a movement of dipoles or electric charges due to a changing electric field in the frequency range of 10^2 - 10^{10} Hz. This mechanism is a relatively slow process when compared with electronic transitions or molecular vibrations which have frequencies above 10^{12} Hz. Maximum polarization, corresponding to the highest observable dielectric constant is realized in a material when sufficient time is allowed for the orientation to attain equilibrium, after the application of an electric field. If sufficient time is allowed, then the observed dielectric constant is the static dielectric constant, ϵ_s . If the polarization is measured immediately after the field is applied, not allowing time for dipole orientation, then the instantaneous dielectric constant, ϵ_∞ is observed. The relaxation time occurs somewhere in between these two extremes. The relaxation time for this energy-absorbing process is $T = \frac{1}{2\pi f_{max}}$, where f_{max} is frequency corresponding to the maximum dielectric losses.

Polarization of dielectric materials may be categorized as electronic, orientational, displacement and interfacial.

- **Electronic Polarization**

Electronic polarization occurs in neutral atoms when an electric field displaces the nucleus with respect to the electrons that surround it. The displacement resulting from this polarization is quite small because the applied field is usually very weak compared with the intra-atomic field caused by the nucleus.

- **Orientation Polarization**

In molecular dielectrics, bound charges (electrons, ions) can also form permanent dipoles. The molecular dipoles can only be rotated by an electric field. Without an external electric field, their dipole moments are randomly oriented. However, in an external electric field, these dipoles tend to be aligned to give a net polarization in the field direction. This process is called orientation polarization.

- **Displacement Polarization (Atomic or Ionic Polarization)**

Arrangement of atomic nuclei in a polymer molecule may be distorted by an electric field and this phenomenon is called displacement polarization. Displacement polarization occurs at lower frequency compared to electronic polarization due to movement of heavy nuclei which is more sluggish than that of electron movement.

- **Interfacial Polarization**

Electronic, displacement and orientation polarization are all caused by charges that are locally bound in atoms, molecules on the structure or liquid. In addition, charge carrier usually exists and may migrate for some distance through the dielectric. However,

when the charge carriers are impeded in their motion, either because they are trapped in the material or at interface or because they cannot be freely discharged or replaced at the electrode, this results in space charges and macroscopic field distortions. Such distortion appears to increase the capacitance of the sample and may be indistinguishable from real rise of the dielectric permittivity. Normally, this mechanism of polarization occurs at a boundary or interface; hence, it is called interfacial polarization.

In the dielectric spectroscopic technique, AC electrical signal is applied to the sample and the real and imaginary components of the complex response are observed as the function of AC frequency. The response may be presented in terms of impedance $Z(\omega)$, capacitance $C(\omega)$, admittance $Y(\omega)$ or modulus $M(\omega)$ which is interrelated to each other by Equation 5.3.

$$Z(\omega) = \frac{1}{Y(\omega)} = \frac{1}{i\omega C(\omega)} = \frac{M(\omega)}{i\omega} \quad (5.3)$$

where ω is the frequency in radians or equal to $2\pi f$ with f the frequency in Hz.

Most dielectric measuring equipment presents the output in the form of the capacitance; therefore, here we use the capacitance as the dielectric response. From Daniel, 1967, we have complex capacitance $C(\omega)$

$$C(\omega) = C'(\omega) - iC''(\omega) \quad (5.4)$$

$$= \frac{\epsilon_0 A}{L} [\epsilon'(\omega) - i\epsilon''(\omega)] - \frac{i\sigma A}{\omega L} \quad (5.5)$$

where $i = \sqrt{-1}$

ϵ_0 is the absolute permittivity of free space, $8.854 \times 10^{-12} \text{ Fm}^{-1}$

A = area of the electrode

d = thickness of the sample and σ = DC conductivity in Sm^{-1}

The frequency-domain response of the dielectric medium may be written in terms of the dielectric permittivity, $\varepsilon(\omega)$.

$$\varepsilon^* = \varepsilon(\omega) = \varepsilon'(\omega) - i\varepsilon''(\omega) \quad (5.6)$$

The classic Debye model (Daniel 1967) gives

$$\varepsilon^* = \varepsilon_\infty + \frac{\varepsilon_s - \varepsilon_\infty}{1 + i\omega\tau} \quad (5.7)$$

$$\varepsilon'(\omega) = \varepsilon_\infty + \frac{\varepsilon_s - \varepsilon_\infty}{1 + \omega^2\tau^2} \quad (5.7a)$$

$$\varepsilon''(\omega) = \frac{(\varepsilon_s - \varepsilon_\infty)\omega\tau}{(1 + \omega^2\tau^2)} \quad (5.7b)$$

τ is the relaxation time of the dipole,

ε_∞ is very high frequency permittivity or induced permittivity

ε_s is very low frequency permittivity or static permittivity

The relaxation described by Debye occurs in about a single order of magnitude in the frequency domain, while the dielectric relaxations in polymers are typically much broader. In order to accommodate this broadening, Cole and Cole (Cole K.S., 1941) modified the Debye expressions with an exponent, α ($0 < \alpha \leq 1$), such that

$$\varepsilon^* = \varepsilon_\infty + \frac{\varepsilon_s - \varepsilon_\infty}{1 + (i\omega\tau)^\alpha} \quad (5.8)$$

From equation 5.8, the real and imaginary permittivities are generated as stated in equation 5.8a and 5.8b.

$$\varepsilon'(\omega) = \varepsilon_\infty + (\varepsilon_s - \varepsilon_\infty) \frac{1 + (\omega\tau)^\alpha \cos(\alpha\pi/2)}{1 + 2(\omega\tau)^\alpha \cos(\frac{\alpha\pi}{2}) + (\omega\tau)^{2\alpha}} \quad (5.8a)$$

$$\varepsilon''(\omega) = (\varepsilon_s - \varepsilon_\infty) \frac{(\omega\tau)^\alpha \sin(\alpha\pi/2)}{1 + 2(\omega\tau)^\alpha \cos(\frac{\alpha\pi}{2}) + (\omega\tau)^{2\alpha}} \quad (5.8b)$$

$\alpha = 0$ has the effect of making the permittivity independent of frequency and $\alpha = 1$ produces the sharp transition of the Debye equation.

As further modification, Davidson and Cole gave the Cole-Davidson equation in 1950 as

$$\epsilon^* = \epsilon_{\infty} + (\epsilon_s - \epsilon_{\infty}) \frac{1}{(1 + i\omega\tau)^{\beta}} \quad (5.9)$$

Havriliak-Negami is another empirical modification of the Debye relaxation model, accounting for the asymmetry and broadness of the dielectric dispersion curve. Havriliak and Negami (1966, 1967) proposed their equation to fit data on amorphous polymers and polymer solutions which were intermediate in character between the Cole-Davidson or Williams-Watts behaviour on the one hand and the circular-arc or Fuoss-Kirkwood descriptions on the other. The model was first used to describe the dielectric relaxation of some polymers (Havriliak S., et al., 1967). The principal use of this function has been for polymers and it can fit results for many amorphous polymers and polymer solutions very satisfactorily over considerable ranges of frequency (RH Cole, 1980).

Their relation for the complex permittivity is a combination of the Davidson-Cole and Cole-Cole functions:

$$\epsilon^* = \epsilon_{\infty} + \frac{\epsilon_s - \epsilon_{\infty}}{(1 + (i\omega\tau)^{1-\alpha})^{\beta}} \quad (5.10)$$

It is obvious that equations 5.9 and 5.10 are both a generalization of the Cole-Cole equation, to which it reduces to $\beta = 0$ and a generalization of Cole-Davidson equation to which it reduces to $\alpha = 0$. Separating the real and imaginary parts of the Havriliak-

Negami (HN) equations give rather intricate expression for ϵ' and ϵ'' (Havriliak S., et al., 1966):

$$\epsilon'(\omega) = \epsilon_{\infty} + (\epsilon_s - \epsilon_{\infty}) \frac{\cos(\beta\varphi)}{(1 + 2(\omega\tau)^{1-\alpha} \sin(\frac{\beta\pi}{2}) + (\omega\tau)^2(1-\alpha^2)^{\beta/2}} \quad (5.10a)$$

$$\epsilon''(\omega) = (\epsilon_s - \epsilon_{\infty}) \frac{\sin(\beta\varphi)}{(1 + 2(\omega\tau)^{1-\alpha} \sin(\frac{\beta\pi}{2}) + (\omega\tau)^2(1-\alpha^2)^{\beta/2}} \quad (5.10b)$$

where $\varphi = \arctan\left\{\frac{(\omega\tau)^{1-\alpha} \cos(\frac{\beta\pi}{2})}{1 + (\omega\tau)^{1-\alpha} \sin(\frac{\beta\pi}{2})}\right\}$

The exponents α and β are the shape parameters describing the asymmetry and broadness of the corresponding shape of the Cole-Cole plots and the τ is the HN relaxation time.

5.2.2 Experimental setup

The prepared PUR films were cut mechanically into circular discs 38 mm in diameter and about 0.5 - 1.0 mm in thickness. The dielectric measurements were carried out over the frequency range of 100 Hz to 40 MHz using Hewlett Packard 4194A Impedance/Gain-Phase Analyzer equipped with a HP 16451B Dielectric Material Test Fixture. The capacitance C_p , and dissipation factor, D of PUR samples were determined and the real and imaginary permittivity is calculated from Formula 5.1 and 5.2 as a function of frequency. The measurements and calculations were performed following the ASTM D150 method (Annual Book of ASTM standards, Vol. 10, 1994). This test method is based on placing a specimen of material in an electrode system with a

vacuum capacitance that can be calculated accurately. The electrode system used in the research comprised micrometer electrodes. This electrode system eliminates the error caused by series inductance and resistance of the connecting leads and of measuring capacitor at high frequencies. A built in vernier capacitor is also provided for use in the system. The area of the test specimen may be equal to or less than the area of the electrodes. The specimen should be as flat and uniform in thickness as possible and free of voids, wrinkles and other defects. The test specimens were cleaned by toluene and allowed to dry thoroughly and were placed in the electrode. Then, the capacitance and ac loss were measured.

5.2.3 Results

Figure 5.1 shows the plot of real and imaginary permittivity of PUalk28 (1.6). This figure illustrates typical frequency dependence of dielectric constant in the material. PUR exhibits similar dielectric function (ϵ^*) spectra for all the samples at room temperature. In order to compare the effects of oleic acid content and NCO/OH ratios on dielectric constants of PUR, the real and imaginary permittivity of all PURs were plotted separately. Figures 5.2 to 5.7 show plots of the real and the imaginary parts of dielectric permittivity, ϵ' (Figure 5.2 to 5.4) and ϵ'' (Figure 5.5 to 5.7) of dielectric function (ϵ^*) respectively, against log frequency, f (Hz) for the PUR at room temperature. Overall, the real permittivity ϵ' results are in the range of 1.90 to 2.48 and imaginary permittivity ϵ'' are in the range of 0.02 to 0.08. In general, most PUR have ϵ' values in the range of 1.5 to 7.0 and ϵ'' in the range of 0.001 to 1.0 (A Korzhenko et al., 1999, J Gowri Krishna et al., 1982, CP Chwang et al., 2004, Kanapitsas A et al., 1999) which indicate that the dielectric values obtained for oleic acid based PUR are comparable to those mentioned above. However, the wide variation of the results in

dielectric is due to many factors such as the change in AC frequency, preparation methods, raw material used, thickness of samples, types of electrode used and etc.

The decrease of ϵ' with increasing of frequency is observed for all the PUR samples. This phenomenon may have occurred due to the Maxwell-Wagner-Sillars (MWS) effect. MWS effect is explained in detailed in 5.2.4.3. MWS effect causes the charge carriers trapped at the boundaries of conducting and non conducting matrix, thus forming the space charges. The space charges orient along the direction of the applied field when the external electric field is applied. As the frequency is increased, the external field is increased and thus decreases the polarization in the material (J Gowri Krishna et al., 1982). Consequently, the real dielectric permittivity is decreased. This type of behaviour is common and is observed in Figures 5.2 to 5.4 and many other polymeric systems. Another observable phenomena in Figures 5.2 to 5.4 is that the ϵ' spectra increases as the NCO/OH ratios increase.

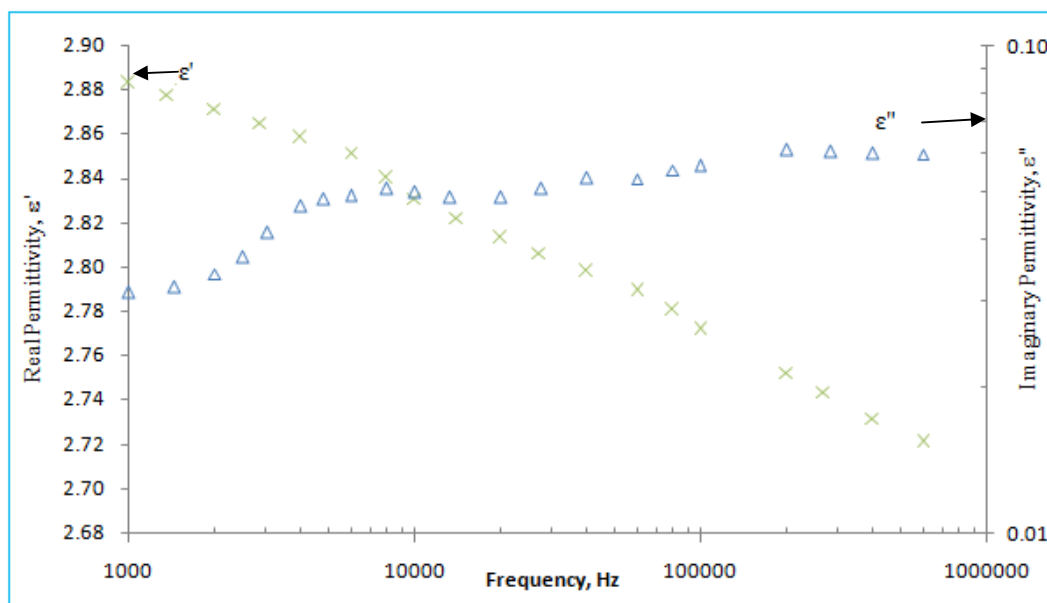


Figure 5.1 Frequency dependence of real and imaginary components of the dielectric permittivity for PUalk28 (1.6) measured at room temperature.

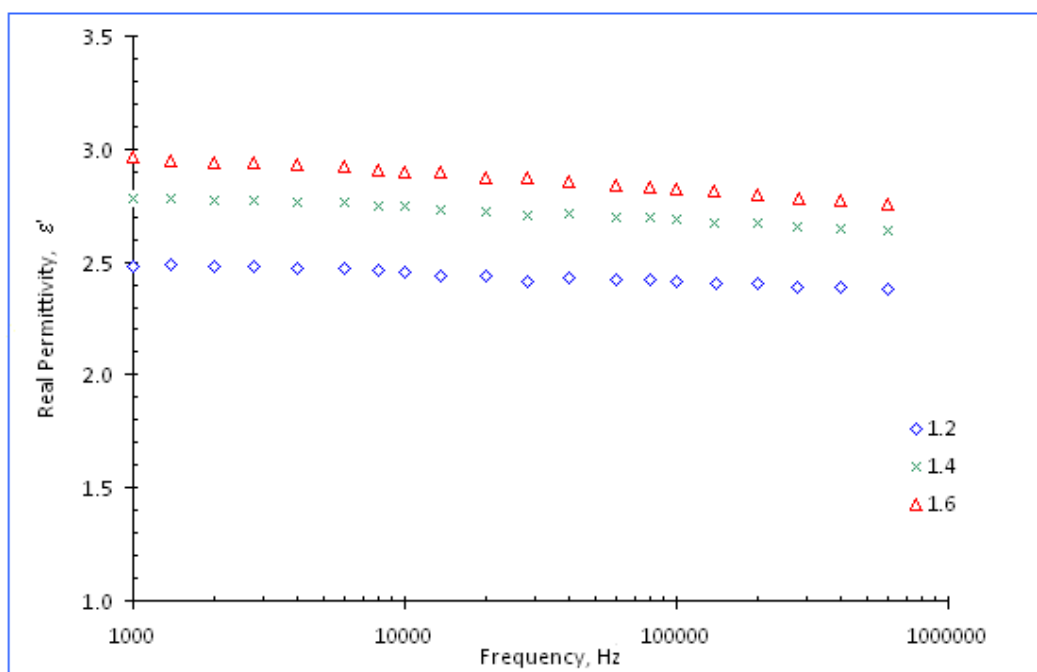


Figure 5.2 Variation of real permittivity (ϵ') with frequency for PUalk28 with NCO/OH ratio 1.2, 1.4 and 1.6. measured at room temperature.

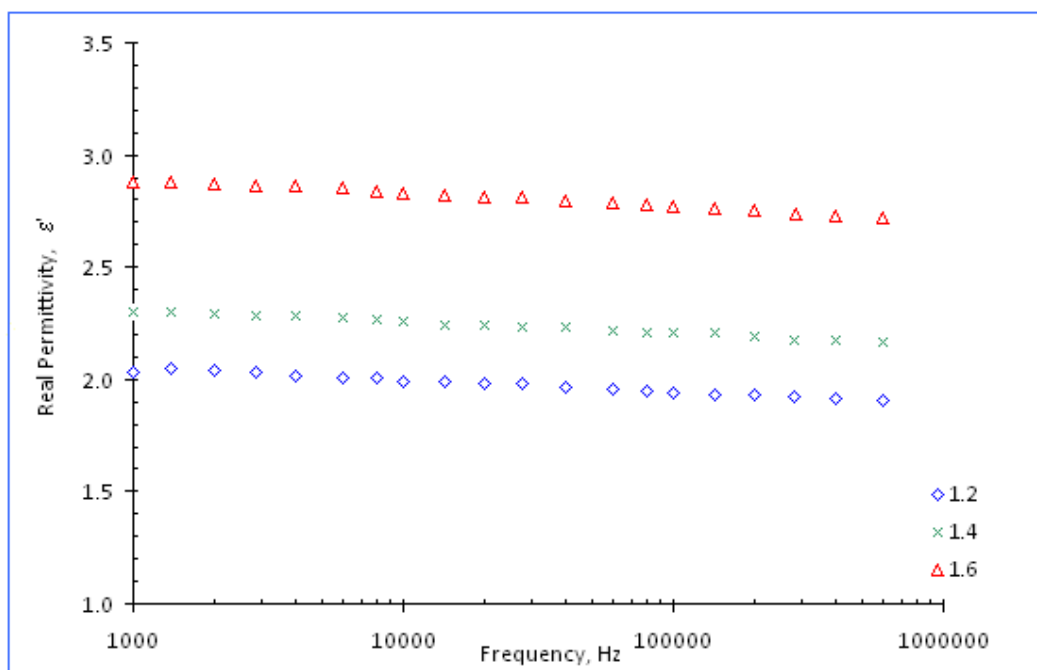


Figure 5.3 Variation of real permittivity (ϵ') with frequency for PUalk40 with NCO/OH ratio 1.2, 1.4 and 1.6 measured at room temperature.

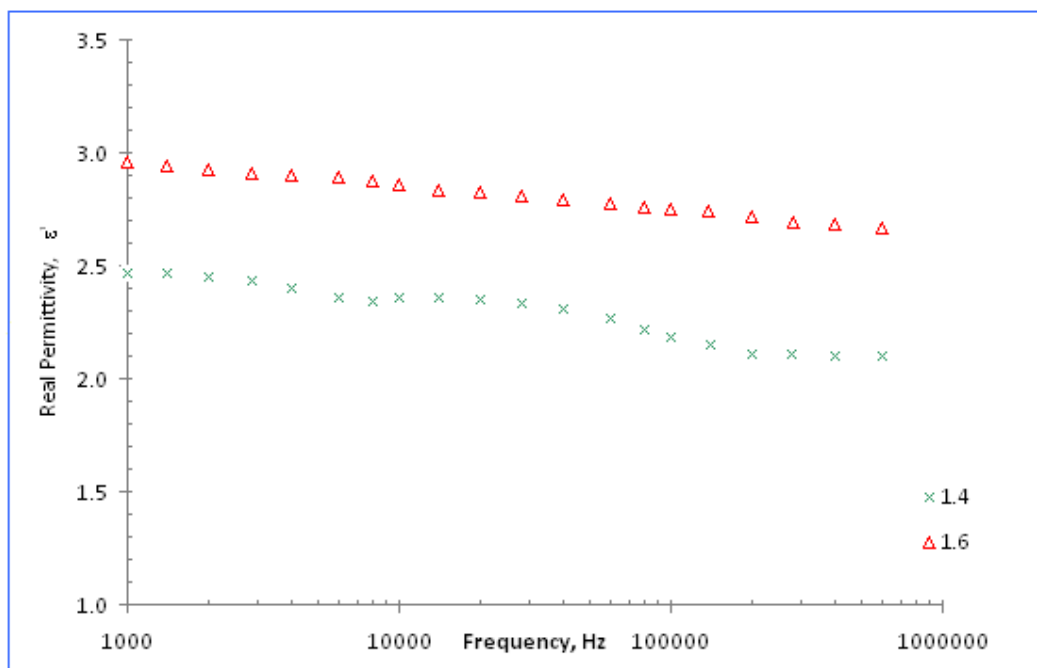


Figure 5.4 Variation of real permittivity (ϵ') with frequency for PUalk65 with NCO/OH ratios 1.4 and 1.6 measured at room temperature.

In Figures 5.5 to 5.7, a corresponding change in the behaviour of ϵ'' can be observed where distinct loss peaks at the frequency range of 4000 to 20000 Hz are obtained for all the nine samples at room temperature. At the frequency range, the relaxation mechanism observed could be related to orientational polarization and will be discussed in detail in the subsequent paragraphs. Basically, the imaginary permittivity value of the samples increases as the NCO/OH ratio increases except for the case of PUalk40 where the value of imaginary permittivity for the ratio of 1.2 overlaps with that of the ratios of 1.4 and 1.6. However, the peak position remains the same or shifts in a small increment as the ratio increases for all the cases.

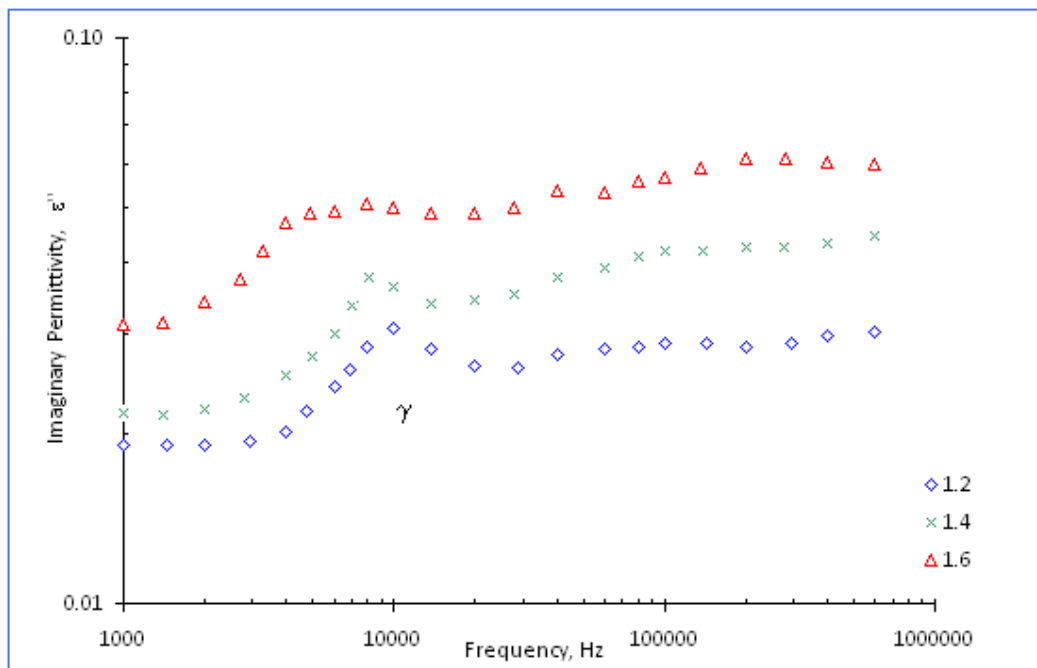


Figure 5.5 Frequency dependence of the imaginary permittivity (ϵ'') for PUalk28 at NCO/OH ratios 1.2, 1.4 and 1.6 measured at room temperature.

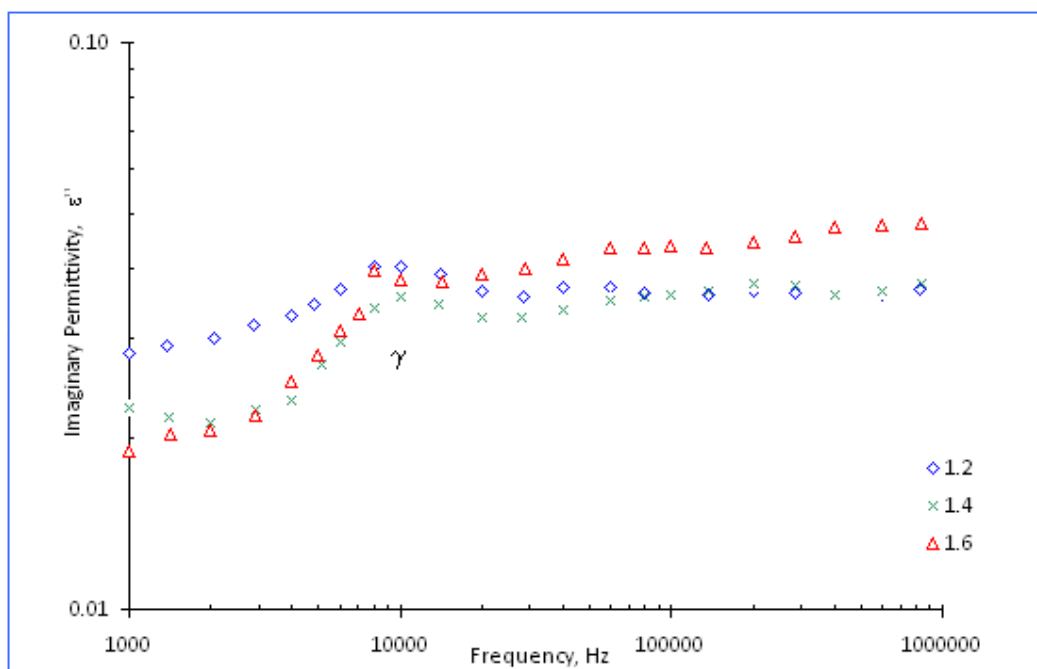


Figure 5.6 Frequency dependence of the imaginary permittivity (ϵ'') for PUalk40 at NCO/OH ratio 1.2, 1.4 and 1.6 measured at room temperature.

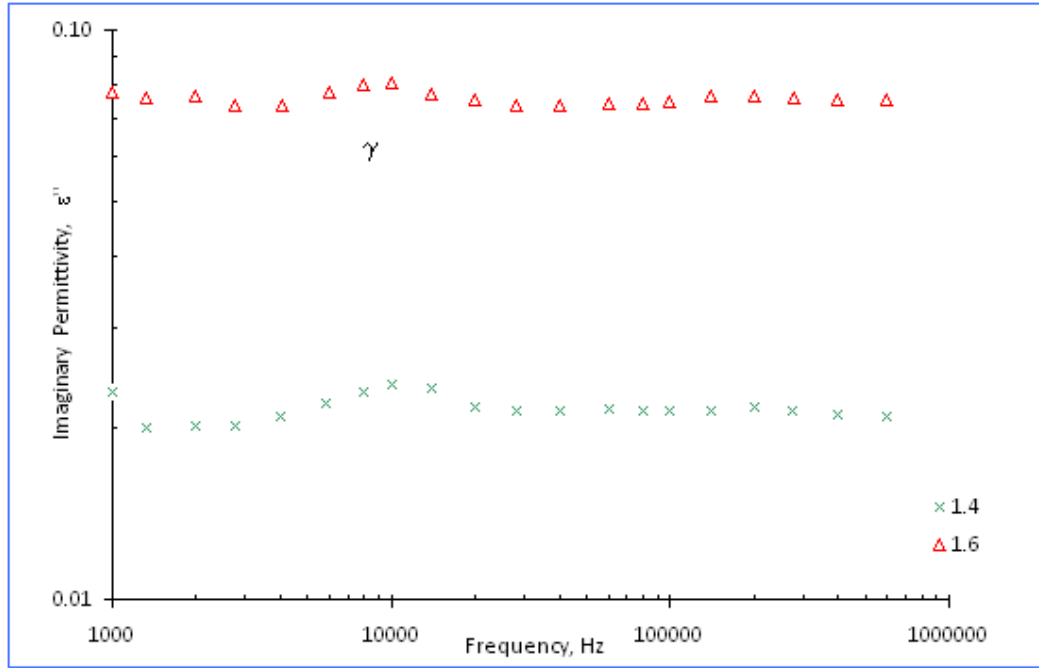


Figure 5.7 Frequency dependence of the relative permittivity (ϵ'') for PUalk65 at NCO/OH ratio 1.4 and 1.6 measured at room temperature.

In order to study the oleic acid content effects on the dielectric constant of the material, the NCO/OH ratio of the material was fixed at 1.6. The PUR dielectric properties with a constant NCO/OH ratio of 1.6 are shown in Figure 5.8 and 5.9. Figure 5.8 demonstrates that at low frequency, PUalk28 has the highest real permittivity ϵ' spectrum followed by PUalk65 and PUalk40. However, the sequence changed to PUalk28 followed by PUalk40 and PUalk65 at high frequency. The number of hydroxyl groups in the polyols, their distribution on fatty acid and position on fatty acid chain affect the network properties on the cross-linking density of PUR material.

Figure 5.9 shows that PUalk65 has the highest imaginary permittivity ϵ'' spectra followed by PUalk28 and PUalk40. A slight shift of the dielectric relaxation peak to the higher frequency is observed for PUalk65 compared to PUalk28 and PUalk40. The relaxation time, τ which corresponds to the critical frequency can be obtained from $\tau = 1/2\pi f_{\max}$.

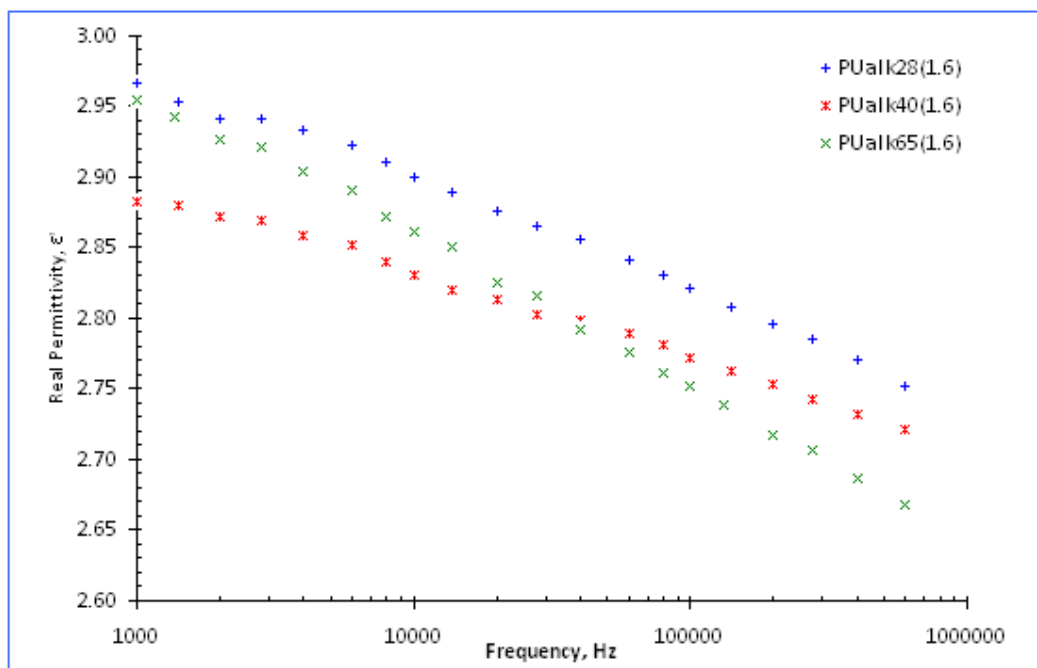


Figure 5.8 Real permittivity ϵ' vs frequency for PUalk28, PUalk40 and PUalk65 at NCO/OH ratio 1.6 measured at room temperature.

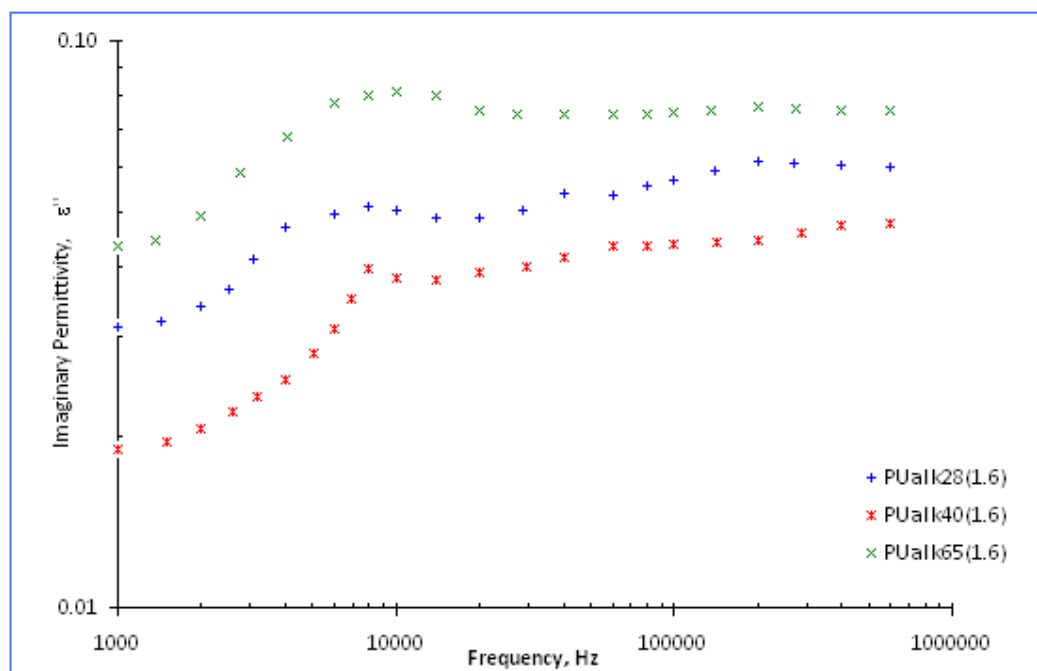


Figure 5.9 Imaginary permittivity ϵ'' vs frequency for PUalk28, PUalk40 and PUalk65 of NCO/OH ratio 1.6 measured at room temperature.

The calculated τ value for PUalk28 (1.6), PUalk40 (1.6) and PUalk65 (1.6) are 1.99×10^{-5} , 1.59×10^{-5} and 1.06×10^{-5} s respectively. This phenomenon can be related to the flexibility of PUR. In the case of orientation of molecular segments or segmental groups, the presence of cross-links should overall increase the relaxation time because the mobility is reduced (J Gowri Krishna et al., 1982). In the case of samples reported in this research, the overall relaxation time increased as the cross-linking increased especially for PUalk28 compared to PUalk65 which is more flexible than the rest of the sample. This shows clearly that the dielectric loss observed is due to the orientational polarisation. Further explanation is given in Section 5.2.4.3.

As mentioned in Section 5.2.1, the classical dielectric relaxation equation offered by Debye is often used to model single dielectric relaxation events as a function of frequency. The major drawback with this equation (Equation 5.7) is that it generally does not fit well to empirical data because the relaxation described by Debye occurs in about a single order magnitude in the frequency domain, while dielectric relaxations in polymers are much broader. The symmetrical Cole-Cole expression describes the shape of the segmental relaxation in the frequency domain. However, Cole-Cole expression does not fit the experimental results obtained from the PUR samples in this research and therefore other models are tested. The best fit is obtained from the asymmetrical Havriliak-Negami (HN) expression (Equation 5.10) and is used successfully to describe the relaxation phenomenon in the frequency domain. This strategy of analysis has been used in many PUR systems which can be found in literatures such as ^bPissis P et al., 2002, Georgoussis G et al., 2000, ^aPissis P et al., 1996, Korzhenko AA et al., 1999 and etc. The HN fit for the relaxation phenomena measured at room temperature is illustrated in Figure 5.10.

The parameters, ε_{∞} , ε_s , $\Delta\varepsilon = (\varepsilon_s - \varepsilon_{\infty})$ and τ , obtained from the experimental HN plots and the shape parameters α and β derived from the HN relaxation model for the relaxation, are tabulated in Table 5.1. Figure 5.10 shows that, except for PUalk28 (1.4 and 1.6) the HN plot of PUR shifts to the right of the graph as the NCO/OH ratio increases. The dielectric strength ($\Delta\varepsilon \pm 0.02$) also increases as the ratio increases.

The parameters α and β can be used to specify the asymmetry and broadness of experimental relaxation peaks even though the exact form of the distribution of relaxation times in the HN equation is not based on any specific model (Blythe AR, 1977). The internal degrees of freedom of the molecules which lead to smaller inter-molecular interaction can be related to the parameter α . Increased α values indicates decreases in the internal degrees of freedom or less molecular interaction in the dielectric. From the Table 5.1, α value for PUalk28 increases as the NCO/OH ratio increases. Theoretically, as the NCO/OH ratio increases the cross-linking of the materials increases and hence, it can be assumed that the internal degree of freedom of the molecules decreases. Therefore the α parameter should increase as the ratio of the formulation increases which is true for the case of PUalk28. However, PUalk40 and PUalk65 contradict the assumption stated due to the higher percentage oleic acid content in the polyol has presumably produced the higher amount of flexible side chain and thus making the polymer become less compact.

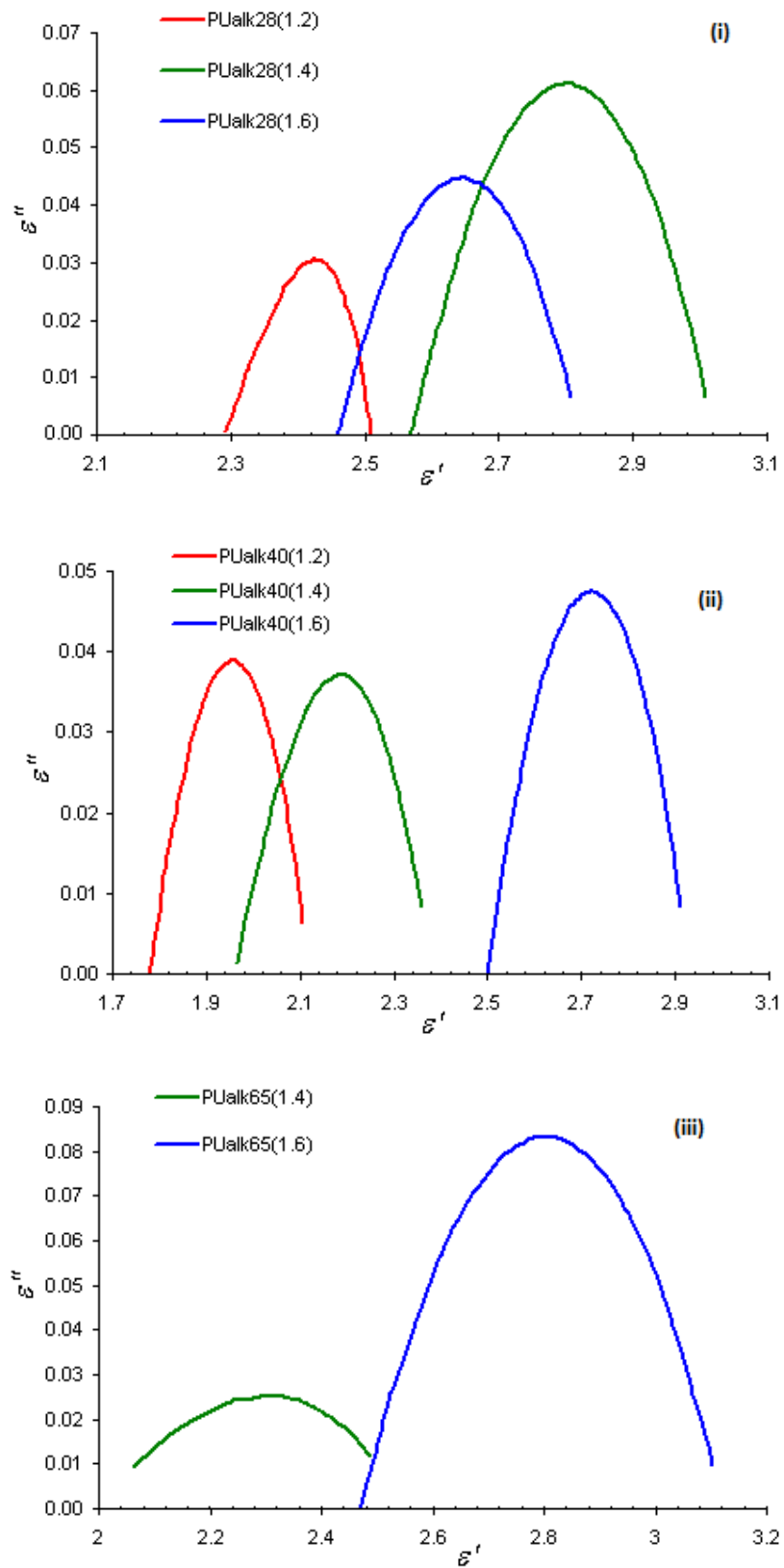


Figure 5.10 The asymmetrical Havriliak-Negami plots of the dispersion curves for (i) PUalk28 (ii) PUalk40 and (iii) PUalk65 measured at RT

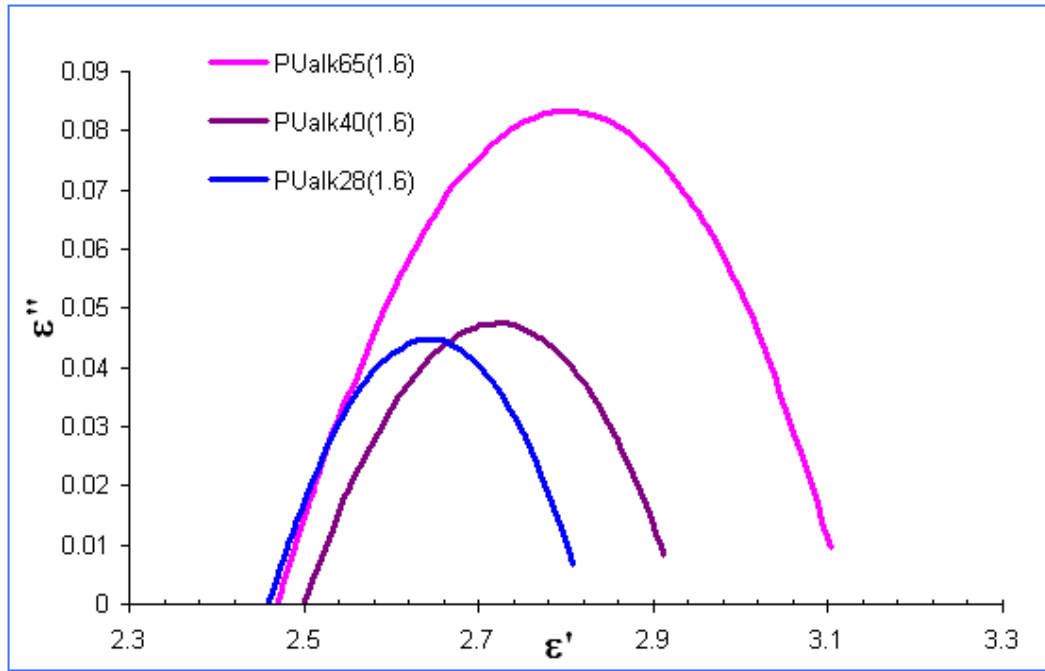


Figure 5.11 The asymmetrical Havriliak-Negami plots of the dispersion curves for PUalk28, PUalk40 and PUalk65 at fixed ratio of 1.6 measured in RT

Table 5.1 The static permittivity ϵ_s , induced permittivity ϵ_∞ , dielectric strength, $\Delta\epsilon$, α and β parameters at room temperature derived from HN Plots.

	PUalk28 (1.2)	PUalk28 (1.4)	PUalk28 (1.6)	PUalk40 (1.2)	PUalk40 (1.4)	PUalk40 (1.6)	PUalk65 (1.4)	PUalk65 (1.6)
α ± 0.01	0.50	0.65	0.68	0.70	0.75	0.71	0.86	0.67
β ± 0.001	0.390	0.890	0.900	0.860	0.710	0.860	0.550	0.901
ϵ_∞ ± 0.01	2.29	2.57	2.46	1.78	1.96	2.50	2.00	2.47
ϵ_s ± 0.01	2.51	3.02	2.82	2.12	2.38	2.93	2.55	3.12
$\Delta\epsilon$ ± 0.02	0.22	0.45	0.36	0.34	0.42	0.43	0.55	0.65
τ (s) \pm $0.01e^{-5}$	$1.35e^{-5}$	$1.98e^{-5}$	$1.99e^{-5}$	$1.77e^{-5}$	$1.45e^{-5}$	$1.59e^{-5}$	$1.77e^{-5}$	$1.27e^{-5}$

It is a well-known factor that in PUR system, the cross-linking increases as the NCO/OH ratio is increased. However, in our case the flexibility of the PUR also increases as the oleic acid content of polyols increases. Therefore it seems as though there is a competing effect of cross-linking with flexibility which can be related to α parameter or internal degrees of freedom. The increase in oleic acid content in polyols and thus the increase in flexibility in PUR has caused the effect of cross-linking to be ineffective or less effective. This clearly shows, the α parameters in PUalk40 and PUalk65 decreases although the NCO/OH ratios increased in the samples.

Molecules of long chain polymers have much broader dispersion lines and this could be explained through β parameters. Supposedly, the β parameter increases as the molecular chain increases. When the β values of PUalk28 (1.6) are compared with that of PUalk40 (1.6) and PUalk65 (1.6), they do not show any particular trend. This phenomenon may have occurred because the main chain of the PUR polymer remains the same but the amount of flexible side chain increases which does not affect the length of the molecules.

Figure 5.12 shows the frequency dependence of conductivity $\sigma(\omega)$ for all the PUR samples at room temperature. The plot exhibits typical behaviour of ionic materials, i.e. the dc plateau and the frequency dependent region. Theoretically, at low frequency, σ_{ac} approaches frequency-independent plateau values and extrapolation to zero frequency gives dc conductivity (^bKanapitsas A et al., 2000). The conductivity is found to be frequency independent in the low frequency region and it is equal to the bulk conductivity of the sample. The onset of the conductivity relaxation phenomenon has been indicated by change over from the frequency independent to the dependent region. The observed behaviour in general agrees with the prediction of the jump model (PS

Anantha et al., 2005). According to this model, at low frequency an ion jumps from one site to its neighbouring vacant site successfully contributing to dc conductivity. The observed conductivity relaxation at high frequencies can be due to the probability of the correlated forward-backward hopping together with the relaxation of the ions.

The total frequency dependent conductivity at given temperature and frequency can be described Jonscher's universal power law (AK Jonscher, 1970) as

$$\sigma(\omega) = \sigma_{dc} + \sigma_{ac}(\omega) \quad (5.11)$$

where σ_{dc} is the dc electrical conductivity and the $\sigma_{ac}(\omega)$ is the ac conductivity. At particular temperature, the frequency variation of $\sigma_{ac}(\omega)$ obeys the law

$$\sigma_{ac}(\omega) = A\omega^s \quad (5.12)$$

where A and s are material dependent constant (Hsing-Lung Wang et al., 2004).

Table 5.2 The experimental and fitted results of dc conductivity at room temperature derived from power law plots.

	NCO/OH ratio	Experimental σ_{dc} values ($\times 10^{-11}$) $\pm 0.1 \text{ Sm}^{-1}$	Fitter σ_{dc} values ($\times 10^{-11}$) $\pm 0.02 \text{ Sm}^{-1}$
PUalk28	1.2	31.6	33.90
	1.4	36.6	35.30
	1.6	37.8	36.80
PUalk40	1.2	3.6	3.31
	1.4	3.3	2.94
	1.6	3.9	3.32
PUalk65	1.4	4.0	3.85
	1.6	7.4	7.15

The experimental frequency range used in the research was from 100Hz to 40MHz. The equation 5.11 and 5.12 has been used to fit the ac conductivity data. In the fitting procedure, A and s values have been varied simultaneously to get the best fits. The fitted curves are shown in Figure 5.12. It was found that the fit was satisfactory in all cases. Extrapolation of the fitted results in zero frequency giving dc conductivity σ_{dc} , as tabulated in Table 5.2. Dc conductivity values measured experimentally at room temperature. The fitted σ_{dc} results shows the validity of the σ_{dc} values which have been obtained experimentally, by using Keithley Source Measurement Unit (SMU 236) where both are in good agreement.

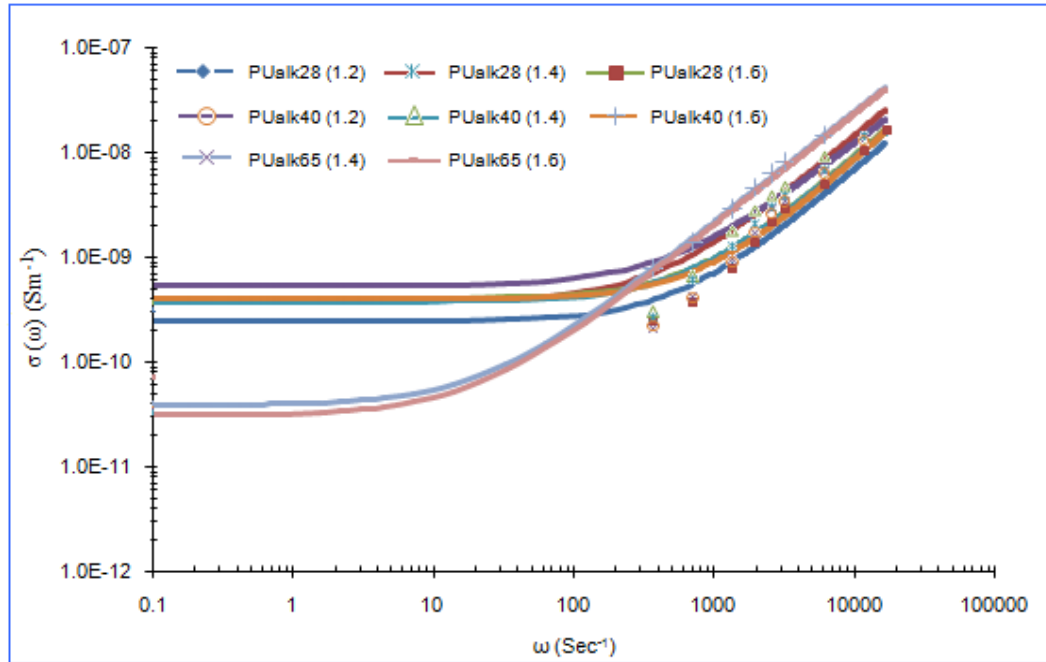


Figure 5.12 Frequency-dependent conductivity, $\sigma(ac)$ vs frequency for PUR at room temperature. Dots are experimental points and continuous lines corresponds to simulated fit.

5.2.4 Discussion

Generally, PURs have poor dielectric properties due to intrinsic limitation of the material itself. Polyurethanes contain many polar groups that tend to orient in an electrical field and most PUR molecules have enough flexibility to permit their polar groups to orient in this way producing high dielectric constant or dielectric permittivity. The Clausius-Mosotti equation indicates that polar groups act to increase the dielectric permittivity of PUR materials (Alex Perrotta et. al., 2003). On the other hand, molecular flexibility and the resulting polar groups' mobility are very sensitive to frequency and temperature, so dielectric constants are far from constants and electrical and mechanical hysteresis produce considerable and variable dielectric loss.

In PUR system there are primary chemical bonds and the weaker intermolecular forces such as hydrogen bonding, polarizability, dipole moments and Van der Waals forces. The weaker bonds are affected by temperature and stress. The effect of intermolecular forces will be reduced if there is repulsion between similar charges or bulky chains or if there is high cross-link density. Aromatic isocyanate (TDI) and phthalic anhydride in polyol which is used in forming PUR contribute to the aromatic ring in the molecular structure of the polymer. Molecular flexibility is affected by the presence of aromatic rings in the PUR system. Aromatic rings stiffen the polymer chains and causes high melting point, hardness and decrease in elasticity. Molecular flexibility depends on freedom of rotation about the single bonds in the main chain of the polymer molecule. Restriction of rotation reduces the molecular flexibility. As noted earlier, molecular flexibility permits polar groups to orient in an electrical field, producing high dielectric constant. On the other hand, molecular rigidity prevents orientation producing low

dielectric constant. Therefore, the dielectric values of PUR varied from system to system depending on the molecular structure of the material.

5.2.4.1 *The effect of oleic acid content*

The electrical property of a polymer very much depends on the molecular structure of the raw material. Chain length of polyols changes the properties of PUR. PUR are generally made of polyol segments of lower polarity plus PUR and or polyurea segments of higher polarity (Szycher Michael, 1999). When the polyol segments are fairly short, the polymer may have a fairly random homogeneous structure. When the polyol segments are longer the resulting copolymer will tend to separate into microphases.

The phase present in larger amount tends to form the continuous matrix and control most of the properties while the smaller amount phase will tend to be segregated as discrete domains and contribute specific properties to the composite structure. In our case, polyols of Alk65 are predicted to have more branched chain length followed by Alk40 and Alk28. Therefore, it is assumed that PUalk28 may have a fairly random homogeneous structure and PUalk65 have copolymer that separate into microphases.

Higher percentage of fatty acid is present in Alk65 polyol compared to Alk28 polyol, therefore PUR formed from Alk65 has more flexible polyblocks with lower polarity compared to PUalk28. Polyblocks with lower polarity have lower dielectric constant compared to that polyblocks with higher polarity. The results obtained in Figure 5.8

verifies the explanation above in which PUalk65 has lower dielectric permittivity compared to PUalk28 and PUalk40 in the high frequency range.

However, below the frequency range of 20 kHz the ϵ' for PUalk65 is higher than PUalk40. This phenomenon occurs presumably due to higher percentage of oleic acid in PUalk65 (protons originating from oleic acid) which dominates the dielectric relaxation mechanism at lower frequency range than that of higher frequency range (SSN Murthy., 1988).

In a polymer chain - $(CH)_n$ - the delocalization of the electron tends to level off all C-C bonds. By quantum mechanical treatment of the system, i.e.: as a particle in a box-type potential well, one finds the energy required to transfer an electron from ground state to the first excited state to be $E_a \sim (n + 1) / n^2$, where n is the monomer or number of molecular chains in the polymer. Thus, when n increases the activation energy for carrier formation decreases and conductivity has to increase with chain length (Ion Bunget et al., 1984). As mentioned earlier, PUalk65 has the highest σ_{ac} conductivity compared to the rest of PUR which confirms the theory explained by Ion Bunget et al., 1984 which links conductivity to the chain length. Oleic acid contributes to flexible side chain of the PUR. Higher percentage of oleic acid content in the polyols attributes to more side chain in the PUR molecular structure. The conductivity of PUalk65 is higher than that of PUalk40 and PUalk28. The polymer with longer length of flexible side chain has higher dielectric constant and thus ac conductivity depends on the dielectric permittivity, the value increases with the side-chain of the polymer.

5.2.4.2 *The effect of NCO/OH ratio*

As discussed in the earlier chapters of this thesis, the prepolymer has isocyanate groups as the end groups. Three different NCO/OH ratios are selected and since the NCO/OH ratio is greater than 1, the PUR formed will be NCO terminated. NCO/OH ratios in PUR relates to cross-linking, where, as the ratio increases the cross-linking increases (Bor-Sen C. et al., 2002). Excess diisocyanate may first react with polyol to form isocyanate-terminated prepolymer. The free NCO groups will react further to form three-dimensional allophanate or biuret cross-links or polar urea structure thus increasing the number of urethane groups (S. Desai et al., 2000). The existence of three dimensional allophanate or biuret structure restricts the mobility of molecular chain (Huang SL et al., 1997). When the NCO/OH ratio is low, the branching will occur at the urethane linkage. At higher NCO/OH ratios, the probability for the formation of urea linkages will be high and, thus, branching will occur at the urea linkage. The cross-linking increases the effective molecular weight of PUR which in turn increases the melting point (Billmeyer, 1971). With the increase in cross-linking, the sample becomes more and more brittle. Evidence is obvious in PUR sample from this research in which the samples of PUalk28, PUalk40 and PUalk65 with NCO/OH ratio 1.6 is more brittle than that of 1.2 or 1.4 as discussed in Section 6.5. This indicates that the higher the NCO/OH ratio, the higher the cross-linking in the polymer.

The important fact of cross-linking in a polymer material is that it changes the electrical properties considerably. For instance, in this case as the NCO/OH ratio of the samples increases from 1.2 to 1.6, the cross-linking of the samples increases too. As a result, the dielectric permittivity of the samples increases as the NCO/OH ratio increased. This phenomenon can be observed in Figures 5.1 to 5.7.

5.2.4.3 Polarization

Dielectric relaxations in polymers are contributed by various factors. Four types of dielectric relaxation are common for PUR which is clearly seen in typical PUR thermally stimulated depolarization currents (TSDC) thermogram (Spathis et al., 1990, ^aPissis P et al., 1996, Korzhenko A et al., 1999). The types of dielectric relaxation are α , β and γ and Maxwell-Wagner Sillars (MWS) or interfacial polarization effect. The γ relaxation has been associated with local motion of $(CH_2)_n$ sequences and β relaxation to the motion of the polar carbonyl groups with attached water molecules (Apekis L et al., 1992, ^{c,d}Kanapitsas A et al., 1999, ^cPissis P et al., 1998). The β transition is very weak in the dry polymers but is greatly increased by increasing moisture content. The α transition occurs near 50°C and corresponds to the glass-rubber transition of the amorphous phase. MWS relaxation is associated with accumulation of the charges at the interfaces between hard microdomains and soft micro phase (^aPissis P et al., 1996).

The α peak dominates the spectra in the kHz range and is associated with the glass-rubber transition. The glass-transition temperature T_g is usually taken as the temperature at which the α -relaxation peak in the dielectric spectrum is at 0.01Hz (Hedvig 1977, McCrum NG et al., 1967 and Ngai KL 1991). Secondary β peak observed at higher frequency range (10 to 1000Hz) and it corresponds to the local motions in the glassy state of polymer (Hedvig 1977, McCrum NG et al., 1967). The α relaxation peak is due to segmental motion and the secondary β transition is due to smaller scale mobility.

In PUR the intergrain boundaries are zones where free charges such as interstitial ions, vacancies, injected electron and etc may accumulate, which causes polarisation of crystallites. These accumulated charges induce image charges on electrodes and

produce a polarization that is superimposed over the distortional and dipolar polarization. This mechanism was studied by Wagner for nonmagnetic crystalline insulators (Ion Bunget et al., 1984). MWS polarization was reported for a commercial PUR elastomer, five PUR (Dev et al., 1972) and three polyether PUR (North et al., 1972). Usually, the α -relaxation is accompanied with the MWS relaxation process (Hanai T, 1968) and was described for PUR as related to the ionic polarization in the diffuse interface boundary region between hard and soft based on dielectric relaxation spectroscopic (DRS) and thermally stimulated depolarization currents (TSDC) measurements (^{a,b,c}Pissis P et al., 1996, 2002 & 1998).

The γ -relaxation is associated with motions of $(-\text{CH}_2-)_n$ units and usually observed at frequency range of 10 kHz. γ -relaxation is proposed and labelled in Figure 5.5 to 5.7. The frequency range of dielectric relaxation which occurring in the Figures 5.5 to 5.7 are in the range of 10kHz as mentioned for γ -relaxation and therefore γ -relaxation is proposed as the probable mechanism for the dielectric behaviour of PUR in the research. γ -relaxation mechanism is attributed to the local motion of the chain segments located between the hydrogen bonds. These chain segments mainly consist of a polar CH_2 and C-O groups where the transition can be observed dielectrically. The existence of CH_2 and C-O groups in PUR can be confirmed from the FTIR spectrum (refer to Figure 3.3). In the spectra, the characteristic carbonyl stretching was observed at 1734 - 1745 cm^{-1} and the band observed at 2930-2940 cm^{-1} was due to the $-\text{CH}-$ stretching. The main factor in determining the transition is the hydrogen-bond chain structure and not the structure of the main polymer chains. However, it is difficult to give an appropriate explanation for the behaviour of γ -relaxation in terms of conception (Hedvig 1977, Jacobs H et al., 1961).

5.3 DC conductivity studies

5.3.1 Theory of conductivity

All materials conduct electricity to a certain extent and all suffer some form of breakdown in a sufficiently strong electric field. For low field strength, the conduction process in most materials is ohmic but as the electric field increases the conductivity become field dependent. Further increase in the field strength causes some form of destructive irreversible conduction.

Ohm's law gives the relation of the current I , to the applied voltage, V as

$$V = IR \quad (5.13)$$

where R is the resistance of the material through which the current passes.

Resistivity is the resistance to the conduction of electricity. The resistivity, ρ is independent of specimen geometry but related to R through

$$\rho = \frac{RA}{l} \Omega \text{ m} \quad (5.14)$$

where l is the distance between two points at which the voltage is measured and A is the cross-sectional area perpendicular to the direction of the current. Electrical conductivity σ is used to specify the electrical characteristics of a material and it is simply the reciprocal of the resistivity,

$$\sigma = \frac{1}{\rho} (\Omega \text{ m})^{-1} \quad (5.15)$$

In addition to Equation (5.13), Ohm's law can be expressed as

$$J = \sigma E \quad (5.16)$$

where J is the current density and E is the electric field intensity.

The conductivity of dielectrics may be either ionic or electronic or both. It may be a matter of great difficulty to separate these components experimentally, particularly at high field strength; however, the basic theoretical ideas are quite distinct. The basic expression for all electrical conductivity is

$$\sigma = \sum_i n_i e_i \mu_i \quad (5.17)$$

where n_i is the density of carriers of the i th species, and e_i and μ_i are the corresponding charges and mobility respectively. The field-dependence of ionic mobility should be small, but the concentration of charge carriers could be strongly influenced by an electric field.

Electronic conduction is a current which arises from the flow of electrons in solid materials which exist in all conductors, semiconductors and many other insulating materials. The magnitude of electrical conductivity is dependent on the number of electrons available to participate in the conduction process. The electrical property of a solid material depends on its electron band structure. The band containing the highest energy or valence electron is termed as valence band and the next higher energy band is termed as conduction band. Fermi energy (E_f) is the highest energy filled state at 0 K. There are four possible different types of band structure at 0 K.

The first type of band structure is the valence band partially filled with electrons. The second type of band structure is the valence band is full but it overlaps with the conduction band. The third and fourth are similar, in which all states in the valence band are completely filled with electrons, however, there is no overlap between the valence band and conduction band and the conduction bands are empty. The four different types of band structure are shown schematically in Figure 5.13. The second

band structure can be found in most metals, the third band structure will be found in insulators and the fourth band structure is for semiconductors. The electrons that participate in conduction process are free electrons which have energy more than Fermi energy and can be accelerated in an electric field. *Hole* can be found in insulators and semiconductors which have energy less than E_F . The electrical conductivity depends on the numbers of free electrons and holes.

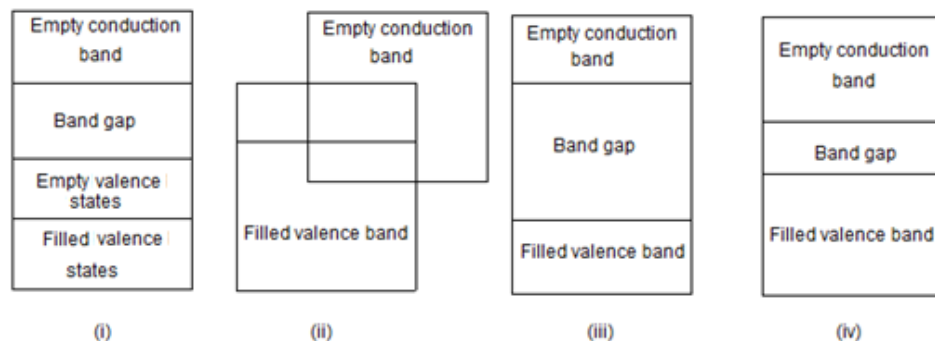


Figure 5.13 Four possible electrons band structures in solid at 0 K

Ionic conduction in a dielectric is the process in which an electric current is carried by the motion of ions. This conduction may arise in a dielectric in two different manners; in an ionic crystal where the basic constituents are ions, while in a non-ionic substance chemical imperfection is required to supply the mobile species.

In most polymeric materials it is very difficult to observe any electronic conductivity at all, and whatever conductivity exists usually depends on the movement of adventitious ions. Ionic conduction in polymers presents by default or added as a separate ingredient to the material. However, some polymers are inherently conductive in having at least one ionisable group per monomer unit. Examples are cellulose and its derivatives,

polyamides and nylon-6,6 (results of the dissociation of amide groups to give protons). Consequently, any improvements in the quality of the insulation are by careful preparation and purification to avoid any ionic impurities such as catalyst residues and dissociable end groups. However, special high conductivity polymers have been made based on certain organic molecular structures which are known to exhibit electronic conduction.

The mechanisms responsible for dc conduction have been variously identified as electrode polarization, dipolar orientation, charge injection due to space charge effects, hopping of charge carriers between trapping sites and tunneling of charge carriers. A range of models have been proposed to discuss behaviour of insulating material. These include the following (AA Alagiriswamy et al., 2002):

A) Ionic hopping

$$J = J_0(T) \exp\left(\frac{q a E}{2 k T}\right) \quad (5.18)$$

where a is the ionic jump distance, k is the Boltzmann constant, T is the absolute temperature and E is the applied field.

B) Poole Frenkel effect

$$J_{PF} = B E \exp\left[\frac{q}{k T} \sqrt{\frac{q E}{\pi \epsilon_0 \epsilon}} - \frac{q \Phi_B}{k T}\right] \quad (5.19)$$

C) Schottky effect

$$J_S = A T^2 \exp\left[\frac{q}{k T} \sqrt{\frac{q E}{4 \pi \epsilon_0 \epsilon}} - \frac{q \Phi_B}{k T}\right] \quad (5.20)$$

where A and B are constants, ϵ , ϵ_0 , q , E , k , and T are the high-frequency dielectric constant, permittivity in vacuum, electronic charge, electric field, Boltzmann constant, and temperature in kelvins, respectively. Φ_S is the barrier height for the injecting electrons for the Schottky emission while Φ_{PF} is the barrier for the trapped electrons for the Poole-Frenkel emission.

D) Space Charge limited current (SCLC)

$$J_{SCLC} = \frac{q\mu\epsilon_0\epsilon F^2 V_{app}^2}{8X_t^3} \quad (5.21)$$

where μ is the mobility of the free carriers, x_t is the effective width of the space charge region, V_{appl} is the applied voltage and θ is the fraction of free carrier concentration to trap carrier concentration.

E) Ionic conduction by migration of ions by hyperbolic sine function (Ikezaki K et al., 1981, DW Kim et al., 2000)

$$J = (2ne\lambda\delta) \exp\left(-\frac{\phi}{kT}\right) \sinh\left(\frac{\lambda q E}{2kT}\right) \quad (5.22)$$

where n is the concentration of ion, e is the electronic charge, λ is the hopping distance of ion, δ is the attempt-to-escape frequency, ϕ is the barrier height, E is the electric field, k is the Boltzmann constant and T is the absolute temperature.

The electrical conductivity of many materials is found to obey the Arrhenius relation,

$$\sigma = \sigma_0 \exp \left(-\frac{E_a}{kT} \right) \quad (5.23)$$

where σ is the value of the electrical conductivity at an absolute temperature T , σ_0 is the conductivity value at absolute zero as obtained by extrapolation and E_a is the activation energy of the conduction process. Arrhenius plots which are obtained when $\ln \sigma$ is plotted as a function of reciprocal temperature can be observed for polymers and consist of two, or sometimes three, joined straight line regions. The same Arrhenius relations can be used to describe the electrical conductivity over the various straight-line regions of the plots.

5.3.2 Experimental setup

The prepared PUR films were cut mechanically into circular discs with diameter of 9.12 mm in diameter and about 0.5 - 1.0 mm in thickness. Measurements of dc conductivity as a function of temperature were performed and the conductivity determinations were carried out using the technique described in ASTM D257 (ASTM, 1994). The measurements were performed on the samples placed in the cryostat connected to the temperature controller (Lakeshore 330 Autotuning Temperature Controller) covering a broad temperature range from 28 °C to 120° C with a resolution of $\pm 0.04^\circ$ C. The equilibrium time for each temperature was at least 10 min. The samples were sandwiched between the two brass electrodes, one of which was provided with a guard ring. The experiment was performed in vacuum to ensure good electrical contact with the samples. The steady currents were measured by varying the voltage level in the range of 0 -100 V with Keithley Source Measurement Unit (SMU 236)

which was connected to a computer and controlled by Labview software to interpret the data obtained from the test.

5.3.3 Results

Polyurethane like many urethane acrylates polymers is electrically nonconductive with a volume conductivity of less than 10^{-16} S/cm in dry state at room temperature (Geoffrey O et al., 2008). This is consistent with the magnitude of an insulator. Although a relatively great number of papers have been published on dc conductivity in plastics, there is no unanimous point of view which supports the experimental facts on the mechanism of conduction for PUR. This state of matters occurs due to the fact that transient polarization superimposed on the weak dc conduction and sometimes with parasitic leakage current which cannot be easily separated in an experimental work.

Two phase structures and phenomenon such as glass transition, characteristic of the amorphous phase affects the temperature dependency of the electrical conductivity for PUR. There is a gradual increase in conductivity as the temperature increased and this phenomenon is expected to occur due to thermal activated conductivity (^aTsonos C et al., 2001 & 2004). The Arrhenius dependence suggests a charge carrier diffusion-controlled conductivity mechanism (^bKanapitsas A et al., 2000) rather than a mechanism governed by the motion of the polymeric chain. Measurement in several PUR systems have shown that σ_{dc} (T) is described by a Vogel-Tammann-Fulcher (VTFH) type equation in the system with high values of σ_{dc} (σ_{dc} in the range of 10^{-10} to 10^{-6} Sm⁻¹) and for the systems with low σ_{dc} (σ_{dc} in the range of 10^{-8} and below) the conductivity is described by Arrhenius equation (^cPissis P et al., 1998, ^aKanapitsas A et al., 1998). VTFH equation states that

$$\sigma_{dc}(T) = A \exp \left(\frac{-B}{T - T_0} \right) \quad (5.24)$$

where A is the pre-exponential parameter, B is the activation energy parameter and T_0 is the ideal glass transition temperature ($T_0 \approx T_g - 50$) (McCrum NG et al., 1967). For comparison, E values of 0.30 and 0.34 eV were determined for σ_{dc} in PUR based on oligotetramethylene glycol (^cPissis P et al., 1998) and of 0.57 and 0.67 eV in the interpenetrating networks of PUR based on a three-functional oligoglycol (^aKanapitsas A et al., 1998). The conductivity mechanism which is governed by the cooperative motion of polymer chain segments similar to polymer electrolytes (Fontanella JJ et al., 1986), is also observed for PUR of higher degree of microphase separation.

The higher dc conductivity is observed for the samples because of its stronger tendency of hard segments for self-association. The reason is due to long-range electrostatic interaction between negatively charged cavities of crown ethers or esters and proton donating soft fragments. However, in our case, Arrhenius equation was used to explain the conduction mechanism since the σ_{dc} is at the lower range (10^{-9} to 10^{-12} Sm^{-1}). Therefore, the conduction is not due to the above reason. The explanation is given in Section 5.3.4.

The Arrhenius plots, $\ln \sigma$ versus reciprocal temperature for the three PUR of varying the NCO/OH ratios are shown in Figures 5.14 to 5.16. The linear relationship in this figures indicate the activation type behaviour of conductivity with the change of temperature. In the range of temperatures investigated, the plots consist of a straight line segments.

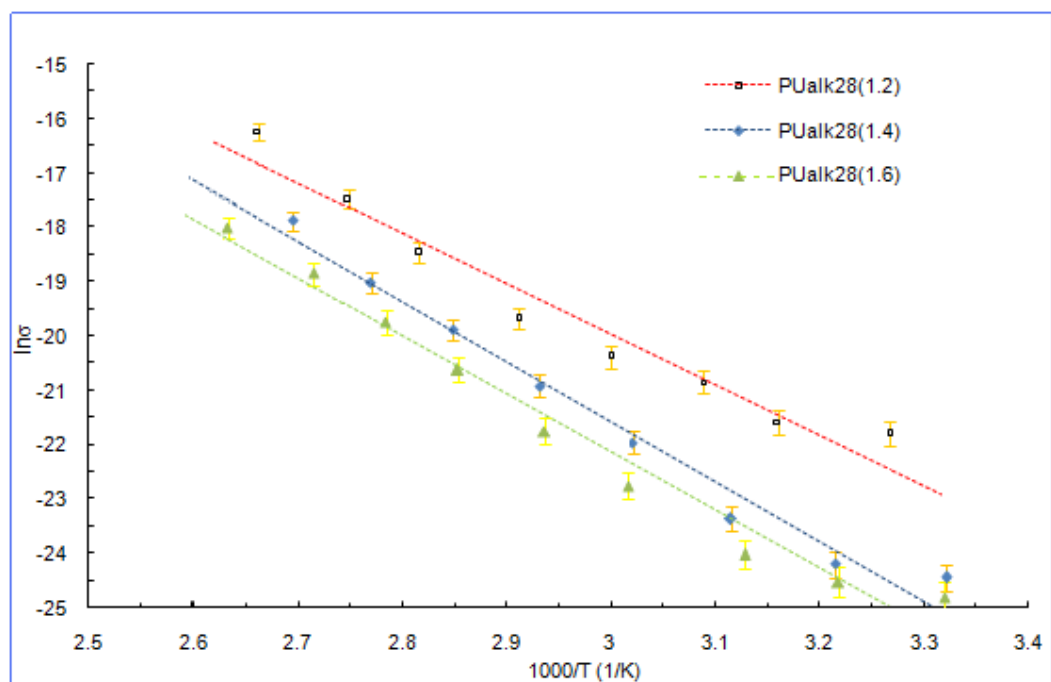


Figure 5.14 Arrhenius plots of PUalk28 with NCO/OH ratio of 1.2, 1.4 and 1.6

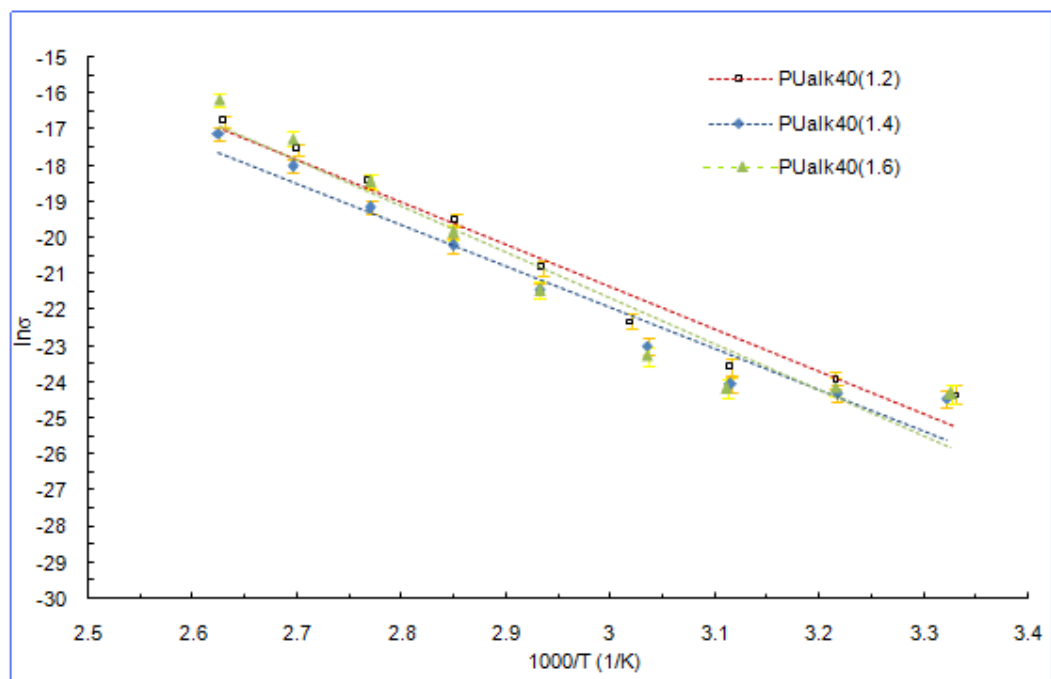


Figure 5.15 Arrhenius plots of PUalk40 with NCO/OH ratio of 1.2, 1.4 and 1.6

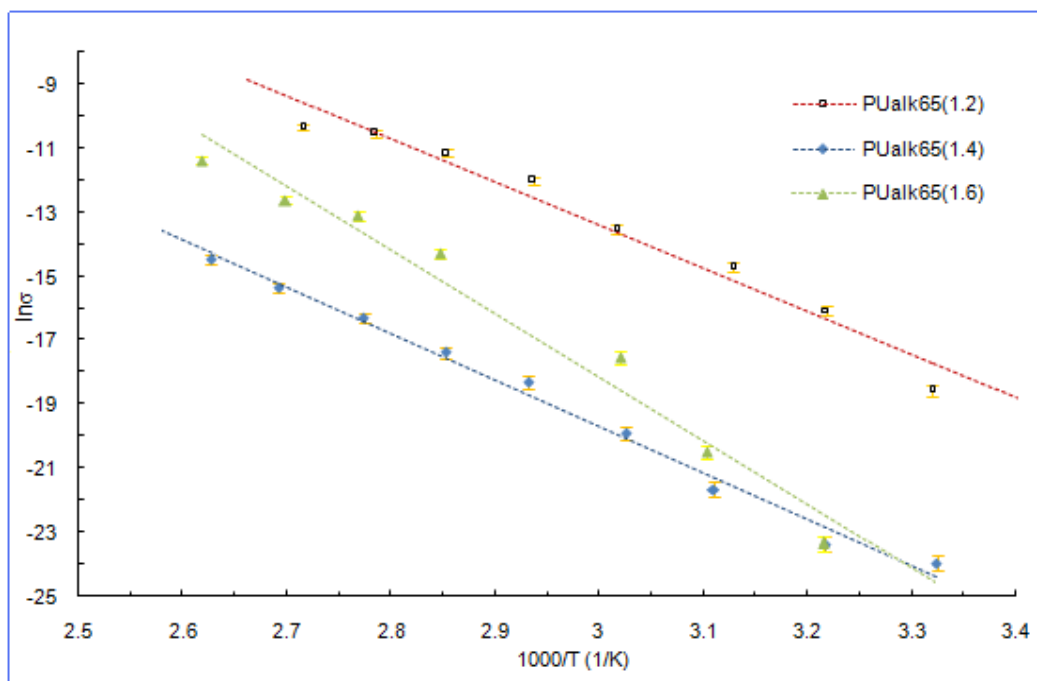


Figure 5.16 Arrhenius plots of PUalk65 with NCO/OH ratio of 1.2, 1.4 and 1.6

From the slope of the straight lines of Arrhenius plot in Figure 5.14 to 5.16, activation energies E_a were evaluated. Values of the activation energies obtained from the curve are reported in Table 5.3. According to reference (VG Shteinberg et al., 1980), the activation energy of a cross-linked PUR is 27 kcal/mole or ~ 1.2 eV. The activation energies obtained for the PUR samples in this work range between 0.8 - 1.7 eV. The activation energies are markedly changed from lower to higher values as the oleic acid content of the polyols of the sample increased suggesting that there is a change in the conduction mechanism.

Table 5.3 Activation energies derived from Arrhenius plot

	NCO/OH ratio	E_a (eV)
PUalk28	1.2	0.80 ± 0.07
	1.4	0.95 ± 0.06
	1.6	0.92 ± 0.05
PUalk40	1.2	1.01 ± 0.08
	1.4	1.0 ± 0.1
	1.6	1.1 ± 0.1
PUalk65	1.2	1.16 ± 0.09
	1.4	1.25 ± 0.04
	1.6	1.7 ± 0.1

In order to clarify conduction mechanism at the specified field, a wide variety of plots of the current versus voltage relationship have been tried in the present work (Mott and Gurney, 1948 (exponential plot), Lampert and Mark, 1970 (space-charge limited conduction (SCLC) plot), Lengyel, 1966 & Jonscher, 1967 (Schottky plot), Hill, 1971 (Poole plot), Ieda et al., 1971 (Poole-Frenkel plot)). Of these, the exponential and Schottky plots are shown in Figures 5.17 and 5.18.

The effect of oleic acid percentage in conductivity mechanism in PUR determined with NCO/OH ratio constant at 1.6. Figure 5.17 shows the typical field dependence of current density, $J(E)$ at various temperatures for PUalk28, PUalk40 and PUalk65 of NCO/OH ratio 1.6. Figure 5.17, shows that $J(E)$ is ohmic at low electric field and non-

ohmic at high fields. This feature indicates the lowering of lifetime of the trapped carriers in defect or localized states with increasing temperature, which increases the density of free carriers. Consequently, the transition from ohmic to non-ohmic behaviour occurs at high temperature and field.

Figure 5.18 shows the plot of current density as function of $E^{1/2}$ (Schottky plot) at various temperatures ranging from 28⁰C to 110⁰C. The Schottky emission mechanism is an electrode-limited conduction, occurring at low voltages at which the electrons on the surface of the injecting electrode transit above the potential barrier. The experimental results does not show a linear variation of $J(E)$ with respect to $E^{1/2}$ over a wide range of temperature and fields. The non-linear behaviour cannot be solely explained on the basis of either Schottky or Poole-Frenkel type of charge transport mechanism. However, the experimental results suggest that the carriers trapping and re-trapping events subsequently play an important role in determining the type of transport mechanism at different temperatures and fields.

Figures 5.19 to 5.21 show the typical hyperbolic sine function model fit performed on PUalk28, PUalk40 and PUalk65 for NCO/OH ratios 1.2 and 1.6 at various temperatures. The experimental values are represented by the dotted points and continuous lines correspond to simulated fit. The experimental data are well-matched particularly at high field regions with hyperbolic sine function Equation 5.20. This phenomenon suggest that ion hopping is presumably the predominant conduction mechanism at high field region for the PUR.

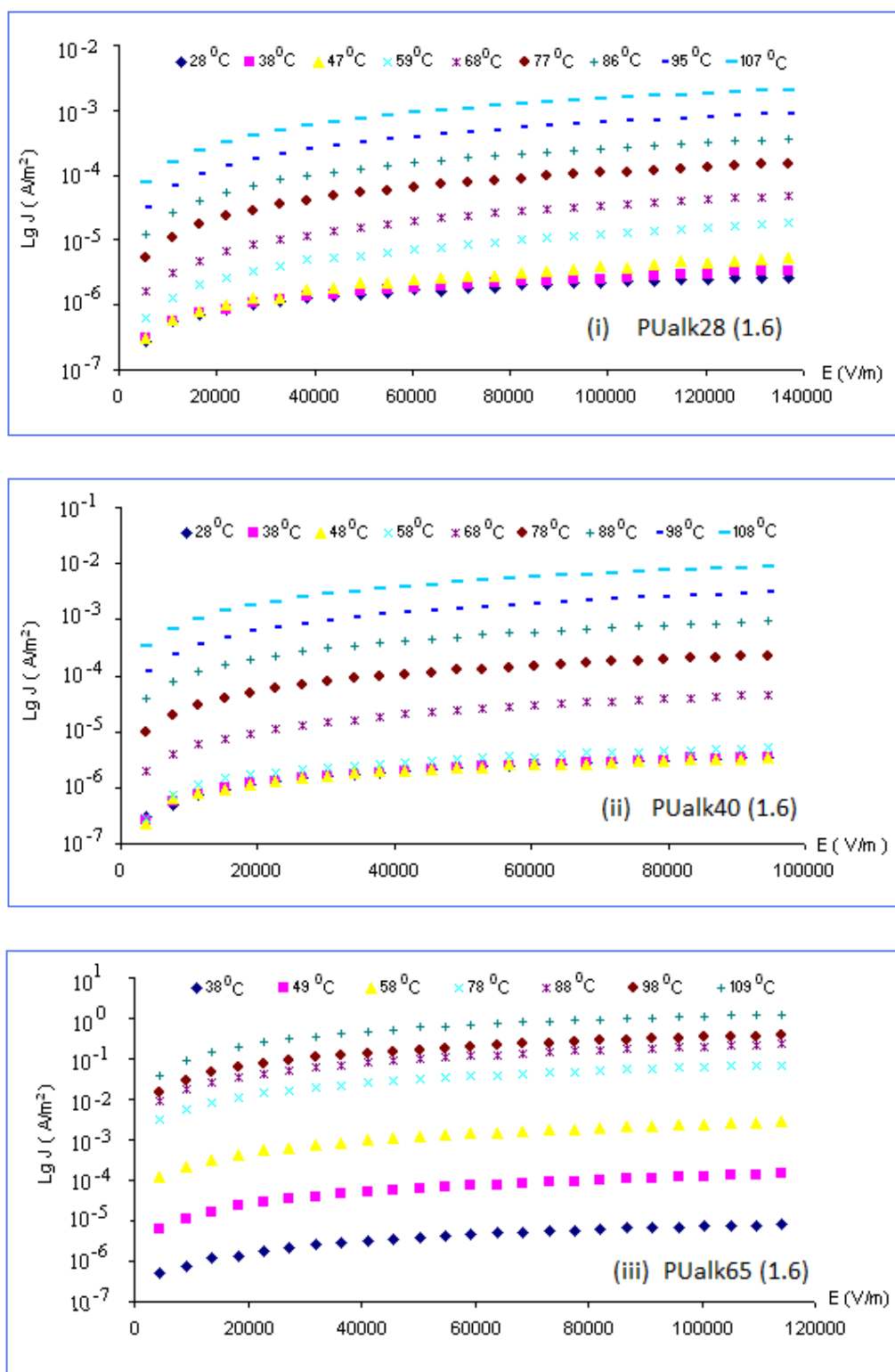


Figure 5.17 Exponential plot at various temperatures for (i) PUalk28 (1.6), (ii) PUalk40 (1.6), (iii) PUalk65 (1.6)

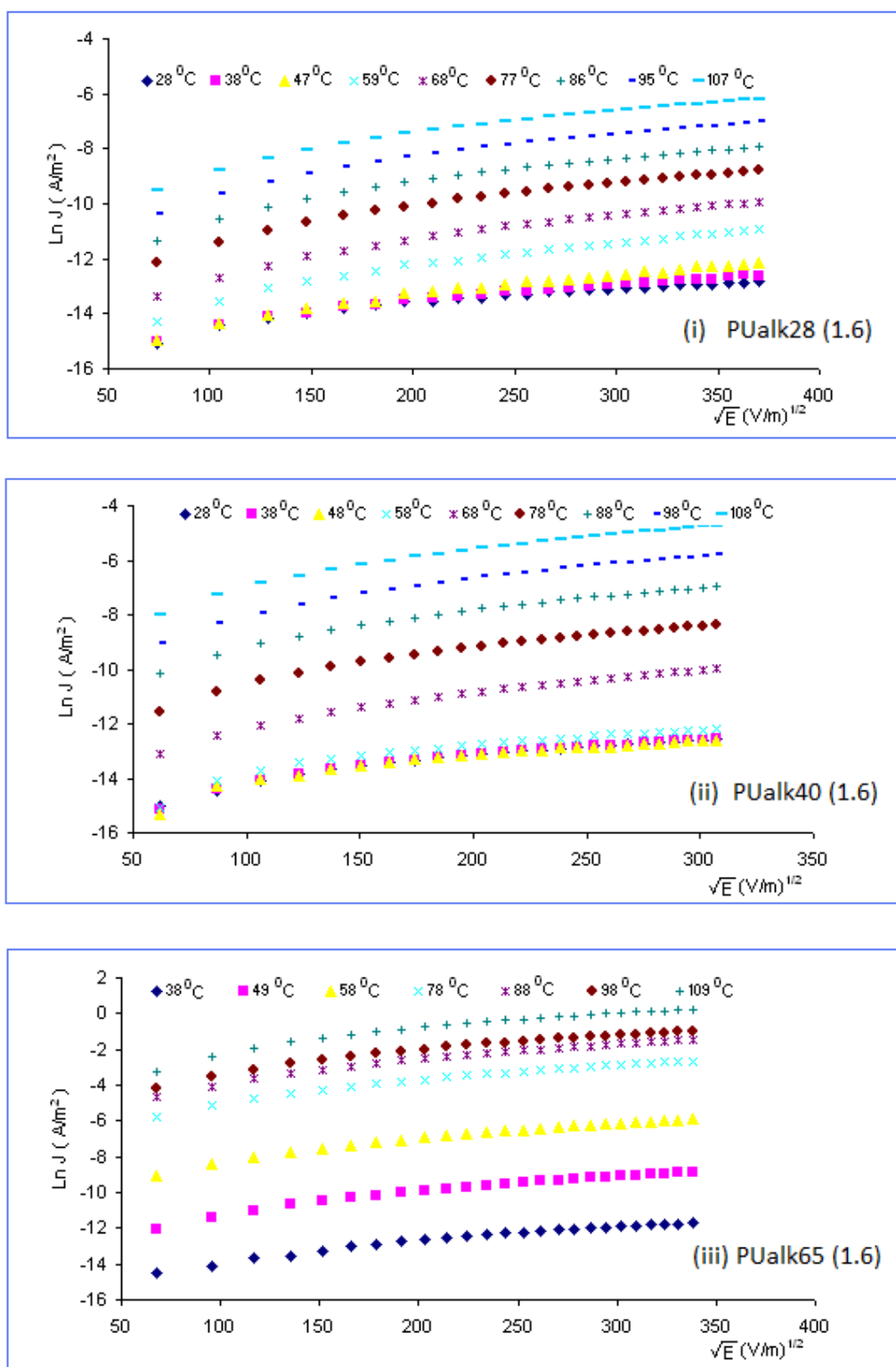
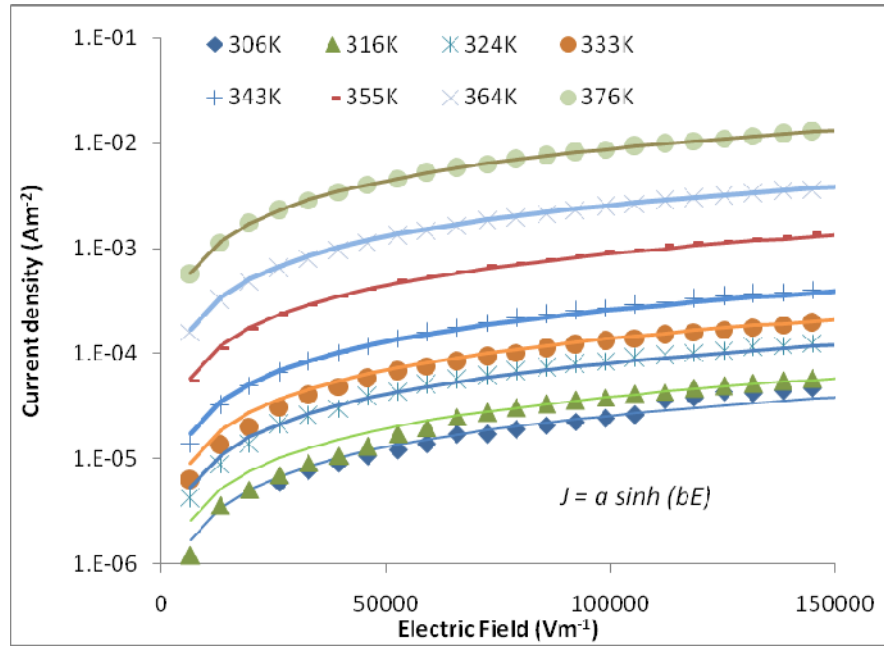
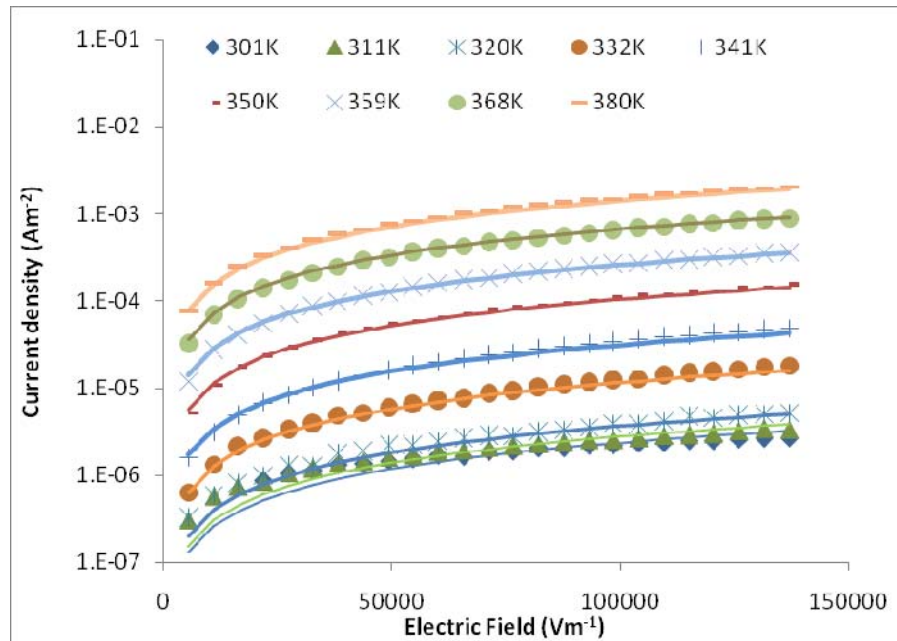


Figure 5.18 Schottky plot of (i) PUalk28 (1.6), (ii) PUalk40 (1.6) and (iii) PUalk65 (1.6) at various temperatures

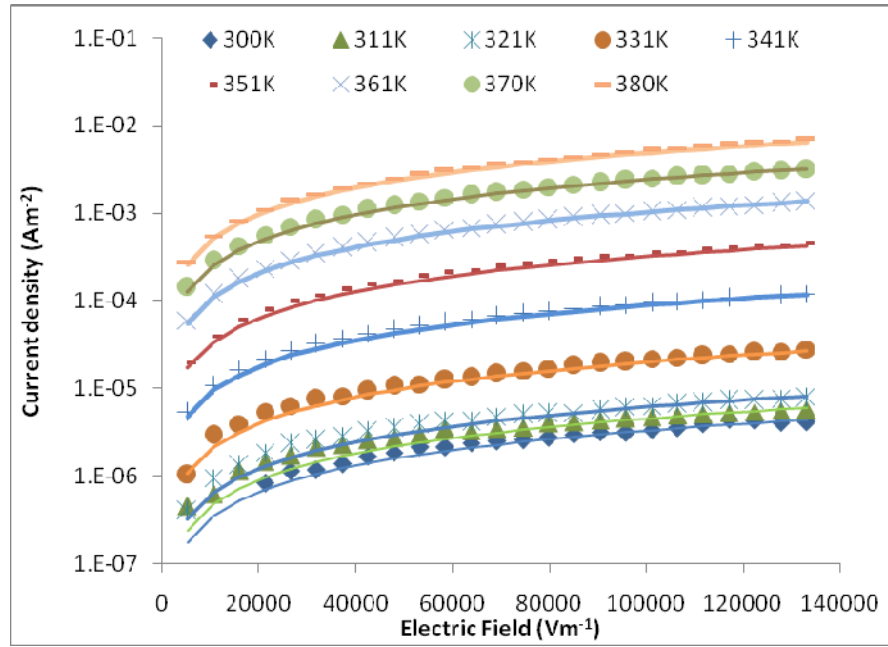


(i)

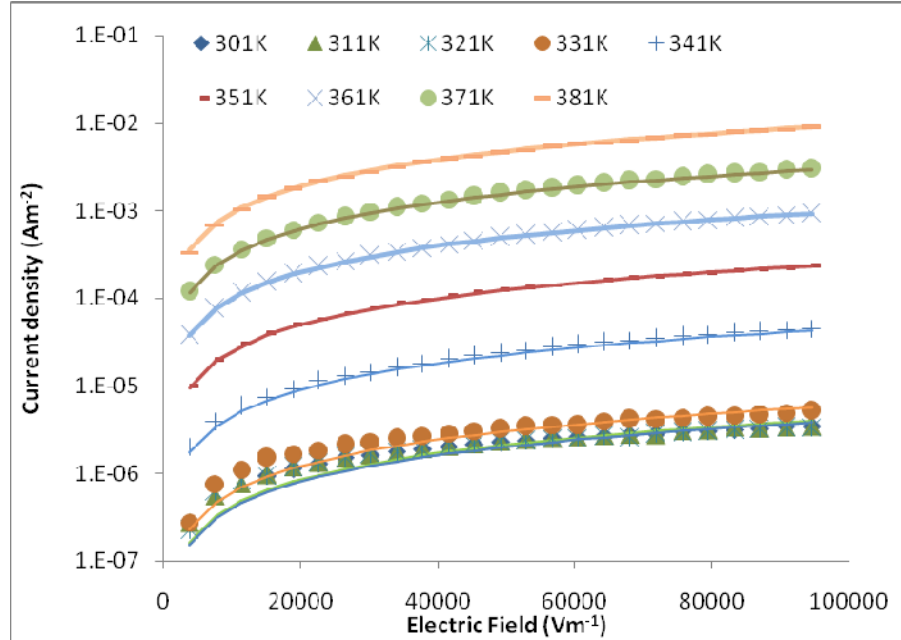


(ii)

Figure 5.19 Typical hyperbolic sine function model fit performed on (i) PUalk28 (1.2) (ii) PUalk28 (1.6). Dots are experimental points and continuous lines corresponds to simulated fit.

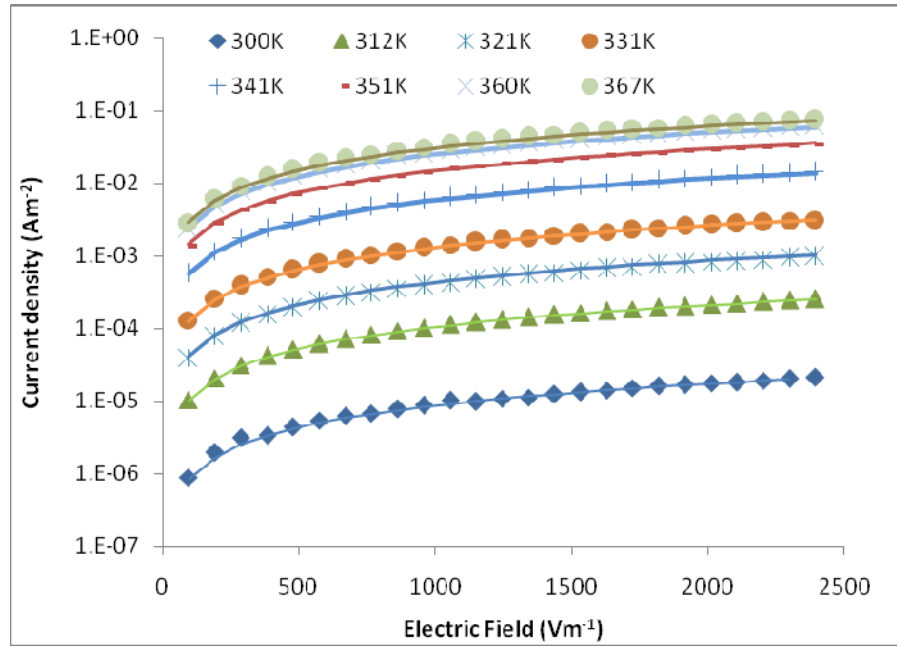


(i)

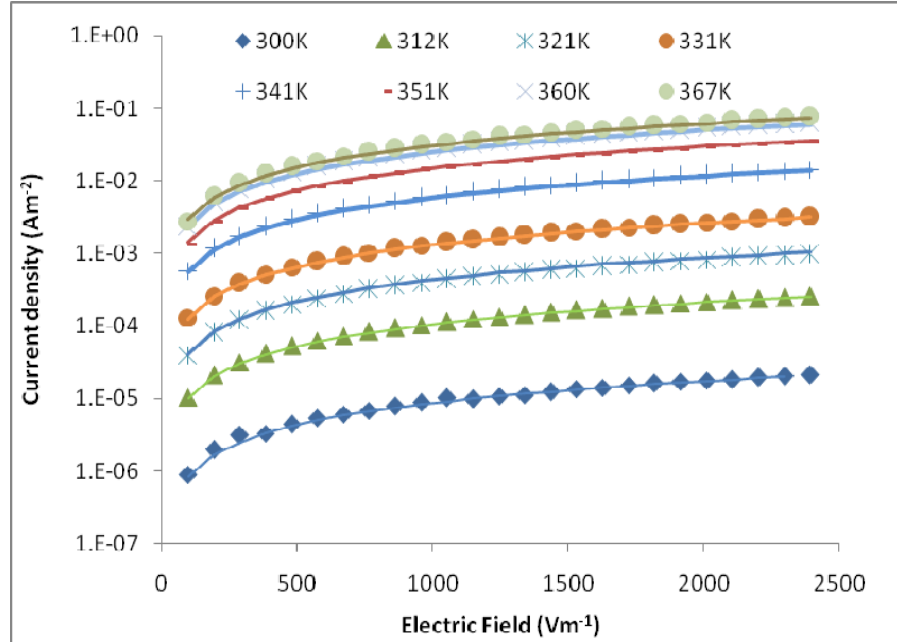


(ii)

Figure 5.20 Typical hyperbolic sine function model fit performed on (i) PUalk40 (1.2) (ii) PUalk40 (1.6). Dots are experimental points and continuous lines corresponds to simulated fit.



(i)



(ii)

Figure 5.21 Typical hyperbolic sine function model fit performed on (i)PUalk65 (1.2) (ii) PUalk65 (1.6). Dots are experimental points and continuous lines corresponds to simulated fit.

When conduction by an ionic mechanism takes place, the conduction ion moves from one interstitial position to the next as when it acquires sufficient energy to overcome the potential energy barrier. The jump distance from one position to the next was calculated from the hyperbolic sine relationship between the current and voltage of PUR. From these results, the hopping distance is evaluated. Figure 5.22 shows the plot of hopping distance λ as a function of T ranging from 300 to 380K. In the present case, $\lambda(T)$ increases gradually as T rises.

Figures 5.22 (i), (ii) and (iii) show the effects of NCO/OH ratios on the hopping distance of PUR. From the observations of the plots, it is noticed that for PUalk28, the hopping distance is almost the same below 360K for all the NCO/OH ratios. Above 360K, PUalk28 (1.2) has the highest hopping distance followed by PUalk28 (1.6) and PUalk28 (1.4). As for PUalk40, a similar trend is observed as in PUalk28, where the hopping distance is almost the same for all the samples below 360K, but above 360K, the hopping distance is higher for PUalk40 (1.2). However, as the temperature increased further, the hopping distance of PUalk40 (1.6) eventually increased above that of PUalk40 (1.2) and PUalk40 (1.4). As for PUalk65, PUalk65 (1.2) has the highest hopping distance followed by PUalk65 (1.6) and PUalk65 (1.4) along the investigated temperature range.

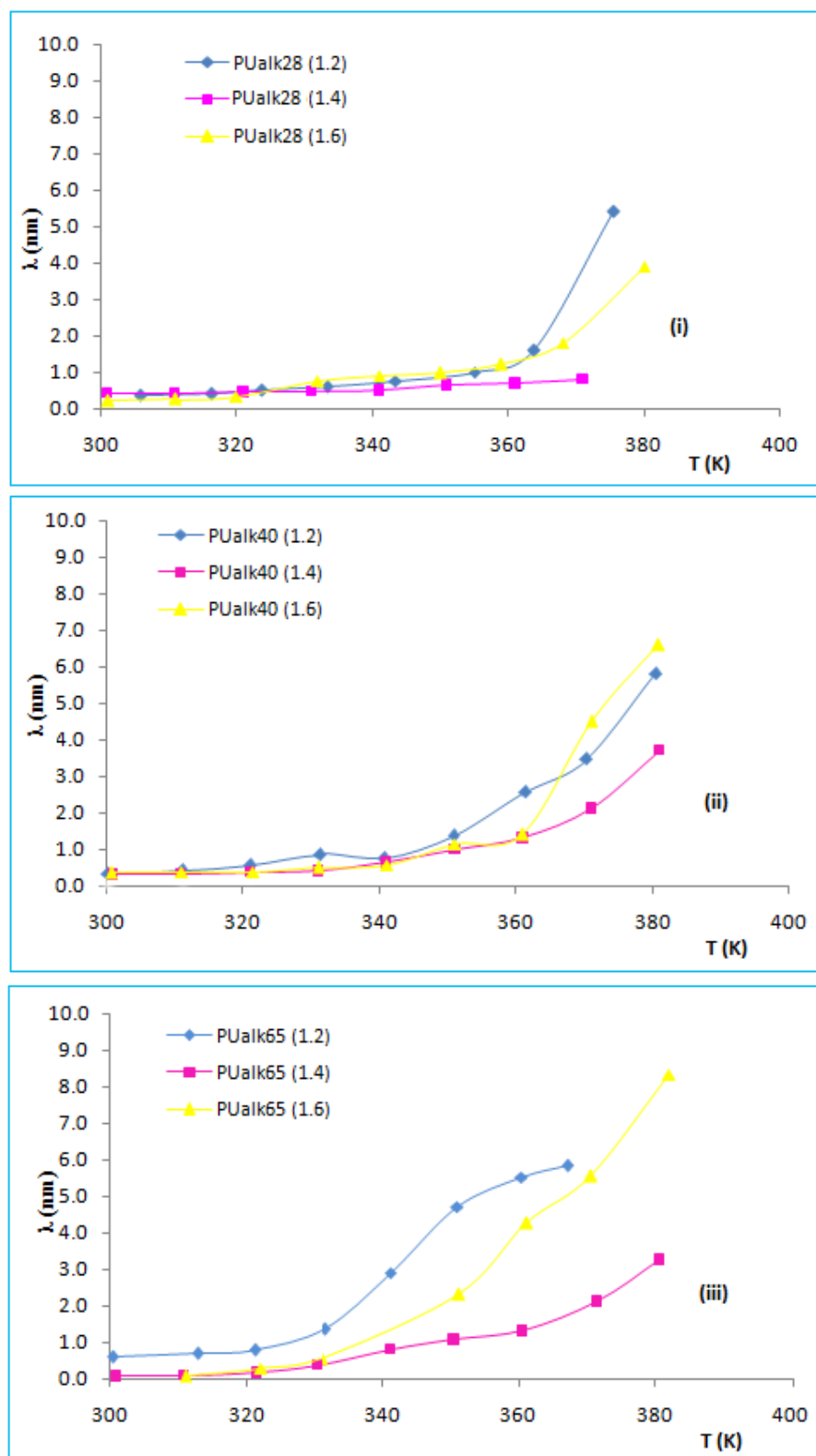


Figure 5.22 Plot of hopping distance, λ as a function of temperature (i) PUalk28 (ii) PUalk40 (iii) PUalk65 for NCO/OH ratio 1.2, 1.4 & 1.6.

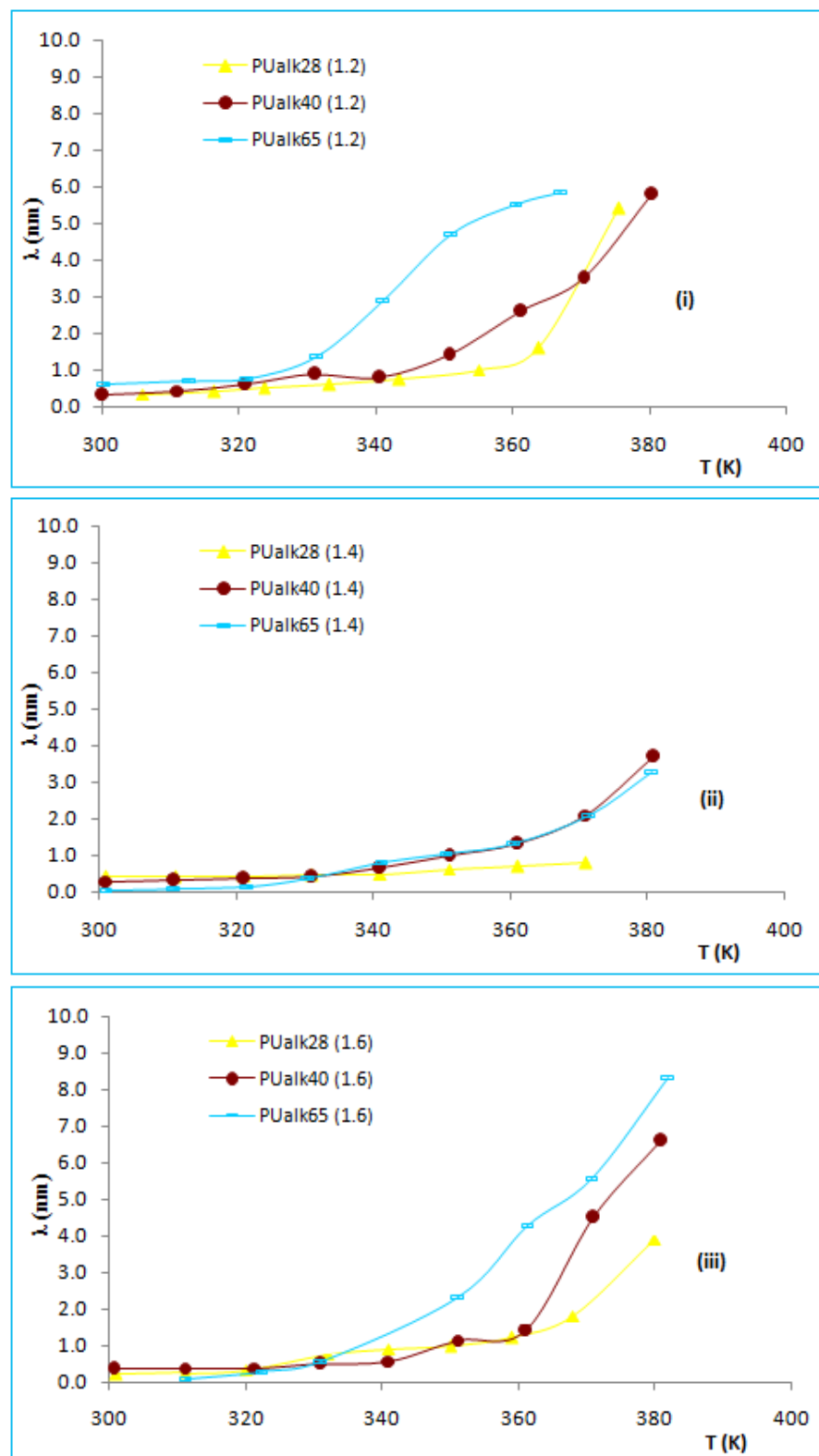


Figure 5.23 Plot of hopping distance, λ as a function of temperature at fixed ratios (i) 1.2 (ii) 1.4 (iii) 1.6 for all the PURs

Figure 5.23 shows the effects of oleic acid content at fixed NCO/OH ratios for the hopping distance of the ions. At fixed NCO/OH ratios of 1.2 and 1.6 (refer to Figure 5.23 (i) and (iii)), below 330K, the λ is the same for all the samples. Above 330K, the λ value follows the range as PUalk65 > PUalk40 > PUalk28. However, the λ value is almost the same for all the PUR samples along the investigated temperature range for fixed NCO/OH ratio of 1.4. Therefore, from the above observation it can be concluded that the higher the oleic acid content in polyols the higher the λ in the samples at the temperature above 330K.

5.3.4 Discussion

Dc conduction for some polymeric materials is not identical for below and above T_g ; a temperature at which physical properties undergo sudden changes. However, electrical conduction for polymeric materials not only depends on the T_g of the material but also on chemical composition, structural features associated (Leonard E. Amborski, 1962) with the degree of molecular order and of the physical significance due to the polymer preparation (MD Migahed et al., 1982).

Below T_g , motions of α type are no longer possible and the molecular configurations are frozen, the volume of free space or voids remain constant. At T_g a constant ratio between the volume of the voids and the total free volume is achieved independently. Free volume represents the sum of the volumes assigned to molecular vibration and of free space between the molecules. Assuming for the motions producing the maximum α , a minimum void volume is necessary (A Lupu et al., 1974).

For every thermally activated segmental motion of the polymer chain, which produces the dielectric α and β absorption, there exist some probability that a favourable configuration will be realized for hopping of the carrier in the direction of the electric field. In such hopping the carrier passes from a site corresponding to a minimum potential to another similar site possibly situated on another molecule. Thus, the molecular motions responsible for the dielectric absorption also allow dc conduction. The probability of the carrier hopping is presumably lower for motion below T_g involving smaller parts of the molecular chains than for motions taking place above T_g . This may account for greater conductivity in region above T_g . However, this discussion will be only on region below T_g since the T_g for all PUR samples are around $123^\circ \pm 0.2^\circ\text{C}$ (refer to Table 3.6).

According to the proposed conduction mechanism, the observation reported above may be interpreted as follows:

1. Decrease in NCO/OH ratio shows a trend of decrease in the activation energy for all the samples. A decrease in NCO/OH is accompanied by an augmentation or expansion of the free volume. This brings about an increase in the frequency of the motions which favours the hopping of the carriers. For example, with reference to Figure 5.14 (PUalk28), for NCO/OH ratio 1.2, the free volume is considered to be high which favours the hopping and therefore the conductivity is higher compared to the ratio of 1.6 where the free volume is less and thus reduces the conductivity of the samples. As a result, conductivity should increase as NCO/OH ratio decreases. Furthermore, the slopes depending on NCO/OH ratio, suggest that the ratios do modify the height of potential barriers

and the rate of hopping. Hence, as the NCO/OH ratio increased the E_a , activation energy increased too.

2. The E_a also increases as the oleic acid content of the polyols increased. As the oleic acid content increases, the phase present in larger amount will form continuous matrix and control most of the properties of the sample. For PUalk65, the polyols contain a higher percentage of oleic acid and thus, presumably the higher amount of side chain resulting copolymer separate into microphase. The conduction mechanism occurs in PUalk65 is dependent on the oleic acid content and cross-linking and there is also a competing effect between them. The carriers in the microphase segments no longer possess the freedom of movement, being trapped or more firmly bound, thus reducing the overall number of carriers. Thus, potential barrier increases causing the E_a to increase.
3. In PUR it is understood that the charge carrier are pre-existent in the polymer and not being thermally created (J Gowri Krishna et al., 1982). Consequently, the temperature only influences the rate of hopping i.e. the carrier mobility.
4. The free carriers which exhibit electrical conductivity in polymers may be ions or electrons. These free carriers may have exist in the polymer molecules and they can either hop from site to site or move through a conduction band under the influence of an applied electrical field. If an ionic mechanism is assumed, the greater conductivity at the elevated temperature can be accounted for by the presence of a greater number of ions (Leonard E Amborski, 1962). The source of this may be ionic dissociation; the number of ions increasing exponentially with temperature. Another possibility is that the mobility of the ions is also enhanced due to a reduction in the internal viscosity of the polymer as the temperature is increased.

The non-linear behaviour of the Schottky plot in Figure 5.18 at the high fields and temperature can be considered in terms of the hopping mechanism (Das Gupta et al., 1976 & 1980). Generally, a free volume of polymer is increased with an increase in temperature. The increase in free volume can facilitate the motion of ionic charges in the bulk. By the high external field, ionic carriers move to the electrode and accumulate on the interface between the bulk and electrode, resulting in a diminishing ionic concentration in the bulk and decrease in the conduction current (DW Kim et al., 2000).

The conduction mechanism in the PUR samples presumably to be ionic due to protons originating from oleic acid content in the samples. In ionic conduction, the current is determined by the migration of ions and expressed by hyperbolic sine function (Equation 5.22). In the present case, the conduction mechanism at higher field in PUR analyzed by hyperbolic sine function model gives a better fit compared to the other models. Figure 5.19 to 5.21 show the results of theoretical (solid line) and experimental data under the ionic conduction at various temperature. The experimental data are fairly well matched with the Equation 5.22 at high field regions. This phenomenon suggest that in this case, at higher field region, presumably ion hopping is the predominant conduction mechanism for PUR.

The charge carriers acquire energy and hop between sites. The variation of λ in temperature has been often observed in the case of other organic polymer (AA Alagiriswamy et al., 2002, Leonard E Amborski, 1962, Miyamoto T., 1974). Furthermore, the values estimated by different authors vary considerably and the ionic jump distance may show strong or moderate variation with T depending on the charge carriers. An electron can travel over a large distance particularly in regular lattice but an ion is a relatively massive particle which hops into an adjacent site, unlikely to travel

over a large distance. In summary, the results obtained in this research support the ionic conduction by migrations of ions since the hopping distance obtained for all the PUR samples are below 10 nm which is considered as a small distance (AA Alagiriswamy et al., 2002).

The charge carriers or ions are from the system itself. Self ionization of urethane groups (SSN Murthy, 1988) and protons originating from oleic acid can be a potential source of ions other than water. The protons from self ionization of urethane groups can contribute to conduction above glass transition temperature of hard segments where their mobility is greater. When the temperature increases their contribution to conductivity also increases. Protonic contribution increases with temperature due to the gradual removal of constraints on proton mobility (SSN Murthy, 1988).

Basically, as NCO/OH ratio increases, the cross-linking increases and thus the localized bonding force between neighbouring chains also increases. This could result in small spacing for movement of ions in the bulk with the ion hopping becoming easy. Therefore, it is assumed that the hopping distance is higher for PUR with lower NCO/OH ratio compared to PUR with higher ratios. Moreover, the hopping distance is also affected by the contribution of protons from the oleic acid content in the polyols. As the oleic acid content increases in the samples, the protonic contribution may increase. Consequently, as the temperature increases, the number of protons increases with temperature thus increasing the hopping distance. Another possibility is that the mobility of the ions is increased by the reduction of internal viscosity of the polymer as the temperature increases.

5.4 Conclusion

The ac conductivity and dielectric behaviour of PUR have been studied as a function of frequency at room temperature. Dielectric parameters are in the range of 2.0 to 3.0 for real permittivity ϵ' and 0.02 to 0.08 for imaginary permittivity, ϵ'' . Cole-Cole plot was fitted successfully using Havriliak-Negami model. The γ -relaxation is proposed as the probable mechanism for the dielectric behaviour of PUR in the research. The dielectric constant and loss mechanism of the material are found to be dependent on variation of frequency, NCO/OH ratios and polyols used in synthesizing the PUR. The frequency dependent permittivity shows dielectric dispersion and variation of dielectric constant with frequency is ascribed to the contribution of charge carriers. The frequency dependent conductivity of PUR materials has been analyzed using a Jonscher's power law expression.

DC conductivity study on PUR and the Arrhenius dependence suggest a charge carrier diffusion-controlled conductivity mechanism. From the Arrhenius plots, the activation energies of the material below T_g were obtained. The activation energies increase as the oleic acid content and NCO/OH ratio increases. DC conductivities obtained for the samples are in the range of 10^{-8} to 10^{-12} Sm^{-1} . There are several conduction mechanisms occurring in the material. The analysis of dc conductivity data shows that the transport of charge carriers in the investigated system is through ionic hopping mechanism. The hyperbolic sine function was used to estimate the hopping parameters $\lambda(T)$ for PUR of this study. It is presumed that the conduction mechanism is assisted by ions for all the PURs. The ions are contributed by oleic acid due to dissociation of protons which originated from oleic acid content and highly polar urethane groups in the PURs.

References

- A Korzhenko, M Tabellout, JR Emery, 1999. Influence of a metal-polymer interfacial interaction on dielectric relaxation properties of polyurethane. *Polymer*, **40**, 7187-7195.
- AA Alagiriswamy, KS Narayan, Govinda Raju, 2002. Relaxation processes in aromatic polyimide. *Journal of Physics D: Applied Physics*, **35**, 2850-2856.
- A K Jonscher 1970. Free-carrier Poole-Frenkel effect in crystalline solids. *Journal of Physics C: Solid State Physics*, **3**, L159-L162.
- Alex P, Lynn D., 2003. The role of materials properties in antenna performance. Motorola. <http://rf.rfglobalnet.com/library/Papers/files/2/perrotta.htm>
- Annual Book of ASTM Standards, 1994. D150, Standard Test method for AC loss characteristics and permittivity of solid electrical insulation. Vol 10, pg 31-48
- Apekis L., Pissis P., Christodoulides C., Spathis M, Niaounakis E, Kontou E., Schlosser E., Schoenhals A, Goering H., 1992. *Progress Colloid Polymer Science*, **90**, 144.
- Billmeyer FW Jr, 1971. A Textbook of Polymer Science. New York: Wiley, p 241.
- Blythe AR, 1977. Electrical properties of polymers, Cambridge University Press.
- Bor-Sen Chiou, Paul E. Schoen, 2002. Effects of cross-linking on thermal and mechanical properties of polyurethanes. *Journal of Applied Polymer Science*, **83**, 212-223.
- Cole K S, Cole R H, 1941. Dielectric constants of aliphatic ketones. *Journal of Chemical Physics*, **9**, 341.
- CP Chwang, CD Liu, SW Huang, DY Chao, 2004. Synthesis and characterization of high dielectric constant polyaniline / polyurethane blends. *Synthetic Metal*, **142**, 275-281.
- Daniel V, 1967. Dielectric relaxation. New York: Academic.

Das-Gupta DK, Doughty K and Brockley RS, 1980. Charging and discharging currents in polyvinylidene fluoride. *Journal of Physics D: Applied Physics*, **13**, 2101-14.

Das-Gupta DK, Joyner K, 1976. A study of absorption currents in polypropylene. *Journal of Physics D: Applied Physics*, **9**, 2041-48.

Dev SB, AM, Reid JC, 1972. Dielectric Properties of Polymers. FE Karasz (new York: Plenum) p 217.

Dissado L A, Green P W, Hill R M and Strivens T A, 1989. Power-law decay of conductance during the drying of latex paints. *Journal of Physics D: Applied Physics*, **22**, 713.

Fontanella JJ, Wintersgill MC, Smith MK, Semancik J, Andeen CG, 1986. Effect of high pressure on electrical relaxation in poly(propylene oxide) and electrical conductivity in poly(propylene oxide) complexed with lithium salts. *Journal of Applied Polymer Science*, **60**, 2665.

Froix MF, Pochan JM, 1976. *Journal of Polymer Science Physics Ed.*, **14**, 1047.

Geoffrey O, Ju-Young K, 2008. Conductive graphite/polyurethane composite films using amphiphilic reactive dispersant: Synthesis and characterization. *Journal of Industrial and Engineering Chemistry*, **article in press**.

Georgoussis G., Kyritis A., Bershtein VA., Fainleib AM., Pissis P., 2000. Dielectric studies of chain dynamics in homogeneous semi-interpenetrating polymer networks. *Journal of Polymeric Science B*, **38**, 3070.

Gowri Krishna J, Josyulu OS, Sobhanadri J, Subrahmaniam R., 1982. Dielectric behaviour of isocyanate-terminated polymers. *Journal Physics D: Applied Physics*, **15**, 2315-2324.

Hanai T, Sherman P (editor), 1968. Emulsion Science, London :Academic Press, p 353

Havriliak S., Negami S., 1966. A complex plane analysis of a-dispersion in some polymer systems. *Journal of Polymeric Science., Polymer Symposium*, **14**, 89.

Havriliak S., Negami S., 1967. A complex plane representation of dielectric and mechanical relaxation processes in some polymers. *Polymer*, **8**(4), 161.
Hedvig P, 1977. Dielectric spectroscopy of polymers. Adam Hilger Ltd., Bristol, 293-296.

Hill RM, 1971. *Philosophical Magazine*, **23**, 59-86.

Hsing-Lung Wang, Chao-Ming Fu, A. Gopalana, Ten-Chin Wena, 2004. Frequency dependent conductivity of the thin film blend of electroluminescent poly(p-phenylene vinylene) with waterborne polyurethane as ionomer. *Thin Solid Films* **466**, 197– 203.

Huang SL., Lai JY, 1997. Structure-tensile properties of polyurethane. *European Polymer Journal*, **33**, 1563-1567.

Ieda M, Sawa G, Kato S, 1971. A Consideration of Poole-Frenkel Effect on Electric Conduction in Insulators. *Journal of Applied Physics*, **42**, 3737-40.

Ikezaki K, Kanebo T and Sakakibara T, 1981. Effect of Crystallinity on Electrical Conduction in Polypropylene. *Japanese Journal of Applied Physics*, **20**, 609-615.

Ion Bunget, Mihai Popescu, 1984. Physics of Solid Dielectric. In: Material Science Monographs, 19, New York: Elsevier; (chapter 5, pg 164-165)

Jacobs H, Jenckel E., 1961. *Macromolecular Chemistry*, **38**,168.

Jonscher AK, 1967. Electronic properties of amorphous dielectric films. *Thin Solid Films*, **1**, 213-34.

^aKanapitsas A, Pisis P, Karabanova L, Sergeeva L, Apekis L.1998. Broadband dielectric relaxation spectroscopy in interpenetrating polymer networks of polyurethane-copolymer of butyl methacrylate and dimethacrylate triethylene glycol. *Polymer Gels Networks*, **6**, 83.

^bKanapitsas A, Pisis P, 2000. Dielectric relaxation spectroscopy in cross-linked PUR based o polymer polyols. *European Polymer Journal*, **36**, 1241-1250.

^cKanapitsas A., Pisis P., Garcia Estrella A., 1999. Molecular mobility in polyurethane/ styrene-acrylonitrile blends studied by dielectric techniques. *European Polymer Journal*, **35**, 923.

^dKanapitsas A., Pissis P., Gomez Ribelles JL, Monleon Pradas M, Privalko EG, 1999. *Journal of Applied Polymer Science*, **71**, 1209.

Kim DW, Yoshino K, 2000. Morphological characteristics and electrical conduction in syndiotactic polypropylene. *Journal of Physics D: Applied Physics*, **33**, 464-471.

Korzhenko AA, Tabellout M, Emery JR., 2000. Dielectric relaxation properties of the polymer coating during its exposition to water. *Material Chemistry and Physics*, **65**, 253-260.

Lampert MA, Mark P, 1970. *Current Injection in Solids*. New York, Academic Press.

Lengyel G, 1966. Schottky emission and conduction in some organic insulating materials. *Journal of Applied Physics*, **37**, 807-10.

Leonard E Amborski, 1962. Structural dependence of the electrical conductivity of polyethylene terephthalate. *Journal of Polymer Science*, **62**, 331-346.

Lupu A, Baltog L, 1974. Mechanism of dc electrical conductivity in Poly (vinyl Chloride). *Journal of Polymer Science: Polymer Physics Edition*, **12**, 2399-2407.

McCrum NG, Read BE, Williams G, 1967. *Anelastic and dielectric effects in polymeric solids*. John Wiley, New York.

MD Migahed, A Tawansi, NA Bakr, 1982. Relaxation phenomena and electrical conductivity of some polymeric films. *European Polymer Journal*, **18**, 975-980.

Mott NF and Gurney RW, 1948. *Electronic Processes in Non-Crystalline Materials*. London: Oxford UP.

Ngai KL., 1991. Test of expected correlation of polymer segmental chain dynamics with temperature-dependent time-scale shifts in concentrated solutions. *Macromolecules*, **24**, 4865.

North AM., Reid JC., 1972. Dielectric relaxation in a series of heterophase polyether polyurethanes. *European Polymer Journal*, **8**, 1129-1138.

^aPissis P., Apekis L., Christodoulides C., Niaounakis, Kyritis A., Nedbal J., 1996. Water effects in polyurethane block copolymers. *Journal of Polymeric Science B: Polymer Physics*, **34**, 1529.

^bPissis P., Georgoussis G., Bershtein VA., Neagu E., Fainleib AM., 2002. Dielectric studies in homogenous and heterogeneous polyurethane/polycyanurate interpenetrating polymer networks. *Journal of Non-Crystalline Solids*, **305**, 150-158.

^cPissis P., Kanapitsas A., Savelyev YV, Akhranovich ER, Privalko EG, Privalko VP., 1998. Influence of Chain Extenders and Chain End Groups on properties of Segmented Polyurethanes II. Dielectric Study. *Polymer*, **39**, 3431.

PS Anantha, K Hariharan, 2005. Ac conductivity analysis and dielectric relaxation behaviour of NaNO₃-Al₂O₃ composites. *Material Science and Engineering*, **B 121**, 12-19.

RH Cole, 8-11 September 1980. Molecular correlation function approaches to dielectric relaxation. *Institute of Physics Conference series No. 58, Invited paper presented at Physics of Dielectric Solids, Canterbury*.

S. Desai, I.M. Thakore, B.D. Sarawade, S. Devi, 2000. Effects of polyols and diisocyanates on thermo-mechanical and morphological properties of polyurethanes. *European Polymer Journal*, **36**, 711-725.

Spathis G, Kontou E, Kevalas V, Apeki L Christodoulides C, Pissis P, Olivon M, Quinquenet S., 1990. Relaxation phenomena and morphology of polyurethane block copolymers. *Journal of Macromolecular Science Physics*, **29**, 31-48.

SSN Murthy, 1988. The temperature dependence of DC conductivity in some hydrogen-bonded polymers. *Journal of Physics D: Applied Physics*, **21**, 1171-1181.

Szycher Michael, 1999. Szycher's Handbook of Polyurethane. CRC Press LLC. Chapter 3, pg 17-32.

^aTsonos C, Apekis L, Viras K, Stepanenko L, Karabanova L, Sergeeva L, 2001. Electrical and dielectric behaviour in blends of polyurethane-based ionomers. *Solid State Ionics*, **143**, 229-249.

^bTsonos C, Apekis L, Zois C, Tsonos G., et al., 2004. Microphase separation in ion-containing PUR studied by dielectric measurements. *Acta Materialia*, **52(5)**, 1319-1326.

VG Shteinberg, Yu. A. Ol'Khov, AG Melent'ev, SM Baturin, 1980. The effect of cross-linking density on dielectric relaxation in PUR elastomers. *Polymer Science U.S.S.R.*, **22**, 269-274.

Zuo M, Takeichi, 1999. Preparation and characterization of poly(urethane-imide) films prepared from reactive polyimide and polyurethane prepolymer. *Polymer*, **40**, 5153-5160

Zilg C, Thomann R, Mülhaupt R, Finter J, 1999. Polyurethane Nanocomposites Containing Laminated Anisotropic Nanoparticles Derived from Organophilic Layered Silicates. *Advanced Material*, **11**, 49-52.

Zoran S. Petrovic, Dragica Fajnik, 1984. Preparation and properties of castor oil based polyurethanes. *Journal of Applied Polymer Science*, **29**, 1031-1040.

6.1 Introduction

Mechanical properties of polymers are usually described with parameter such as modulus elasticity, yield and tensile strengths. A simple stress-strain test is essential in characterizing some of these mechanical parameters for many polymeric materials [ASTM D638]. Polymer chain microstructure, the relationship between morphology, bulk properties, chain conformation and inter chain effects have profound effect on the mechanical properties of a material. At low strain (i.e., <1%), the deformation of most polymers are elastic. The deformation is homogeneous and full recovery can occur over a finite time. However, at higher strains, the occurrence of polymers deformation depends on the characteristic of the polymers.

As for PUR, generally the mechanical properties are mostly controlled by molecular flexibility, crystallinity and cross-linking. For instance, the introduction of cross-links between PUR molecules produces restriction of molecular mobility. At low degrees of cross-linking where long segments of the backbone molecule are still free to move with a little loss of soft flexible rubbery behaviour, there is a distinct improvement in strength and creep resistance. At increased degree of cross-linking, modulus increases and extensibility decreases, giving tough flexible products. At higher degrees of cross-linking, the polymer molecules are immobilized and become rigid thermoset polymer. Thus cross-linking alone can develop a broad spectrum of PUR properties and products (Szycher M., 1999).

The structure of the paint is determined through studying the properties of the detached films. The determination of ultimate values for extension and tensile strength followed by the study of creep and recovery which involves smaller stresses on the film will have a relation to adhesion characteristic in forecasting the service life of the film (Taylor CJA. et al., 1965). The mechanical properties of oleic acid polyol based polyurethanes are addressed in this chapter. Basically, two types of testing are performed. First is the tensile measurement where the tensile strength and extensibility of the material are investigated. Secondly, the creep and recovery of material at constant load and time are determined. The literature review, theory, experimental details, results and discussion on the mechanical testing performed will be outlined and discussed in this chapter.

6.2 Literature review

The mechanical properties of a material depend very much on the effect of stress on the material. Materials may react in various ways to an applied stress. Laboratory tests for measuring mechanical properties are static test, cyclic test and impact test. In the static test, loads are applied slowly so that the quasistatic equilibrium of forces is maintained and in the cyclic test, loads are applied partly or wholly and then removed or reversed for a sufficient number of times to cause the material to behave differently. As for the impact test, loading is applied rapidly so that the material absorb the energy given rather than resist a force (Szycher M., 1999).

Studies on the mechanical properties of PUR are not new in PUR industry. Structural properties of the material are investigated depending upon the raw materials used in preparing the PUR. In 1978, Yuji M. et al., have studied the cross-linking and

mechanical property of polyurethane elastomer derived from liquid hydroxyl-terminated polybutadiene (HTPB), low molecular weight aliphatic diol, and diisocyanate system. ^{a,b}Zoran S. et al., 1984 have researched the mechanical properties of PUR elastomer synthesized using diphenylmethane diisocyanate (MDI) and castor oil as the polyol. Results have shown considerable influence on the type of MDI, the excess isocyanate and the preparation temperature on the properties of the PUR synthesized. In another study, Manjari R et al., 1994 investigated the structure-property relationship of HTPB-based propellant with varying molecular weights, hydroxyl values and levels of diol and triol contents of the material. They have concluded that diol-triol ratio and their level constitute a useful tool for controlling the mechanical properties of HTPB based propellants in addition to the NCO/OH ratio. Another article investigated the effect of NCO/OH ratio of PUR prepolymer based on castor oil and polymethyl methacrylate (PMMA). From their results, Vilas A. et al., 1997 concluded that the material showed significant enhancement in the mechanical properties and it was possible to design the most desirable material for a specific end use requirement. Hamid Y. et al., 2004, investigated castor oil based PUR elastomer and reported that these elastomers could be tailor made in order to fulfil industrial needs.

Microphase separation and surface properties of segmented PUR based on MDI 1,4 butanediol as hard segments (HS) and poly(propylene glycol) as soft segments were studied by Katsuhiko N. et al., 1996. Their results show that optimum hard segment content of segmented PUR leads to good mechanical properties. Another study on segmented PUR elastomers containing chemical cross-links in the hard segment was done by Petrovic Z S. et al., in 1998 and furthermore, Sung HL. et al., 2004 reported

the tensile cyclic loading behaviour of shape memory PUR having cross-links in the soft and hard segments.

In 1999, Mutsuhisa F. and his subordinate studied the mechanical properties of polyesterurethane elastomers with alkyl side groups. They stated that the polyurethane elastomers with alkyl side groups have good mechanical properties comparable to those of general purpose polyester urethanes. Tensile strength, elongation at break, hardness and elastic modulus of waterborne PUR dispersion with ions in the soft segments were investigated by Li-Hong B. et al., 2006. They have used maleic anhydride modified castor oil (MCO) to prepare aqueous PUR dispersion. Overall, the mechanical properties of the material increase as the mass ratio of MCO and polyether glycol increase but at a certain point the properties deteriorate due to excessive phase mixing.

Aliza Z. et al., 2004 reported that cross-linking density and physical state of material at test temperature affect tensile strength. They have synthesized six PUR networks from MDI and polyols based on midoleic sunflower, canola, soybean, sunflower, corn and linseed oil. ^aKrupicka A. et al., 2003 stated that mechanical surface characterization was a promising procedure to screen organic coatings. In another paper, ^bKrupicka A., et al., 2003 studied the effect of long-term recovery and storage on the mechanical response of ductile polyurethane coatings. The effects of storage have been measured in terms of variations in the mechanical response with time. Their study demonstrates the potential of contact tests combined with sensitive surface imaging tools for monitoring long-term processes in coatings.

The mechanical properties of PUR composites also very frequently investigated in PUR industry. For example, the elongation at break and electrical conductivity of PUR filled

with two different grades of graphite, Ag-coated basalt particles were investigated (Novak I. et al., 2002). The correlation between the electrical conductivity and elongation at break was observed in each case as a consequence formation of the internal network particles within a matrix. Another example is the investigation on PUR composites produced based on rice husk and polyethylene glycol. The effects of weight percentage of rice husk on tensile and other properties were investigated (Rozman HD. et al., 2003).

6.3 Background

6.3.1 Polymers classification

Polymers have been classified in many ways. It can be assigned according to the mechanism of polymerization or upon their thermal characteristics. If we look at the polymerization mechanism, there are two types; addition or condensation. In the addition polymerization method, high polymer is formed very early in the polymerization and the locus of the polymer is only on those few chain containing an active propagating centre. Polyurethane is classified as condensation polymer where the repeat unit of the finished polymer does not contain the same structures as the monomers from which it was prepared.

Polymers can be divided into two categories relating to their elevated temperature characteristics. Polymers are usually either thermoplastic or thermosetting. A thermoplastic material will flow at elevated temperature and solidify as temperature is reduced. These polymers can be reheated as many times as desired and when it is cooled again, they reversibly regain their solid or rubbery state. Thermoplastic

materials are mostly linear polymers which consist of long polymer chains. However, thermosetting polymers once their shape has been made could not be reshaped or melt on reheating. In other words, thermosetting materials cannot be recycled easily. These polymers have three dimensional network structures (Kenneth GB et al., 1999).

6.3.2 Molecular forces and chemical bonding

Most of the organic materials are hydrocarbon material which consists of hydrogen and carbon atoms. These atoms are joined together by intra molecular forces which are very strong. Polyurethanes are characterized by forces at work within and between molecules. Among these forces, covalent bonds are the strongest and most significant. In order to fully understand the nature of polyurethanes, an explanation of the secondary bonding forces that act between individual polymer molecules is important. The secondary bonding forces directly affect a material's physical properties such as viscosity, surface tension, frictional forces, miscibility, volatility and solubility. These secondary forces are categorized as van der Waals forces, dipole interaction, hydrogen bonding and ionic bonding as shown in Figure 6.1.

van der Waals forces are responsible for short-range natural attraction of molecules that are similar to each other. When overcoming van der Waals forces, slightly stronger dipole forces by polar groups in the backbone or side chains, are generated. The third category of the secondary bonding forces is hydrogen bonding which is associated with the group in backbones and the -OH or NH₂ groups in the side chains. Lastly, the strongest of all, ionic bonds are forces between positively and negatively charged ions (Szycher M., 1999).

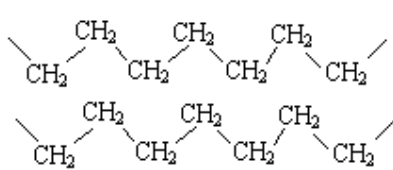
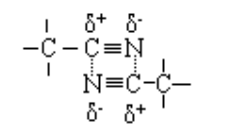
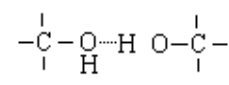
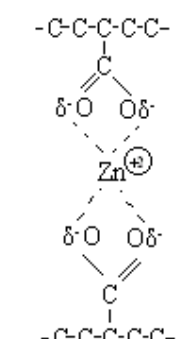
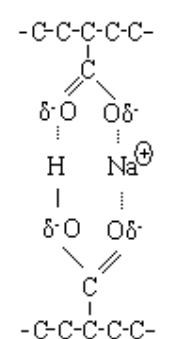
Type	Example	Dissociation energy (kilocalories per mole)
Van der Waals forces		0.5 to 2
Dipole interaction		1.5 to 3
Hydrogen bonding		3 to 7
Ionic bonding	<div style="display: flex; justify-content: space-around;"> <div style="text-align: center;">  <p>100 percent ionized</p> </div> <div style="text-align: center;">  <p>50 percent ionized</p> </div> </div>	10 to 20

Figure 6.1 Secondary bonding (Adapted from Szycher M., 1999)

6.3.3 Solid state properties of polymers

There are three different states of intermolecular order in polymer science: crystalline, amorphous and segmented solids. Polymer molecules arranged in highly oriented structure are described as crystalline state and when the polymer is arranged in an unordered structure is known as amorphous state. Polyurethane can be in many forms. For example it can be crystalline solids, segmented solids, amorphous glasses or viscoelastic solids. Polyurethane elastomers are a two-phase structure, where the hard segments separate to form discrete domains in a matrix of soft segments and this arrangement is termed as segmented or phase-separated polyurethane. The probability of a polymer exhibits crystalline structure is determined by chemical nature of the

polymer chains. Polymer with low molecular weight and high flexibility favour crystallinity. Polyurethane elastomers are mixtures of crystalline and amorphous regions.

Physical characteristic of polymer depends on molecular structure of the material. Structure of the molecule can be linear, branched, cross-linked or network. A polymer built from strictly difunctional monomers has linear polymer chain. The chains are long, flexible, and one-dimensional structure. If intentionally or by chance in the polymerization reaction, a chain continues to grow concurrently as two chains, it is said to have a branched structure. Many elastomers have branched type of structure which cause them to be resilient and able to withstand significant stretch without breaking. As for cross-linking structure, during the polymerization reaction we are able to get the individual chains to form chemical bonds with each other and the resultant structure is very strong and rigid. Cross-linking phenomenon involves primary bonds between polymer chains and in fact happens in most thermosetting polymers. The polymers cannot be remelted because the bonds between chains are too strong. The rigidity of the material also increases as the degree of cross-linking increases. Fully cross-linked polymers do not exhibit melting point, however they do have a glass transition when heated above glass transition temperature, T_g .

6.3.4 Mechanical properties

Mechanical properties are important in selecting materials for structural machine components. If a load is applied uniformly over a cross-section or surface of a body, the mechanical behaviour may be obtained by a simple stress-strain test. There are three principal ways in which a load may be applied: namely tension, compression and shear

(William D. Callister, 2004). In a tensile test, a stress is applied to a material and the response of the material to this stress will be recorded. The mathematical definition of stress (shown in formula (6.1)) is instantaneous load (F) applied perpendicular to the specimen cross-section over the original cross-sectional area (A_0).

$$\sigma = F / A_0 \quad (6.1)$$

Strain, ϵ , is defined as in formula (6.2), in which l_o is the original length before any load applied, and l_i is the instantaneous length. Deformation elongation or change in length at some instant referenced to original length is denoted as Δl .

$$\begin{aligned} \epsilon &= (l_i - l_o) / l_o \\ &= \Delta l / l_o \end{aligned} \quad (6.2)$$

The degree to which a structure deforms depends on the magnitude of stress applied. A typical plot of stress versus strain curve is shown in Figure 6.2. Deformation in which stress and strain are proportional is called elastic deformation. The slope of this linear segment corresponds to the modulus elasticity, E. The stiffness of a material increases as the E increases. Elastic deformation is non-permanent and will return to its original length when the load is removed. Some materials exhibit nonlinear behaviour hence modulus of the initial elastics portion is determined by either tangent or secant modulus. For plastic materials, the tensile strength is taken as a maximum on the curve which occurs just beyond the termination of the linear-elastic region. The stress at this maximum is the tensile strength. Fracture strength is the stress at which fracture occurs. Other parameters such as elongation at break, ϵ_{Fmax} and E modulus are shown in Figure 6.2.

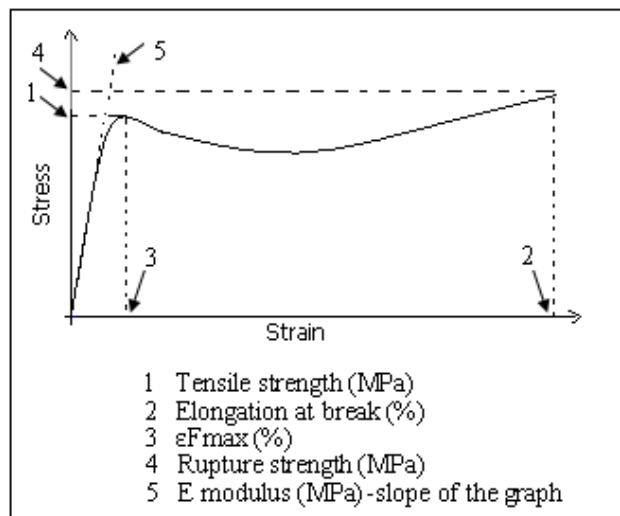


Figure 6.2 Schematic stress-strain curve for a plastic polymer showing how tensile strength, elongation at break, ϵ_{Fmax} , rupture strength and E modulus are determined.

Figure 6.3 sketches some representatives of stress-strain curves for three types of polymers (William D. Callister, 2004). Curve (a) in the figure refers to rigid and brittle type of polymers. These materials will fail while deforming elastically. Examples of this class of polymer material are polystyrene, polymethyl methacrylate and most thermoset. Curve (b) represents rigid and tough materials which behave similarly to many metallic materials. These materials have high modulus, tensile strength and hardness. Initially, these materials undergo elastic deformation which is followed by yielding and a region of plastic deformation. Examples of this type of materials are polycarbonates, cellulose ester and nylons. Finally, the deformation displayed by curve (c) represents elastomers: flexible and tough polymers. These materials have high elongation but low modulus and tensile strength. Examples of this type of materials are low and medium density polyethylenes.

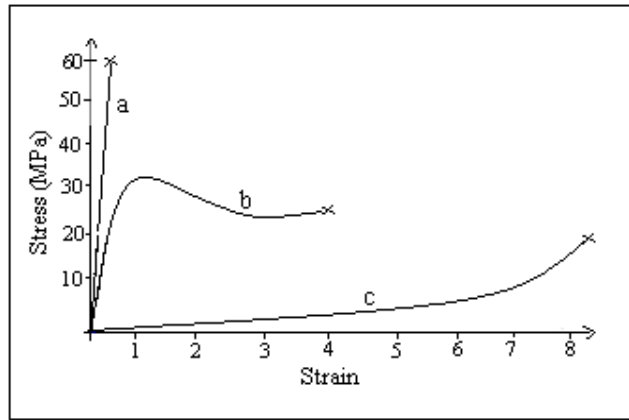


Figure 6.3 Typical stress-strain curves for (a) rigid and brittle, (b) plastic, (c) highly elastic (elastomeric) polymers

Creep is a time-dependent deformation that happens when metals or other materials are subjected to stress over a period of time. The applied stress in creep is always less than the yield strength as measured in a tensile test, yet creep causes permanent deformation. Creep at room temperature is more common in polymeric materials and is called deformation under load. The plastic strain is time-dependent in the creep deformation.

Creep studies at a constant load and time can be determined to relate elasticity and toughness of coating material. These determinations are made on detachable films formed from coating materials. Load is applied to the film at a pre-determined interval and the extension is measured. After 15 minutes, the load will be removed and the recovery of the material will be measured. Percentage recovery of the material is calculated from Equation 6.3 (Taylor et al., 1965).

$$\text{Percentage recovery} = \{(E_{15} - E_F) / E_{15}\} \times 100 \quad (6.3)$$

where E_{15} is the extension of film after a period of 15 minutes under load

and E_F is the extension of film after removing the load for a period of 15 minutes

From the results obtained the extension-time curves can be drawn. A typical extension-time curve is shown in Figure 6.4.

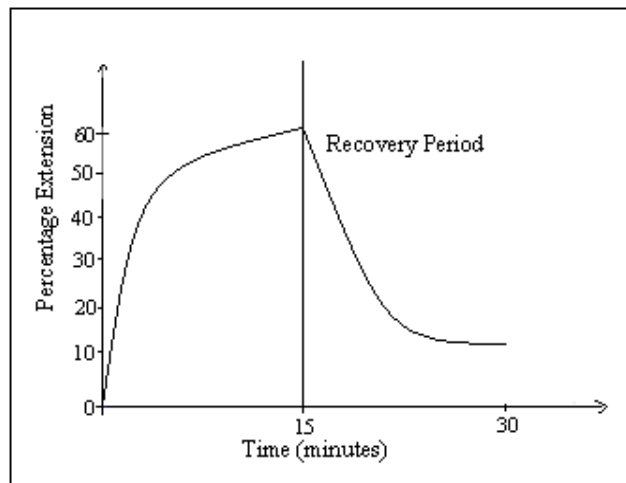


Figure 6.4 Typical extension-time curve for creep studies

6.4 Experimental setup

6.4.1 Tensile testing

i. Apparatus

The tensile measurement of the oleic acid polyol based polyurethane is done according to the test method stated in ASTM D638. The instrument used for the measurement is Zwick Z050 Universal Testing Machine. The machine is connected to a computer and controlled by special software called TestXpert to interpret the data obtained from the test. The machine consists of a stationery member carrying one grip and a movable member carrying the second grip. The grips are for holding the test specimen between the fixed and movable member respectively in such a

manner that they will move freely into alignment as soon as any load is applied such that the long axis of the test specimen will coincide with the direction of the applied pull through the center line of the grip assembly. The test specimen shall be held in such a way that slippage of specimen from the grip is prevented. The grips used in the testing are deeply serrated with a pattern found satisfactory for most plastic materials. The specimens are aligned as perfectly as possible with the direction of the pull to avoid any rotary motion that may induce slippage or breakage in the grips.

ii. Test specimen

The test specimen conforms to the dimension shown in Figure 6.5 following the specification stated in ASTM D638 type IV. Specimen is prepared by die cutting. The die is specially designed in dog bone shape, type IV by manufacturer. The die will be placed on the test specimen (thick film) and pressed using pressure machine to cut into the desired shape. Test is conducted on samples which are free from visible flaws, scratches or imperfection and in standard laboratory atmosphere of $(23 \pm 2) ^\circ\text{C}$. The thickness of the specimen is measured using micrometer with an accuracy of 0.01 mm. Thicknesses of the specimens ranged from (0.55 ± 0.01) to (1.00 ± 0.01) mm. For each sample, at least five specimens are tested and any specimen that breaks at some obvious fortuitous flaw or that do not break between predetermined gauge marks are discarded and another retest is made. The speed of motion is fixed at 5mm /min following the specifications stated in ASTM D638 standard method for rigid and semi rigid plastic.

The tensile and creep measurements are carried out on eight different samples. The PUR samples are prepared from polyol Alk28, Alk45 and Alk60 by varying the NCO/OH ratio 1.2, 1.4 and 1.6. PUalk65 (1.2) is omitted from the mechanical testing due to difficulty in forming the sample in film form. The samples are hard to cure or take more than 2 weeks to cure in room temperature. The cured samples are very sticky, uneven and unsuitable for the mechanical testing.

iii. Procedure

The width and thickness of the specimen is measured using a micrometer. The width of the specimen is the distance between the cutting edges of the die in the narrow section and is recorded in computer to calculate the cross-sectional area of the specimen. Then, the specimen is placed in the grips of the testing machine, taking care to align the long axis of the specimen and the grips with an imaginary line joining the points of attachment of the grips to the machine. The distance between the ends of gripping surface is 64 mm as stated in Figure 6.5. The grips are tightened evenly and firmly to the degree necessary to prevent slippage of the test specimen during the test but not to the point where the specimen would be crushed. The test speed is set in the machine and the machine is initiated. Results of the testing are recorded in the computer and discussed in Sections 6.5 & 6.6.

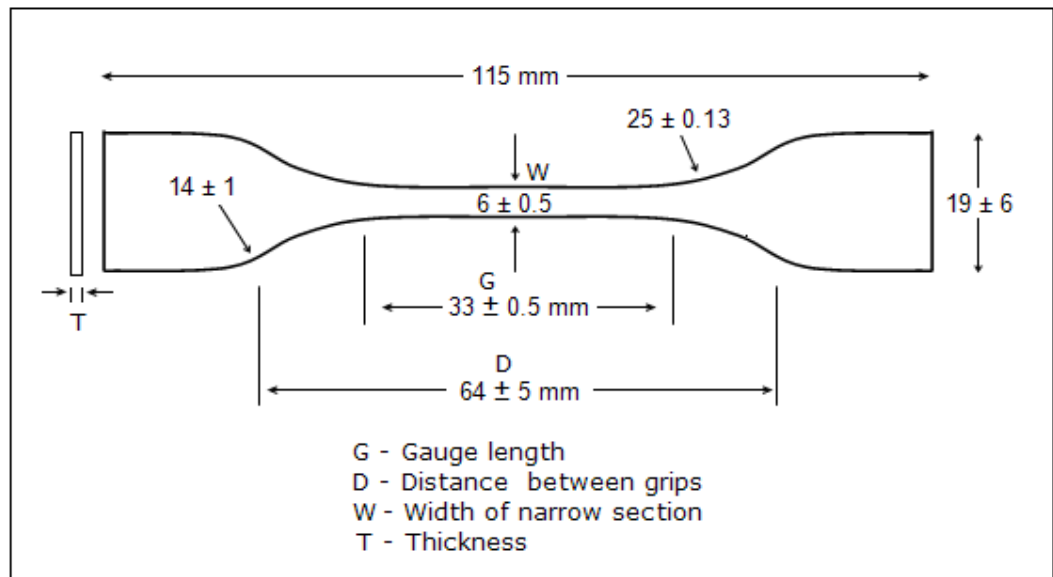


Figure 6.5 Specimen dimension according to ASTM D638 – type IV. The entire dimension is in mm.

6.4.2 Creep and recovery testing at constant load and time

i. Apparatus

The apparatus used for creep measurement is extremely simple as suggested in Taylor CJA et al., 1965. A grip is attached to a panel which is fixed and free from any movement. The second grip is attached to a weight pan and capable of perpendicular movement with minimum friction. The testing specimen is clamped in between the grips. The dimension of the test specimen and the clamping procedure of the specimen are similar as is the tensile measurement. Reproducibility of the results on a number of films are determined and found to be

quite satisfactory and within 5%, providing that the applied load is greater than 50 g and that the extension produced exceeded 25% of the original length.

ii. Procedure

The gauge length and thickness of the specimens are measured and recorded. The thickness of the specimen is measured using micrometer with an accuracy of 0.01mm. The load is applied to the film by adding a suitable weight to the pan and the extension produced in the film at predetermined intervals is assessed by measuring the distance between the gauge length using a vernier calliper capable of reading to within 0.05mm. After 15 min the added load is removed from the weight pan and the film is allowed to remain in a 'slack' condition at standard laboratory atmosphere. The recovery is measured at intervals up to 15 min after the removal of the load, by using a vernier calliper. Care is taken to ensure that no tension is applied to the film during the recovery process. The stress applied is calculated using Formula 6.1 as stated in Section 6.3.4. Each sample is tested for the stress ranging from 0.5 MPa to 36.0 MPa at the interval of 0.5 MPa depending upon their ability to withstand the stress applied within the first 15 min.

6.5 Results

6.5.1 Tensile studies

Stress-strain (%) curves obtained from the tensile tests are displayed in Figure 6.6. The resultant curves are compared with Figure 6.3 in Section 6.3.4, and the characteristics of PUR are predicted. PUalk28 (1.2) to PUalk28 (1.6) show the trend of curve (a) in Fig. 6.3, which is rigid and brittle, a characteristic of thermoset polymer.

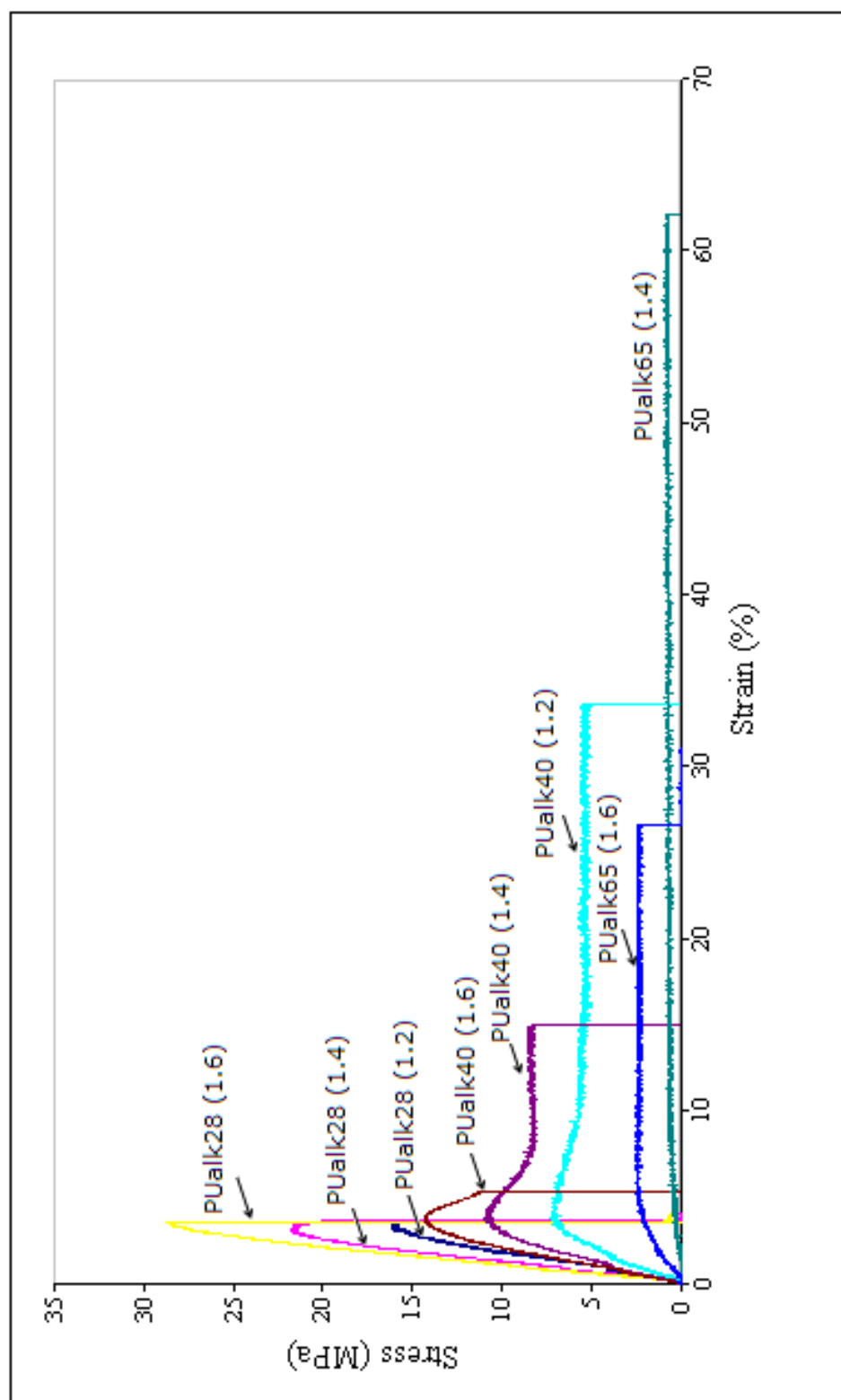


Figure 6.6 Stress (MPa) versus Strain (%) curves for oleic acid polyols based PUR

These materials failed while deforming elastically. However, PUalk40 (1.2) to PUalk40 (1.6) follow the trend of curve (b) which is rigid and tough material. These materials have high modulus, tensile strength and hardness and initially undergo elastic deformation followed by yielding and region of plastic deformation. As for PUalk65, this material follows the trend of curve (c) which is an elastomer. These materials are very flexible and tough polymer with high elongation but low modulus and tensile strength.

The average tensile mechanical properties at room temperature are summarized in Table 6.1. The summary consists of values such as E modulus (MPa), tensile strength (MPa), rupture strength (MPa), ϵF_{max} (%) and elongation at break (%). The modulus values are found to be 683, 805, 1033, 221, 343, 473, 30 and 71 MPa for PUalk28 (1.2), PUalk28 (1.4), PUalk28 (1.6), PUalk40 (1.2), PUalk40 (1.4), PUalk40 (1.6), PUalk65 (1.4) and PUalk65 (1.6) respectively. The modulus values showed the largest variability with the variation of NCO/OH ratio 1.2 to 1.6. For PUalk28, when the NCO/OH ratio increases from 1.2 to 1.6, the modulus increases about 51.4%, and as for PUalk40 the increment is much higher, 114.1%. PUalk65 also displays increment of 135.1% when the NCO/OH ratio increases from 1.4 to 1.6.

The variability exhibited in the tensile strength and elongation at break, indicated as bar diagrams in Figures 6.7 and 6.8. If the mechanical properties of the materials are discussed individually in term of polyol, the PUR films prepared from polyol Alk28 have the highest tensile strength (30 MPa), tensile E modulus (1033 MPa) and the lowest elongation at break (3.5%) than that of the PUR films prepared from polyol Alk40 and Alk65. Consequently, in terms of NCO/OH ratios, the tensile strength, E

modulus and rupture strength increase and ductility decreases as NCO/OH ratio increases for all the three samples.

Table 6.1 Summary of results from tensile measurement

Samples	Emod (MPa)	Tensile Strength (MPa)	Rupture Strength (MPa)	ϵ_{Fmax} (%)	Elongation at break (%)
PUalk28 (1.2)	683 ± 3	17 ± 2	16 ± 2	2.9 ± 0.3	3.2 ± 0.3
PUalk28 (1.4)	805 ± 2	22 ± 1	22 ± 1	2.97 ± 0.09	3.6 ± 0.3
PUalk28 (1.6)	1033 ± 4	30 ± 4	29 ± 4	3.5 ± 0.5	3.5 ± 0.5
PUalk40 (1.2)	221 ± 5	7 ± 4	5 ± 3	4 ± 2	34 ± 8
PUalk40 (1.4)	343 ± 1	11.2 ± 0.3	8.4 ± 0.2	3.82 ± 0.02	15 ± 1
PUalk40 (1.6)	473 ± 4	14 ± 1	11.0 ± 0.8	3.8 ± 0.2	5.4 ± 0.6
PUalk65 (1.4)	30 ± 1	1.1 ± 0.1	0.81 ± 0.03	56 ± 1	60 ± 3
PUalk65 (1.6)	71 ± 2	2.61 ± 0.02	2.46 ± 0.07	7 ± 1	26 ± 1

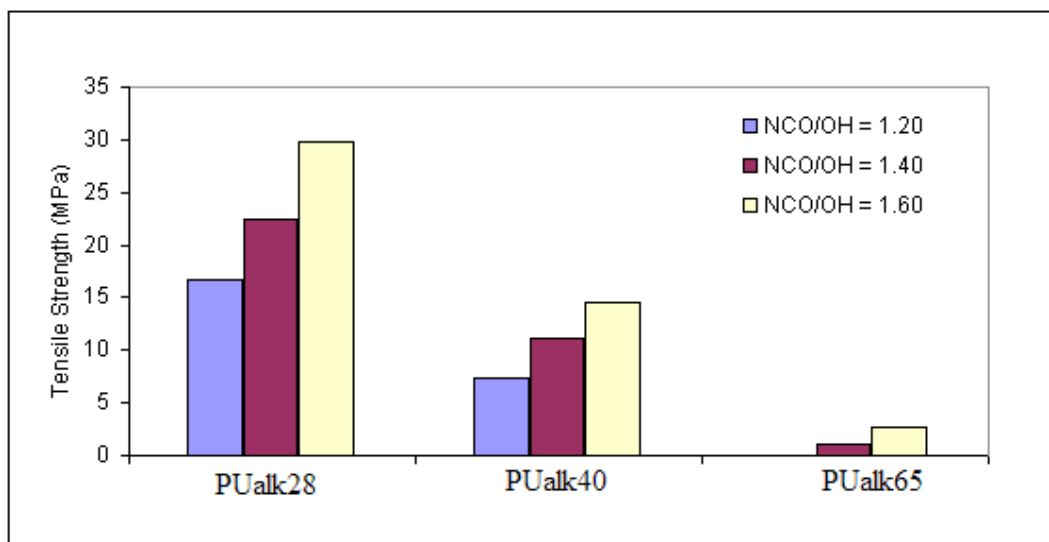


Figure 6.7 The effect of NCO/OH ratios on the tensile strength for PUR

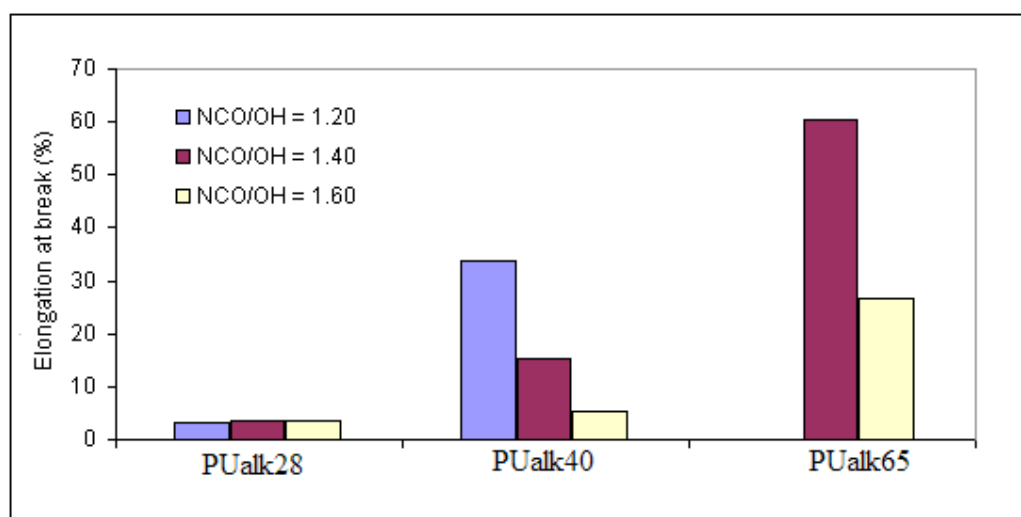


Figure 6.8 The effect of NCO/OH ratios on the elongation at break for PUR

6.5.2 Creep and recovery studies

The experimental short term creep and recovery curves for PUalk28 (1.2), PUalk28 (1.4), PUalk28 (1.6), PUalk40 (1.2), PUalk40 (1.4), PUalk40 (1.6), PUalk65 (1.4) and PUalk65 (1.6) are presented in Figures 6.9 to 6.16 respectively. The stress applied depends on the fracture strength of the sample within the first 15 minutes after loading weight on the weight pan.

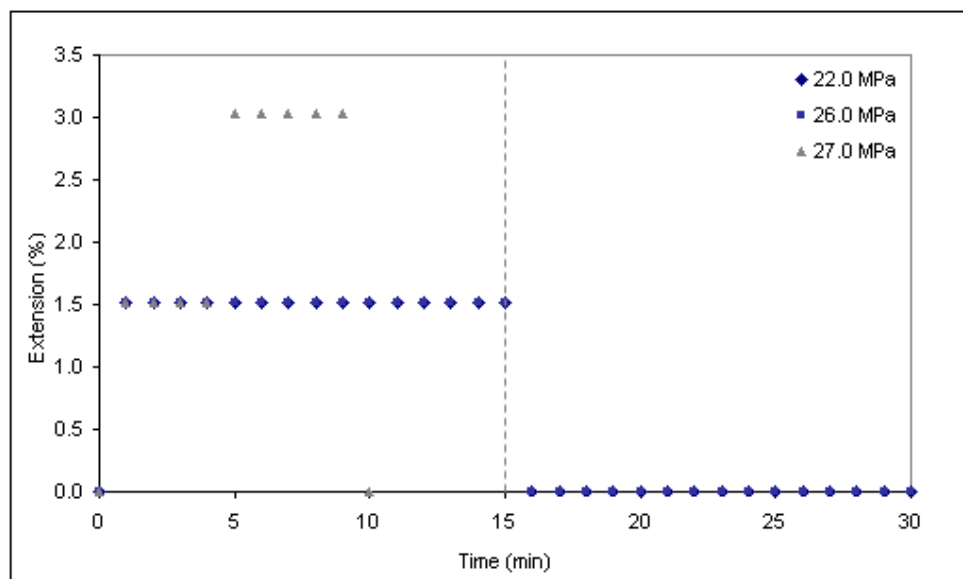


Figure 6.9 Extension (%) versus Time (min) curve for PUalk28 (1.2)

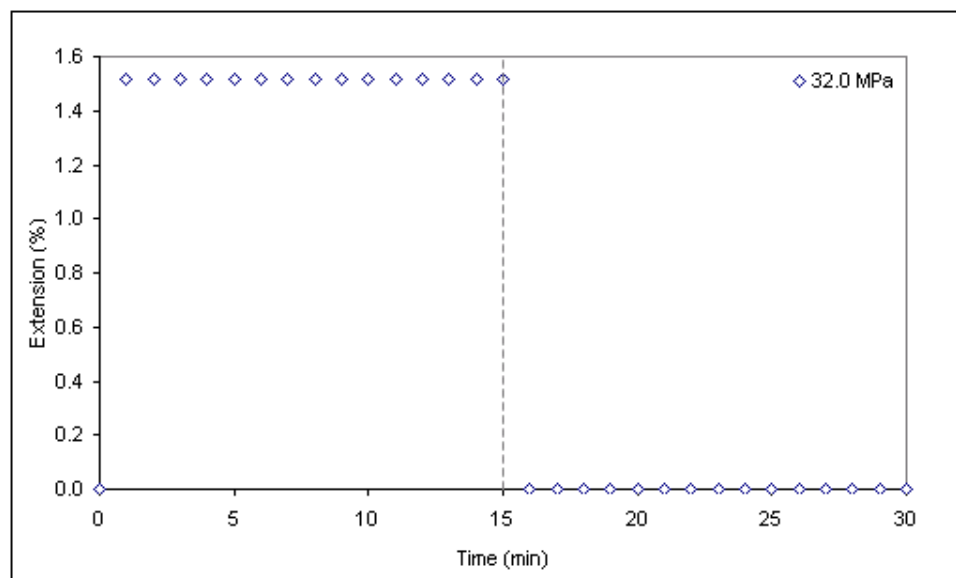


Figure 6.10 Extension (%) versus Time (min) curve for PUalk28 (1.4)

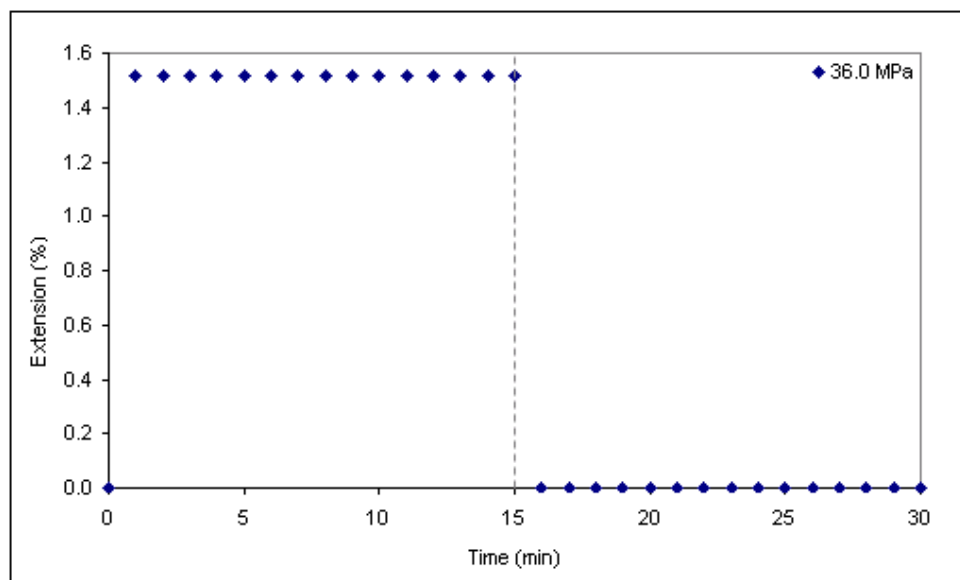


Figure 6.11 Extension (%) versus Time (min) curve for PUalk28 (1.6)

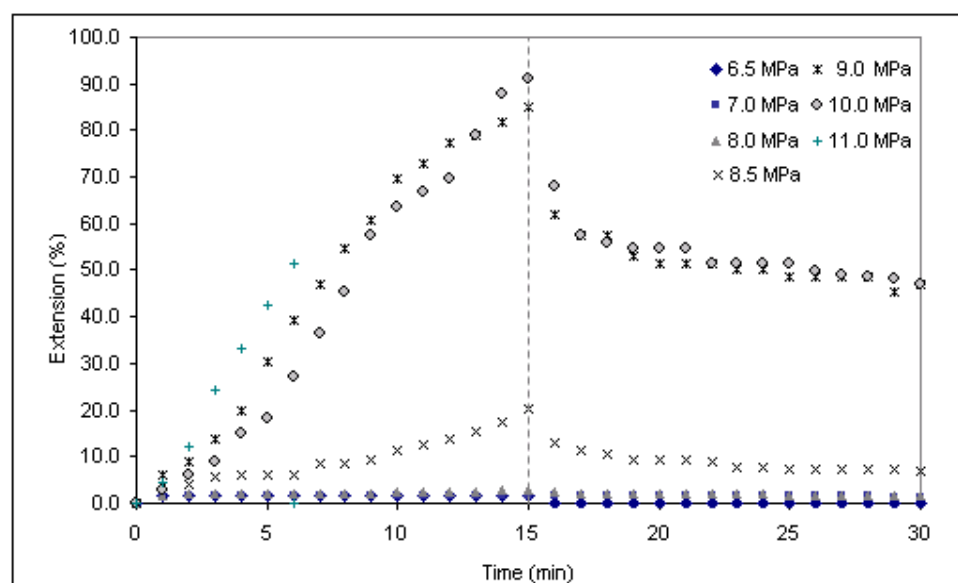


Figure 6.12 Extension (%) versus Time (min) curve for PUalk40 (1.2)

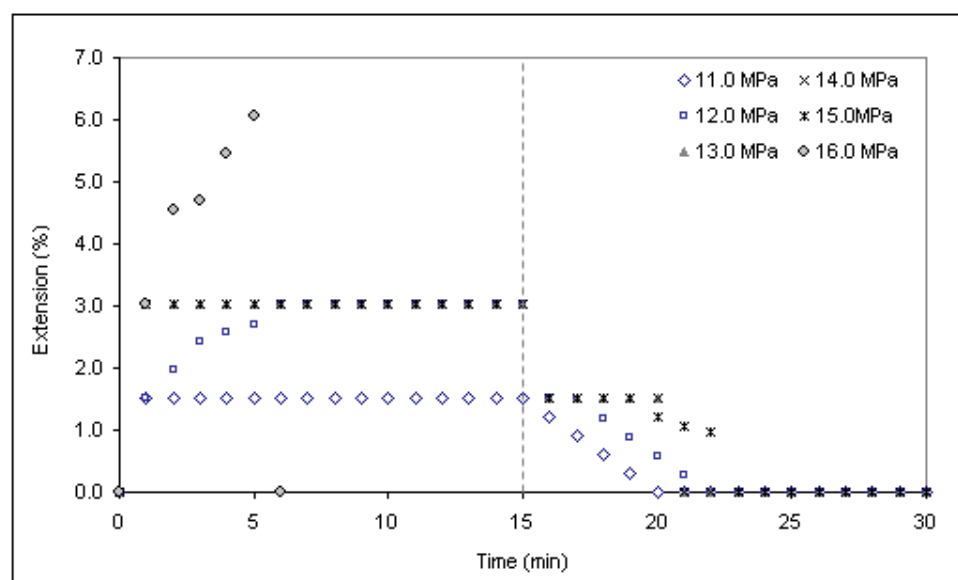


Figure 6.13 Extension (%) versus Time (min) curve for PUalk40 (1.4)

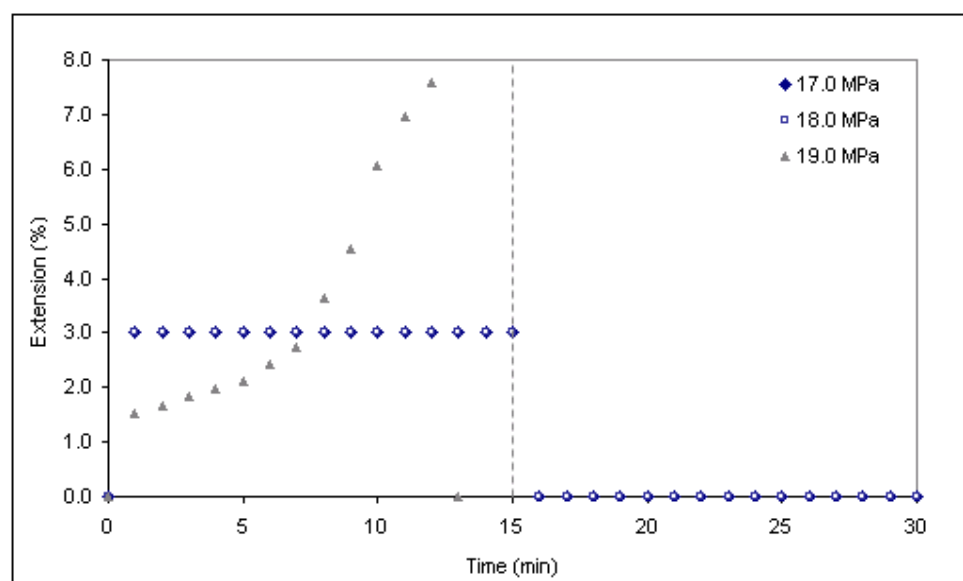


Figure 6.14 Extension (%) versus Time (min) curve for PUalk40 (1.6)

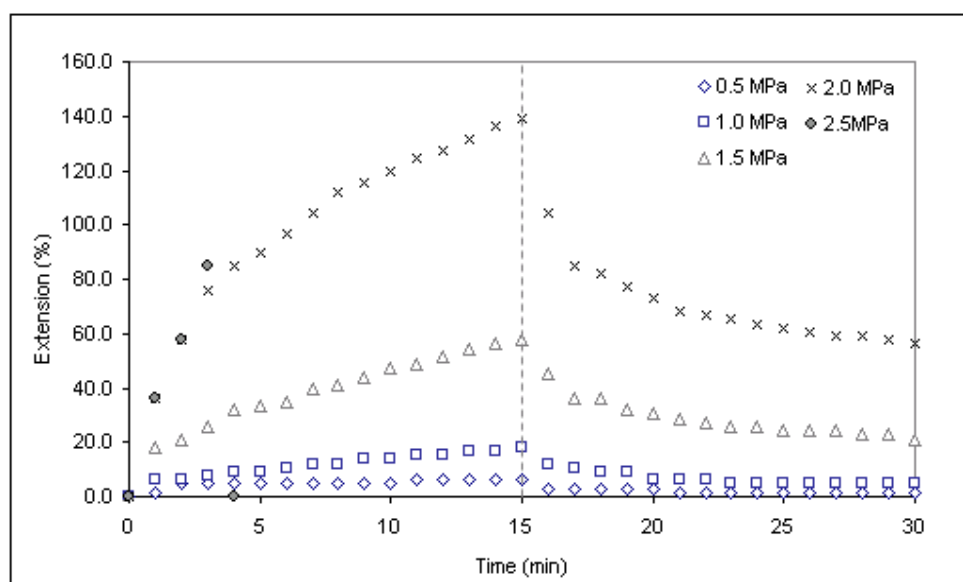


Figure 6.15 Extension (%) versus Time (min) curve for PUalk65 (1.4)

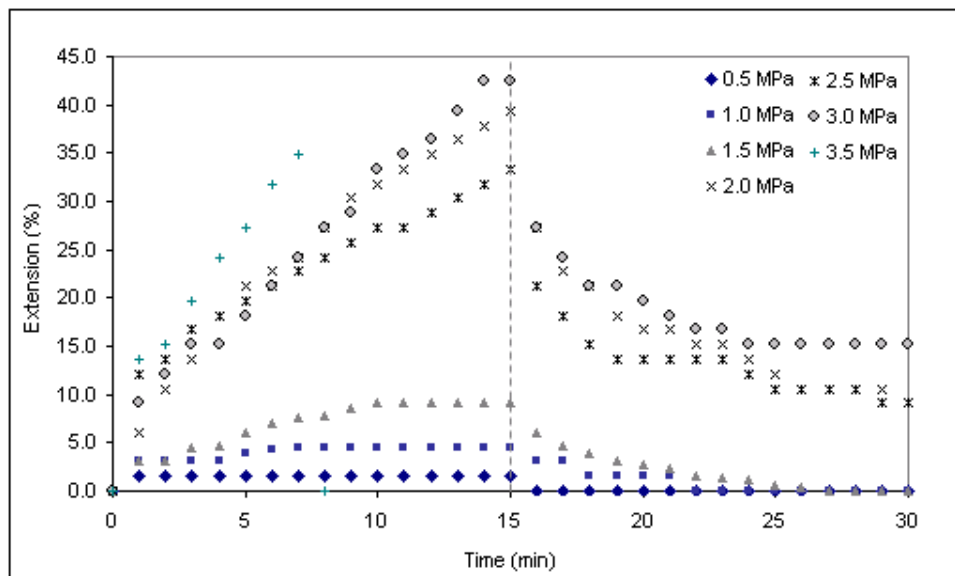


Figure 6.16 Extension (%) versus Time (min) curve for PUalk65 (1.6)

The summary of the materials characteristic during the creep test is reported in Table 6.2. Data from the Table 6.2 clearly indicates that the rupture strength of the oleic acid polyol based PUR depends upon the oleic acid content of the polyols and NCO/OH ratio. As the oleic acid content of polyols increases (from Alk28 to Alk65), the rupture strength decreases. Comparing the rupture strength of PUR samples at constant NCO/OH ratio 1.4, the rupture strength decreases 59% from PUalk28 to PUalk40 and decreases further 32% from PUalk40 to PUalk65. The characteristic of PUR materials also changes from tough and brittle to soft and elastic as the oleic acid content of polyols increases. However, the samples become tough and stiff again as the NCO/OH ratio increases. Similar results are obtained for the rest of PUR samples.

The main difference in percentage recovery between the PUR samples is the characteristic of the material. When the tough samples are loaded, the increment of the strain is less, in the range of 1.5 to 3%, and the strain fell immediately almost to zero (percentage recovery = 100%) when the specimen is unloaded. However, when the

materials are soft and elastic the percentage recovery is dependent upon the stress applied. Recovery curves from the creep under constant stress indicate that at any selected time the extent of recovery is directly proportional to the stress applied.

Table 6.2 Material's characteristic and percentage recovery during the creep test

Samples	Materials Characteristic	Stress Applied ($\sigma \pm 0.3$) MPa	Percentage Recovery ($E_r \pm 0.5$) %
PUalk28 (1.2)	Very hard, brittle, stiff, elongate ~1.5%	0.5 - 26.0	100.0
		27.0	F
PUalk28 (1.4)	Very tough and brittle, elongate ~1.5%	0.5 - 32.0	100.0
		33.0	F
PUalk28 (1.6)	Very tough, brittle, elongate ~1.5%	0.5 - 35.0	100.0
		36.0	F
PUalk40 (1.2)	Elastic, elongate ~ (10 - 90)%	0.5 - 8.0	100.0
		8.5	65.7
		9.0	44.6
		10.0	48.3
		11.0	F
PUalk40 (1.4)	Tough, elongate ~ 3%	0.5 - 15.0	100.0
		16.0	F
PUalk40 (1.6)	Tough, brittle, elongate ~3%	0.5 - 18.0	100.0
		19.0	F
PUalk65 (1.4)	Soft, elastic, elongate ~ (5 - 140)%	0.5	24.3
		1.0	74.9
		1.5	63.6
		2.0	59.8
		2.5	F
PUalk65 (1.6)	Soft, elongate ~ (5 - 43)%	0.5 - 1.5	100.0
		2.0	76.9
		2.5	72.7
		3.0	64.3
		3.5	F

F- Fractured

6.6 Discussion

6.6.1 Tensile test

Polyurethanes are heterophase system composed of alternating aromatic urethane and macroglycol segments (Jung HC et al., 2000). The macroglycols segments are usually the polyols. Incompatibility between the chemically dissimilar blocks prevents formation of homogeneous mixture, the urethane and macroglycol segments cluster into separate domains forming a two-phase system. The existence of two phases in PUR has been proven by electron microscopic studies conducted by Koutsky JA et al., in 1970. Polyols of low glass transition temperature are designated as soft segment while diisocyanate as hard segment. The hard segments act as filler particles and cross-links to restrain the motion of the soft segment chains. This mechanism enhances the mechanical properties of polyurethane. The hard segments give high mechanical strength whereas the soft segments give high extensibility and resilience.

On the other hand, PUR may be a cross-linked polymer depending upon the raw material and preparation method used in preparing the samples. Therefore, it is also quite reasonable to expect the presence of cross-links in a segmented system could restrain the chains from achieving necessary configurations for phase separation (Lagasse RR, 1977). This hypothesis is supported by the results obtained by Cooper and Tobolsky, 1967 who modified linear thermoplastic elastomer by adding various cross-linking agents. They have inferred that the domain structure initially present in the linear systems could be either maintained or destroyed when cross-links are introduced, depending on the number and location of the cross-links in the segmented copolymer chains. In this research, the PUR is predicted to have either a cross-linked or

segmented structure which may act differently to the mechanical properties obtained from the tensile result.

Isocyanates used in the preparation of PUR also play a big role in the properties of the end use material. For example, TDI-based PUR possess higher stress and lower strain property behaviour due to the fact that there is an aromatic ring in the main chain of TDI, which has higher intermolecular interaction between the hard segments. Direct association of two isocyanate groups with the same phenyl ring in TDI contributes to the higher rigidity of a material (Petrovic ZS et al., 1984). In this research, TDI is used as isocyanates, therefore it is predicted that the rigidity and toughness of the PURs in the research is due to TDI.

Another factor that contributes to the mechanical properties of PUR is NCO/OH ratio. Three different NCO/OH ratios are selected and since the NCO/OH ratio is greater than 1, the PUR formed will be NCO terminated. NCO/OH ratio in PUR relates to cross-linking, where, as the ratio increases the cross-linking increases (Bor-Sen C. et al., 2002). The excess diisocyanate may first react with the polyol to form the isocyanate-terminated prepolymer and the free NCO groups will react further to form three-dimensional allophanate or biuret cross-links or polar urea structure thus increasing the number of urethane groups (S. Desai et al., 2000). The mobility of the molecular chain in the PUR system is restricted by the existence of three dimensional allophanate or biuret structure (Huang SL et al., 1997). When the NCO/OH ratio is low, the branching will occur at the urethane linkage. At higher NCO/OH ratios, the probability for the formation of urea linkages will be high and, thus, branching will occur at the urea linkage. The branching will be further increase at higher atmospheric pressure and humidity; hence percentage of urea to urethane will be higher.

Results obtained from the study indicate that the tensile strength, E modulus and rupture strength increase progressively with NCO/OH ratios while elongations decrease. This phenomenon is attributed to the fact that increased chemical cross-linking leads to a change in morphology which affects the mechanical properties. The introduction of cross-linking in PUR molecules produces restriction to the mobility of the molecular structure. The long segment of the backbone molecule is still free to move at low degree of cross-linking where soft flexible rubbery behaviour occurs. The strength and creep resistance are improved at this stage. With increasing the degree of cross-linking, the modulus increases and the extensibility decreases giving tough, flexible products. A higher degree of cross-linking, the polymer molecules are completely immobilized and become rigid thermoset plastic. The increased NCO/OH ratio also increases the intermolecular attraction of hard segments which in turn increase the tensile strength and decreases elongation. The intermolecular attraction between the hard segments occurs because of the hydrogen bonding between -NH and -C=O of the hard segments. Increased hydrogen bonding of the carbonyl group increases the phase mixing of the soft and hard segments and in return increases the stress property and decreases the strain property.

The oleic acid content in the polyols is also a factor that has contributed to the observed mechanical properties of the PURs. As mentioned in Section 6.5, the tensile strength, E modulus, rupture strength of PUR increases as the oleic acid content of the polyol reduces but the elongation at break or strain properties of the materials decrease. This phenomenon occurs probably due to the fact that PUalk65 with the highest content of oleic acid in polyols have more flexible side chain in the PURs compared to Alk28 with the lowest oleic acid content. PUalk65 exhibits flexibility compared to that of PUalk28 which is brittle. As the oleic acid content increases, more flexible side chain exist in the

polymer which presumably function as plasticizers, and consequently decrease the modulus and tensile strength of the material. This may explain why the PUalk65 has lower tensile properties and higher elongation compared to PUalk28. As for PUalk40, it displays medium tensile properties compared to the rest of PURs due to the moderate oleic acid content in the polyols.

The hydroxyl value of the polyols is 142, 142 and 143 (as stated in Chapter 3, Table 3.1) for Alk28, Alk40 and Alk65 respectively. In general, the greater the excess of hydroxyl content, the greater is the number of sites available for cross-linking and subsequent cures. The number of hydroxyl groups in the polyols, their distribution in the fatty acid and the position in fatty acid chain (in the middle or closer to the end of the chain) will affect the network properties on the cross-linking density of PUR (Alisa Z. et al., 2004). Polyol with the highest hydroxyl value has the large number of reactive sites available for reaction with isocyanate compared to that of the lowest hydroxyl value. The rate of reaction between the hydroxyl groups with the isocyanate groups from TDI is dependent on the amount of hydroxyl groups. However, in this case, since the hydroxyl value of the polyols is almost similar, this factor may not contribute much to the mechanical properties of the PUR.

The functional groups in polyols determine chain extension and network formation in the PUR polymer (S. Desai et al., 2000). According to them, reaction of difunctional components with TDI results in chain extension while that of tri-functional components lead to network formation. The network formation reduces flexibility and gives rise to tensile strength of the polymer. The functionality of the polyols obtained from oleic acid polyol based is most probably due to the content of glycerol in the formulation. Glycerol has three functional groups. Therefore, the network formation is predicted to

occur in the structure of PUR in the research. However, as the oleic acid content increases in the series of the PURs, flexibility of the material increases. Furthermore, as the NCO/OH ratio increases the cross-linking increases which causes the increment on the mechanical properties of the material.

Lower reactivity of secondary hydroxyl group could lead to poor mechanical properties of the PUR sample (V. Sekkar et al., 1996, Yuji M et al., 1978, Davis TL et al., 1934). Reactivity of the secondary hydroxyl groups towards isocyanate groups is lesser than the primary hydroxyl group. This difference could lead to defective network formation and incomplete cure reaction which could lead to poor mechanical properties.

6.6.2 Creep test

At low stresses the creep behaviour of polymers can be represented by a linear time dependent factor. As the creep stress is increased the relation between creep strain and applied stress becomes nonlinear (E. Krempl et al., 2003). For rigid plastic, shear stress is the main activating stress for creep, and normal stresses have a secondary effect. The effect of shear stress is to bias, in the direction of the stress, the random interchange of bond forces resulting from thermal vibration. This permits a shearing displacement of individual atoms of a molecule or chain segments to occur. The displacement allows normal stress to alter the shape of molecules by straightening, uncoiling or stretching. In polymers with a tightly coiled molecular configuration, normal stress may act to extend the coil with much less contribution from slip being required. Normal stress may influence to increase or decrease the shearing stress parallel to the plane of atoms, molecular segment or sheet of molecular segments that occurs in this plane. In polymers where tightly coiled molecular configuration is found, the normal stresses

may act to extent the coil with much less contribution from slip being required (O'Connor et al., 1962). The structure of PUR that permits cross-linking by means of hydrogen bonds at intervals along the molecular chain prevents the other portion of molecular adjacent to the bonds from packing as closely to neighbouring molecules and might have greater influence on normal stress in PUR.

The results from creep and subsequent strain recovery curves are found to have general form showing an instantaneous elastic strain on loading that is followed by a period of slow linear deformation. These two regions are separated by a transition zone (at $t = 15\text{min}$) that is more pronounced at high load level. As expected, high loading stress resulted in large creep strain. Creep and recovery measurements indicate that the PUalk28 (1.2), PUalk28 (1.4), PUalk40 (1.4) and PUalk40 (1.6) have relatively good creep properties (lower creep strains) at higher load levels. The residual strains after recovery are also lower, showing almost full recovery after removal of creep load of 0.5 to 35MPa (see Figure 6.9 to 6.14). In general, full recovery of the cross-linked polymers is expected at low creep strains. Large creep strain in the creep process results in higher residual strain in the subsequent recovery (Nielsen LE et al., 1994, Ward IM et al., 1993).

In order to elucidate these results, it is necessary to analyze the structure of these thermosetting polymers. Most of the bulk polymers have highly cross-linked structures. In general, full recovery of the cross-linked polymer is expected at low creep strains (Nielson LE et al., 1994, Ward IM et la., 1993). In this study, the loading level used is between 0.5 to 10.0MPa (lower stress level), and some measurement results showed the presence of irreversible strains (ex. PUalk40(1.2) at stress value of 9.0 and 10.0MPa, PUalk65(1.4) at stress value of 1.5 and 2.0MPa, PUalk65(1.6) at stress value 2.5 and

3.0MPa). These irreversible strains become pronounced when high loading is employed. The observed residual strains are ascribed to the non-identical cross-linking structure obtained from various percentage of oleic acid content in the polyols. The matrix of bulk polymer consists of highly cross-linked molecules and these substances do not produce any irreversible strains after creep and recovery processes. However, the interface between these substances is composed of many lightly cross-linked molecules. These molecules at the interfaces are easier to deform upon loading at room temperature. The existence of free oleic acid chain molecules in the bulk polymer prefer to reside in the interfaces which facilitate movement of the interfacial molecules under loading. When the stress is removed, these lightly, cross-linked molecules tend to turn to their original state. The driving force for this recovery is from the stored elastic energy in the creep process. Due to their viscoelastic nature, these molecules cannot completely return to their original state like the perfectly cross-linked molecules, and as a result, various amounts of irreversible strains are observed.

6.7 Conclusion

Tensile and short term creep properties of oleic acid polyol based PUR are investigated and reported in this chapter. From the tensile measurement, it is concluded that PUalk28 is a thermosetting polymer with higher degree of cross-linking. Increment of NCO/OH ratio from 1.2 to 1.6, further increased the cross-linking and produced rigid and brittle polymer with higher modulus and lower extensibility. PUalk40 is rigid and tough material behaves similar to many metallic materials. These materials have high modulus, tensile strength and hardness. Initially, this material undergoes elastic deformation which is followed by yielding and plastic deformation. However, cross-links are induced into the polymer as the NCO/OH ratio is increased and produced rigid

and brittle polymer (PUalk40 (1.6)). PUalk65 behaves as an elastomer which has lower modulus and higher extensibility. These materials are very flexible and tough. From creep test results, it is concluded that PUalk28 (1.2), PUalk28 (1.4), PUalk40 (1.4) and PUalk40 (1.6) have relatively good creep properties at higher load levels. The residual strains after recovery are also lower, showing almost full recovery after removal of creep load. Furthermore, study on the effects of oleic acid content in the polyols of the PUR shows significant changes on mechanical properties of the samples. PUR with the lowest oleic acid content polyols (Alk28) have the best mechanical properties followed by medium (Alk40) and the highest oleic acid content (Alk65). Hence, it can be concluded that the oleic acid content of the polyols and the NCO/OH ratios of the PUR samples influence the mechanical properties of the samples.

References

- Alisa Zlatanic, Charlene Lava, Wei Zhang, Zoran SP., 2004. Effect of structure on properties of polyols and polyurethanes based on different vegetable oils. *Journal of Polymer Science Part B: Polymer Physics*, **42**, 809-819.
- ASTM D638, 1972. Standard Method of Test for Tensile Properties of Plastic, 186-199.
- Bor-Sen Chiou, Paul E. Schoen, 2002. Effects of cross-linking on thermal and mechanical properties of polyurethanes. *Journal of Applied Polymer Science*, **83**, 212-223.
- Cooper SL, Tobolsky AV., 1967. Anomalous depression of rubbery modulus through cross-linking. *Journal of Applied Polymer Science*, **11**, 1361.
- Davis TL, Farmun JM, 1934. Relative velocities of reaction of amines with phenyl isocyanate. *Journal of American Chemical Society*, **56(4)**, 885-886.
- Erhard Krempf, Fazeel Khan, 2003. Rate (time)-dependent deformation behaviour: an overview of some properties of metals and solid polymers. *International Journal of Plasticity*, **19**, 1069-1095.
- Hamid Yeganeh, Mohammad Reza Mehdizadeh, 2004. Synthesis and properties of isocyanate curable millable PUR elastomers based on castor oil as renewable resource polyol. *European Polymer Journal*, **40**, 1233-1238.
- Huang SL, Lai JY, 1997. Structure-tensile properties of polyurethane. *European Polymer Journal*, **33**, 1563-1567.
- Jung HC, Kang SJ, Kim WN, LeeYB, Choe KH, Hong SH, Kim SB, 2000. Properties of cross-linked polyurethanes synthesized from 4,4'-Diphenylmethane Diisocyanate and polyester polyol. *Journal of Applied Polymer Science*, **78**, 624-630.
- Katsuhiko Nakamae, Takashi Nishino, Seiji Asaoka, Sudaryanto, 1996. Microphase separation and surface properties of segmented PUR-effect of hard segment content. *International Journal of Adhesion & Adhesive*, **16(4)**, 233-239.

Kenneth G. Budinski, Michael K. Budinski, 1999. Engineering Material. Sixth edition, Prentice Hall, Chpt 3, 56-110.

^aKrupicka A, Johansson M, Hult A., 2003. Mechanical surface characterization: A promising procedure to screen organic coatings. *Journal of Coatings Technology*, **75(939)**, 19-27.

^bKrupicka A, Johansson B., Johansson M., Hult A., 2003. The effects of long-term recovery and storage on the mechanical response of ductile poly(urethane) coatings. *Progress in Organic Coatings*, **48**, 14-27.

Laggasse RR, 1977. Domain structure and time dependent properties of a cross-linked urethane elastomer. *Journal of Applied Polymer Science*, **21**, 2489-2503.

Manjari R, Pandureng LP, Somasundaran UI, Sriram T, 1994. Structure-property relationship of HTPB-based propellants, Optimization trial with varying levels of diol-triol contents. *Journal of Applied Polymer Science*, **51**, 435-442.

Mutsuhisa Furukawa, Tetsuro Shiiba, Shegeru Murata, 1999. Mechanical properties and hydrolytic stability of polyesterurethane elastomers with alkyl side groups. *Polymer*, **40**, 1791-1798.

Nielsen LE, Landel RF, 1994. Mechanical properties of polymers and composites, New York, Marcel Dekker.

Novak I, Krupa I, Chodak, 2002. Investigation of the correlation between electrical conductivity and elongation at break in polyurethane based adhesives. *Synthetic Metals*, **131**, 93-98.

O'Connor, Findley WN, Oct. 1962. Influence of normal stress on creep in tension and compression of polyethylene and polyvinyl chloride copolymer. *SPE Transactions*, 273-284.

Petrovic ZS, Fajnik D, 1984. Preparation and properties of castor oil based polyurethanes. *Journal of Applied Polymer Science*, **29**, 1031-1040.

Rozman HD, Yeo YS, Tay GS, Abubakar A., 2003. The mechanical and physical properties of polyurethane composites based on rice husk and polyethylene glycol. *Polymer Testing*, **22**, 617-623.

S. Desai, I.M. Thakore, B.D. Sarawade, S. Devi, 2000. Effects of polyols and diisocyanates on thermo-mechanical and morphological properties of polyurethanes. *European Polymer Journal*, **36**, 711-725.

Sung Ho Lee, Jin Woo Kim, Byung Kyu Kim, 2004. Shape memory polyurethane having cross-links in soft and hard segments. *Smart Materials and Structures*, **13**, 1345-1350.

Szycher Michael, 1999. Szycher's Handbook of Polyurethane. CRC Press LLC. Chapter 3, 17-32.

Taylor CJA, Marks S, 1965. Paint Technology Manual ; Part Five, The Testing of Paints. Chapman & Hall, London. Chapter 3, 86.

V. Sekkar, Rama Rao M, Krishnamurthy VN, Jain SR, 1996. Modelling of polyurethane networks based on hydroxyl terminated polybutadiene and poly(12-hydroxy stearic acid-co-TMP) ester polyol: Correlation of network parameters with mechanical properties. *Journal of Applied Polymer Science*, **62**, 2317-2327.

Vilas Athawale, Suresh Kolekar, 1998. Interpenetrating polymer networks based on polyol modified castor oil PUR and PMMA. *European Polymer Journal*, **34**, 1447-1451.

Ward IM, Hadley DW, 1993. An introduction to the mechanical properties of solid polymers. New York, Wiley.

William D. Callister, 2004. Material Science and Engineering, An Introduction. Sixth Ed., John Wiley & Sons, Chapter 6, 113-151.

Yuji M, Shinzo Yamashita, Hiroshi Okamoto, Tadao Matsuo, Michiaki Izawa, Shun-ich Kohmoto, 1978. Cross-linking and mechanical property of liquid rubber, Curative effect of aliphatic diols. *Journal of Applied Polymer Science*, **22**, 1817-1844.

^aZoran SP, Dragia F, 1984. Preparation and properties of castor oil-based polyurethanes. *Journal of Applied Polymer Science*, **29**, 1031-1040.

^bZoran SP, Ivan Javni, Gyorgi B, 1998. Mechanical and dielectric properties of segmented PUR elastomers containing chemical cross-links in the hard segment. *Journal of Polymer Science Part B: Polymer Physics*, **36**, 237-251.

CHAPTER 7: CONCLUSION AND SUGGESTION FOR FUTURE WORK

There are many types of PUR in the market. The research studies presented in this thesis focussed on palm olein oleic acid polyol based PUR coating which is new in the market and presumed to have good prospect in the future. This work is mainly aimed at investigating the physical characteristic of the PUR coatings. The molecular structure of the coating has been varied by percentage of oleic acid content in polyols and NCO/OH ratios above 1. By varying the oleic acid content in polyols, the amount of flexible side chains incorporated in the polymer was varied. In addition, the NCO/OH ratios of the PURs samples are varied to see the cross-linking effects as the ratios increased. As the NCO/OH ratio becomes greater than 1, excess diisocyanate introduce allophanate or biuret bond between polymer chains which consequently increase the cross-linking in the samples forming a more stable physical network. The effect of both variations on the physical characteristic of the PUR samples are discussed and concluded in this chapter.

Polyols

Percentages of oleic acid content varied in the polyols are 28, 40 and 65. In this series of polyols, there is a great excess of glycerol over the phthalic anhydride at the initial stage which lead to a mixture of oligomers with hydroxyl groups. Some of these hydroxyl groups would react with the calculated amounts of oleic acid to form the final products with the required hydroxyl values. The oleic acid is incorporated as flexible side chains. The resulting low molecular weight polyols are viscous liquids that do not air-dry by itself, as there were insufficient C=C unsaturation through the incorporation

of oleic acid. Presence of free hydroxyl groups in the polyols are confirmed by FTIR analysis. The transmittance of $3460 - 3480\text{ cm}^{-1}$ (presence of free hydroxyl groups) disappears as a result of cross-linking with isocyanate to form PUR.

The polyols synthesized has color, viscosity and acid value which decreased as the oleic acid content is increased. The melting temperature, T_m remains the same for the three alkyds. The polyols may have similar main chain structure, formed from the reactions of phthalic anhydride and glycerol. The attachment of some oleic acid as flexible side chains has not caused any significant changes to the T_m .

The presence of oleic acid and glycerol from palm olein contributes tinge of yellowness to the end product of polyols due to the nature of palm oil itself. As the oleic acid content increased in the formulation of polyols, the yellowness of the end product (PUR) increased too.

Polyurethanes

Free hydroxyl groups in the polyols are reacted with isocyanate to form PUR. The FTIR analysis confirms the reaction occurring by the disappearance of OH band and the appearance of NH band in the PUR spectrum.

This research has discovered that PUR coatings have adhered well on mild steel panel regardless the oleic acid content. Excess NCO present in the formulation of the coatings apparently remains well-distributed within PUR to give cross-linked network having good adhesion strength. Generally, the alkali has greater detrimental effect on the coating performance than acid. The lowest oleic acid content polyol PURs coatings

formed the best appearance and cured rapidly. Polyols, which have higher percentage of oleic acid content has lower hydroxyl number, are proven to have a longer dry hard time. However, the curing time decreases further as the NCO/OH ratios of the PURs were increased. It has been observed that the hardness of the coating films, water, solvent and acid resistance are at satisfactory level for this type of PUR. These properties are further enhanced by increasing the NCO/OH ratios of the samples.

The nature of the PUR samples is investigated through the XRD analysis. The PURs are in amorphous nature where the small amount of crystallinity is overshadowed by the presence of long hydrocarbon chain of the polyols and hydrogen bonding – OCONH- groups of PUR. However, it should be noted that the amorphous nature of the samples decreases as oleic acid content is increased. Furthermore, percentage of hard segments increases as the NCO/OH ratio of the sample is increased thus the samples become less amorphous.

Thermal transition of the samples was investigated through DSC analysis and from the analysis it has been concluded that both phase separation and crystalline formation may have been inhibited by the presence of chemical cross-links. The PURs with a higher percentage of oleic acid content have higher percentages of flexible side chains which hinder cross-linking. All the alkyds have almost identical T_m values around -28°C . PUR samples exhibit single broad T_g suggesting that there are less visible phase separations between soft and hard domains. The T_g values remain at 123°C regardless the NCO/OH ratios and the increment of oleic acid percentage. The only significant change in the structure of main PUR chain is the side branch of oleic acid and in this case the side chain does not contribute significantly to the T_g of the sample.

Thermostability of the PURs was determined through TGA analysis. The TGA studies show that the weight loss of PUR samples starts around 170°C with the expulsion of the gaseous compounds such as water, CO and methane. Eventually, urethane starts to degrade followed by isocyanate (360°C) and finally the carbon backbone of the polymers degrades between 500°C to 700°C. It has been observed that the thermostability of PURs increased as the oleic acid content of the polyols is increased. Thus, it has been anticipated that the decomposition of oleic acid fragment may cause the thermostability to increase. Furthermore, the increased NCO/OH ratio also increased the thermostability of the samples. The presence of urea groups presumably increase the thermostability as the thermostability of PUR samples reported are in the order of isocyanate > urea > urethane > biuret > allophanate.

Another aspect of the research has been directed towards characterizing the electrical properties of the PUR samples. AC and DC electrical testing were performed. The real permittivity ϵ' and imaginary permittivity ϵ'' values were obtained and the results are in the range of 1.90 to 2.48 and 0.02 to 0.08 respectively. These values are comparable to that of other polyurethane in the market. One must therefore realise the possible prospect of obtaining PUR from palm olein oleic based polyurethanes which are compatible to PURs obtained from petroleum derivatives.

It has been found that the frequency and oleic acid content are factors which govern the dielectric properties of the samples. The ϵ' values decrease with increasing frequency due to decreased polarization in the material. Distinct loss peak is also observed in ϵ'' spectra at the frequency range of 4000 to 20000 for all the samples. In our case the Cole-Cole plot was fitted using Havriliak-Negami model. The γ -relaxation due to

orientational polarization is proposed as the probable mechanism for the dielectric behaviour of PUR in the frequency range of 1000 – 1000000 Hz.

Frequency dependence of conductivity $\sigma(\omega)$ for all the PUR samples at room temperature exhibits typical behaviour of ionic materials. The frequency dependent conductivity of PUR materials has been analyzed using a Jonscher's power law expression. From the fitting and extrapolation of the Jonscher's power law the dc conductivity is obtained. ϵ' spectra increases as the NCO/OH ratios increased. ϵ'' value of the samples increases as the NCO/OH ratio increases except for the case of PUalk40 where the value of imaginary permittivity for the ratio of 1.2 overlaps with that of the ratios of 1.4 and 1.6. The peak position remains the same or shifts in a small amount as the ratio increases for all the cases. Another property which increased as the NCO/OH ratio increases is the dielectric strength of the material.

Analysis of dc conductivity studies agrees to Arrhenius plot and gives the dc conductivity in the range of 10^{-8} to 10^{-12} Sm^{-1} . Ionic conduction mechanism is predicted to be the main conduction mechanism in the PUR samples which also agrees well with the analysis of ac dielectric studies. The charge carriers are assumed to be contributed by ions due to dissociation of protons from oleic acid and dissociation of urethane groups in the samples. The hyperbolic sine function was used to estimate the hopping parameters $\lambda(T)$ for the PURs. Hopping distance of the charge carriers are in range of below 9 nm for all the PUR samples in the research.

This research has also focussed on the mechanical properties of the PUR samples. From the studies, it has been observed that the modulus values, tensile strength and rupture strength decreased but elongation increased with the oleic acid content of the samples.

It has been speculated that there exists more dangling chain of oleic acid in the bulk of PUR polymers which function as plasticizers as the oleic acid content is increased in the PURs thus decreasing the modulus, rupture strength and tensile strength of the material. However, as the NCO/OH ratio increased, the modulus values and tensile strength increased. This characteristic of the materials occurs due to the presence of increased three-dimensional allophanate, biuret cross-links and polar urea structure. The three-dimensional allophanate or biuret structure restricts the mobility of the molecular chain and consequently, increases the stress property and decrease the strain property.

The studies presented can be considered as the groundwork in preparing the PUR coating from palm oil. Much work remains to be accomplished and many formulation possibilities can be utilized in improving the research results. In this context there are a number of topics that deserve further investigation in preparing the PUR coatings with better properties and several possibilities are discussed in the section below.

1. Presently the polyols with lower oleic acid content are very viscous, which requires heating during handling of the material. In order to overcome this problem, the oleic acid polyols could be modified with other unsaturated anhydride such as maleic anhydride and citronic anhydride to improve the viscosity of the polyols.
2. The PUR coating obtained from palm oil based PUR is slightly yellow in colour. This can be overcome by incorporating colour pigment in the coating formulation. Thus, to fully evaluate the usefulness of the pigmented PUR

coatings, the properties of coatings should be investigated and compared with the current clear PUR coatings.

3. Solventborne PUR coatings have been used successfully for several years. These formulations of PUR coating can be modified to aqueous PUR dispersions which is free from low-boiling organic solvents for coating applications as well as for two-component PUR casting applications. Both hydrophilic and hydrophobic polyisocyanate can be used as a cross-link for two-component waterborne PUR films. Much of the work with this technology has been done with hydrophilically modified polyisocyanates made by partially reacting a polyisocyanates with a monofunctional hydrophilic polyether. The technology can be modified to prepare the oleochemical based waterborne PUR coating. The aqueous PUR coating based on oleochemical polyols in application, such as industrial flooring PUR system can offer an interesting alternative to classical epoxy systems.
4. Another aspect to consider in furthering the work is by choosing various aromatic and aliphatic isocyanates as a cross-link with the current polyols to study their effects on the performance of PUR coatings. Generally, aromatic isocyanates can yield excellent cross-linked films but will down-gloss on outdoor exposure and aliphatic isocyanates yield coatings with excellent gloss and colour retention on outdoor exposure. Some of the commercially available aliphatic and aromatic isocyanates which can be considered are Methane Diphenyl Diisocyanates (MDI), Hexamethylene Diisocyanate HDI, Isophorone Diisocyanate (IPDI) and Hydrogenated MDI (H12MDI).

A lot of experience and achievement has been obtained during the research work and preparation of this thesis. Being a physicist it was not an easy task to formulate and synthesize the PUR coatings. Substantial amounts of literature have been reviewed throughout the research to obtain deep knowledge on the material. The formulation and experimental set-up was prepared with great awareness in reducing the effect of impurities such as water. The PUR coatings were successfully synthesized and physically characterized with full determination and courage. Various characterizing techniques utilized have been covered in this thesis. It has been demonstrated that these polymers could be highly promising for many technological uses because of their chemical versatility, stability, processability and low cost. Improving the synthesis, characterization and optimising the palm oil polyols paves the way for the production of the PUR coating with reproducible quality.

APPENDIX

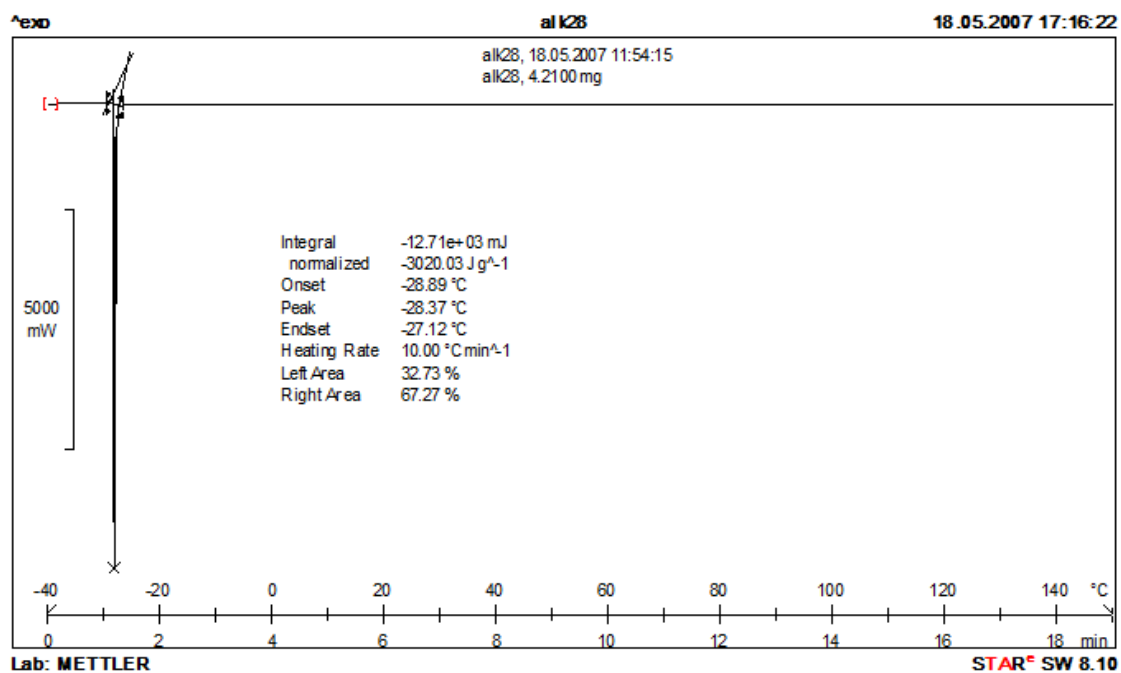


Figure X DSC thermograms of Alk28

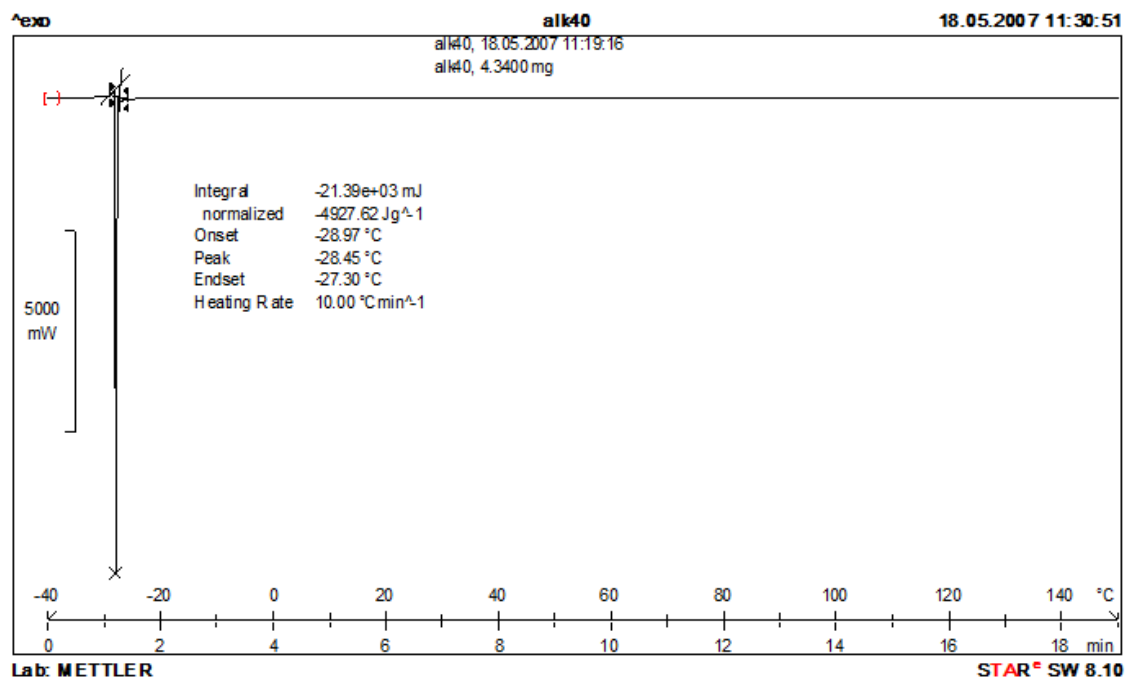


Figure XI DSC thermograms of Alk40

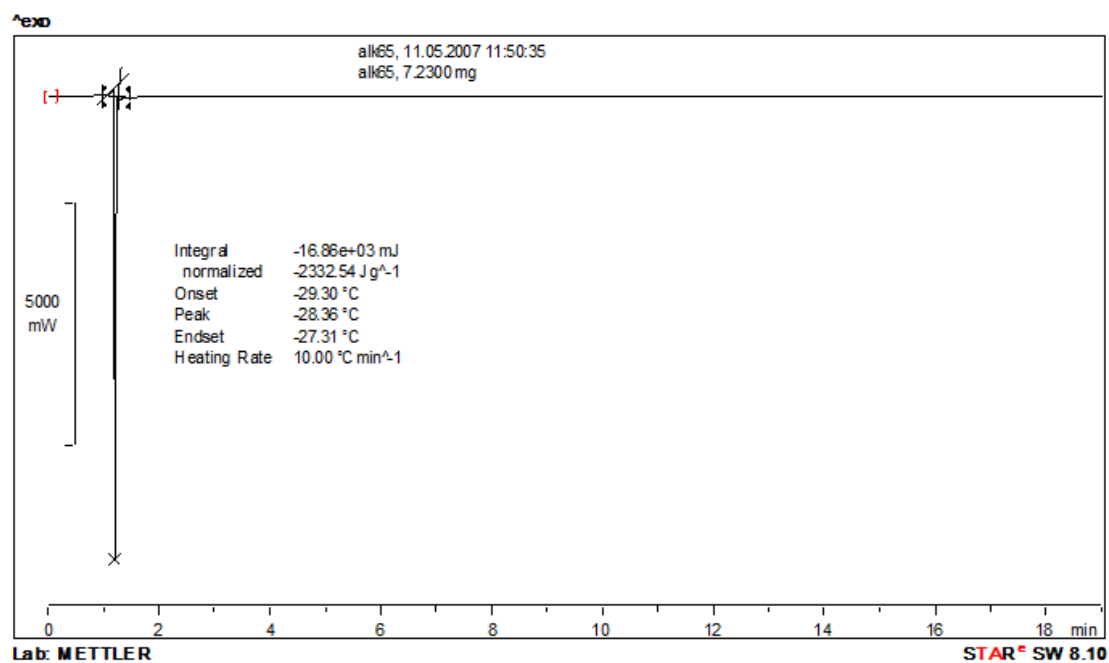


Figure XII DSC thermograms of Alk65